
Universitat
de les Illes Balears

**DOCTORAL THESIS**

**2017**

# REAL-TIME MONITORING OF BIOACCESSIBILITY TESTS FOR SOLID SAMPLES USING AUTOMATIC FLOW METHODS

**David Jaime Cocovi Solberg**


Universitat
de les Illes Balears

**DOCTORAL THESIS**

**2017**

**Doctorado en Ciencia y Tecnología química**

# REAL-TIME MONITORING OF BIOACCESSIBILITY TESTS FOR SOLID SAMPLES USING AUTOMATIC FLOW METHODS

**David Jaime Cocovi Solberg**

**Director: Manuel Miró Lladó**

**Doctor per la Universitat de les Illes Balears**

# List of papers derived from this doctoral thesis

- David J. Cocovi-Solberg, Manuel Miró, Victor Cerdà, Marta Pokrzywnicka, Łukasz Tymecki, Robert Koncki - Towards the development of a miniaturized fiberless optofluidic biosensor for glucose - Talanta, 2012, 96, 113–120.
- David J. Cocovi-Solberg, Maria Rosende, Manuel Miró - Automatic Kinetic Bioaccessibility Assay of Lead in Soil Environments using flow-through microdialysis as a front end to electrothermal atomic absorption spectrometry - Environ. Sci. Technol. 2014, 48, 6282-6290.
- Marta Fiedoruk, David J. Cocovi-Solberg, Lukas Tymecki, Robert Koncki, Manuel Miró - Hybrid flow system integrating a miniaturized optoelectronic detector for on-line dynamic fractionation and fluorometric determination of bioaccessible orthophosphate in soils - Talanta, 2015, 133, 59-65.
- David J. Cocovi-Solberg; Manuel Miró - CocoSoft: educational software for automation in the analytical chemistry laboratory - Anal. Bioanal. Chem 2015, 407, 6227-6233.
- Alexandra Sixto, Marta Fiedoruk-Pogrebniak, María Rosende, David J. Cocovi-Solberg, Moisés Knochen, Manuel Miró - Mesofluidic platform integrating restricted access-like sorptive microextraction as a front-end to ICP-AES for determination of trace level concentrations of lead and cadmium as contaminants in honey - J. Anal. At. Spectrom., 2016, 31, 473-481.
- Ana C.F. Vida, David J. Cocovi-Solberg, Elias A. G. Zagatto, Manuel Miró - Rapid Estimation of Readily Leachable Triazine Residues in Soils Using Automatic Kinetic Bioaccessibility Assays followed by On-line Sorptive Clean-up as a front-end to Liquid Chromatography - Talanta, 2016, 71–78.
- Daniel Kremr, David J. Cocovi-Solberg, Petra Bajerová, Karel Ventura, Manuel Miró - On-line monitoring of in-vitro oral bioaccessibility tests as a front-end to liquid chromatography for determination of chlorogenic acid isomers in dietary supplements – Talanta, 2017, 166, 391–398.
- David J. Cocovi-Solberg, Astrid Kellner, Stine N. Schmidt, Andreas Loibner, Manuel Miró, Philipp Mayer - Membrane Enhanced Bioaccessibility Extraction (MEBE): A novel platform for determining accessibility of nonpolar species in environmental solids without sink constraint (In preparation)
- David J. Cocovi-Solberg, Manuel Miró - Coupling of dynamic accessibility tests to liquid-chromatography using bead-injection mesofluidic analysis for monitoring of the leaching kinetics of xenobiotics in environmental solids (In preparation)

Universitat de les Illes Balears

Dr. Manuel Miró Lladó, profesor titular de química analítica, vinculat al Departament de Química de la Universitat de les Illes Balears

DECLARO:

Que la tesi doctoral que porta per títol 'Real-time monitoring of bioaccessibility tests for solid samples using automatic flow methods', presentada per David Jaime Cocovi Solberg per a l'obtenció del títol de doctor, ha estat dirigida sota la meva supervisió i que compleix amb els requisits necessaris per optar al títol de Doctor Internacional.

I perquè quedi constància d'això signo aquest documen

Palma, 20 de març de 2017

# Acknowledgements

Several scientific works reveal the benefits of being grateful [1–3]. I am grateful to the Spanish Ministry of Science and Competitiveness (MINECO), former Spanish Ministry of Science and Innovation (MICINN) for PhD fellowship allocation (BES-2011-044253) through project CTM2010-17214, and for mobility grants for research stays in Danmarks Tekniske Universitet (Technical University of Denmark, DTU) (EEBB-I-14-08721) and in Universität für Bodenkultur in Vienna (University of Natural Resources and Life Sciences in Wien, BOKU) (EEBB-I-15-10182). I am also grateful to the MINECO for financial support through project CTM2014-61553-EXP. Many thanks also to the Faculty of Pharmacy in Hradec Králové of the Charles University in Prague, for the financial support through the project entitled 'TEAB- Establishment of Research Tema Focused on Experimental and Applied Biopharmacy', and to 'Banco Santander' for the financial support through the award to the best PhD students of the UIB (2013).

I also acknowledge the institutions that allowed me to bring my thesis to a successful conclusion: The Universitat de les Illes Balears (UIB), the Danmarks Tekniske Universitet (DTU) and the Universität für Bodenkultur in Vienna (BOKU).

I extend my gratitude to the territories I wandered and the lovely people I found there, who favored physically, mentally or morally my work, leaving an indelible fingerprint in this joyous journey of mental stimulation that are life and science respectively. The techniques described in this thesis may or may not be applied in the future, but the human and social baggage acquired in this thesis time will last a long time.

Many many many thanks to my mother, Isabel Solberg, because of her unconditional help and conditional approval during this long journey, there are no words for expressing how grateful I am for all the work and sacrifices she made for allowing me to be here. Many thanks also to my little sister Myriam Cocovi, who happens to be a scientist too. Her interest in my work makes me keep hoping that it's useful for something or someone. Twelve dozens of red thanks and yellow tulips to Camila Cela, my girlfriend, for the limitless advices about how to manage and balance my work, free time and future from a pretended objective point of view. Sorry for coming late from the lab, happiness is made of love and work. Not last and for sure not least, I want to extend my gratitude to Lady Elisabeth Taylor a.k.a. Lilifrut, our Cavalier King Charles spaniel because her plant-eating promenades, countless naps along the day, indecorous sniffing habits and random saturday-night firework sympathetic crisis

make me focus on really important things – watching the sea defiantly with the wind on the face, holding a hot mug of coffe with milk. 'On my lap sleeps one who possesses beauty with vanity, courage against cats and birds without cruelty, and the virtues of all human beings without any of their vices'. To all of you, I promise I will try to be closer in this treacherously pretended stressless age to come.

Many thanks go also to my friends Tofol Gomez, Gabi Noguera, Javi Perez de Diego, Roberto Vich and Jordi Coll. They have been pointing out how worthless is my work and trying to make me quit it for years. They will love to be in this acknowledgement.

Many many thanks to Manuel Miro, my supervisor during 7 years. With him I actually learned that with patience, perseverance and deep understanding about what we do, we can get wherever we want to, science is more related to dreams than to cables and tubing. I'm also very thankful to the closest members of the chemistry department, namely Maria Rosende, Susana Gutierrez, Miquel Oliver, Alberto Hernández, Cristina Cerezo, Javi Llorente, Ruth Suarez, Sabrina Clavijo, Toni Serra and Luis Laglera, as well as the lovely visitors I coworked with: Marta Pokrzywnicka, Marta Fiedoruk, Sira Nitiyanontakit, Valentina Manzo, Victoria Manuel, Tania Rodriguez, Alexandra Sixto, Alejandra Herrera, Ana Vida, Daniel Kremr, Michał Michalec, Kateřina Fikarova, Maite García and Olivia Han, we had a nice time together. Special thanks to Burkhard Horstkotte for his stimulating endless engineering feedback from the distance as well as advices and cheerful contributions about possibilities of the designed systems.

My thanks also go to Jose Gonzalez, and Maribel Cabra for their hours and hours helping me with the ETAAS and the HPLC respectively, always with good humor, and also to Josep Agusti Pablo for helping me repairing the HPLC when it stopped working. Many thanks also to Neus Piña and Sergio Prats regarding all the unspecific help I received from them in so many different fields. My appreciation also goes to Raul Santos Sanchez Torres for the help in the mechanical workshop, for being at least as perfectionist as I am and for the zoomout regarding the thesis and the university life, use and abuse.

Many many thanks to the bar crew: Tomeu, Cati, Lianka, Dina, Emil, Marga and Nuri. While ideas are the limiting reagent of science, coffee and jokes are an indisputable catalyzer. Many thanks also to the bedels Rafel, Sion, Pedro and Carmen as well as to the housekeepers Mati and Cati, who spread their good humor and actually cleaned, allowing me to work by placating my obsessions-compulsions.

Many thanks to Philipp Mayer for being my supervisor in Copenhagen, as well as to Christina Maj, Mikael Olson, Monna Refstrup, Suzanne Kruse and Jens Schaarup for the help in the chromatography lab, and specially to Stine Nørgaard Schmidt for the

help in the lab and her collaboration in the research. Without them this work could not be presented. Many thanks also to Aiga Mackevica, Laura Roverskov, Umut Savacı, Kosan Roh, Sayana Tsushima, Rosella Onofrio, and Angel Marrero for the social program.

I am very grateful also to to Stephan Hann for being my supervisor in Vienna, I enjoyed the time there. Thanks also to Christina Troyer for sitting with me and demonstrating that Van Deemter's equation has some real and immediate applications, and is a great tool for everyday use. Limitless thanks go also to Philipp Tondl for giving away many hours helping me with everything related to the GC-QqQ, to Simone Panholzer and Teresa Mairinger for further help with the GC and putting into perspective the analysis and the research itself and to Marianna Vitkova for the time spent setting up the brittle-tip GX-271 ASPEC. I also appreciate very much the Schönbrunn garden for keeping me fit and inspired and to Cafe Landtmann and Palmenhaus for being the lovely places where I wrote down disrupting and revolutionary ideas and uncanny manifolds about future work watching the sunset. Some dreams made me forget what those systems were designed for, but the pictures should be still revisited.

My gratitude goes also to the most technical section of the big family of flow injection analysis, specially to Marcela Segundo, Antonio Rangel, Hana Sklenářová, Petr Solich, Spas Kolev, Aristidis Anthemidis, Graham Marshall, Ilkka Lähdesmäki, Purnendu K. Dasgupta, Moises Knochen, Mirek Macka, Elo H. Hansen, Paweł Kościelniak, and Olaf Elsholz for their discussions in the corridors of the conferences, they made me think what I do is clever and encouraged me to keep working hard. They will probably never know that they are in this acknowledgement, but however they should be here.

Finally, I would also acknowledge the technical team that allowed me to deposit flawlessly this thesis, including once again my supervisor, the external evaluators and the administrative and management staff of the Universitat de les Illes Balears.

# List of abbreviations

| | |
|---|---|
| AcOH | Acetic acid |
| ADC | analog-digital converter |
| ASTM | American Society for Testing and Materials |
| BARGE | BioAccessibility Research Group of Europe |
| BCR | Community Bureau of Reference |
| BI | Bead Injection |
| CAN | Controller Area Network |
| CRM | Certified Reference Material |
| DMSO | DiMethyl SulphOxide |
| ECTS | European Credit Transfer System |
| EDTA | EthyleneDiamineTetraAcetate |
| EHEA | European Higher Education Area |
| EPA | Environmental Protection Agency |
| ESD | Equilibrium Sampling Device |
| ETAAS | ElectroThermal Atomic Absorption Spectroscopy |
| FEP | Fluorinated Ethylene Propylene |
| FI | Flow Injection |
| FIA | Flow Injection Analysis |
| FLD | Fluorescence Detector |
| FPEDD | Fluorometric Paired Emitter-Detector Diodes |
| GUI | Graphic User Interface |
| HC | Holding Coil |
| HOC | Hydrophobic Organic Chemicals |
| HPCD | 2-hydroxypropyl-β-cyclodextrin |
| HPLC | High Performance Liquid Chromatography |
| ICP-OES | Inductively Coupled Plasma Optical Emission Spectrometry |
| ID | Inner Diameter |
| ISO | International Organization for Standardization |
| ISO/TS | International Organization for Standardization - Technical Specification |
| IV | Injection Valve |
| IUPAC | International Union of Pure and Applied Chemistry |
| $K_D$ | solid to water distribution coefficient |
| LDPE | Low Density PolyEthylene |
| LED | Light Emitting Diode |

| | |
|---|---|
| $L_{ef}$ | effective length |
| LOC | Lab-On-Chip |
| LOD | Limit Of Detection |
| log $K_{ow}$ | Logarithm of the 1-Octanol-Water distribution coefficient |
| LOQ | Limit of Quantification |
| LOV | Lab-On-Valve |
| L/S | Liquid to Solid ratio |
| MEBE | Membrane Enhanced Bioaccessibility Extraction |
| MWCO | Molecular Weight CutOff |
| µTAS | microTotal Analysis System |
| n | number of observations |
| NIST | National Institute of Standards and Technology |
| NMR | Nuclear Magnetic Resonance |
| OD | Outer diameter |
| p | number of parameters |
| PAH | Polycyclic Aromatic Hydrocarbons |
| PDA | PhotoDiode Array |
| PDMS | PolyDiMethyl Siloxane |
| PEDD | Paired Emitter-Detector Diode |
| PEEK | PolyEther Ether Ketone |
| PES | PolyEtherSulphone |
| PP | Peristaltic Pump |
| PTFE | PolyTetraFluoroEthylene |
| PVC | Poly(Vinyl chloride) |
| PVDF | Polyvinylidene fluoride |
| QC | Quality Control |
| $Q_d$ | perfusate flow rate |
| QuEChERS | Quick, Easy, Cheap, Effective, Rugged and Safe |
| $R^2$ | coefficient of determination |
| $R^2_{adj}$ | adjusted coefficient of determination |
| RAM | Restricted Access Material |
| $R_d$ | Resistance to mass transfer through dialysate |
| $R_e$ | Resistance to mass transfer through external medium |
| $R_m$ | Resistance to mass transfer through membrane |
| rpm | revolutions per minute |
| RR | Relative Recovery |
| RS | Recommended Standard |
| RSD | Relative Standard Deviation |
| SD | Standard Deviation |
| SEM | Scanning Electron Microscopy |
| SFA | Segmented Flow Analysis |

| | |
|---|---|
| SI | Sequential Injection |
| SIC | Sequential Injection Chromatography |
| SMT | Standards Measuring and Testing Program |
| SP | Syringe Pump |
| SPE | Solid Phase Extraction |
| SPME | Solid Phase MicroExtraction |
| SRM | Standard Reference Material |
| $SS_{RES}$ | Sum of Squared variance of the residuals |
| $SS_{TOT}$ | Sum of Squares of total variance |
| SV | Selection Valve |
| TE | Trace Element |
| TFF | Tangential Flow Filtration |
| UBM | Unified Bioaccessibility Method |
| USB | Universal Serial Bus |
| VBA | Visual Basic for Applications |

# Index

# Abstract (English)

Total extraction methods for risk assessment/exposure of potentially contaminated solid samples of environmental interest tend to overestimate the actual hazard of such samples. Bioaccessibility tests have been developed during the past few decades in order to assess the real hazard of environmental solid samples more closely by resorting to mild extractions in environmentally mimetic conditions. Those tests present however a series of drawbacks, including the operationally defined conditions that should be adapted between samples (but are not), the risk of readsorption and redistribution processes, and the lack of sink capacity of the extraction media. A novel insight into the fundamentals of bioaccessibility of organic pollutants is presented in this dissertation by the so-called Membrane Enhanced Bioaccessibility Extraction (MEBE) approach (chapter 3), which uses semipermeable membranes in order to separate the extraction medium and the final acceptor of the pollutants, and thus foster maintaining the desorption flux from the matrix.

To assess the suitability of the operationally defined conditions and detect readsorption and redistribution processes the international community proposed dynamic extraction tests and kinetic monitoring of the ongoing extraction processes, in spite of complicating and lengthening the analyst workload. In this dissertation, we propose the development of automatic methodologies resorting to low pressure flow methods for simplification of bioaccessibility tests from solid matrices followed by extract clean-up and preconcentration (whenever needed) for monitoring the kinetics of the leaching of nutrients, trace elements and organic pollutants. To control this instrumentation and to ease the data treatment, CocoSoft, an automation suite has been developed (chapter 4). At-line and on-line hyphenation of flow-based bioaccessibility tests to appropriate detectors allows for real time leachate monitoring with added benefits of deconvolution of several bioaccessible pools, early prediction of pollutant content or test duration. Those hyphenations have been applied to molecular fluorimetry (chapter 5), atomic spectrometry (chapters 6 and 7) and reverse phase HPLC (chapters 8, 9 and 10).

# Resumen (Castellano)

Los métodos de extracción total utilizados en la evaluación de riesgos de muestras sólidas de interés ambiental potencialmente contaminadas tienden a sobreestimar el peligro real de estas muestras. Los ensayos de bioaccesibilidad se han desarrollado durante las últimas décadas para evaluar el peligro real de muestras sólidas de interés ambiental recurriendo a extracciones suaves en condiciones ecomiméticas. Estos ensayos presentan de todas formas una serie de desventajas, que incluyen condiciones operacionalmente definidas, que deberían adaptarse entre muestras (pero no lo hacen), el riesgo de readsorción y redistribución, y la falta de solubilidad de los analitos en el medio de extracción. En esta disertación se presenta una nueva visión fundamental de la bioaccesibilidad de contaminantes orgánicos mediante la aproximación llamada Extracción Bioaccesible Mejorada con Membrana (MEBE por sus siglas en inglés) (capítulo 3), que utiliza una membrana semipermeable para separar el medio de extracción del aceptor final de los contaminantes, y por ello ayudan a mantener el flujo desortivo desde la matriz.

Para evaluar la idoneidad de las condiciones operacionalmente definidas y detectar procesos de readsorción y redistribución, la comunidad internacional propuso ensayos de extracciones dinámicas y la monitorización cinética de los procesos de extracción, a pesar de complicar y alargar la carga de trabajo del analista. En esta disertación, proponemos el desarrollo de métodos automáticos que recurren a técnicas fluídicas de baja presión para simplificar los ensayos de bioaccesibilidad de matrices sólidas, seguidos de limpieza y preconcentración del extracto (cuando sean necesarios) para monitorizar la cinética de lixiviación de nutrientes, elementos traza y contaminantes orgánicos. Para controlar la instrumentación y facilitar el tratamiento de datos, se ha desarrollado CocoSoft, un paquete de automatización (capítulo 4). El acople at-line y on-line de los ensayos fluídicos de bioaccesibilidad a los detectores adecuados permite la monitorización a tiempo real del extracto, con los beneficios añadidos de deconvolucionar diversas fracciones bioaccesibles y la anticipación del contenido de contaminante o la duración del ensayo. Estos acoples se han aplicado a fluorimetría molecular (capítulo 5), espectroscopia atómica (capítulos 6 y 7) y HPLC de fase reversa (capítulos 8, 9 y 10).

# Resum (Català)

Els mètodes d'extracció totals emprats a l'avaluació de riscos de mostres sòlides d'interès ambiental potenciament contaminades tendeixen a sobreestimar el veritable perill d'aquestes mostres. Els assaigs de bioaccessibilitat s'han desenvolupat durant les darreres dècades per avaluar el perill real de mostres sòlides d'interès ambiental recorrent a extraccions suaus en condicions ecomimètiques. Aquests assaigs presenten de totes maneres una sèrie de desavantatges que inclouen condicions operacionalment definides que s'haurien d'adaptar entre mostres (i no es fa), el risc de readsorció i redistribució, i la manca de solubilitat dels analits al mitjà d'extracció. En aquesta dissertació es presenta una nova visió fonamental de la bioaccessibilitat de contaminants orgànics mitjançant l'aproximació anomenada Extracció Bioaccesible Millorada amb Membrana (MEBE per les seves sigles en anglès) (capítol 3), que empra una membrana semipermeable per separar el mitjà d'extracció de l'acceptor final dels contaminants i per això ajuda a mantenir el flux desortiu des de la matriu.

Per avaluar la idoneïtat de les condicions operacionalment definides i detectar processos de readsorció i redistribució, la comunitat internacional va proposar assaigs d'extraccions dinàmiques i la monitorització de la cinètica dels processos d'extracció, encara que compliqui i allargui la càrrega de treball de l'analista. A aquesta dissertació, proposem el desenvolupament de mètodes automàtics que recorren a tècniques fluídiques de baixa pressió per simplificar els assaigs de bioaccessibilitat de matrius sòlides, seguits de neteja i preconcentració de l'extracte (quan sigui necessari) per monitoritzar la cinètica de lixiviació de nutrients, elements traça i contaminants orgànics. Per controlar la instrumentació i facilitar el tractament de dades, s'ha desenvolupat CocoSoft, un paquet d'automatització (capítol 4). L'acoblament at-line i on-line dels assaigs fluídics de bioaccessibilitat als detectors adients permet la monitorització a temps real de l'extracte, amb els beneficis afegits de deconvolucionar diverses fraccions bioaccessibles i l'anticipació del contingut de contaminant o la duració de l'assaig. Aquests acoblaments s'han aplicat a fluorimetria molecular (capítol 5), espectroscòpia atòmica (capitols 6 i 7) i HPLC de fase reversa (capítols 8, 9 i 10).

# 1. Introduction

## 1.1 Risk assessment: Aims and needs

Chemical risk assessment of soil for regulative purposes relies on the total amount of pollutants [4]. However, in the last decades many studies highlighted that the total amount of pollutant overestimates the real hazard to biota, because the toxicity of a given substance is not intrinsic to the isolated molecule but affected by its local environment: speciation, isomerism, complexation, adsorption, immobilization, binding to organic matter and soil components… This local environment information is partially or completely lost when using total extraction procedures endorsed by international regulations such as acidic digestion at high temperature, matrix solid-phase dispersion, pressurized liquid extraction, soxhlet extraction, ultrasound and microwave assisted extractions or QuEChERS [5]. For evaluating the actual hazard of a potentially contaminated soil sample, the evaluation has to be done under ecomimetic conditions. While this aspect has been discussed for quite a long time in the research domain, is has not made its way to the regulatory realm and only a few technical documents, as the International Organization for Standardization (ISO) norm 17924:2007 on soil quality and oral bioaccessibility or 17402:2008 [6] on soil quality and methods for assessing bioavailability and those related, tackle this issue. The tests that offer information about the local pollutant environment by resorting to mild extractions are known as accessibility tests. Figure 1.1 shows a close-up of the complex environment that accessibility tests have to tackle with.

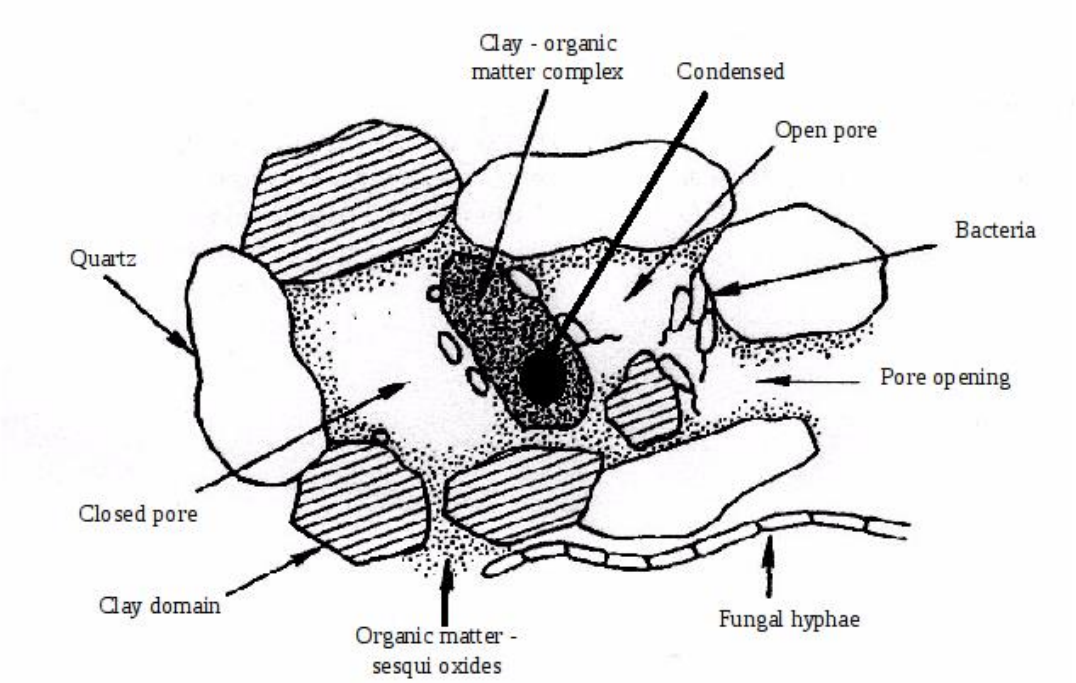


*Figure 1.1. Close-up of the local environment involved in ecological conditions that accessibility tests have to simulate.*

## 1.2 Accessibility

While total pollutant concentrations values are used to identify worst case scenarios, they tend to overestimate the potential hazard of the sample in real human/biota exposure conditions because no real biotic environment has the eluotropic power, matrix disaggregation properties or chemical reactivity of the chemicals used in total extraction methodologies. Since the pollutant has to cross several interfaces and diffuse through several compartments before reaching the bioactive target, not all the total mass of pollutant will reach the target organ or tissue, contrariwise it will distribute into all the available ecological compartments. Nevertheless only some species present in a given compartment might be potentially toxic to biota. While speciation could seem to be more suitable for quantifying the target pollutant species, the interconversion due to the dynamic equilibrium in each environmental compartment and during the sampling process itself make fractionation approaches more adequate. To quantify the maximum amount of pollutant able to cross those natural barriers, bioaccessibility tests, *viz.* tests that study the pollutant solubility from soil particles under biomimetic and environmentally simulated leaching conditions have been trendy over the past decades. ISO 17402:2008 defines and describes the processes relevant to, three ecological compartments: soil particles, liquid phase and biota inner medium, and the two interfaces that separate them:

soil/liquid interface and cellular membrane. Down here we present a short discussion of those three compartments, which are summarized in figure 1.2.

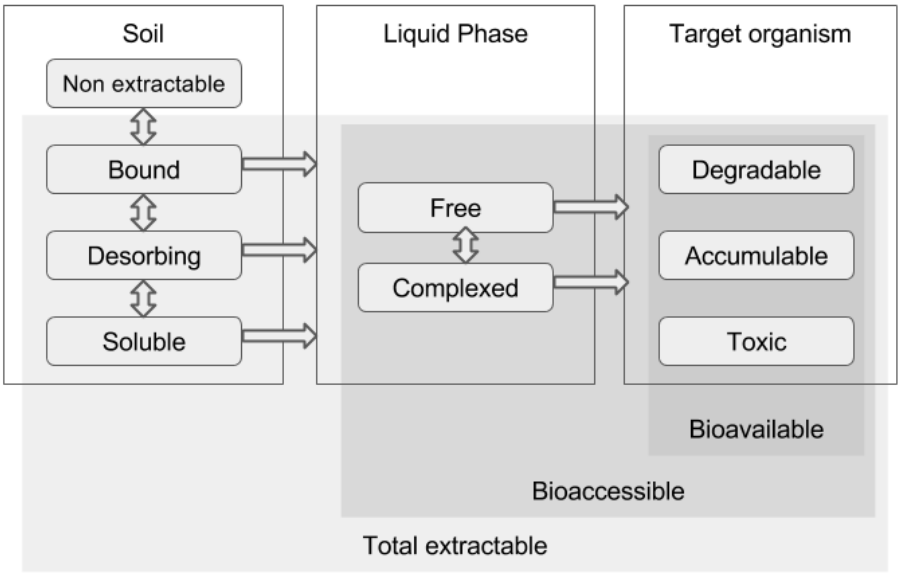


*Figure 1.2. Summarized environmental processes concerning accessibility of different substances in three ecological compartments separated by two interfases.*

The first step for the pollutant to reach the target organ or tissue in a bioavailability and ecotoxicological framework is to pass from its reservoir (e.g., soil material) to a liquid phase by means of desorption or extraction in ecomimetic conditions, which determines the bioaccessible fraction. If the pollutant is not able to get into the liquid phase (e.g., interstitial soil pore water), it will not be available to reach the target organism membranes. Several tests based on mild extraction schemes (slightly acidic or complexing leaching agents for polar/ionic compounds and mild solvents for organic compounds) try to mimic liquid ecological compartments in order to simulate their eluotropic power or aggressiveness and thus mimic real leaching conditions e.g. rainwater, pore water, acidic rain. These tests consist usually on a fractionation, *viz.* a separation of the target species in several solubilized fractions or phases, representing ecological relevant compartments. Several leaching schemes are designed for specific pollutants and environmental samples (e.g. Tessier [7], McLaren-Crawford [8], Kersten-Förstner [9], Krishnamurti [10] or the former three-step Community Bureau of Reference(BCR) method [11], now Standards Measuring and Testing (SMT) scheme for trace elements, or the Hieltjes-Lijklema [12] for orthophosphate). Some of them are single step extraction methods in which the soil is extracted once with a given leaching agent, while other are sequential extraction in which leaching agents of increasing chemical aggressiveness are applied consecutively

to the residue of former extractions, thus allowing a further fractionation of the target species. The aforementioned ISO norm calls this fraction the environmental available, but is best known as the bioaccessible fraction by the early paper of Semple in 2004 [13]. A lot of research has been done under the bioaccessibility of trace metals subject [14] and several extraction schemes are referenced in the ISO norm 17402:2008.

The second environmental relevant interface that the pollutant has to cross in order to reach the target organ or tissue is the external membrane of target organism (cytoplasmic membrane for simple organisms or those derived from the ectoderm or endoderm in complex ones, depending on the type of exposure (oral, transdermal…)). The fraction able to enter the target organism is called bioavailable fraction. Those tests consist briefly in feeding young model animals e.g. swine, monkeys, etc., with a controlled dose of contaminated soil [15]. After the end of the experiment the animals are slaughtered, and the biological samples are extracted, characterized, and analyzed, through total extraction for organic or mineralization for inorganic analytes. The total amount of pollutant fed is known because is prepared from standards and if not, it can be calculated through total extractions or mineralization of the food. The bioavailable fraction is calculated as a ratio of the found in the animal tissues and the total fed. *In-vivo* tests need to be performed on animals, but recent economic and ethical considerations [16,17] as the weaning, fasting and caging of piglets, fostered the study of thermodynamically based correlations between the so called bioavailable fraction obtained from *in-vivo* ecotoxicological tests (or environmental bioavailable, according to the ISO norm) and *in vitro* chemically partitionable fractions. From the initial bioaccessible fraction, only a subfraction will be able to cross membranes, so additional tests have to be performed on the accessible fraction with further *in-vitro* partitioning based on physiologically relevant processes, referred to e.g. filterable [18] through a given pore size [19,20], dialyzable [21], (electro)labile [22] or freely dissolved species (simulating passive transport in chordate intestine) or directly correlating some mild extraction results with *in-vivo* tests for mammals.

Once the pollutant has entered the target organism it can affect several biological pathways by modifying them, or incorporating itself to the target organism metabolome. The exact number of processes affected and the endangering consequences can only be studied in vivo for each pollutant, each organism and each exposition mode. ISO 17402:2008 defines as the toxicologically bioaccessible fraction, the fraction of pollutant able to experiment biological processes, such as absorption, distribution, metabolism, excretion or accumulation. If the target substance or its metabolites are toxic to the target organism, that is, jeopardize the target organism self-sustainability at relatively low concentrations, the focus should be put onto the organism: only ecotoxicological tests can assess lethal doses. If contrariwise the analyte or its metabolites are not causing acute toxicity, the target molecule might be transformed or degraded and thus, its concentration decreases in target organism and

its ecosystem, while the concentration of metabolites for which the toxicity needs to be estimate will increase. This could be named the “biodegradable” fraction. If the target molecule is not metabolized, it will enter and exit the target organism at different rates until it is equilibrated with the medium (due to different solubility and thus partitioning coefficients of the molecule between the medium and the organism tissues). The amount of pollutant from a sample that is retained in the biota is called the bioaccumulable fraction. When a pollutant accumulates in an organism, it leads to biomagnification, *viz.* increasing concentrations at increasing trophic chain level. Toxicity, biodegradation and bioaccumulation are processes of utmost environmental and economic interest and many experimental works have been carried out to quantify the biodegradation and bioaccumulation of model pollutants by model organisms. As in the case of the bioavailable fraction, some correlations have been studied for biodegradable and bioaccumulable fractions between *in-vivo* ecotoxicological tests and *in vitro* mild extractions under operationally defined conditions, based on mimicking the biotic medium with extractants that match chemical parameters of physiological interest, such as the complexing capacity, dielectric constant or polarity. These correlations allow including *ex-vivo* tests in routine analysis for assessing the biodegradation and bioaccumulation of target model pollutants by target model organisms of environmental interest. Examples of biodegradation or bioaccumulation tests include the 24h extraction with 2-hydroxypropyl-β-cyclodextrins (HPCD) that correlates with the biodegradable fraction of Polycyclic Aromatic Hydrocarbons (PAH) by soil microbiota (Pseudomonas sp) [23–35] or the 24h extraction with n-butanol that correlates with the accumulation of PAH by *Eisenia foetida* (red worm) [36–40]. Regarding organic pollutants only tests for PAH are tackled in the ISO 17402:2011, but their natural origin and broad log $K_{ow}$ range make them very good case examples for other organic compounds with similar reactivity, such as halogenated hydrocarbons with endocrine disrupting properties, namely the twelve persistent organic pollutants endorsed by the Stockholm Convention from 2001, those added in further Conference of Parties and those proposed for inclusion in the next conferences. Some examples are: Aldrin, chlordane, dieldrin, endrin, heptachlor, hexachlorobenzene (HCB), mirex, toxaphene, polychlorinated biphenyls (PCB), dichlorodiphenyltrichloroethane (DDT), polychlorinated dibenzo-p-dioxins (PCDD), polychlorinated dibenzofurans (PCDF), alpha-hexachlorocyclohexane (αHCH), beta-hexachlorocyclohexane (βHCH), chlordecone, hexabromobiphenyl (HBB), polybrominated diphenyl ethers (PBDEs), lindane, pentachlorobenzene, perfluorooctanesulfonic acid (PFOS), perfluorooctane sulfonyl fluoride (POSF), endosulfan, hexabromocyclododecane (HBCD), polychlorinated naphthalenes (PCN), hexachlorobutadiene (HCBD) and pentachlorophenol (PCP)), to name a few.

The mechanisms underlying accessibility tests based on mild extractions are deemed to be thermodynamically biomimetic, but the lack of legislation as well as

broad literature proposing different conditions adapted from one to another researcher can obscure the ecological mechanism and relevance. Only resorting to the real thermodynamic and kinetic basis accessibility tests would be useful tools in risk assessment and exposure investigations of environmental pollutants.

## 1.3 Thermodynamic considerations

As stated in the previous sections, the main drawback of the proposed accessibility tests is their operationally defined nature and the adaptation of extraction conditions among different researchers without evaluating their actual environmental significance in every given assay. Ecological processes rely upon a constant dynamic redistribution of pollutant molecules onto countless natural phases through diffusion and dissolution/permeation processes. Comparing a biphasic (soil-extractant) model with such a natural system is a clear simplification and the prescribed fixed time kinetic measurements (operationally defined conditions aimed to ascertain a thermodynamic equilibrium, but not always accomplish it) controvert the aforementioned dynamic process: Rarely an ecological compartment will be in equilibrium with all surrounding phases simultaneously. To ameliorate the mimicry of the model with the ecological conditions researchers resorted to the dynamic extraction concept as a substitute to equilibrium-based extraction, namely packing the solid sample in a container and perfusing it continuously with the desired extractant. By doing so, leaching equilibriums are shifted, and a faster exhaustion of the deemed accessible fraction occurs as is expected in the accessibility concept. If no further equilibrium readjustment occurs, the total extracted amount can be termed the accessible fraction, however, kinetic information requires further data interpretation as the results are not directly comparable to those of batch extractions. Dynamic extraction tests are usually found in the research realms, but only some discrete cases are transferred to regulations [41].

Ecological leaching conditions imply seldom completely shifted equilibria, but a constant reequilibration of the analyte in the sample and dissolved medium. While dynamic extraction can be considered an improvement of batch extractions, both of them rely on exhausting the accessible fraction from the sample, either because of the high solubility of the analyte in the extractant or the high amount of the later (high L/S ratio). Mayer and Reichenberg [42] took a different approach by resorting to the chemical activity instead of absolute concentrations. Using activity as endpoint of the ecological measurement does not return information about the analyte mass, but of its tendency to move from its current phase or compartment, ranging the activity between 0, that is, the substance is not present or at the minimum possible chemical potential, to 1, where the substance will do its best to react, precipitate or diffuse, and thus, become available for the biota. The bioavailable concentration and activity are hence complementary measurements.

Mass transport in a system with several compartments is driven by activity so the analyte will diffuse from the compartment where its activity is higher to the one where it is lower, reaching the thermodynamic equilibrium when the activity in all compartments is the same. Therefore, in thermodynamic equilibrium, calculating the activity coefficient in one of the compartments allows to know the activity in the other compartments.

Activity measurements are usually obtained by resorting to equilibrium sampling devices [43,44] (ESD), using e.g. solid-phase microextraction (SPME) fibers [45] or the so-called coated jar method [46,47], where vials are coated with a microfilm of sorbent. In all ESD methodologies, a minute amount of an external phase (polydimethylsiloxane (PDMS) in the previous examples) presenting a good solubility for the target analyte is introduced in the extracting medium. The system is let reach the equilibrium, the external phase is removed, and the analyte content is measured by ordinary means. This implies usually a back extraction, as in the coated jar method [43], or directly in the GC injector as in the SPME methodology, using the same ESD method for constructing the external calibration curve through the partitioning standards technique [48], where briefly, the standards of known concentrations are prepared in the same medium as the ESD, and the ESD 'samples' the standard, e.g. PDMS SPME sampling the headspace of a calibration prepared in liquid PDMS. Advantages of the EDS are that the external phase is easy to separate from the extraction medium (against the common examples of depletive sampling methodologies as tenax beads [26,49,50]) and that the amount of analyte withdrawn is so small that it can be considered negligible, so the equilibrium between the sample and leaching medium can be studied with minimal influence by the external phase.

Another pitfall of accessibility tests is that even if they reach a steady state, it may be due to artifacts. The most illustrative example is a lipophilic pollutant extraction in which the limited L/S ratio is kept under operationally defined conditions, but the limited solubility of the pollutant in the leaching agent prevents its further desorption, reaching a fast thermodynamic equilibrium that does not reflect the real hazard of the sample. This is called the 'sink problem' (referencing the lack of solubility, the small acceptor volume or similar solubility of the pollutant in the soils and in the leaching agent) [51]. Using different L/S ratios those problems might be shed to light: The amount of pollutant released in a given timeframe should be only proportional to the amount of soil extracted, neglecting the volume of extractant. If lower L/S ratios lead to lesser amount of available fraction, a sink problem is encountered. Usual solutions imply the inclusion of an extra heterogeneous sink into the extraction medium, namely a given amount of mass in which the analyte is more soluble than the extraction medium [52]. Several approaches have been developed during last years for increasing the sink capacity of extraction medium in tests for lipophilic organic compounds, such as the inclusion of tenax beads [49,50,53,54],

silicone rods [55,56] or active carbon loaded silicone, *viz.* the so-called 'contaminant trap' [57]. While they successfully increase the sink capacity, some drawbacks are also introduced, as the difficulty of separation of the formed slurry with the beads, the need of back extraction from the silicone rod, or the impossibility of retrieving the analytes and thus the need for a mass balance with total extraction in case of the contaminant trap. A recent improvement in methodologies for tackling the sink effect is the so-called Membrane Enhanced Bioaccessibility Extraction (MEBE) test which was developed during this thesis work and is further explained in chapter 3. It basically consists of confining the bioaccessibility extraction process (sample and a low volume of leaching reagent) inside a semipermeable bag (membrane). This bag is placed in a vial containing an extracting solvent in a L/S ratio of ca. 20 that will act as a sink because of having a larger affinity for the analytes than the leaching reagent. In our case the liquid was ethanol and the analytes PAHs. In MEBE, the analytes are extracted inside the bag, they migrate across the membrane wall and accumulate in the ethanol, so the extraction medium does not get saturated and an aliquot of the sink can be directly sampled and analyzed directly without any further pretreatment. More advantages and characterization schemes can be found in chapter 3

## 1.4 Kinetic considerations

Regarding kinetic considerations, the first pitfall in accessibility tests is that even if the extraction test could correlate with an ecological partition, the kinetic monitoring of the pollutant release showcases that in many cases the operationally defined conditions are not enough to reach a steady state, that is, the deemed equilibrium is reduced to a fixed time measurement. Because every author uses different conditions, the results are thus not comparable. Examples of errors for trace metals involve soils with unexpected mineralogical phases that linger dissolution more than expected, keeping captured a pool of metal that would be released under different conditions, or in case of lipophilic pollutants, a slower kinetic release due to e.g. the occurrence of pores deeper than expected in soil particles from which the pollutant has to diffuse, or the inadequate soil grinding.

A second problem is that shaking conditions in laboratories such as magnetic stirrers may differ in some cases from gentle mixing as expected under ecological conditions, even if the former are deemed to be ecomimetic. In this way, a too aggressive shaking may lead to an overgrinding of the sample and creation of new surfaces that influence adsorption processes. The previously released pool of target molecule can be readsorbed in the newly created surfaces, and affect its (or other target molecules) partition in a redistribution process. Orbital or end-over-end shakers operated at low speeds may be deemed gentle enough to be compared with fluidizing conditions caused in the topsoil by rain, however they are not so common labware as the traditional magnetic stirrers. While in this thesis the magnetic stirrer has been

used, the end-over-end shaking is preferred for future work.

For those reasons, the kinetic monitoring of the extraction process and the use of different L/S ratios are key approaches for assessing the suitability of test conditions. Readsorption and redistribution can be documented by a decrease of signal vs time.

In case of not reaching the steady state, the kinetic measurements can predict the real steady state by fitting the experimental release data to the theoretical mathematical model. All fractions start leaching at the initial moment, and all tend to be completely extracted at infinite time following a first order kinetic model:

$$C = A(1 - e^{-kt})$$

Where A is the bioaccessible pool and, k is the kinetic releasing constant and t is time. A common interpretation of the duration it takes to extract a given fraction is to calculate the time needed to extract the 95% of that pool ($t_{95\%}$), because for a first order model, the 100% will take infinite time. The $t_{95\%}$ can be calculated from the kinetic constant as follows:

$$t_{95\%} = \frac{\ln(20)}{k}$$

Very often in single extraction procedures using highly eluotropic extracting agents e.g. ethylenediaminetetraacetate (EDTA) [58], citrate [59], there is a fraction overlap, that is, the readily leachable fraction is extracted along with the more immobile fraction. However, because fractions have a different extraction constant, the bulk of the readily leachable fraction is released at early times, where the slowly leaching fractions contribution is still negligible, and the later can be studied at longer times, where the readily leachable pool has been completely extracted. If several fractions with different releasing constants coexist, their kinetic profiles can be deconvoluted by fitting to a multiple first order releasing model [60–63].

$$C = \sum_{i=1}^{n} A_i(1 - e^{-k_i t})$$

Adding extra compartments and thus variables to the model increases always the goodness of fit of the model; statistical parameters taking into account the extra number of variables should be thus used, as the $R^2$ adjusted. The difference between the $R^2_{adj}$ and the original $R^2$ coefficients is shown below:

$$R^2 = 1 - \frac{\frac{SS_{RES}}{n}}{\frac{SS_{TOT}}{n}} \qquad R^2_{adj} = 1 - \frac{\frac{SS_{RES}}{n-p-1}}{\frac{SS_{TOT}}{n-1}}$$

Where $SS_{RES}$ is the sum of the squared variance of the residuals, $SS_{TOT}$ the sum of squares of the total variance of the data, *n* the number of measurements and *p* the number of parameters of the regression. As can be seen in the formula above, the only difference between $R^2$ and $R^2_{adj}$ is that the $R^2_{adj}$ includes the number of parameters in the degrees of freedom, so with increasing number of parameters, the $R^2_{adj}$ will decrease unless the fit is the best without an excess of regressive parameters, so the maximum $R^2_{adj}$ indicates the model that has to be chosen.

The mathematical compartments in the model (each with its own pool (A) and releasing constant ($k_A$) can be related to real ecological compartments. The readily leachable are water extractable, pore water soluble, immediate extraction with leaching agents that possess higher eluotropic power than water, weakly adsorbed substances. The easily leachable require diffusion through pores, more time, or bounded to secondary mineralogical phases, leachable with weak solvents (organics) or with electrolytes or weakly acidic extractants. The bound or slowly leachable take more time and/or stronger extractants and the immobile fraction do not leach with strong eluents.

Notwithstanding the fact that the monitoring of the leaching kinetics offer indisputable information about readsorption, redistribution, proper extraction time and relevant insight into several partitioning compartments, only two types of manual methodologies have been proposed nowadays ad hoc [14]:

- Starting several parallel extractions and stopping them each at a given time for analysis. This multiplies the needed of labware, sample amount, sampling frequency and includes a representativeness factor into the analysis (has to account for irreproducibility between samples)
- Scaling up the extraction and sampling at predefined intervals. Multiplies the sample amount and sampling frequency. Sampling the extraction medium changes the L/S ratio during the extraction time. Results are less reliable than the previous method [58].

Because both methodologies need multiple analysis per sample, they increase greatly the analyst work for each sample, leading to more expensive analysis, and are more prone to errors (human and instrumental). If no alternative concepts or technologies are developed, an immediate solution is the automation of extraction test by mechanized approaches, namely the sample preparation step. By doing so, most crass errors are avoided and the sample will be ready for analysis. The main drawback of kinetic monitoring methods is that the number of analysis will be sample number multiplied by the number of points of the desired kinetic profile, however if the aliquots can be analysed at real time, the reported feedback can help the decision making even before the prefixed duration time of the test.

## 1.5 Automation

Apart of the required performance of unsupervised operations, flow through automatic approaches offer a plethora of advantages compared to batchwise counterparts, most of them derived from the volume reduction (from the range of dL to mL in the batchwise fashion to the range of mL to µL in the automatic fashion): Less reagent and sample consumption, manipulation of hazardous reagents and samples, increased sample throughput for discrete analysis, increased number of analyte determined per sample, decrease of instrumental and human costs, increased precision and trueness, data generation, unsupervised data processing, miniaturization, portability, less power consumption and flexible and versatile manifolds.

From all available options for automating accessibility tests and performing kinetic studies, flow approaches, namely, those based on the pressure driven manipulation of liquids, gases and slurries in closed manifolds are the better suited for bioaccessibility tests because they allow handling of several extractants, monitoring of wet chemical reactions and are flexible to incorporate a plethora of physical unitary operations related to the sample pretreatment to the analysis, as described in the literature [64–68].

An alternative to flow methodologies is the automation by batch analysis, in which samples are kept in individual reservoirs, but are usually limited to mixing, shaking, direct detection or titration, or handled unattended by robotic stations, where a specialized robot has a plethora of modules in which unitary operations can be accommodated [69]. Robotic stations have lasted till nowadays for some sample preparation operations that do not involve a continuous flow, often hyphenated to chromatographic equipment [70] and automating the injection of samples, diluting, adding internal standards, cleaning of the injection mechanism, controlling temperature (both cooling and warming), shaking, headspace sampling, SPME, etc...

Flow approaches appeared and developed during the second half of the 20th century, starting from Segmented Flow Analysis (SFA) designed by Skeggs in 1957 and published in 1964 [71], and evolving through several generations of flow analysis. The flagship of the so-called first generation of flow analysis techniques is Flow Injection Analysis (FIA), launched by Ruzicka and Hansen in 1975 [72], based on a computerless, reagent-sample mixing, diffusion-controlled, fixed-time kinetic measurements that relied on peristaltic pumps (PP) and injection valves (IV) as depicted in figure 1.3. This methodology yielded a high sample throughput of colorimetric, potentiometric or other diffusion-based assays.

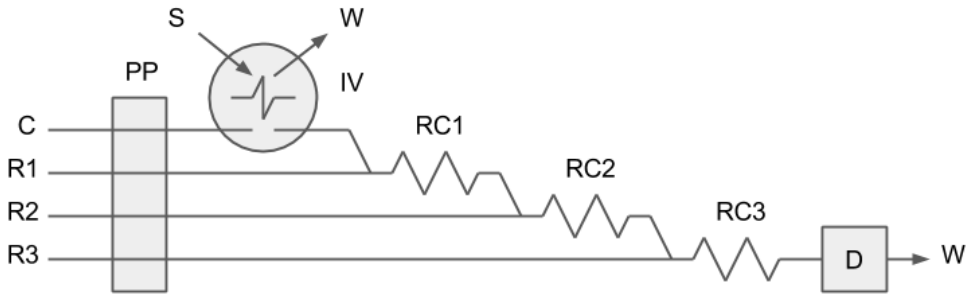


*Figure 1.3. Conventional FIA setup showing PP: Peristaltic Pump, IV: Injection Valve, D: Detector, RC: Reaction Coils, S: Sample, W: Waste, C: Carrier and R: Reagents*

Advances in microelectronics led to the second generation of flow analysis, whose flagship is the Sequential Injection Analysis (SIA) by Ruzicka and Marshall in 1990 [73,74]. The conventional SIA scheme contains a syringe pump (SP) connected to the central port of a selection valve through a tube length called holding coil (HC) (figure 1.4). Sample and reagents are sequentially aspirated, mixed and sent to a detector for measurements. SIA is a more flexible and robust alternative to FIA, but its main drawback is that reagent and sample are mixed only by axial diffusion of adjacent segments, so mixing is incomplete and analytical signal and sample throughput tend to be lower than FIA.

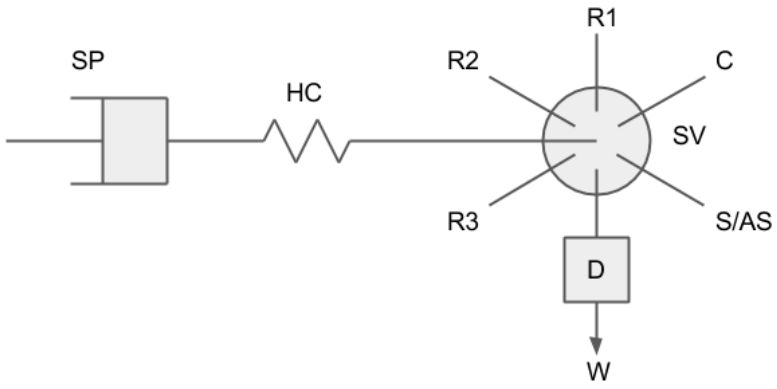


*Figure 1.4. Conventional SIA setup showing SP: Syringe Pump, HC: Holding Coil, SV: Selection Valve, D: Detector, C: Carrier, S/AS :Sample or AutoSampler port, R: Reagents and W: Waste.*

Many other flow approaches based also in computer-controlled bidirectional fluid manipulation can be also included in the second generation, as the Multi-Commutated Flow Analysis (MCFA), based on a peristaltic pump and several solenoid valves [75], Multi-Syringe Flow Injection Analysis (MSFIA), based on a syringe pump furnished with several syringes with synchronous plunger movement [76], Multi-Pumping Flow Systems (MPFS), which substitute each channel of a peristaltic pump

with a solenoid pump, and can thus be driven computerless [77], All Injection Analysis (AIA), based on a plethora of injection valves both for recirculation of reagents and sample in an equilibrium-based reaction model [78], Stepwise Injection Analysis (SWIA) as a combination of flow and batch methods, exploiting a computer-controlled bidirectional peristaltic pump, a selection valve and a mixing chamber [79], Cross Injection Analysis (CIA), exploiting fluid mixing in several crossing channels controlled by a conventional peristaltic pump [80], Loop Flow Analysis (LFA) which exploits two peristaltic pumps and a specially designed proportional injector [81] in order to mix and trap a sample and reagents in the detection cell of a non-destructive optical detector, with the potential monitoring of kinetics processes [82], Simultaneous Injection Efficient Mixing Analysis (SIEMA), that uses several injection coils for aspirating reagents or sample through solenoid valves and syringe pumps, and mixing them efficiently in a flow confluence while dispensing them to the detector [83] and Flow Batch Analysis (FBA), that adds plugs of reagents and samples to a common mixing chamber [84].

The inclusion of additional unitary operations along with advances in miniaturization, micromachining and material science yielded the third generation of flow analysis, whose flagship is the Lab-On-Valve (LOV) [85–89]. The LOV is basically an SIA mesofluidic setup with channel dimensions of 0.5-1,5 mm ID where apart from reagent and samples, many laboratory unitary operations are miniaturized and included in the valve monolithic body, thus reducing distances, sampling times, and sample and reagent volumes down to the µL range. A depiction is shown in figure 1.5. Operations included can be as simple as physical preparations: filtration, shaking, mixing or diluting, or analyte detection using analytical techniques integrated in the valve: optical techniques such as photometry, fluorimetry and chemiluminescence [90–92], or electrical techniques such as potentiometry [93–95], amperometry [96] and voltammetry [97–99], without mentioning the hyphenations to instrumental equipments. The most analytically relevant applications resort to the incorporation of partitioning setups between solid, liquid and gaseous phases, and among them the Bead Injection (BI) and Sequential Injection Chromatography (SIC) have to be highlighted because of their outstanding potential. The bead injection technique [100] resorts to solid phase extraction (SPE) resins suspended in liquid and manipulated as slurries in the fluidic manifold in order to perform sorptive partitioning separations in a renewable fashion, dismissing some of SPE drawbacks such as the irreversible absorption of matrix components in the resin, and using several different partitioning mechanisms: anion and cation exchange, adsorption, reverse and normal phase, molecular imprinting and size exclusion, or even mixed mode. Sequential Injection Chromatography (SIC) exploits the use of short monolithic columns [101–103] for achieving acceptable analyte resolution without resorting to high pressure separation [104–107].

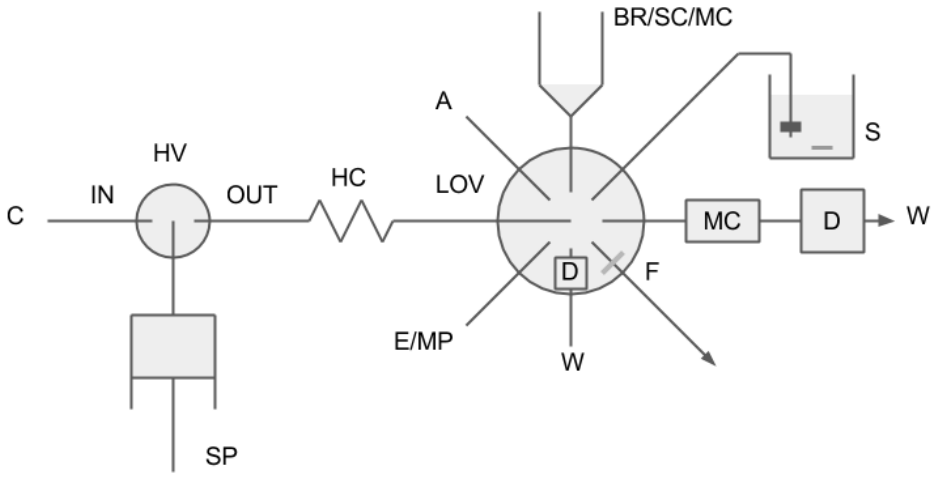


*Figure 1.5. Illustration of a Lab-On-a-Valve (LOV) setup showing the typical components as the Syringe pump, with a Head Valve (HV) of two positions: IN, connecting to the Carrier, and OUT, connecting to LOV monolithic manifold through the Holding Coil (HC). This particular valve has a Bead Reservoir (BR), that could be used as Sampling Cup (SC) or Mixing Chamber (MC), an Air input (A), Eluent or Mobile Phase (E/MP), a Monolithic Column (MC) used in the sequential injection chromatography (SIC) mode, a Frit in one port in order to retain a sample preparation resin in the bead injection (BI) mode, Detectors (D) in the integrated or external configuration, a Sample port (S) for real-time sampling and a Waste outlet (W).*

Further miniaturization of the analytical setup evolved the so called Lab-On-Chip (LOC) concept. LOC systems integrate in a miniaturized device with channel dimensions down to 100 µm some dedicated microfluidic operations for performing a given (bio)analysis. They leave aside the selection valves, and the flow is usually driven either by electrophoretic motion or with a large number of syringe pumps. The reagent consumption is minimal, very small spatial resolution can be achieved (e.g. manipulation of single cells or DNA chains) and the chip is customizable and disposable. Those systems however are usually not flexible enough to accommodate different analysis in the same chip, are not small enough (including the liquid drivers) for in-situ measurements and the volumes used (nL) are not suitable for environmental monitoring where volumes of several mL are needed for trace analysis [108].

In order to further integrate fluid handling and detection, micro Total Analysis Systems (µTAS) have arisen by integrating in the LOC a sort of micropumps, electronics for control, detectors and in general all necessary laboratory operations needed for a given analysis and are thus perfect regarding portability, but the sample volumes are still too low for proper environmental analysis and fixing the fluidic part to a dedicated analysis reduces drastically the system flexibility.

Thus, SIA and LOV are deemed the flow methods of choice for automation of accessibility tests in environmental samples, on the basis of their features in sample

preparation capabilities and portability. Adaption of accessibility tests to an automated fashion solves some drawbacks of classical accessibility tests but introduces both a series of new instrumental issues (e.g., handling of the solid sample) and theoretical/practical modifications of the classical test. Solid sample introduction and detection in those systems require further discussion.

### 1.5.1 Sampling

While methodologies of liquid sample introduction in fluidic manifolds have been standardized since the origin of flow analysis by aspirating from the sample vial or medium directly or through an autosampler, flow approaches might not be well suited for handling of solid samples as those described in this thesis. Several methodologies have however been introduced in the past few decades for sampling external extraction vessels, or for integrating the solid sample in the main fluidic path.

When the accessibility test involves a single step batch extraction with an elevated soil mass for the sake of sample representativeness and a high volume of leaching agent in order to not to limit the sink capacity of the medium, slightly invasive microsampling techniques have been developed to minimize both the volume and the analyte mass sampled so as to minimally disturb the leaching equilibria. The main microsampling techniques for on-line/in-line sampling of soil leachates include microfiltration, microdialysis and diafiltration as described below.

Microfiltration consists on the use of a small filter to withdraw a minute extraction medium volume by negative pressure. Syringe filters (figure 1.6) are intensively used in the analytical chemistry laboratory because of their standard luer connection, the assortment of filtering surfaces, pore sizes and filter chemistries. Their use has been automated with the aid of micro/mesofluidic techniques in order to introduce the filtered samples in the manifolds [109]. The main drawbacks of syringe filters for on-line handling of soil extracts are the progressive pressure increase, potential clogging, dead volume and disturbance of the extraction equilibria if the sample volume aspirated is significant. The pressure drop issue can be avoided by using low flow rates, other drawbacks can be prevented by a very simple trick adopted in the experimental part of this dissertation (see chapters 6 and 8): aspirating through the filter a volume higher than the dead volume, analysing only the distal plug, and returning to the extraction vessel the volume withdrawn plus an extra volume of fresh leaching agent, thus compensating the neat volume analyzed [110]. By doing so, the volume in the extraction vessel remains virtually unaltered, the filter is unclogged in the step where the volume is returned to the vessel and the fraction analysed corresponds to the concentration at the current time of sampling. Microfiltration is by now the simplest methodology for in-line sampling in batch extractions.


*Figure 1.6. Examples of syringe filters with different pore sizes (0.22 and 0.45 µm), filtrating surfaces 15 and 25 cm), and chemistries (Nylon, Polyethersulphone (PES), Polyvinylidene fluoride (PVDF))*

Microdialysis [111–115] sampling involves introducing in the extraction vessel a semipermeable membrane that is perfused through its lumen with the extracting medium. Two main types of microdialysis probes have been received much attention so far, namely, the linear and the concentric type configurations (figure 1.7 and figure 6.1 in chapter 6). The equations modelling their behavior on the basis of the chemical and geometrical considerations of the probe have been extensively evaluated and validated as indicated in Chapter 6. All analytes of low molecular weight permeable through the membrane will diffuse across it. If the perfusate flow rate is low (usually in the 1-5 µL/min range), the inner volume is small and the membrane is long enough, the output flow, namely, the dialysate, will be equilibrated with the sampling medium, thus operating under dialytic equilibrium medium, for which dialysis efficiency is close to 100%. For monitoring of kinetic processes, it should be taken into account that the low flow-rate allows for a limited time resolution, and the dialysate concentration may be proportional to the integral of the concentration in the sampling vessel during the sampling time. The most relevant aspect of microdialysis sampling is the fact that membranes with pore size in the upper range of nm or lower µm allow for a very clean matrix, free from macromolecules and humic substances.

*Figure 1.7. Commercial concentric dialysis probe showing the central body with a metal outlet and a GC capillary column as inner cannula serving as perfusate inlet. Note the step at the left of the probe, used for fixing the dialytic membrane. More details on chapter 6.*

Diafiltration (figure 1.8) or tangential filtration is an alternative microsampling technique encompassing dialysis and ultrafiltration concurrently, that has been used in chapter 10. A sample is recirculated between the extraction vessel and a module containing a dialysis membrane of appropriate molecular weight cut-off. The sample only contacts one side of the dialysis membrane. Adding a flow-rate restrictor to the output of the sample flow provokes an increased pressure on the sample side of the membrane and thus, a minute amount of volume is forced to cross the membrane towards the acceptor compartment and is recovered for analysis, that is, the diafiltrate. Passive diffusion between the donor and acceptor sides of the dialysis membrane equilibrates the concentrations of molecules smaller than the molecular weight cutoff in both sides in a dialysis like process. As only a slight pressure is applied to the sample, only a minute volume of sample containing low molecular species is withdrawn.


*Figure 1.8. Diafiltration cassette used in chapter 10 with details of input/output connections, composition and molecular weight cutoff (MWCO)*

While microsampling techniques have been proved to be extremely useful for *in-situ* sampling of batchwise extractions, they also offer some limitations for automation in flow systems. A mechanical limitation can be exemplified with sequential extractions, in which consecutive extracting agents are applied to the residues of the previous extractions. In this case all of the previous extracting agents need to be removed by filtration or centrifugation, and this would be difficult to automate. Dynamic extractions, where the solid sample is packed in a container with low dead volume and the leaching agent is perfused through the sample, apart from mimicking closely the dynamic processes occurring in the ecosphere, offer a perfect integration with flow analysis due to their flow-through nature. Packed columns or stirred chambers are the main alternatives for in-line handling of solid substrates. Further details are available in chapters 5,7 and 9.

Packed columns [116,117] (see figures 1.9 and 1.10) usually consist of an inert housing that holds a quantity of soil in the milligram to gram range between a fluidic input and output. Those input and outputs are fenced by filters, and allow connecting the housing to the fluidic setup (usually peristaltic pump) without extractant leak. Flow-through macrocolumns (figure 1.9) for soil quality assessment are endorsed by the ISO/TS norm 21268-3:2007. Microcolumns on the other side contain a lesser amount of solid (hundreds of milligrams). They offer less dead volume and are deemed especially convenient when the sample is scarce or the analyte is very concentrated. The flagship of those microcolums is the so-called biconical column [116,118–120] (figure 1.10), whose central body has a biconical shape, creating a gradient of linear speed that maintains the solid sample fluidized and thus enhances the extractability of available fractions. A dedicated microcolumn could be also assembled by holding the solid sample in the dead space between two serially connected syringe filters [121].

*Figure 1.9. Disassembled packed macrocolumn showing (left to right) the outer cap, o-rings for air proofing, a support for the commercial filter, polytetrafluoroethylene (PTFE) washer and central body.*

*Figure 1.10. Packed microcolumn showing the outer caps, airtight o-rings, filter support, Nylon membrane and washer and low-volume central biconical body.*

Stirred flow chambers [116,122] (see figure 1.11) consist on a glass or plastic bottom housing with a tobacco-pipe-like shape where the solid sample is loosely extracted (see Chapter 7). Its dimensions allow introducing a magnetic stirrer in its bottom part in order to maintain the sample suspended during the leaching test. A filter and a flow-through lid close the system, so when the bottom part is perfused with the leaching agent, the filtrate is recovered through the lid. The main drawback is

that the large inner volume causes a high dead volume, so poor temporal resolution can be expected.

*Figure 1.11. Disassembled and closed stirred flow cell showing the upper and bottom glass parts, as well as PDMS washers for holding the commercial filter membrane in place.*

## 1.5.2 Hyphenation to instrumental analysis equipment

The detection step is usually performed in flow analysis through in-line molecular spectrometry or electrical techniques, from bulky benchtop classical instruments in FIA till miniaturized in-valve dedicated schemes for LOV. These detection techniques have however in most cases a limited selectivity and sensitivity for raw samples and rely on proper derivatization chemistry for obtaining selective and sensitive analytical signals. Hyphenation to bulk instrumental analysis equipments, especially to chromatographs for organic analytes or atomic spectrometers for inorganic species, allows for a sensitive multiresidue analysis. In those configurations, the flow analysis platform automates the sampling and sample pretreatment, the commercial instrument takes upon the analysis and detection, and the hyphenation between both parts is the most delicated step. In the academic or industrial realm, the dedication of an instrumental equipment to a given setup for a long time is usually not possible due to the different analysis that have to be performed or the elevated number of samples that have to be analysed in a short timeframe, that is, the instruments have to be kept flexible and thus, versatile interfaces need to be designed. For the sake of clarity, the nomenclature used to describe the coupling of the fluidic part and the commercial or dedicated detection system is described below:

- Off-line hyphenation (figure 1.12) is not considered as an automation approach: the analyst gets the sample from one instrument and introduces it into another.


*Figure 1.12. Off-line hyphenation*

● At-line hyphenation (figure 1.13) uses the instrument's autosampler to introduce the sample into the detection system. The invasiveness of this procedure is negligible, and is especially suited when the detector operates in discontinuous mode e.g. ETAAS.

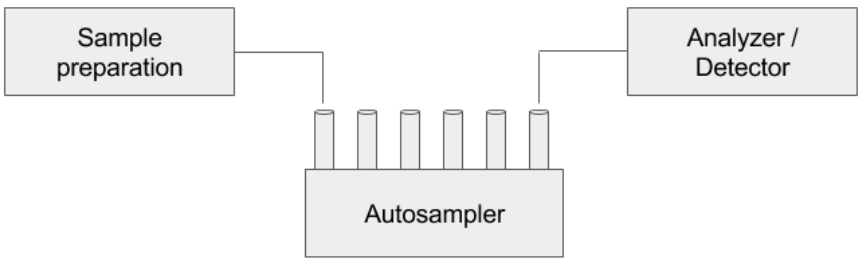


*Figure 1.13. At-line hyphenation*

● On-line hyphenation uses an injection valve to insert a plug of pretreated sample into a carrier solution. The injection valve has to be set up, but this is a fast operation as it only requires changing the connections from the usual instrument's autosampler to an external injection valve. This is useful for continuous detectors/analyzers such as ICP, FAAS or HPLC, where a carrier flow is passing constantly through the instrument. The way in which the injection coil content enters the analyser/detector allows differentiating 4 modes of operation of on-line hyphenations:

○ Fixed loop (figure 1.14). In this simplest approach, the injection loop is overfilled with a homogeneous sample. Offers best repeatability.

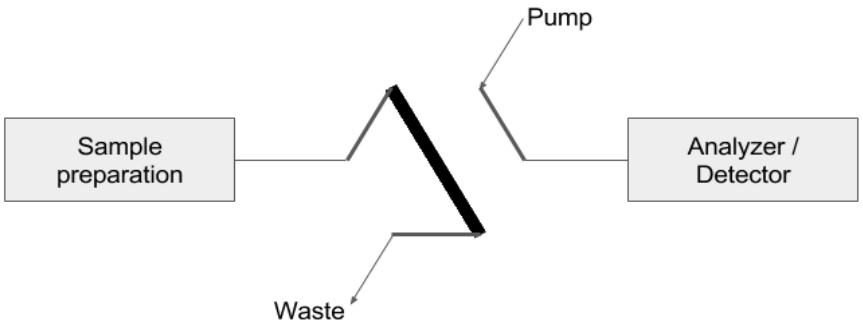


*Figure 1.14. On-line fixed-loop hyphenation*

○ Metered volume (figure 1.15). As in most common autosamplers, the injection loop is partially filled with a syringe pump. Its reproducibility is as good as the injection conditions are, because diffusion in the injection loop can change the resulting peak profile, area, height, front or tail shapes.

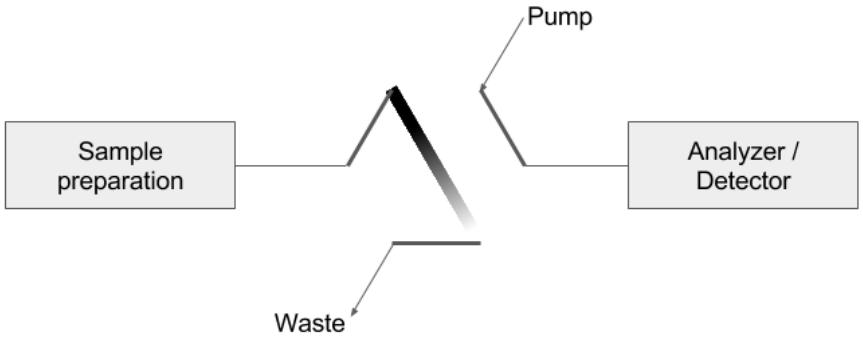


*Figure 1.15. On-line metered volume hyphenation*

○ Heart-cut (figure 1.16). If the sample is not homogeneous (e.g., in the case of eluates with a concentration gradient) and its volume is higher than the loop volume admitted for the instrument, only a segment with the volume of the injection loop can be injected. Usually, the sample volume (e.g. SPE eluate) is pumped in the injection loop until the maximum analyte amount will be injected.

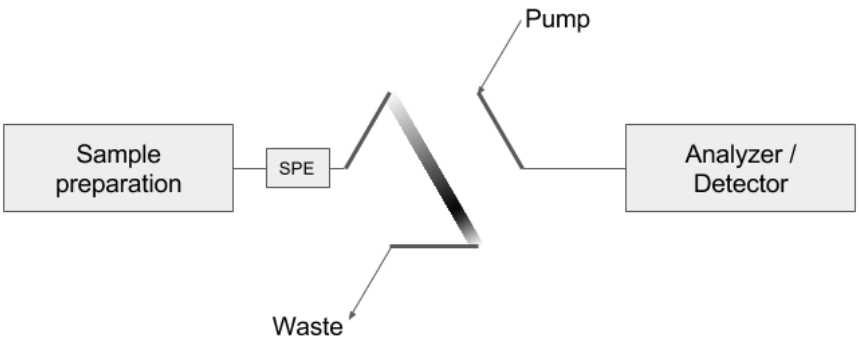


*Figure 1.16. On-line heart-cut hyphenation*

○ Switching valve (figure 1.17). For avoiding the analyte loss inherent to the heart cut operation, sometimes the SPE column or unit operation (e.g., in-tube microextraction) is directly placed on the injection coil. In a first step, the analyte is preconcentrated and the sample matrix washed away. Turning the valve elutes the sorbent directly into the analyser/detector. Configuration of the injection valve connections allows to either benefit of the minimal chromatographic separation occurred in the SPE cartridge when eluted in the same direction of the loading, or to focus the analyte on the separating column head if eluted in a back-flash mode.

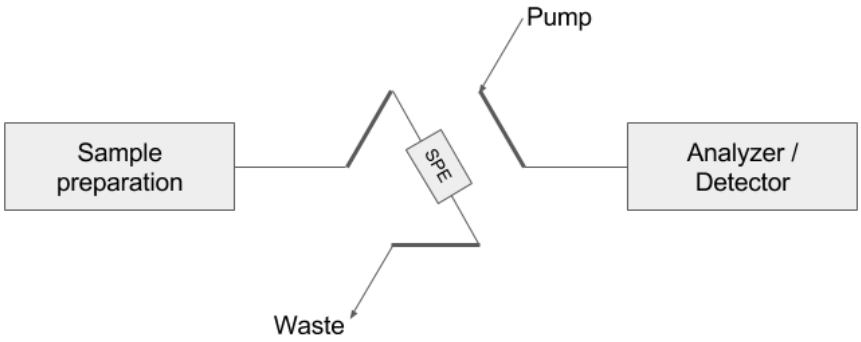


*Figure 1.17. On-line switching valve hyphenation*

● In-line hyphenation (figure 1.18) means that the continuous output of a given equipment will feed another through a single transfer line. This implies a complete dedication of the detector and is thus not commonly used, except for electrochemical detectors or molecular spectrometric detectors where the (pretreated) sample is introduced in a flow through cuvette.

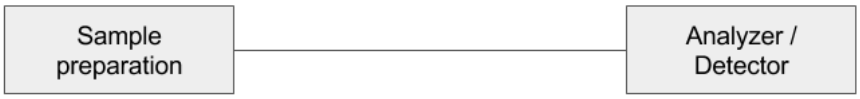


*Figure 1.18. In-line hyphenation*

## 1.5.3 Software and data flow

Besides FIA, for its simplicity of operation, all other mainstream flow techniques, as SIA, LOV and its sequels require software control for allowing reproducible flow rates and timing in valve switches. Usually all fluid drivers are controlled by standard communication standards, such as Recommended Standard 232 (RS232), RS485, Controller Area Networc (CAN) or Universal Serial Bus (USB). Knowing the communication protocols and the electrical standards allows coding custom programs for dedicated analysis, however those programs have to be customizedfor any desired change in the method workflow. Some commercial programs allow for controlling a vast number of standard devices and instruments, as FIASoft [123] and SIASoft [124] from Fialab Instruments Inc [125], AutoAnalysis [126,127] from Sciware Systems SL [128] and FloZF [129] from Global FIA [130], giving them a similar functionality as the softwares controlling commercial instrumental equipments but with the increased flexibility typical of low pressure flow approaches. Even if the software allows a high degree of flexibility in the control of devices, the number of devices controlled by each software are usually limited and related or directly produced by each enterprise. Adding new hardware usually involves changing the program or getting in touch with the manufacturer.

Regarding the control of instrumental equipment, they can usually be controlled only by their own software, because those equipments are designed to operate as standalone laboratory equipment. Furthermore, instrument manufacturers seldom provide solutions to tackle this issue because of commercial strategies and the lack of communication between manufacturers and final users. Various approaches can be exploited when addressing communication issues in instrumental control:

- The most appropriate alternative is to communicate programmatically with the detector, but the communication protocol is usually closed by the

manufacturer.

- Other alternative is the use of a program that simulates the behaviour of a human being in front of the computer, that is, mimicking the use of the keyboard and mouse in order to control the instrumental analysis equipment in the same way the analyst would do (graphic user interface (GUI) automation) but requires installing second or third party software on the same computer as the detector software, and is sensitive to screen layout, so it is difficult to get it working properly: While the real user would easily find the options needed or avoid or close some popup menus, the automated GUI will only repeat mechanically some clicks on predefined screen positions.
- The most common alternative is to control the detector via contact closure, that is, triggering a preprogrammed action (e.g. start injection) through automatic shorting of two cables. To this end, fluidic equipment usually bears some inputs and relay outputs, controllable with their standard communication protocol.
- If the contact closure is not available, time synchronization is the last alternative, where the fluidic equipment and the instrumental analysis equipment are controlled by different computers, software or instances of the same software, and are not wired together: the methods executed have some delays inserted in order to synchronize them.

Regarding data acquisition, small footprint detectors such as the most usual handheld molecular spectrometers [131], potentiostats [132], multimeters [133], conductometers and potentiometers offer their communication standards and protocols to their final user, so if the software that controls the fluidic setup has access to real time data, the execution method can be adapted at real time for fitting the specific needs of a given sample, e.g. customized dilution. This real time adaption offers an added value to the analysis, inasmuch as replaces the analyst contribution. In this frame, the International Union of Pure and Applied Chemistry (IUPAC) qualifies 'automated' [134] to a mechanical and instrumental system that replaces human manipulative effort and faculties in the performance of a given process and is regulated by feed-back of information, so that the apparatus is self-monitoring or self-adjusting. If a system does not possess this feedback regulated operation, the correct word would be 'mechanized': Use of mechanical devices to replace, refine, extend or supplement human effort.

In the case of instrumental equipment and because of the drawbacks described in the control section, getting data at real time is a very difficult task, usually the analysis is only mechanised, and all the data is recovered at the end of analysis. Sometimes it is possible to exploit some scripts or macros (e.g. Python or Visual Basic for Applications in Excel) or specific programs for getting relevant figures from raw data; if not, they are retrieved manually. There are quite few methodologies that can

be used for getting data at real time from instrumental equipment for adjusting in an unsupervised fashion the execution of an automatic workflow:

- Installing a program in the instrumental equipment that access a file where the data is stored temporarily, processes the data and provides it to the control program. It can be the same control program. This program can be installed in the same computer as the control program, or provide the data through some communication protocol.
- In many software packages, the transient signal is displayed on the screen at real time. A program could read the data directly from the screen and process it. As in case of the control by GUI automation, this approach is screen-layout-sensitive and is thus not robust.
- Getting the raw signal directly from the detector is an alternative if the analog signal can be intercepted but requires specific electronics and re-implementing the signal treatment.

# 2. Objectives

The objectives of this PhD dissertation can be summarized in three main aims for which a number of milestones are expected as described below:

- To develop batch-flow or on-line approaches for unsupervised monitoring and investigation of kinetics of accessibility extraction tests (bioaccessibility, bioavailability, biodegradation…) of solid samples by:
    - Sampling of leachates of accessibility tests, either by probing an external vessel with microdialysis, microfiltration or diafiltration, or by resorting to dynamic extractions included in the manifold as flow-through packed macrocolumns, microcolumns, or stirred flow chambers.
    - Automatic conditioning of the leachates if required e.g. filtration, dilution and addition of internal standard.
    - Automatic extraction, separation or preconcentration of target analytes in leachates through SPE if required.

- To hyphenate the previously described flow manifolds to molecular spectrometric techniques for on-line determination of nutrients in leachates (as case example of macrocomponent), to atomic spectrometric techniques for the determination of bioaccessible trace elements (TE) and to HPLC for the determination of bioaccessible legacy pollutants (as case example of trace organic compounds).

- To develop software tools for minimizing the analyst intervention in the analytical workflow of accessibility tests of environmental pollutants or nutrients performed in the flow manifolds by automating:
    - The control of the fluidic sample preparation equipment.
    - The control of the analyzer or detector or synchronization with the sample preparation manifold.
    - Data acquisition if possible.
    - Data treatment and reporting, by coding scripts that not only transform the raw analytical signal into relevant analytical figures, but also perform without analyst intervention other advanced procedures that are usually supervised, eventhough mechanic, as outlier removal, smoothing, fitting to theoretical equations, statistical tests or plotting, all of them with quick integrated QC procedures.

# 3. Membrane Enhanced Bioaccessibility Extraction (MEBE): A novel platform for determining accessibility of nonpolar species in environmental solids without sink constraint

## 3.1. Introduction

Evaluation of environmental exposure of hydrophobic organic chemicals (HOCs) in solid samples of environmental interest is increasingly associated with accessibility tests because they provide data related to the potential hazard of contaminated samples against overestimating total extraction methods [14]. Bioaccessibility tests are typically mild extractions aiming at desorbing the accessible fraction but without directly extracting or even disintegrating the solid matrix [53]. Environmental regulations (e.g., ISO 17402:2008 [6]) usually aim at worst-case scenarios or at least a high degree of conservatisms, and underestimations of bioaccessibility need consequently to be avoided. However, during the last 5 years several researchers have shown that the bioaccessibility of HOCs can be markedly underestimated when the capacity of the extraction medium is insufficient for a given sample [51,56,135,136]. The traditional approach for avoiding such underestimations is to set the L/S ratio high enough, which for heavy metals often is set to 100 L/kg. Unfortunately, such L/S ratios are often not sufficient for bioaccessibility extractions of HOCs in solid samples with very high solid to water distribution coefficients ($K_D$) that for PAHs in soot, soil, sediment and biochar can exceed $10^6$ L/kg [136].

Several attempts reported in the literature to ameliorate the sink capacity usually involve the incorporation of sorptive sinks in a three-phase extraction model [51] so as to maintain concentration gradients driving the desorption process via the so called ‘contaminant trap [57] using a composite of PDMS and active carbon as infinite sink, the ‘silicone rod’ based sorptive bioaccessibility extractions [55,56] in which a solid sample is incubated in a medium containing a large silicone rod with high surface or slurry solid-phase extraction using poly(diphenylphenylene oxide) (Tenax) or poly(styrene-divinylbenzene) copolymeric (e.g., Amberlite XAD-2) beads [25,49,53]. Depletive sampling of target compounds from soils by the above sorptive-based

procedures is however not free from drawbacks. Accumulated HOC species cannot be retrieved easily from contaminant traps due to their high retention in PDMS-activated carbon composite [57], and thus, the bioaccessible fraction can only be estimated by subtraction of the non-desorbable pool from the total concentrations, which both have to be measured by exhaustive extraction. As for sorptive bioaccessibility extractions with silicone rods, sorbent with large mass (≥ 16 g) is needed to ensure a high sorptive capacity and the analytical workflow is lengthened by the back extraction of target analytes out of the silicone sink [55,56]. Recent research has also demonstrated that sorptive bioaccessibility extraction with PDMS as sink can be insufficient for measurement of accessible PAHs in solid samples with extremely high $K_D$ values [136]. Tenax beads can be difficult and sometimes even impossible to separate properly from the solid matrix in bead-based extractions and dedicated configurations are usually called for [137].

A very fundamental challenge in bioaccessibility extraction is to provide relevant desorption conditions and avoid exhaustive extractions while at the same time providing sufficiently high sink capacity [136]. Maximizing L/S ratios or including sorptive sinks are two strategies to cope with this challenge, at least to some degree. However, it would be even better to find an approach where the desorption conditions and the sink capacity can be varied and set almost independently. The present study introduces such an approach, where a semipermeable membrane is applied as physical barrier between two media: The sample is suspended in an aqueous medium that sets the desorption conditions, whereas an organic solvent serves as an infinite sink and analytical acceptor phase. This “Membrane Enhanced Bioaccessibility Extraction (MEBE)” is inspired by nature, since biological contaminant uptake generally involves the transfer of the contaminant through a semipermeable membrane. It is also based on the progress made within analytical chemistry on membrane extractions in general [138] and specifically a very simple clean up method using lay flat low density polyethylene (LDPE) bags for the removal of lipids from solvent extracts by Strandberg and co-workers [139].

The main aim of this study was to generate the proof of concept of the MEBE approach. First we aimed for finding the simplest possible configuration for MEBE. We selected β-cyclodextrin solution as desorption medium and PAHs as model contaminants, whereas several acceptor solvents were considered and tested. We then conducted a number of simple dynamic and mass balance experiments, before the approach was applied and tested on a polluted soil containing native rather than spiked contaminants. The main hypothesis of the study was that MEBE allows the independent control of desorption conditions and dimensioning of the sink capacity, can facilitate the analytical work and can be applied to field contaminated soils in a very simple way.

# 3.2. Experimental

## 3.2.1. Materials

The certified reference material CRM 47940 (Standard PAH mixture) was purchased from Sigma-Aldrich. It contained 16 priority U.S. Environmental Protection Agency (EPA) PAHs at the 10 mg/L level in acetonitrile. The 20-cm long LDPE bag was made from a 1 inch x 70 µm thick lay flat LDPE band (Brentwood Plastics Inc., St. Louis, Missouri) by double-hot-sealing. Different qualities of ethanol were used in the initial experiments, and all final experiments were conducted with ethanol of analytical grade (99.98%, VWR Chemicals). The initial method development was conducted on a heavily contaminated soil with incurred PAHs from a scrapyard in Vienna.

## 3.2.2. Working principle and design of MEBE test

The sample and some milliliters of HPCD solutions are added to a lay flat LDPE bag that is heat sealed in one end. The other end is heat sealed before the LDPE device is introduced in a flask (or vial) containing a larger volume of acceptor solvent. The flask is placed on a rolling table during the extraction process.

On a molecular scale, PAHs desorb from the sample matrix and are co-transported by the cyclodextrins (inclusion complexes) to the LDPE membrane [56,140], which acts as a sorptive sink that maintains the desorption gradient. The PAH molecules then diffuse through the LDPE before they partition into the solvent acceptor [139], which in turn maintains the gradient driving the diffusion through the membrane.

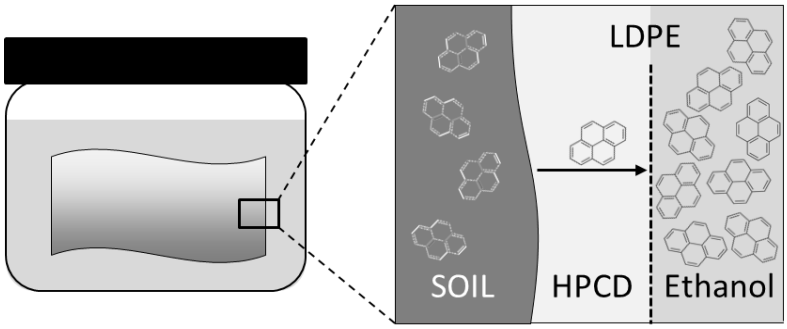


*Figure 3.1: Schematic representation of the Membrane Enhanced Bioaccessibility Extraction (MEBE) concept.The so-called MEBE mimics nature's clever use of membranes, in which the extraction medium and the final target/sink remain separated by a hydrophobic barrier. MEBE has been proved to overcome shortcomings of conventional batchwise bioaccessibility tests for organic pollutants in terms of improved extraction rate, better estimation of worst-case scenarios by augmentation of the sink capacity and as a collateral effect yielding a cleaner matrix due to the membrane clean-up effect.*

MEBE is deemed applicable by untrained personnel and easily applied in parallel to any sample size because the method uses a simple setup available in any laboratory with no specialized instrumentation.

Benefits of the proposed setup as compared to the classical bioaccessibility test include a much higher and scalable sink capacity, a cleaner extract that can be injected directly into the analyzer, drastic reduction of sample manipulation and possibility of processing many samples simultaneously since the setup is readily arranged in standard GC/LC vials that can be automatically processed (control of shaking and temperature) or/and analyzed by conventional autosamplers (automatic injection), thus minimizing analyst workload and interaction with the sample.

## 3.2.3. Solvent selection experiments

A first experiment was conducted to assess the general compatibility of solvents with MEBE. Several 20 cm x 1 inch lay-flat LDPE bags were filled with solvents that are known to dissolve lipophilic compounds: 1-hexanol, hexane, 1-octanol, 2,2,4-trimethylpentane, ethyl acetate, ethanol and acetone. Bags were sealed on both ends and stored in 50 mL Schott-Duran flasks closed with Teflon-lined caps that were opened regularly during 2 weeks and checked visually for leakage, membrane swelling, change of appearance of the bag and solvent losses based on weighing. Finally, the evaporative loss was assessed gravimetrically. Based on these two experiments, ethanol was selected as acceptor medium.

## 3.2.4. Sink dimensioning

MEBE devices were filled with 0.5 g soil and 2 mL of 75 g/L HPCD solution containing 0.5 g/L of $NaN_3$ as a biocide to circumvent biotic degradation of organic species. The loaded devices were then immersed in 22 mL, 100 mL and 1000 mL bottles that contained respectively 5 mL, 50 mL and 500 mL mL of ethanol yielding solid to acceptor phase ratio of 1:10, 1:100 and 1:1000. The bottles were shaken on an orbital shaking table at 80 revolutions per minute (rpm) during 28 days (triplicates, protected against light). Aliquots of 100 µL of ethanol were sampled and analyzed by HPLC at 1, 2, 4, 8 h, 1, 2, 4, 7 d) and then weekly up to 28 d without replenishing the volume probed. The PAH content profile in ethanol was compared for the suite of solid to acceptor ratios aimed at evaluating the sink capacity of the MEBE setup.

## 3.2.5. Diffusive mass transfer though LDPE membrane

The time required for a quantitative PAH transfer through the LDPE membrane was determined. 100 µL of CRM 47940 (10 mg/L PAH mix standard) was added to the MEBE device (no soil, no cyclodextrin solution) and the PAH transfer into 50 mL of

ethanol acceptor phase was monitored in time (triplicates, orbital shaking, 80 rpm). The same was repeated, but for standard volumes of 200 µL and 300 µL inside the bag. Aliquots of 100 µL of ethanol were sampled at 1, 2, 4, 8, 16 h, 1, 2 and 4 d without replenishing the sample volume. The transfer of each PAH was plotted against time, fitted to a simple first order model and the time to transfer 95% of the initial mass was estimated.

### 3.2.6. Shaking influence

In order to determine the influence of the shaking mode on the extraction rate, four sets of MEBE contained in 22 mL vials with 15 mL of ethanol acceptor were subjected to four different shaking conditions (triplicates): unshaken, vortex shaking (500 rpm), rolling table and gentle orbital shaking board (80 rpm). Aliquots of 100uL were sampled at 2, 4, 8, 24 and 48 h without replenishing the volume removed during the experiment.

### 3.2.7. Enhancement of the extraction speed

The mass transfer kinetics of the proposed MEBE method was compared against that of the classical HPCD test. To this end, 0.5 g of soil were introduced in triplicate in a 20 cm x 1 inch lay-flat LDPE bag along with 2 mL of 75g/L of HPCD and 0.5 g/L $NaN_3$. The bags were squeezed in a 100 mL SCHOTT-DURAN bottle along with 50 mL of ethanol and subjected to shaking on an orbital shaking table at 80 rpm. Aliquots of 100 µL of ethanol were transferred to 1.5 mL HPLC vials at 1, 2, 4, 8, 16 h and 1, 2, 4, 7, 14 and 21 d, without replenishing the volume uptaken and analyzed by HPLC without further treatment.

In parallel, 0.5 g of soil were extracted for 28 days in a 100 mL Schott-Duran bottle with 50 mL of 75 g/L HPCD solution containing 0.5 g/L $NaN_3$ and sampled at the same time intervals as for the proposed MEBE method. Approximately 1 mL of the extraction medium was taken up with a 1 mL syringe, filtered through a 0.45 µm nylon filter into an HPLC vial until approximately 100 µL of clean extract were sampled. The syringe plunger was then pulled back to recover the non-filtered extract and the retained soil for returning them to the extraction medium. In this way, only ca. 100 µL of extract were collected in every discrete sampling step and only a minute quantity of soil was lost.

### 3.2.8. Instrumental PAH analysis

Concentrations of 16 PAHs were determined by HPLC in all phases using an Agilent HPLC 1260 series equipped with Zorbax Eclipse PAH column (4.6 mm x 50 mm, 5µm), a 4 channel fluorometric detector (FLD) and photodiode array detector (PDA).

Ethanol extracts from MEBE were injected directly into the HPLC system without any further treatment, whereas soil containing-cyclodextrin extracts were filtered through nylon syringe filters before injection. Whenever the samples could not be immediately analyzed, they were preserved at -18ºC.

The Agilent HPLC software package (ChemStation, B.0403) was used for controlling the chromatographic equipment as well as for processing chromatograms. The injection volume was 10 µL and column flow was 0.7 mL/min (40°C) operated during 17 min under this acetonitrile/water gradient: (%acetonitrile) 10% (t = 0), 10% (t = 2 min), 30% (t = 4 min), 80% (t = 7 min), 100% (t = 13 min), 100% (t = 15 min), 10 % (t = 16 min) Absorbance measurements were carried out by PDA at 254 nm and 310 nm and FLD at excitation of 260 nm and emissions of 330, 380, 410 and 480 nm. Data analysis was accomplished using Microsoft Excel.

## 3.3. Results and discussion

### 3.3.1. Solvent selection

Out of the various solvent explored as MEBE sinks, ethyl acetate, hexane and acetone showed distinct mass losses after two weeks (1.6%, 15.8% and 3.5% respectively), so were discarded as final acceptors of PAH since experimental results demonstrated their ability to diffuse back to the extraction medium and disturb the mild extraction conditions. The surface of the bag exposed to 2,2,4-trimethylpentane was slightly cloudier after 7 days, but the external texture (transparency, smoothness and stiffness) did not change, signaling moderate solubility into LDPE. Ethanol, 1-hexanol, 1-octanol and 2,2,4-trimethylpentane filled bags showed significantly inferior mass losses in 2 weeks as compared to more non-polar solvents (0.10%, 0.10%, 0.11%, 0.8% respectively), so they were deemed suitable as final sink acceptors. Ethanol was chosen among the alcohol counterparts for being environmental friendly, less toxic and readily compatible with reversed phase HPLC.

### 3.3.2. Sink Dimensioning

The aim behind this assay is to evaluate whether vials containing less volume of acceptor phase undergo a noticeable sink limitation. On the other hand, in the absence of differences in sink capacity, the PAH amount dissolved in the acceptor phase will be steady with increasing ethanol volumes.

Figure 3.2 depicts temporal extractograms illustrating the ratio of PAH leached from soil divided by the total amount PAH obtained by total extraction ($C_0$), that is, the per-unit bioaccessible fraction, plotted against time for distinct sink capacities and individual representatives of each number of rings, namely, phenanthrene (3 rings)

(PHE), fluoranthene (4 rings) (FLT), benzo[b]fluoranthene (5 rings) (BbF), indeno[1,2,3,cd]pyrene (6 rings) (I1P).

For the 2, 3 and 4 ringed PAH representatives; the extractograms indicated no significant differences in the amount of target compounds extracted. For the 5-ringed and especially 6-ringed PAH, a statistically different PAH mass is encountered in the 5mL ethanol vial. This is in agreement with the solubility of different PAHs and reveals a sink limitation for the 5 mL vial configuration for the 5 and 6 ringed PAHs and t > 10 days.

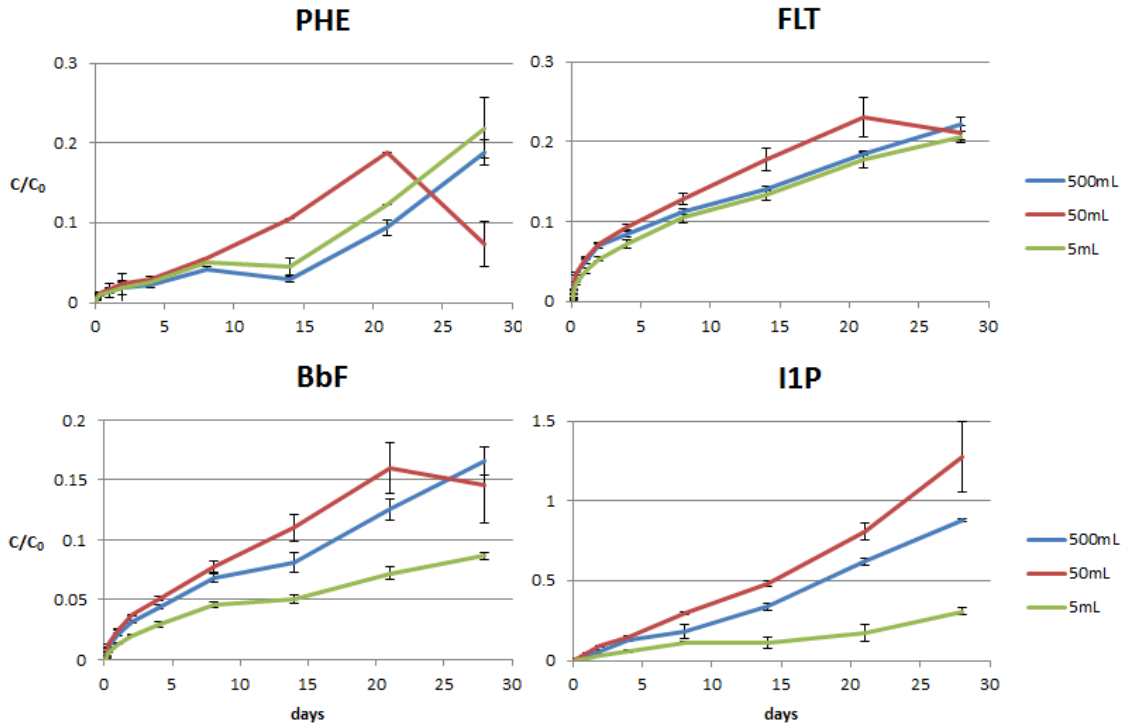


*Figure 3.2. Amount of PAH extracted in 5, 50 and 500 mL of ethanol acceptor phase configurations. The comparison reveals the lack of sink capacity in the 5 mL configuration for 5 and 6 ringed PAH (the less soluble species in polar solvents).*

## 3.3.3. Diffusion characterization

The mass transfer resistance across the hydrophobic LDPE membrane from the HPCD medium into the sink was studied for all 16 priority PAHs using 100, 200 and 300 µL of CRM 47940. Maximum concentrations obtained at the end of experiment were steady and ranged from 86% for PHE to 100% for I1P. The amount extracted at each time was normalized against the maximum amount measured at 96 h and plotted in figure 3.3.

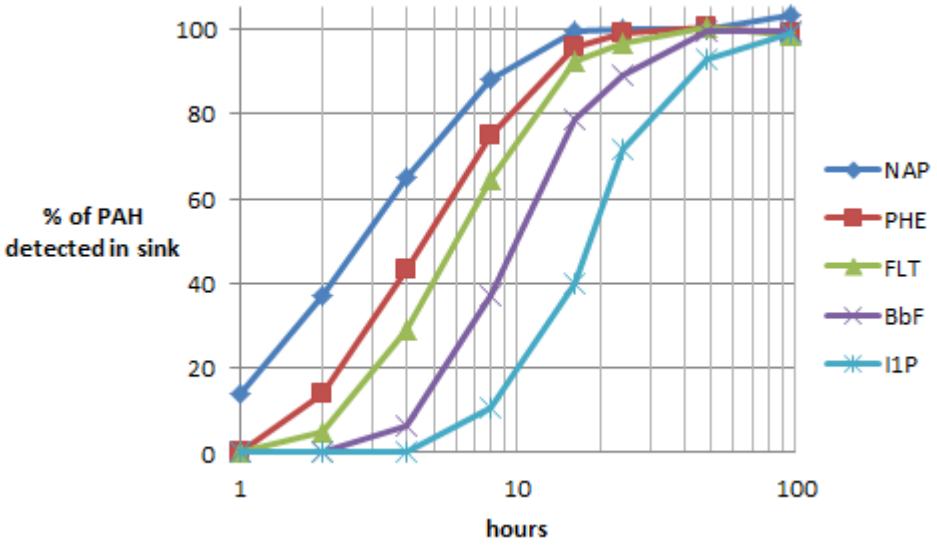


*Figure 3.3. Monitoring of the diffusion of PAH from inside to outside of the bag. The maximum $t_{95\%}$ time is for I1P with 47 h.*

The kinetic constants associated to mass transfer were calculated by fitting the extraction profiles to a first order exponential growth function:

$$C = \begin{cases} 0 & A\left(1 - e^{-k(t-t_0)}\right) \leq 0 \\ A\left(1 - e^{-k(t-t_0)}\right) & A\left(1 - e^{-k(t-t_0)}\right) > 0 \end{cases}$$

Where A is the amount extracted at t=∞, k the kinetic constant in $h^{-1}$ and $t_0$ a correction for the delay of the appearance of the analyte in the final acceptor medium. The $t_{95\%}$ values for estimation of diffusional time for measurement of the 95% of the overall amount that can permeate the membrane ($t_{95\%}$ = ln(20)/k) are shown in table 3.1, along with the $R^2$ coefficient of the regression as the fraction of the total variance explained by the regression for quality control of the fitting. This indicates that all 16 EPA priority PAH are transferred from inside to outside of the bag in 47 h, and thus, the evaluation of the extraction kinetics through the monitoring of the PAH concentration in the acceptor phase has to take this into account.

*Table 3.1. Values of $t_{95\%}$ for each model PAH to cross the membrane along with the $R^2$ parameters as quality control of the fitting.*

| *PAH* | *$t_{95\%}$ ($h^{-1}$)* | *$R^2$* |
|---|---|---|
| *NAP* | *10.2* | *0.9796* |
| *PHE* | *14.5* | *0.9998* |
| *FLT* | *18.1* | *0.9991* |
| *BbF* | *26.4* | *0.9984* |
| I1P | *47.0* | *0.9958* |

## 3.3.4. Shaking influence

In this assay, the amount of PAH extracted from the contaminated soil sample was monitored continuously in the ethanol acceptor phase during 4 days in the 22 mL vial configuration (0.5 g of soil extracted into 10 mL of final acceptor) using FLT as the model compound. The resulting monitored profiles are shown in figure 3.4.

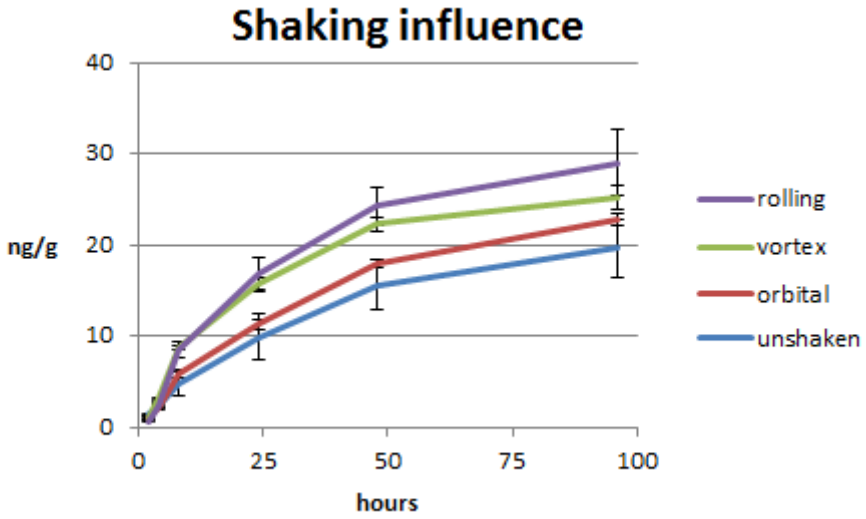


*Figure 3.4. Influence of the shaking mechanism in the extraction efficiency of FLT.*

Experimental results demonstrated that the extraction speed in MEBE is strongly dependent upon shaking of soil with extractant and that it may increase the amount extracted up to a 147% (in this example, for fluoranthene) as compared to quiescent extraction tests. As per the results in figure 3.4 the rolling table and vortex were the shaking method that enhanced the extraction speed best. It should be noted that small air bubbles can be trapped in the LDPE bag while sealing it. Since the LDPE bag is coiled inside the vials, the rolling table is the only method out of the four tested approaches that allows those bubbles to move inside the bag, thus improving the mixing of soil and leaching agent in MEBE, while other methods only shake efficiently the ethanol acceptor phase.

## 3.3.5. Enhancement of extraction speed

The amount of PAH (µg/g) measured in the ethanol acceptor phase by MEBE in the 50 mL-acceptor configuration was compared against that of the classical extraction method, also in the 50 mL cyclodextrin configuration, with both extraction methods per triplicate, using 0.5 g of soil and 24 h of extraction so as to attest for the prescribed time in most of the literature cases. Sampling times were 1, 2, 4, 8 h, 1, 2, 4 d, 1, 2 and

3 w. Extractograms are shown in figure 3.5. Despite the lag introduced by the diffusion through the membrane, the amount extracted by the MEBE, was for each model PAH significantly higher (at 95%, $p<0.05$) than the amount extracted with the classic test as shown in table 3.2, along with the average absolute concentrations found in thee xtractions mediums and their standard deviation (SD) for n = 3 samples

*Table 3.2. Average and standard deviations of concentration ratios in conventional bioaccessibility extraction against the proposed MEBE method*

| $C/C_0$ | | | PHE | FLT | BbF | IP |
|---|---|---|---|---|---|---|
| 24h | Classic | average | 0.008 | 0.026 | <MQC | <MQC |
| | | SD | 0.001 | 0.005 | | |
| | MEBE | average | 0.000179 | 0.00053 | 0.000248 | 0.00049 |
| | | SD | 0.000004 | 0.00001 | 0.000004 | 0.00002 |
| | p (<0.05) | | 0.00002 | 0.00017 | 7E-10 | 5E-11 |
| 21 days | Classic | average | 0.018 | 0.034 | <MQC | <MQC |
| | | SD | 0.011 | 0.001 | | |
| | MEBE | average | 0.18 | 0.23 | 0.15 | 0,81 |
| | | SD | 0.02 | 0.02 | 0.02 | 0,05 |
| | p (<0.05) | | 0.000002 | 0.00003 | 0.00002 | 0.0000007 |

*MCQ: Minimum quantifiable concentration, corresponding to the minimum concentration of standard analyzed in the calibration curve (1 µg/L).*

The amount of PAHs extracted with the new MEBE system in which the sink is separated from the extraction medium is in all instances greater than that of the classical system regarded of the spot sampling time as can be seen in figure 3.5.

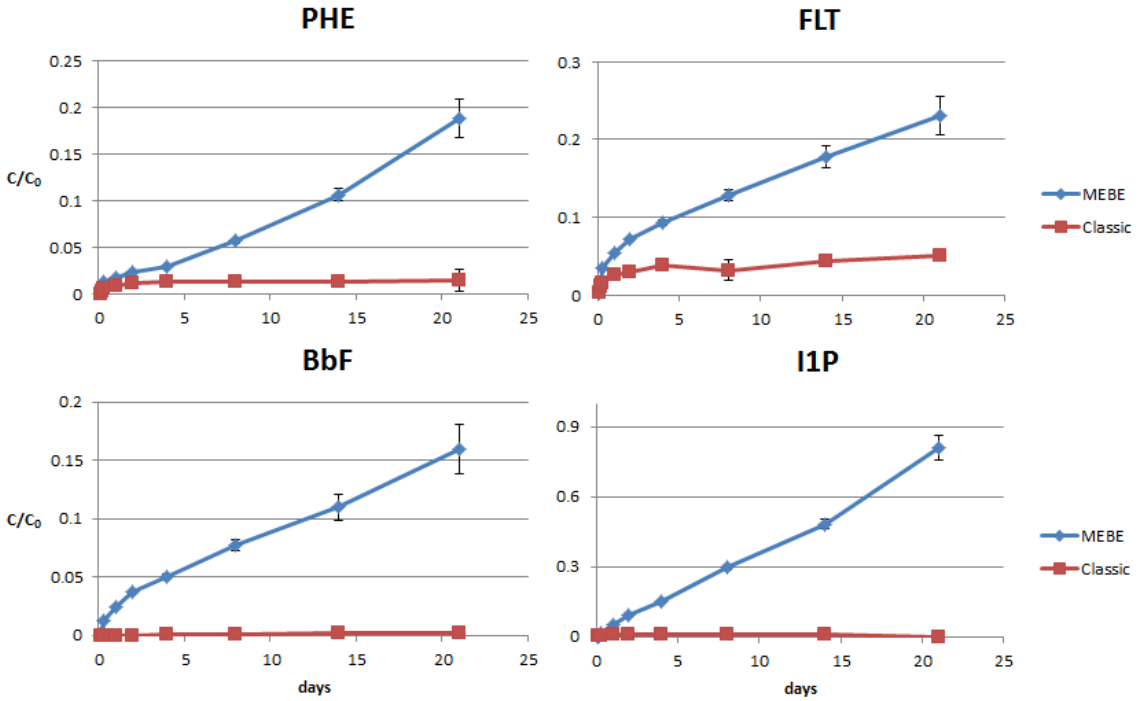


*Figure 3.5. Comparison between classical hydroxypropyl-β-cyclodextrin extraction and the proposed MEBE concept both with 0.5 g of soil and 50 mL of acceptor. While the classic extraction reaches the thermodynamic equilibrium in ca. 3 d, with the MEBE configuration the mass flux from the soil is sustained indefinitely in the studied period.*

While the classic extraction reaches the thermodynamic equilibrium in ca. 3 days, with the MEBE configuration the mass flux from the soil is sustained indefinitely. The most significant differences are found in PAHs of 5 and 6 rings that were deemed to not occur in the contaminated soil sample using the classical setup, but with the MEBE system appeared at levels exceeding 40 ng/g for BbF and 35 ng/g for I1P, respectively. The separation of the extraction medium and the final sink in our configuration showcases the limited sink capacity of HPCD in the conventional assay in which the extracting agent is simultaneously operating as a sink. It can be seen that the short-term alleged steady-state equilibrium in the batchwise conventional medium (usually 20-24 h [23,26,29–34,39,44,142–146]) is actually a consequence of the lack of sink capacity of the HPCD.

Improved sink capacity is deemed imperative in bioaccessible extractions, and operationally defined conditions in classical methods should be revisited or a QC methodology should be introduced to assess that no artifacts arise from faulty setups, as e.g., via the monitoring of release kinetics from scaled sinks, which is in good agreement with earlier researchers [31].

# 4. CocoSoft: educational software for automation in the analytical chemistry laboratory

## 4.1. Introduction

The implementation of European Credit Transfer System (ECTS)-based majors and subject courses has launched a vast number of innovative teaching and learning methods over the recent past [147–151]. Lecturers and students are currently bearing new roles compared with traditional syllabuses in higher education institutions. The lecturer is not tagged anymore as the active and sole element within the knowledge transfer chain in European Credit Transfer System (ECTS) disciplines, yet the vehicle for continuous generation of active knowledge. Students are expected to possess a new role as the actual managers of their own learning in a formative assessment framework [152]. Undergraduate laboratory courses in the analytical chemistry syllabus such as 'advanced chemistry laboratory' or 'integrated chemistry laboratory', to name a few, are now focused on solving real-life scenarios involving chemical tools in which students in a guided-inquiry format shall choose by themselves the analytical techniques that better fit their purpose, learn the fundamentals and basic operational principles of those techniques, and acquire knowledge on how to process experimental data correctly from the mathematical and chemical viewpoints on their own [153]. The limited number of lecturers allocated to every single laboratory exercise and the increasing workload of the ECTS-based analytical chemistry syllabus make these learning objectives become challenging tasks to accomplish. As a result, the course learning objectives are increasingly common calling for straightforward unit operations (e.g., the loading of a preprocessed sample aliquot in a given analyzer) but students might not be aware of the various components of the analyzer and how the instrumental setting is computer controlled, thus lacking the appropriate knowledge to face and track failures in analytical instrumentation, or how to improve the analytical procedure outside the range of predefined experimental conditions. Chemistry students are trained to introduce the experimental data into a macro spreadsheet or statistical software, but they are barely able to understand what algorithms are behind the scenes. An attempt to teach the underlying software, electronics, communications, and mechanics of instrumental analyzers from engineering viewpoints might greatly improve student proficiency in the analytical chemistry laboratory curriculum.

At the postgraduate level, chemometric tools for visualizing relevant figures from datasets are usually well understood by students, but the increasingly larger datasets are making the tracking of errors cumbersome. Courses focused on laboratory control, automation, or data processing are in many instances obsolete, unspecific, and lack real 'hands on' experiments on programming topics, and are merely dedicated to solve focused tasks in ad hoc short sessions, but with difficult adaptation to a broad set of real-life scenarios that are expected in ECTS-based disciplines.

There is actually a quest of open source software packages for basic laboratory control and data processing designed in user-friendly and educational format, in which the algorithms used to solve a given case study might be read directly from the font code, assisting students in acquiring proficiency in the analytical chemistry laboratory. Commercial software packages regrettably are rarely free or open. They tend to be dedicated to a handful of instruments or execute pre-set operations rather than automating the entire analytical process. As a consequence, payware works as a black box, in which the machinery cannot be seen and potential errors are difficult to trace back by users. To understand the math or computing behind the experimental results (or errors), this type of software package is worthless. More importantly, commercially available software packages are expensive, restrain some functions the hardware could do originally and, in some cases, distinct individual software packages are needed to operate various analytical instruments. Experimental data must usually to be exported several times in a humdrum and time consuming manner that prevents users from getting new data or processing results in a timely manner. Default commercial unsupervised algorithms lead to errors, and customized algorithms can only be implemented in customized software packages, not in proprietary ones, so data treatment is not as automatic as it could be. Several approaches toward dedicated software packages for the control of instrumental equipment and/or data acquisition have been published over the past few years. Notwithstanding the fact that the reported software packages are open-source and allow for a 'hands on' startup, they are still deemed to be directed to specific hardware [154–158], rely upon predefined libraries [159], and even if algorithms or communication protocols are known, the addition of new hardware is not straightforward and requires manufacturer's assistance [123,127,129]. Available open-source software packages also bear limited options for data processing, making the implementation of feedback protocols in analytical methods cumbersome, jeopardizing the development of fully automated smart methods.

In this chapter, a novel user-friendly and open educational software package, so-called CocoSoft, is proposed for automation of analytical procedures, including instrumental control, data treatment, and smart method development, in which the font code can be either readily read to get insight into the algorithm or added by the user for controlling new hardware or executing new data processing procedures. This

software package can also serve as a valuable educational tool for introducing coding exercises at the graduate and postgraduate course level so as to trigger problem resolution capabilities of the students as expected in ECTS-based subject matters.

The software package presented herein allows for facile automation of analytical procedures and control of instrumentation as endorsed in the analytical chemistry laboratory curriculum with the additional advantage of processing experimental data at real time, all aided by customized mathematical procedures. It is written in Python programming language. This is a multiplatform that has proven to be extremely readable against other engineering-directed software packages, such as Matlab or Labview [160]. CocoSoft is composed of a friendly graphic user interface (GUI), a file management system, and a tool for highlighting different instructions of the script that allows users to visualize the analytical procedure step under execution at real time. A close-up of the software main window and components thereof is given in figure 4.1. Further details on the working of CocoSoft can be found in section 4.4

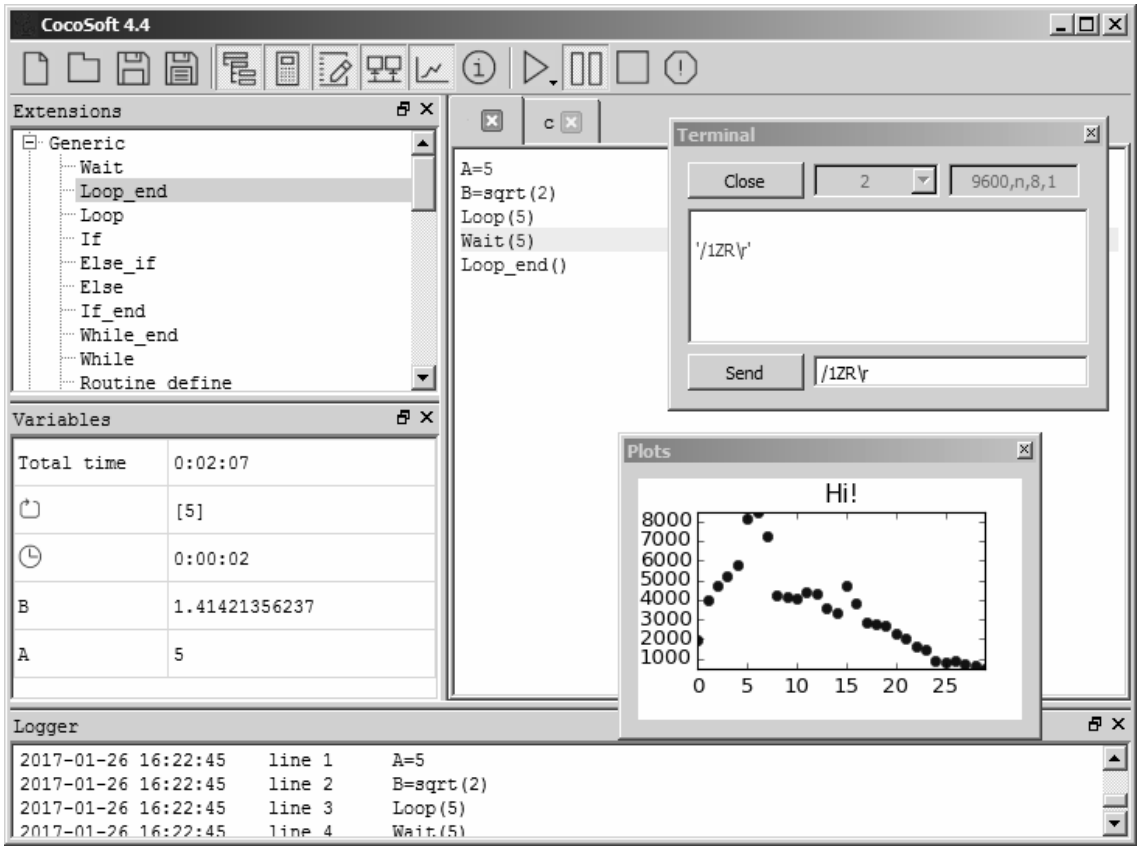


*Fig. 4.1 Screenshot of CocoSoft main window in Windows 7 illustrating the method script and extensions available. The toolbar includes file management, edition of the method, method flow, information, loops, and delay icons.*

Any hardware to be controlled by CocoSoft should have a related extension (Python script) that contains all necessary functions to successfully control it. Any python file ('.py') that is in the same folder than that of CocoSoft will be recognized as an extension, and its functions imported and made available from GUI with a single mouse click. Any native Python syntax is accepted as instruction in the program, thus expanding CocoSoft's functionality far beyond extensions. The program executes the entire set of steps of the analytical procedure in a one-at-a-time format so as to wait for the instrument or function's feedback before pursuing the next instruction. Failures related to inaccurate hardware timing are thus avoided. This is in fact seen as the main drawback of other custom-made software packages [154].

## 4.2. CocoSoft tutorial in undergraduate courses

In order to follow the guidelines set by the European Higher Education Area (EHEA) regarding the use of problem-based learning in the analytical chemistry laboratory curriculum at the undergraduate level, an interpretative lesson about the relevance of monitoring and maintaining the extractant pH in bioaccessibility tests of trace elements in soil environments—harnessing the single-extraction procedure as endorsed by the EU Standards, Measurement, and Testing (SMT) program using 0.43 mol/L AcOH as leaching medium—was taken as a tutorial example. The idea behind is to supplement laboratory assays combining acid-base reaction tests with potentiometric detection. Based upon constructive active learning, students should observe the increase of extractant pH upon dissolution of soil carbonates whereupon they should design appropriate analytical procedures supported by software algorithms to sustain the nominal extractant pH for reliable measurements throughout the extraction test, which, according to SMT, lasts 16 h.

From an educational viewpoint, the pH-stat methodology [161] is to be described first, namely, the addition of minute aliquots of a strong acid to the extraction medium to compensate for the neutralization of the acetic acid by dissolved carbonates, followed by the presentation of the hardware and software employed in the tutorial example: Eutech PC 2700 pH-meter, Cavro XP3000 syringe pump, magnetic stirrer, extraction vessel, 3 mol/L HCl reservoir, and CocoSoft for controlling all of the instrumentation. Figure 4.2 shows a diagrammatic description of hardware connections and the information flow path between hardware and CocoSoft.

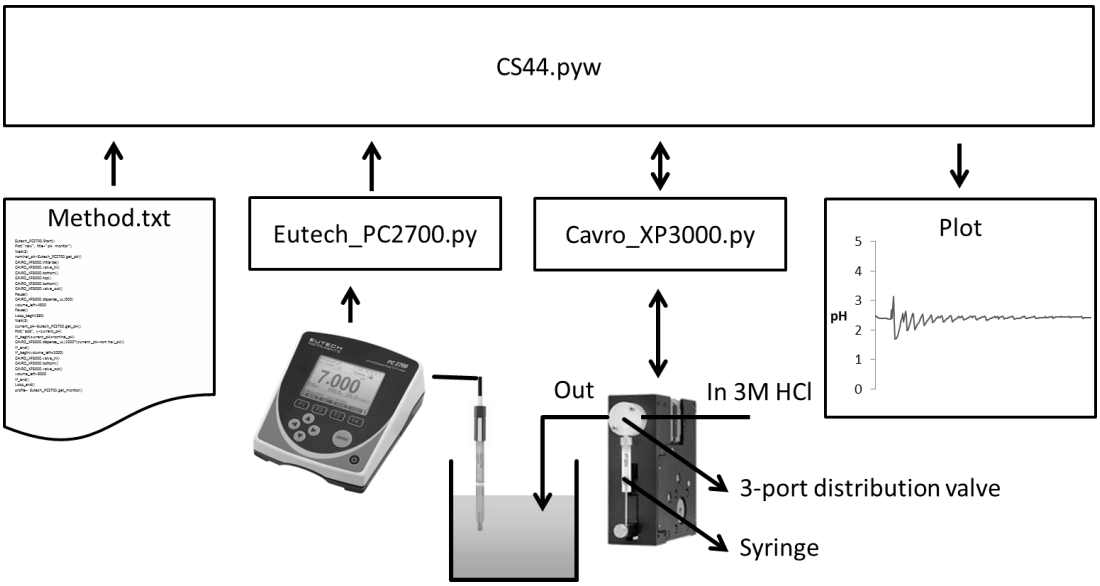


*Fig. 4.2. Conceptual diagram of the distinct instrumental components and connections used in this tutorial. The pH-meter and the syringe pump are connected to the PC through USB-RS232 converter. The main CocoSoft program controls hardware components via their extensions. A text file containing the method is executed automatically. Data is read continuously from the pH-meter and triggers the motion of the syringe pump in due time. The pH profile is plotted in the screen.*

A monitoring algorithm is first taught and provided to the students. This is followed by running the standard SMT method for 15 min while describing the main pitfalls that could stem from the gradual increase of the extractant pH (e.g., the lower extracting capability of the acetic acid and the underestimation of the real hazard of contaminated soils by trace elements) The SMT single extraction test was executed by adding 2.0 g of a calcareous agricultural soil (Palma de Mallorca, Spain) to 80 mL of 0.43 mol/L $CH_3COOH$ subjected to controlled mechanical agitation (500 rpm) throughout.

A simple CocoSoft script is given below as an educational example:

```
Profile= []

Loop(330)

Wait(3)

Profile.append(Eutech_PC2700.get_pH())

Plot(y=Profile)

Loop_end()
```

The role of every single instruction in the automatic analytical method above for continuous monitoring of the pH is to be explained, including setting up of the communications, data acquisition, and data plotting. An illustrative profile of pH monitoring is shown in figure 4.3a.

Upon critical evaluation of the pH profile, students should be asked to search possibilities and write viable scripts for automatic addition of HCl aliquots to the extraction vessel. They are distributed in small groups to trigger collaborative work in line with EHEA recommendations. The lecturer should indicate a number of instructions available of the Cavro XP3000 pump while providing tips and tricks of what could be done with the equipment assembled.

The prevailing answer expected is to add fixed minute volumes of HCl at predefined times aided by the syringe pump. The amount to be added, however, varies from soil to soil, and although this protocol is recommended in the standard CEN/TS 14429:2005, as students have access to smart automatic equipment, no further attention was given to this method. Emphasis was placed on the word 'smart', and on the possibility to further improve the pH monitoring system if we succeed in programming a viable automatic method with feedback from the sample.

After further discussion in a team collaborative environment, the possibility of design of a pH comparison system should come up. This was the case in a last year undergraduate course of advanced analytical chemistry laboratory in which this tutorial example was introduced as an innovative learning tool. The basis of the comparison algorithm is as follows: 'when the extract pH is higher than the nominal pH of the extractant, a given volume of acid should be added (in our case 200 µL (see script below)'. The fluidic system was initialized manually, and four instructions were added to the previous monitoring script:

Before the loop:

```
Initial_pH = Eutech_PC2700.get_pH()
```

And in the loop, before the plotting:

```
If(Eutech_PC2700.get_pH()>Initial_pH)

Cavro_XP3000.dispense_uL(200)

If_end()
```

The time-based pH profile of the SMT test was projected at real time in the class (see figure 4.3b) and synchronized with the visualization of the CocoSoft script. This test served in triggering students' learning outcomes and engagement as a great expectation was observed after the first addition of acid inasmuch as most students

were eagerly waiting for the pH to exceed the nominal extractant pH for the automatic actuation of the syringe pump.

Several teams, however, soon realized that the main drawback of the smart comparative procedure is that once the carbonate pool of the solid material is almost entirely dissolved in the acetic acid milieu, occurring within a few-minute timeframe, the difference of 100th of a pH unit still triggered the addition of an aliquot of 200 µL of 3 mol/L HCl with the consequent sharp decrease in the extractant pH, which is not to be buffered. The lecturer should make students aware that the dissolution of further mineralogical phases that have slower leaching kinetics will be carried out at lower pH values, which will in turn overestimate the pools of bioaccessible trace elements in risk assessment studies of metal contaminated soils. As a result, the students in the laboratory course should identify the need of a different algorithm to tackle this issue. Our experience indicates that at this point the educator should give some further tips and tricks prior to introducing the so-called proportional algorithm in which the volume of the acid aliquot added to the extraction medium is proportional to the difference between the nominal and current pH values rather than adding a steady volume regardless of the absolute pH value, as is the case with the comparator algorithm. The procedure is the same as in the previous example, but the smart conditional line should be replaced from:

Cavro_XP3000.dispense_uL (200)

to:

Cavro_XP3000.dispense_ uL (1000*(Eutech_PC2700. get_pH()-Initial_pH))

This demonstrates the versatility of the CocoSoft software package in method development and optimization of analytical procedures. With the proportional algorithm, two simple demonstrations could be introduced to illustrate the fact that a difference of one pH unit will lead to the addition of a 1000µL acid aliquot to the extraction vessel, whereas a difference of 100th of a pH unit will trigger the automatic addition of a mere 10µL aliquot. The new monitoring profile (proportional algorithm) is compared in figure 4.3c with that of the previous procedure (comparator algorithm).

As a further team collaborative work, students might be asked to enumerate potential improvements to the algorithm. We do expect that they envisage the feasibility of the first derivative for monitoring of the rate of pH change. Optimization of the parameters of the proportional algorithm, including the time between consecutive measurements and the constant of proportionality between the acid volume and the difference between the nominal and actual pH values, needs also to be perceived and illustrated via practical examples in the laboratory.

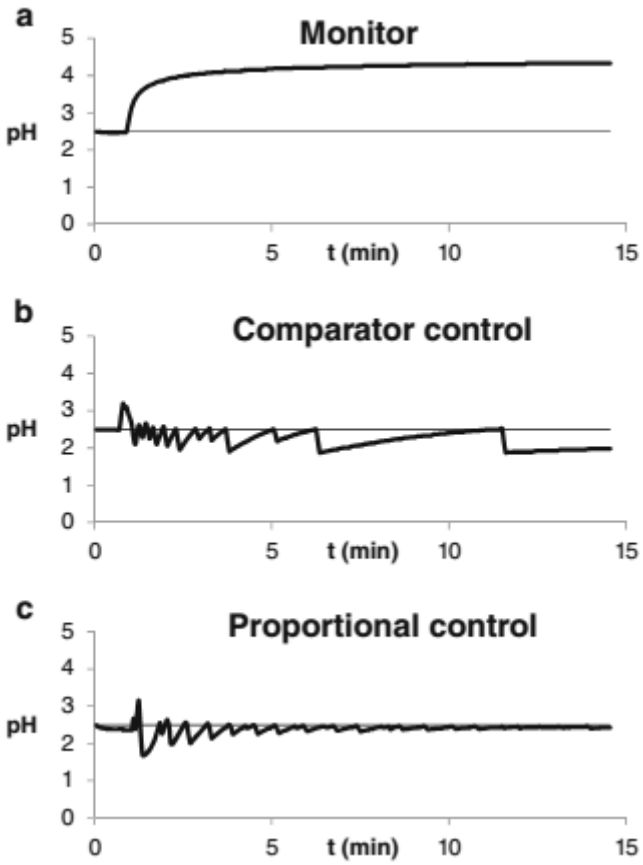


*Fig 4.3. Extraction profiles illustrating the changes of pH values as obtained with (a) monitoring test, (b) comparator algorithm, and (c) proportional algorithm in a 15 min extraction timeframe*

## 4.3. CocoSoft tutorial in postgraduate courses

CocoSoft was also introduced in advanced courses of automation in the analytical chemistry laboratory addressed to Master and PhD students so as to set up computer-controlled fluidic manifolds composed of pressure-driven liquid drivers, sample injection systems, gas-diffusion units, and potentiometric detectors for characterization of agricultural soils in terms of ammonium content [162]. Lecturers should, in a tutorial format, comprehensively pinpoint CocoSoft GUI main components and advanced functions thereof (see figure 4.1 for details). Instructions for writing a basic script serving as analytical protocol should be given to students for interactively learning the underlying principles of programming and features of CocoSoft in the analytical laboratory for operation of syringe pumps, rotary valves, and measurement and processing of potentiometric data from ion selective electrodes. Students should afterwards be actively engaged in writing new analytical procedures using an emerging educational model of laboratory-based formative assessment on the basis of the initial analytical protocol presented before to, for example, move the valve from port 3 to port 4 or wait 30 s rather than 3 s for efficient permeation of evolved ammonia in the

flow system. In both cases, students should realize that a change of the number in brackets would suffice for proper script modification. At this point, lecturer–student interaction is deemed imperative for building a fully automated analytical procedure for determination of ammonium in soil extracts in a flow-based configuration incorporating gas-diffusion separation and understanding the underlying acid-base reactions involved. The lecturer does take the lead here but requires students' feedback on how to code the different instructions. Students are also encouraged to take notes on more specific challenging tasks, for example, replace the communication port and execution of optimization protocols of method parameters such as flow rates, sample/reagent volumes, and delays by straightforward modification of numerical values in the CocoSoft script. In this way, students acquire proficiency in method programming on their own. At this point, we have observed that most postgraduate students merely perform minor changes in the arguments of the instructions, but do not dare writing new instructions. After more than 1 week of full-time hand's-on training on software functionalities taking the flow-based potentiometric system as a tutorial example, we have seen that postgraduate students succeeded in making analytical methods from scratch efficiently by copying groups of instructions of defined functionality from previous methods and incorporating unusual instructions from available extensions.

## 4.4. User guide

CocoSoft is a wrapper around python, that is, the method loaded in CocoSoft will be parsed and executed by Python line by line. So, in principle, the method loaded in CocoSoft is written in Python syntax. The main feature of CocoSoft is that it sets the framework for allowing untrained personnel to develop the control and data treatment methodologies without knowledge of coding. It includes the Graphic User Interface (the windows and buttons), an easy way of writing the instructions, an easy way of adding hardware to the experimental setup, hides the communication protocol from the final user, and provides tools for monitoring the method as well as to create, save and edit the instrumental methods.

### 4.4.1. Installation

CocoSoft is based on Python and some third party modules. It used 'pyserial' for the serial communications, 'numpy' and 'matplotlib' for the plots and 'PyQt4' for the GUI. All those modules have to be installed in order to get full functionality of CocoSoft. However, it is enough to install Python and run CocoSoft for getting help with installing all other modules needed.

The easiest way to get CocoSoft working under Windows environment is to install 'PythonXY' [163] in the full mode (it will include all other modules needed).

Afterwards, the user simply needs to copy the CocoSoft file ('CS44.pyw') in the computer and add to the same folder the extensions he or she wants to use in his/her method. There are currently more than 30 extensions for most common labware as Cavro, Fialab, Vici, Crison, Milligat, CMA, UNI-T, AIM, Ontrak, Gilson, IDEX, Ismatec, and Hamamatsu, to name a few. Other extensions allow for example to proxying mouse and keyboard patterns without human intervention, aiming at setting fully automated smart methods exploiting modern analytical equipments (e.g., chromatographs, atomic absorption or emission spectrometers, mass spectrometers), which do not usually offer the option to be controlled by software other than that of the manufacturer. They are available upon request, and will be soon available for public download. For executing the program, the user should double click the 'CS44.pyw' file.

### 4.4.2. Adding hardware

The configuration of new hardware is straightforward. For each instrument the user wishes to control the appropriate extension has to be added to the same folder of the CS44.pyw file.

For example, if the system consists of a Cavro XP3000 pump and a Crison selection/injection valve module, the user has to include the CS44.pyw, Cavro_XP3000.py and Crison_Valve.py files in the same folder.

If there will be several hardware of the same kind (e.g. two Cavro XCalibur pumps), there will be 2 different extensions for these pumps. The used should only copy the extension with a different name, e.g. Cavro_XCalibur1.py and Cavro_XCalibur2.py

### 4.4.3. Graphic User Interface (GUI)

When double clicking the 'CS44.pyw' file, the program will open and show the CocoSoft window, as can be seen in figure 4.1. It consists of a main window and toolbar. The method window consists in different tabs where the different methods can be opened simultaneously by using the icons located at the left of the toolbar: New, Open, Save and Save as actions. If the mouse is stopped over any icon of the toolbar, its name will appear.

To the right of the toolbar, there will be the icons for Play, Pause, Stop and Emergency stop, that will start the method, pause it (until it is continued by clicking again on the Play or Pause buttons), stopped (the next time the Play button is clicked, the method will restart from the beginning) and emergency stop, that is, the method will be stopped and all mechanical parts halted. If the play button is pressed but not released, the options to start the method from a selected line or to execute only a selected code are also available. Those method related actions are also available by

right clicking on the method window, along with edition related actions (copy, cut, paste, find and replace, comment, uncomment). Nothing is executed in a line after a pad sign (#). This functionality may be of use for adding comments to the methods. The comment action adds a pad at the beginning of all selected lines, Uncomment removes them, one at a time from each line.

In the middle of the toolbar there are the buttons to show or hide different accessory docks. Those docks can be detached from the main window, and allocated in any geometry in the screen, as can be seen in fig. 4.1. Extensions dock shows all the extensions (.py files in the same folder than the main CS44.pyw file) and the functions present on them. Clicking on the extensions name will make the function list to drop down or compress, and clicking on the function will add it to the method window in the current cursor position. Some functions need arguments inside the parentheses, others do not. Letting the mouse be on a function name will show a help tip about the proper syntax. Variables dock shows the current value for the variables used in the method, the total execution time, and if the method is in a loop or a delay, it shows the loops left, and the time left, respectively. In the logger dock are annotated all actions taken during the method execution. Upon method stop this log will be saved in the 'Log' folder of the CS44.pyw location. If the folder does not exist, it will be created. This log can be useful for tracking errors, or keeping information about the method performance. The terminal dock offers a RS232 communication interface in which the user can send and receive data to/from a serial port by specifying the port name from a dropdown list of available ports, and setting the baudrate, databits, parity and stopbits. The sent characters appear in red and the received in green. The window content can be copy pasted in order to save it. Any unicode string can be send by resorting to python syntax. The plots dock represents the plots that have been called from the executed method with the 'Plot()' function. The information button provides a pop up window with information about CocoSoft publication, contact and acknowledgements.

### 4.4.4. Generic Functions

Functions controlling the method structure are included under the 'Generic' title in the extensions dock. Their proper syntax and comments can be seen letting the mouse to stop over the function name. Most important functions are commented down here. For comprehensive description, see the supplementary information of CocoSoft published paper [164]

- Wait(). Sets a delay
- Loop(x), [...], Loop_end(). Repeats the code comprised in between x times.
- If(), Else_if(), Else(), End_if(). Allow for smart method developing by introducing conditionals. The conditions must to be written in python language. See section

about python syntax (section 4.4.6).

- While(x), [...], While_end(). Executes the code in between until x condition is false
- Routine_call(x), Routine_define(x), Routine_end(). Calls a routine that has to be defined.

Other functions that expand the CocoSoft functionality are Send_mail(), for sending an email with e.g. the results of the analysis, Variables() for opening or saving data, Beep() an acoustic signal, Monitor() to acquire data at real time in a different program thread e.g. in a chromatographic mode, Call() to call a method from inside other method (like the routine function but with separate files), Send_RS232() for communicating with instruments when there is no extension available for them, Plot() to plot data and Fit() to fit experimental data to a theoretical equation automatically in the method workflow.

### 4.4.5. Adding extensions

Extensions are python scripts in which some functions are defined. When the scripts are placed in the same folder as CocoSoft, and the software is opened, the extensions are imported and the functions are made fully available to CocoSoft. Modifying the extensions after they have been imported has no effect. CocoSoft has to be reopened for importing the latest version of the extensions. Only two things have to be taken into account when designing custom extensions for CocoSoft:

- If the instruction that is executed contains an equal sign before a parenthesis e.g. 'A=get_pH()', the assignment is done, and the method continues executing next instruction. If there is no assignment e.g. 'Cavro_XCalibur.dispense_uL(1000)', the returned value of the function will be evaluated. If it does not return any value, the execution is continued with next instruction. If it returns any value, the instruction will be called once and again until it does not return any value. This is how the program can be synchronized with instruments: the 'Cavro_XCalibur.dispense_uL(1000)' instruction returns a string until the movement has finished. Afterwards it does not return anything. So the CocoSoft method will not execute next line until the Cavro pump has finished its motion.
- Some particular names can be given to the functions in order to get a special behaviour: if the function name contains '_n_', it will not be added to the extension dock. If it contains '_e_' it will be called when pushing the emergency button, so it should halt all mechanical parts. If it contains '_p_', it will be executed when the Play button is pressed. If it contains '_o_' it will be executed when opening CocoSoft. For example, the function '_e_n_stop()' will not appear in the extension dock and will be executed when pressing the emergency button.

### 4.4.6. Python syntax

Since the CocoSoft method has to be written in python language, here are some tips for the writing of complex methods.

The strings (file names…) should be written between quotes (‘ ‘) or double quotes (“ “).

Variables make coding easy, use them!

Dots separate the integer and decimal part; commas separate the elements in a list.

Python builtins are always available.For more information refer to supplementary information on the published CocoSoft paper [164] or to python builtin functions [165], boolean operations, comparisons, numeric types, bitwise operations, string, lists and dictionaries methods [166] and advances mathematical functions [167]

# 5. Hybrid flow system integrating a miniaturized optoelectronic detector for on-line dynamic fractionation and fluorometric determination of bioaccessible orthophosphate in soils

## 5.1 Introduction

Phosphorus plays an important role in the environment and food web as is contained in fertilizers for supporting the plant growth and in food additives as well. On the other hand, phosphorus is a factor of eutrophication in water reservoirs, such as lakes or rivers, and might pose severe risks to aerobic living organisms [168]. Phosphorus occurs in different forms – both inorganic, namely orthophosphates, metaphosphates and polyphosphates, and organic species [169–171], which include e.g. phospholipids, sugar phosphates, nucleic acids and phosphoproteins [172]. The labile organic forms of phosphorus might hydrolyze on a short notice [173]. Immediate detection is thus needed after sampling or leaching for discrimination between inorganic and organic phosphorus species. This requirement is most likely met with flow analysis methodology [174]. In case of soil analysis in-line microcolumn/chamber extraction coupled to downstream detection allows the simplification of the analytical leaching procedures for orthophosphate and the minimization of the hydrolysis of the organic forms [175,176].

Free inorganic phosphorus forms can be measured using different analytical methods including potentiometry [177], voltammetry [178] and amperometry [179] but the most commonly used are optical methods in combination with the molybdenum blue chemistry. Flow methods have been frequently used in view of their green chemical credentials as a result of miniaturization, automation, and high sample throughput with the extra degree of on-line sample handling at hand [180,181]. A large number of FI and SI methods focused on detection of the yellow heteropolyacid complex (phosphomolybdate acid) generated by reaction of orthophosphate with

molybdate in acidic medium [180,182], yet this method is deemed not sensitive enough in multifarious environmental analysis. Sensitivity amelioration is gained by reducing the heteropolyacid to the molybdenum blue dye using ascorbic acid, hydrazine or tin chloride, hydroquinone [181–183]. The molybdenum blue method was also used in combination with enzymatic reactions based on alkaline phosphatase to determine orthophosphate [184] and flow-based preconcentration setups using anion-exchange reactors [185]. Another existing photometric method for determination of orthophosphate is based on the ion-pair association between the yellow heteropolyacid and Malachite Green, yet it affords poorer repeatability and narrower linear range as compared to the molybdenum blue chemistry [180]. Besides photometric methods, fluorometric detection is also feasible on the basis of the ion-pair formation between the heteropolyacid and fluorophores, such as rhodamine B [180,186] and rhodamine 6G [187,188] for indirect analysis relying upon fluorescence quenching. This procedure has been adapted to a flow-based format as well [180,181,186–188].

In this work, the concept of light-emitting diodes (LEDs) as both emitters and detectors of light (so-called Paired Emitter–Detector Diode (PEDD) device) is applied to fluorometric detection (FPEDD).

### 5.1.1. Paired Emitter-Detector Diodes

A diode is a silicon or germanium crystal doped in a zone with a pnictogen atom in order to have an excess of electrons and in other zone with a earth metal atom for having a defect of electrons, or 'holes'. The electrons and holes diffuse into both zones until the electrostatic forces are equilibrated. When the diode is directly polarized, the electrons of the negative pin repel the electrons from the diode's cathode, pushing them towards the *pn* junction, while the positive pin attracts the valence electrons from the diodes' anode. It's equivalent to push the holes towards the junction. The electrons with enough thermal energy recombine with holes so a net current passes through the diode. In an LED, the recombination energy is liberated in the UV-Vis-IR wavelength. When reversely biased, electrons are removed from the n zone and pushed towards the p zone, producing stable electron configurations in both sides of the junction. When the depletion zone potential equals the power supply voltage, the process is halted and no current passes through the circuit, except a leak current (due to carriers in the crystal surface, because of the coordinative unsaturation).

The initials PEDD resort to the simultaneous use of LED as emitters and detectors in optical measurements. LEDs have long been used as emitters in instrumental methods of analysis [189] for being quite monochromatic (25 nm of width at half height), very affordable, very intense in terms of light flux and they have a very long shelf life. LEDs for special uses have even narrower bandwidth and they are

commercially available for 235 nm and higher in 5 nm [190] intervals until near infrared (4600 nm) [191] The use of LED as detector is documented from 1976 [192], but a very tiny bibliography has been published since then showing their characteristics [193,194] Main difference of the LED against a normal photodiode is that the LED can only detect light with a wavelength smaller than the one it produces (inner filter effect), because this is the minimum energy that achieves a disproportion of electrons and holes in the *pn* junction.

#### 5.1.1.1. Comparison with photodiodes

Critical comparison of LEDs against photodiodes as detectors has been recently reported by Hauser's team [195]. The lower price of LED, the greater shape choice and the ease of mechanical modification are usual arguments in favor of LEDs against photodiodes. Regarding their capabilities as detectors, LEDs generate 1 or 2 orders of magnitude less current than photodiodes. Used in the Warsaw approach (section 5.1.1.3), the voltage generated gives a similar sensitivity than photodiodes and both respond well in the 10 kHz range, but the LED suffers from a narrower dynamic range.

The inner filter effect allows taking optical measures more complicated than the mere measurement of the total photonic flux. Special caution should be taken when buying an LED to know if the emission is truly monochromatic, because some LEDs contain impurities for adding a taint to their main emission peak. Several ways to profit this include:

- The use of a multicolor emitter and detector for quantifying absorbance at different wavelengths without changing the optical setup.
- Using a continuous background source and an LED as a detector can measure the integral of the lower wavelength limit of the source to the upper wavelength limit of the LED. If this is combined with multiple detectors, several integrals of parts of the electromagnetic spectrum can be obtained simultaneously in line with new miniaturization trends [196].
- Optimizing the geometry for simultaneous measures of absorbance, fluorescence [197], turbidimetry, nephelometry and diffuse reflectance are possible because the emitter and detector roles can be changed from measure to measure.

#### 5.1.1.2. Dublin approach

In the approach exploited by the Diamond's group [198] in Dublin, the LED is reverse biased for a given reproducible time in order to accumulate holes and electrons around the *pn* junction. The LED acts like a capacitor. The discharge time is measured. When the LED is discharged in darkness, the holes and electrons migrate

until electrostatic equilibrium is reached, the capacitor is discharged. When the LED discharges under a light flux, the disproportion of electrons and holes injects electrons in the n zone and holes into the p zone, so the discharge is much faster. It can be considered:

$$t = \frac{Q}{i_{dark} + i_{light}}$$

Being t the discharge time, Q the charge separated by the reverse bias, $i_{dark}$ the discharge current in darkness and $i_{light}$ the discharge current due to light. The discharge due to light is faster than the dark one, so the $i_{dark}$ can be usually left out of account. The time of discharge to a given level is inversely proportional to the received light, the expression can be substituted onto the Lambert-Beer-Bouguer law:

$$A = log\left(\frac{I_0}{I}\right) = \varepsilon lC = log\left(\frac{t}{t_0}\right)$$

Being $t_0$ the time that takes the LED to discharge under light conditions without any absorbing species and t the time that takes to discharge through the sample. We can arrange the expression:

$$log(t) = \varepsilon lC + log(t_0)$$

The analytical signal in this case is the time that the charge takes to reach a predefined level and its relation with the colored analyte is logarithmic [199,200].

In practice, Diamond's group strategy is to connect the LED to the analog-to-digital converter (ADC) of a microcontroller (e.g. PIC16F876), powered with a LM7805 voltage regulator, that initially polarized the LED for 500 µs to 5.00 V and after, the measurement mode is triggered: the time until the microcontroller's pin passes from high to low in the TTL system: 1.7 V. The logarithm of this time is obtained and this value is send with serial communications to the computer through a MAX232ACP adapter.

The main drawbacks are that the price of the LED is increased with the electronics to more than 10€ (LM7805, PIC16F876, MAX232ACP), and the chip programmer. In general, the whole measure takes 600 µs in high light flux conditions and up to some ms in low illumination conditions. With this data acquisition rate, it is possible to use this system as detector for flow techniques [201] or HPLC [202].

### 5.1.1.3. Warsaw approach

In the approach exploited by the group of Koncki [203,204] in Warsaw, the LED is kept in a pure photovoltaic mode with zero bias. The voltage between the electrodes due to the creation of pair electron-hole is measured directly with a very high

impedance voltmeter. The Shockley's equation relates the I-V curve for diodes:

$$I = I_S\left(e^{Eq/nTk} - 1\right)$$

Being I the current that passes through the diode, $I_s$ the reverse bias saturation current, E the *pn* junction potential, q the electron charge, n the ideality factor or emission coefficient, T the absolute temperature of the *pn* junction and k the Boltzmann constant. The term Tk/q is called 'thermal voltage'. When the LED is directly polarized at room temperature the exponential term is much bigger than 1, so the second term can be deleted:

$$I = I_S\left(e^{Eq/nTk}\right)$$

With logarithms:

$$log(I) = log(I_s) + \frac{q}{nTk}E$$

The voltage that will be generated when the LED is illuminated directly (blank) or through the sample will be:

$$\Delta E = E_{blank} - E_{sample} = \frac{nTk}{q} log\left(\frac{I_{blank}}{I_{sample}}\right)$$

Because the current that the LED generates (I) is proportional to the light flux it receives ($I_{light}$), the previous equation can be combined with the Lambert-Beer-Bouguer law (A=εlC):

$$\Delta E = \frac{nTk}{q} log\left(\frac{I_{light,blank}}{I_{light,sample}}\right) \propto A = \varepsilon lC$$

So, the difference of voltage measured between the blank and the sample is proportional to the sample concentration. The ideal way to perform the measurement is to use a high impedance voltmeter (R > $10^{12}$ Ω) and successive amplification steps, so the voltage can be measured without the establishment of an external current, achieving a measure constant with time, since the only way charges disappear is the electron-hole annihilation that is already in the equilibrium considered (creation-annihilation).

Another way to perform the measure is with a low impedance voltmeter [204]. In this case it is necessary that the LED is still illuminated and what is measured is actually the voltage maintained in the steady state while three processes are simultaneously happening: charge by illumination, discharge by recombination and discharge through the low impedance voltmeter. Measurements are 1 to 2 orders of magnitude more sensitive than those with the high impedance voltmeter.

### 5.1.1.4. Use of PEDD

PEDDs are predominantly developed for photometric measurements and several research teams utilized this concept to build miniaturized detection platforms for analytical purposes [205–209]. LEDs can also be used as fluorescence inductors in dedicated cell geometries. Only recently, prototypes of FPEDD have been reported [210–215]. FPEDD detectors are greatly cost-effective and miniaturized in comparison to conventional fluorometric spectrometers. These detectors are dedicated to a given analysis by careful selection of the optical properties of the LEDs. Enhancement of sensitivity of measurements is provided by using various diodes (with the same emitting wavelength) as fluorescence inductors and one LED working as detector of induced fluorescence [211]. Such optoelectronic detectors have been successfully used in fluorometric assays of calcium [211], phosphate [212], oxygen [213], riboflavin [214] and proteins [215].

A novel hybrid SI/FI system integrating in-line soil leaching (using the Hieltjes-Lijklema sequential extraction procedure) with flow-through FPEDD detection (using two LED emitters) is herein proposed for expedient bioaccessibility tests of orthophosphate in soils. To the best of our knowledge PEDD detection has not been resorted to the analysis of soil extracts as of yet. As compared to previous dynamic leaching methods for orthophosphate using advanced flow methodology [176,216] the proposed setup is more simple (merely needs one syringe pump instead of five liquid drivers [176] and uses portable and affordable detection systems that are easily constructed in the lab. Combining an SI manifold for automatic leaching and a secondary FI system for on-line detection the phosphorus laden extracts are analyzed at real-time, with the subsequent minimization of the hydrolysis of organic phosphorus in the alkaline or acid fractions that was not avoided in previous studies with off-line detection of leachates [216]. The hybrid flow system also affords in-line dilution upon demand by using automatic flow programming.

## 5.2. Experimental

### 5.2.1 Reagents, solutions, samples

All chemicals were of analytical reagent grade. Solutions were prepared using double distilled water. The stock standard solution (100 mg $PO_4^{3-}$/L in water) was prepared from $KH_2PO_4$ (Merck). Working standard solutions were prepared separately in each extractant milieu ($NH_4Cl$, NaOH, HCl). In this work, the three step Hieltjes-Lijklema (HL) sequential extraction procedure [12] was selected. In the first step, 1.0 mol/L $NH_4Cl$ (Probus) adjusted to pH=7 with $NH_3$ (25%, Scharlau) was used to extract the labile phosphate (water soluble and exchangeable fraction) from the soil sample. In the second step, 0.1 mol/L NaOH (Panreac) was pumped through the column to

extract the Fe- and Al-bound phosphate. The last step, using 0.5 mol/L HCl (37%, Scharlau) as extractant, released Ca-bound phosphate. The derivatization reagent consisted of 12 g/L ammonium molybdate tetrahydrate (Scharlau) in 0.8 mol/L $H_2SO_4$ (Sigma-Aldrich). In some instances oxalic acid (Panreac) was added at the level of 0.25% (w/v). The solution of fluorophore was prepared by dissolving 70 mg of rhodamine B (Merck) in 1000 mL of distilled water. This solution contained 0.05% (w/v) of polyvinyl alcohol (30–70 kDa, Sigma). A standard reference material from the National Institute of Standards and Technology (NIST)–SRM 2711 (Montana Soil) and a surface agricultural soil in Mallorca (Spain) were selected to study the reliability of the hybrid microcolumn-based flow system and validate the FPEDD detection method. Prior to chemical analysis, the soil was oven-dried at 105ºC until constant weight and 2-mm sieved. Soil pH was measured in 0.01 mol/L $CaCl_2$ at a soil to solution ratio of 1:5 (w:v) after 2 h of equilibration using a combined pH electrode as specified by ISO 10390 [217]. The pH value was 7.52 ±0.03. The total organic carbon (TOC) contents of 8.55% were determined by dry combustion at 900ºC after removal of carbonates with a few drops of a 20% (v/v) HCl solution. Particle size distribution of the fraction <2 mm for determination of soil texture was performed with the Bouyoucos hydrometer method (American Society for Testing and Materials (ASTM) type 152H) [218]. The agricultural soil consisting of 51.1% sand (0.05–2.0 mm), 34.5% silt (2–50µm), and 14.4% clay (<2 µm) was classified as loam soil.

## 5.2.2. Flow system

The hybrid flow system for in-line sequential extraction (fractionation) and automatic determination of orthophosphate in soil samples is depicted in fig. 5.1. This integrated SI/FI system is a combination of a µSIA setup (FIAlab Instruments, Seattle, US) furnished with a SP and a 6-port multiposition SV, controlled by its own software (FIAlab Instruments), with a dedicated secondary FI system incorporating a PP (Minipuls 3, Gilson, Middleton, Wisconsin), a rotary IV (IDEX V-1451-DC, Upchurch scientific, Oak Harbor, Washington) and a solenoid valve (Parker Hannifin, Cleveland, Ohio). All components of the FI system are controlled by contact closure from a USB relay plate (ADU200, Ontrak Control Systems, Sudbury, Ontario, Canada), with the FIAlab software akin the SI extraction system. The syringe pump is furnished with a 5-mL glass syringe and a three-way valve at its head (VH). It is connected by a 2.25 mL holding coil (HC, 1.5 mm ID) with the SV. This valve allows also selecting the appropriate extractant which via the SP is delivered to the soil containing microcolumn nested to one of the external ports of SV (see figure 5.1). The IV furnished with 1.0-mL PTFE loop (1 mm ID) enables the connection between the SI and FI systems. The PP uses four channels to pump concurrently the derivatization reagents downstream for fluorometric detection of the heteropolyacid-fluorophore ion pair. An additional solenoid valve (V1) is used for dilution of HCl extracts. The volumes of the PTFE

reaction coils (0.8 mm ID, R1, R2 and R3) are ca. 400mL, 600mL and 400mL, respectively. PP Tygon tubing was of 0.89 mm ID for molybdate, water/sample and rhodamine B and of 1.85 mm ID for the HCl stream as diluent.

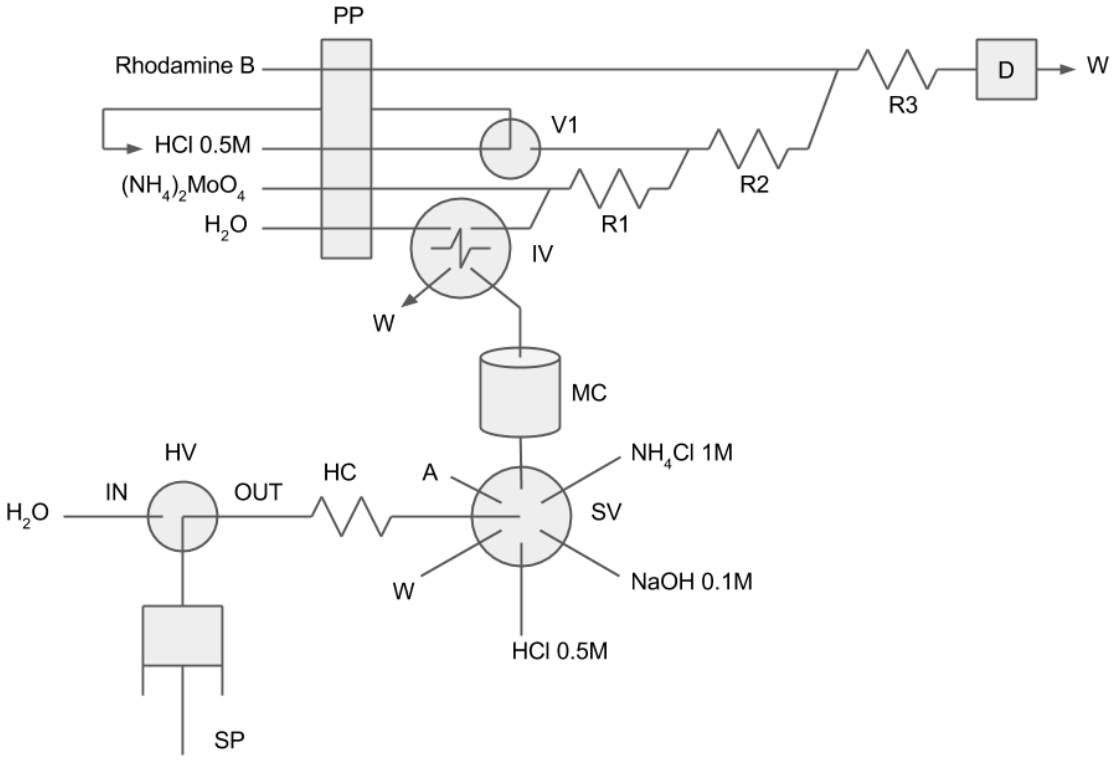


*Fig. 5.1. Scheme of the hybrid flow system for in-line extraction and determination of bioaccessible orthophosphate in soils using FPEDD. SP: Syringe pump; HC: Holding coil; PP: Peristaltic pump; HV: Head Valve, SV: Selection valve, IV: Injection valve, MC: Microcolumn (containing soil); R1, R2, R3: Reaction coil; V1: Solenoid valve; D: Fluorometric paired emitter–detector diode.*

## 5.2.3. Flow-through microcolumn assembly

The polyether ether ketone (PEEK) extraction microcolumn has been described elsewhere [176,216]. It includes a central dual-conical shaped sample container, filters and caps at its both ends. Two different membrane filters (13 mm, FHLP01300, Fluoropore, Millipore) are used – 0.45 mm on the top of the column and 1.0 mm at the bottom to not allow the solid particles to flow freely to the detection part of the system. The free column volume was ca. 250 µL. The column was placed in upright configuration unlike previous dynamic microcolumn-based sequential extraction procedures for orthophosphate in soils [176,216].

## 5.2.4. Flow-through PEDD detector

The dedicated flow-through FPEDD detector has been constructed for fluorometric measurements of orthophosphate (see figure 5.2). The design has been described elsewhere [211,214]. Briefly, a 25 mm long and 15.5 mm diameter PEEK cylinder is used. In the equatorial plane, a 5 mm through hole is drilled so as to accommodate two identical green LEDs as inductors of fluorescence (525 nm Optosupply, China) facing each other. In the same equatorial plane but perpendicular to the LEDs, a 2 mm through hole is drilled for inserting the inlet and outlet tubes (PEEK, 2 mm OD, 1 mm ID, 8 mm protruding) which are glued to the cylinder walls. A 5 mm hole is drilled through the cylinder axis, but the entries are enlarged to 7 mm. The ridge so formed serves to retain the acrylic windows (7 mm diameter), which are blocked by a short tube adapter (7 mm OD, 5 mm ID). The red LED detector (650 nm, Optosupply, China) is press-fitted and held by the tube adapter. The volume of the obtained flow cell is ca. 60µL. Both LED emitters operated at a current of 30 mA. An ordinary low-budget multimeter with RS232 serial communication (model UT70B from UNI-T, China) is used for reading the voltage signal (mV) generated by the FPEDD whereupon it is processed by a PC.

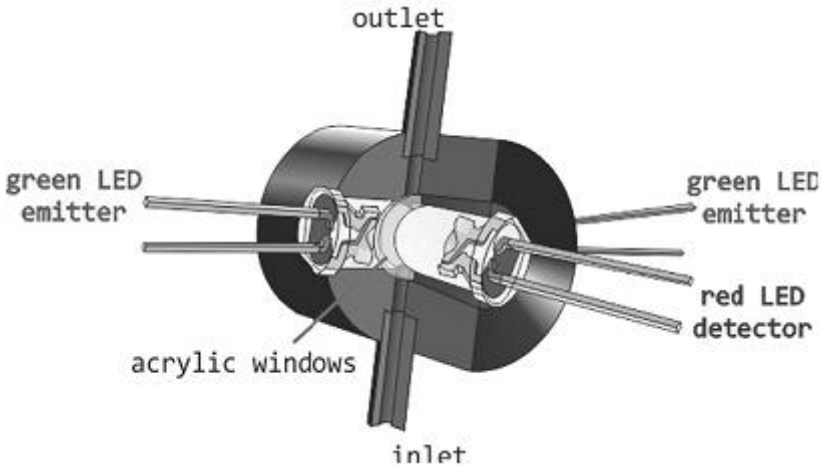


*Fig. 5.2. Schematic illustration of the dedicated flow-through detector based upon FPEDD detection. The flow-cell is confined within the two acrylic windows.*

## 5.2.5. Analytical procedure

The automatic sequential extraction procedure using the SI manifold starts by drawing 100 µL of air into HC to avoid mixing of individual extractants with carrier and filling the free column volume with the first extractant. Then, 1100 µL of 1.0 mol/L $NH_4Cl$ were aspirated into the HC whereupon the flow was reversed and 1000 µL (first subfraction) were dispensed through the soil laden column. Using bidirectional flow the negative influence of flow back pressure is alleviated in the fractionation scheme

and allows faster extraction of orthophosphate. The extractant was aspirated back into the HC and then again dispensed through the column into the injection coil of the FI manifold in a backward–forward mode. All these operations were performed while the injection valve position was set to “load”. Afterward, the injection valve was activated to the “inject” position so as to introduce the first subfraction into the secondary FI system (described below). The subfraction was injected into a water carrier stream to maintain the same flow rate across the detector throughout. The main advantage of combining and synchronizing two flow manifolds in parallel is that on-line analysis of extracts is immediately performed without delay after dynamic extraction. This procedure was repeated several times until the orthophosphate signal was negligible or when the sum of the last 5 consecutive measures is below 10% of the overall extracted orthophosphate so as to obtain the full extraction profile of the first $NH_4Cl$ fraction. The FPEDD detector and FI tubes were then cleaned with ca. 4 mL denatured ethanol containing 0.1% (w/v) benzalkonium chloride to remove the adsorbed ion pair while the HC of the SI manifold was cleaned with double-distilled water (ca. 6 mL). A virtually identical dynamic extraction procedure was repeated for the second fraction (0.1 mol/L NaOH) for a given number of subfractions until no increase in phosphate leaching was detected. After cleaning the detection cell again, the analytical procedure was repeated with 0.5 mol/L HCl but this time using unidirectional flow, that is, the extractant is only pushed once through the column. All solutions of extractants were aspirated and dispensed at 1.5 mL/min.

In the FI manifold each leachate subfraction from the SI microcolumn extraction method merges in the first and second reaction coils (R1 and R2) with ammonium molybdate to generate the phosphomolybdic acid. In case of HCl-fractions, the dilution module is turned on (normally closed on the micro solenoid valve) so as to dilute the subfraction by ca. 3 times in the second reaction coil. The heteropolyacid then reaches the third reaction coil (R3) where the ion pair is formed with rhodamine B. The solution of the rhodamine B exhibits fluorescence and therefore the blank signal was taken as the baseline. As a result of ion pair generation the fluorescence was quenched and negative peak signals were recorded [182,186]. The flow rate of each FI channel was 3 mL/min, except of the dilution stream which was set to 9.4 mL/min.

In-line extraction and analysis of every single subfraction takes ca. 6 min for the $NH_4Cl$ and NaOH fractions and ca. 5 min for the HCl fraction. For calculation of bioaccessible phosphate pools external matrix matched calibration was used

## 5.3. Results and discussion

### 5.3.1. Fluorometric detection of orthophosphate

Before analysis of the agricultural soil and the SRM 2711 (Montana Soil) different

parameters affecting FPEDD detection were investigated in details. For low fluorophore concentrations, the fluorescence yield increases when the exciting intensity does, thus, the exciting LEDs were powered with 30 mA, that is, the maximal current recommended by the manufacturer.

Rhodamine B concentration was investigated so as to obtain the highest full FPEDD scale with appropriate sensitivity for detection of bioaccessible orthophosphate in soils. To this end, a phosphate standard concentration of 1 mg/L was analyzed with rhodamine B concentrations ranging from 20 to 200 mg/L. The highest sensitivity was obtained with a fluorophore concentration at the 70 mg/L level.

To prevent fouling of the flow system by sorption/precipitation of the ion-pair onto PTFE tubing, polyvinyl alcohol (PVA) was added to the fluorophore reagent in the concentration spanning from 0.01% to 0.05% (w/v) (higher concentration is not recommended [186] ). With a concentration of 0.05% (w/v) PVA the baseline drift was significantly refrained while improving simultaneously the analytical signal repeatability.

### 5.3.2. Analytical performance of the in-line dynamic leaching method with FPEDD detection

Different physical and analytical parameters of the hybrid flow system influencing orthophosphate leachability and the reliable analysis of leachates were thoroughly examined. The SI microcolum system was proven to endure flow rates of extractants up to 3.0 mL/min, yet significant backpressure was observed from 1.5 mL/min onwards. As a compromise between system reliability and length of subfraction analysis, the flow rate was fixed to 1.5 mL/min for the three extractants.

A bidirectional (forward–backward–forward) extraction mode was used for both the exchangeable and NaOH fractions for amelioration of extraction profile repeatability while hindering filter clogging by soil particles. Unidirectional flow was however selected instead for the HCl fraction as a consequence of the large pools of P associated to calcite, which are released in the first subfractions. Otherwise undue dilution will be needed for reliable FPEDD measurements.

Triplicate fractionation analysis of either 50 mg of SRM 2711 or the agricultural soil with repeatabilities in all instances ≤8.8% demonstrated that the test portion assayed was representative of the bulk soil medium.

The effect of the soil leachate matrix in the three extractants upon accurate FPEDD orthophosphate quantitation was investigated by off-line collection of subfractions and application of the method of the standard additions using two spikes. Deviations below 12% between the recovered and the expected value revealed the

inexistence of matrix interfering effects.

The potential interfering effect of silicate onto the FPEDD phosphate signal was ascertained by spike recoveries of a phosphate standard at the 1 mg/L level containing increasing concentrations of silicate in the last two extraction milieus (0.1 mol/L NaOH and 0.5 mol/L HCl), as silicate extraction by $NH_4Cl$ is expected to be negligible [176]. Silicate was tolerated up to 400 mg/L in 1.0 mol/L HCl with recoveries above 90%. Without masking agents the hybrid flow system however showed severe interfering effects from silicate in the NaOH medium at the same concentration level than that of orthophosphate. Addition of 0.25% (w/v) of oxalic acid to the molybdate derivatization reagent made the detection system immune to silicate at a Si/P ratio of 400 with recoveries above 87%.

The detection (LOD) and quantification (LOQ) limits of orthophosphate at the 3 and 10s blank level, respectively, using the FI automatic method with FPEDD detection were 0.02 and 0.07 mg P/L for $NH_4Cl$, 0.04 and 0.13 mg P/L for NaOH and 0.013 and 0.043 mg P/L for HCl, respectively. We have proven that the LOQ of the photometric PEDD counterpart using 650 nm red LEDs as emitter and detector, respectively, for determination of orthophosphate in water was 1.9 mg/L. The expected concentrations of bioaccessible orthophosphate in soils are lower than the LOQ thereby making the miniaturized photometric detection inappropriate for analysis of soil leachates.

Dynamic linear ranges (mg P/L) in the three extractant media were 0.019–0.32 mg/L for $NH_4Cl$ (R=0.9967); 0.042–0.32 mg/L and 0.32–1.63 mg/L for NaOH (R=0.9999 and 0.9958, respectively) and 0.045–2.0 mg/L and 2.0–10 mg/L for HCl (R=0.9949 and 0.9946, respectively).

### 5.3.3. Applicability of the SI/FI-FPEDD setup for in-line sequential extraction and determination of orthophosphate in soil leachates

A reference material (SRM 2711-Montana soil) and a real soil (agricultural soil) were analyzed in this work to assess the reliability of the hybrid flow setup. The in-line extractrograms (kinetic extraction profiles) in individual extractants are shown in figure 5.3 for the agricultural soil.

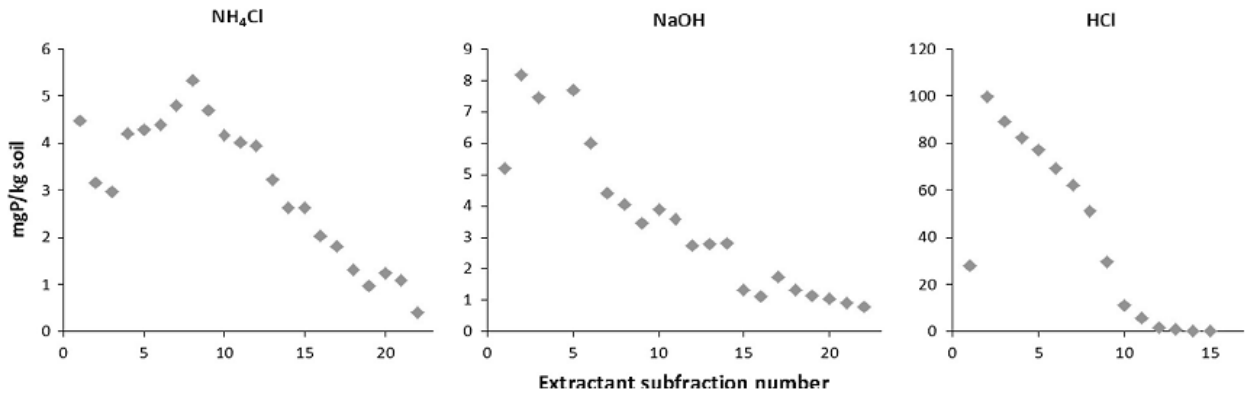


*Fig. 5.3. Profiles obtained for in-line extraction and fluorometric FPEDD detection of bioaccessible orthophosphate in the agricultural soil using the Hieltjes-Lijklema sequential extraction scheme. The subfraction volume is 1 mL.*

The magnitudes of bioaccessible orthophosphate pools in both samples determined by the SI/FI setup with on-line FPEDD detection are listed in table 5.1. The proposed hybrid system allows accurate measurements of inorganic phosphorus, mostly orthophosphate but fast hydrolyzing condensed inorganic phosphates, whenever available, while minimizing the undesirable hydrolysis of organic phosphorus forms because of immediate in-line analysis of the extracts. In the two first extractants the concentrations of bioaccessible orthophosphate are low (below the mg/L level in every subfraction) but the sensitivity of the fluorometric PEDD detector suffices for reliable measurements.

*Table 5.1. Statistical comparison between on-line/off-line detection of orthophosphate in leachates obtained from the SI-microcolumn setup using FPEDD and a reference method based on the molybdenum blue chemistry for the SRM 2711 reference material and an agricultural soil*

| | | *On-line FPEDD (mg P/kg)* | *Off-line FPEDD (mg P/kg)* | *Off-line molybdenum blue photometric method (mg P/kg)* |
|---|---|---|---|---|
| *SRM 2711 (Montana Soil)* | *$NH_4Cl$* | *45 ± 1* | *58 ± 6* | *69 ± 5* |
| | *NaOH* | *102 ± 18* | *68 ± 10* | *58 ± 5* |
| | *HCl* | *671 ± 60* | *581 ± 43* | *574 ± 86* |
| *Agricultural soil (Mallorca)* | *$NH_4Cl$* | *100 ± 24* | *153 ± 49* | *123 ± 65* |
| | *NaOH* | *115 ± 39* | *107 ± 21* | *107 ± 33* |
| | *HCl* | *668 ± 58* | *731 ± 59* | *817 ± 14* |

*Results are expressed as the mean ± standard deviation. Results of paired t-tests: p=0.901 (n=17) for on-line FPEDD against standard photometric method; p=0.946 (n=18) for off-line FPEDD against standard photometric method; p=0.917 (n=17) for on-line FPEDD against off-line FPEDD*

As shown in figure 5.3, the leaching kinetics of orthophosphate in the three extractant solutions are rather different in the agricultural soil. The labile orthophosphate (first fraction) is mostly leached within the first twelve subfractions and decayed in the ensuing sub-fractions. This is actually the most relevant inorganic phosphorus pool for plant uptake, and a sustained labile orthophosphate release is found in the agricultural soil assayed. Conversely, the leaching of the pools of phosphorus associated to hydrous oxides of Al and Fe using a more aggressive extractant (second fraction) takes place in a shorter time period. Similar profile is recorded for Ca-bound orthophosphate (third fraction) as a result of fast acid dissolution of Ca-laden mineralogical phases.

The SI/FI-FPEDD assembly merely detects bioaccessible orthophosphate but organic phosphorus species are also leached under alkaline and acidic extraction conditions [171,219,220]. In addition, organic phosphorus forms are hydrolyzed to inorganic phosphate in (microwave) digestion protocols aimed at measurement of the total phosphorus (or the residual phosphorus fraction after fractionation) in soils [176]. Hence, a mass balance validation usually employed in sequential extraction schemes as a QC tool [122,221,222] is here inapplicable for orthophosphate. Taking this into

account, a flow-through spectrophotometric method based on the molybdenum blue chemistry, reported elsewhere [176],was selected as a reference method using the SRM 2711 and the agriculture soil as model samples to investigate the reliability of the FPEDD detection system. To this end, leachates from the SI microcolumn extraction system were collected off-line and analyzed on a short notice (to circumvent the hydrolysis of organic phosphorus compounds) using both detection techniques. The results of the paired t-tests (see footnote in table 5.1) indicated no significant differences between both methods at the 0.05 significance level ($p>0.05$), thereby demonstrating the lack of biased results.

To investigate the potential hydrolysis of organic phosphorus in the SRM 2711 and the real soil in the different Hieltjes-Lijklema leaching media, the on-line leaching data obtained with the proposed FPEDD method were statistically compared against the results obtained by off-line FPEDD detection of 4 h-aged leachates. No statistically significant differences were found at the 0.05 significance level ($p>0.05$) between on-line FPEDD against offline FPEDD (see footnote in table 5.1) using a paired t-test. Therefore, there was no hydrolysable organic phosphorus detectable in the analyzed soils, at least after a reaction time of ca. 90 s, which equals to the residence time of each extractant volume in the SI microcolumn extraction system and the FI detection part. The pools of bioaccessible orthophosphate in SRM 2711 as obtained by the hybrid SI/FI microextraction setup using the Hieltjes-Lijklema scheme were compared against previous flow-through dynamic sequential extraction methods [175,176,216] (see table 5.2).

*Table 5.2. Bioaccessible phosphate in SRM 2711 using dynamic Hieltjes-Lijklema fractionation assays.*

| | *$NH_4Cl$ (mg P/kg)* | *NaOH (mg P/kg)* | *HCl (mg P/kg)* |
|---|---|---|---|
| *Stirred-flow cell extraction [175]* | *189 ± 6* | *77 ± 4* | *413 ± 6* |
| *SI-microcolumn extraction [216]* | *45 ± 5* | *93 ± 10* | *373 ± 18* |
| *Multisyringe-based microcolumn extraction [176]* | *7 ± 1* | *13.1 ± 0.4* | *324 ± 45* |
| *This work* | *45 ± 1* | *102 ± 18* | *671 ± 60* |

A good agreement is found in both $NH_4Cl$ and NaOH fractions for bioaccessible orthophosphate between the proposed SI/FI manifold and that of a previous SI-microcolumn extraction method [216]. Despite the fast FI detection, the residence time of the leachates in our SI manifold in the bi-directional extraction mode most

likely suffices for hydrolysis of some condensed inorganic phosphates (pyrophosphate and polyphosphates), even in mild leaching conditions [171]. This might explain the increased amount of most readily available orthophosphate (first step in the Hieltjes-Lijklema procedure) with regard to a multisyringe flow injection microcolumn extraction scheme reported earlier [176]. As compared to continuous-flow extraction chamber devices [175], flow-based microcolumn procedures (see table 5.2) afford decreased leachability of readily available orthophosphate because of the lack of mechanical agitation and the lower residence times of the extractant. With regard to the HCl fraction, our SI/FI hybrid assembly leaches significantly higher amounts of orthophosphate associated to calcite compared to previous flow-through microcolumn systems [176,216]. The main difference between our configuration and previous horizontal-type microcolumn arrangements [176,216] is the upright position of the column for up-flow extraction mode that fosters fluidized bed-like leaching with the consequent increase in leachability.

# 6. Automatic Kinetic Bioaccessibility Assay of Lead in Soil Environments Using Flow-through Microdialysis as a Front End to Electrothermal Atomic Absorption Spectrometry

## 6.1 Introduction

The impact of potentially hazardous trace elements in terrestrial environments cannot be evaluated reliably by measuring solely the total concentration of individual metal species, because the effect of anthropogenic compounds on ecological systems and biological organisms largely depends on their bioaccessibility and consequent bioavailability [6,14,221], that is, the fraction of contaminants which could be made available for biota uptake. Single and sequential extraction schemes are frequently used in bioaccessibility tests in which a certain amount of solid sample is subjected to the action of a given number of leaching reagents aimed at releasing particular metal-soil phase associations into the liquid phase under environmentally simulated conditions [223,224]. Though batchwise leaching methods are well accepted in environmental risk assessment scenarios, they are not free from drawbacks, for example, the lack of selectivity of the leaching reagents for nominal phases, and the reprecipitation and readsorption of previously released metals onto undissolved solid components or freshly exposed surfaces within the time frame of the extraction step, which in turn would lead to underestimating the content of bioaccessible contaminants associated with a nominal soil fraction [60,225,226].

The application of batchwise kinetic models [59,61,227] affords the discrimination of metal pools of different lability through the deconvolution of the extraction patterns and assists in overcoming phase overlapping of non-selective extractants (e.g., EDTA [63] ), and exploring potential metal readsorption phenomena. Two possible methodologies for batchwise kinetic extraction have been reported. In the first, leachate aliquots are collected from an individual sample at fixed time frames, but due to the invasiveness of the sampling method this approach tends to be inaccurate. The second one involves the exposure of various sample batches to a given

leaching reagent at different extraction times with the subsequent need of repetition of the classical steps for sample extraction and separation of the supernatant solution in each individual sample [61]. In this case, the results obtained are more reliable in terms of decreased uncertainty but the resulting protocol is very laborious and time-consuming [14].

Microsampling methods, in which small aliquots of the extraction medium are collected and analyzed with minimal impact on the extraction milieu and sample itself, provide an appealing solution to these shortcomings. Microfiltration is a very simple technique in which minute quantities of sample are drawn from the extraction medium across a membrane filter [109].

The main drawbacks of this sampling technique involve the potential membrane clogging by the fine particles of soil, in which case the system might actually not be able of enduring flow backpressure, and the need of further leachate cleanup in troublesome environmental samples.

Flow-through microdialysis [113,115], which emerges from the neurobiological field, is a microsampling method recently introduced in the environmental analytical area [228–232]. A semipermeable hydrophilic hollow fiber is used as a molecular sieve to separate compounds on the basis of molecular weight with the concentration gradient as a driving force. As opposed to microfiltration clogging effects usually are overcome because only ions and molecules below the molecular mass cut off of the membrane are freely diffusing across the membrane. As a consequence of its inherently molecular size discrimination features microdialysis is deemed most suitable as effective cleanup tool for probing intricate soil leachates [228–230]. Further, minimum disturbance of the natural equilibria at the sampling site is guaranteed because the uptake of target species is virtually negligible and the net sample volume remains unaltered, thus working under near-negligible depletion conditions [113,115,228].

Several microdialysis probe configurations have been reported in the literature including the so-called loop, linear, side-by-side and shunt-type arrangements [113]. The concentric probe, however, monopolized the applications as of yet as is commercially available, sturdy, and easy to assemble. On the other hand, commercial concentric microdialysis probes lack the flexibility required during the design and optimization of a new method and they are usually rather expensive and of disposable nature [113,115,228]. To tackle these shortcomings, novel flow-through linear/concentric configurations have been recently devised and optimized for expedient sampling of free metal species and low molecular weight organic acids [228–231,233]. The main asset of the linear-type probe configuration is that physical characteristics are tailor-made, that is, the effective transfer length and the capillary inner and outer diameters are to be selected as per the assay demands in order to

improve the microdialysis efficiency. As acceptable dialysis recoveries are merely obtained by perfusing the hollow fiber at low perfusate flow rates (usually at the low µL range per minute) minute dialysate volumes are thus collected in a time course analysis, which might in turn hamper accurate analysis. Electrothermal atomic absorption spectrometry (ETAAS) is usually the detection technique of choice for micro dialysates inasmuch as the graphite tube platform admits sample volumes ≤ 50 µL. The off-line detection mode relies on the consecutive collection of subfractions of metered dialysate volumes prior to ETAAS detection [112,232–234], but evaporation in the time frame between collection and measurement is a serious concern. To this end, an attempt of in-line coupling of microdialysis with ETAAS for investigation of metal mobility from soils in discrete microenvironments has been reported lately but was not applied to bioaccessibility assays [229]. The outlet of the continuously operating microdialysis system was connected via the autosampler arm to the atomizer at fixed time intervals but the dialysate volume injected into ETAAS could not be accurately measured.

In this work, the proof of concept of smart hyphenation of microdialysis sampling to ETAAS using a flow-programming based interface is herein presented for the first time. The aim behind is to mechanizing batchwise kinetic extractions following the recommended single extraction protocol of the SMT programme of the European Commission for evaluation of bioaccessible trace elements in soils without need of cumbersome manual and laborious protocols. Lead was selected in this work as a model analyte as is largely determined in routine analysis of potentially polluted soils. Different fractions of lead in soil environments, the so-called readily mobilizable and the slowly mobilizable species, are assessed from the kinetic data of the SMT bioaccessibility test via two first-order release model [60]. This model is aimed at estimating the actual time required for acetic acid extraction to reaching steady-state against the 16 h time frame preset by the standard SMT test, the effect of potential lead redistribution over time; as well as the overall bioaccessible lead under equilibrium conditions.

# 6.2. Experimental

## 6.2.1. Reagents, Samples, and Dialysis Membranes

All chemicals were of analytical reagent grade and employed without further purification. Milli-Q water (resistivity > 18 MΩ·cm; Millipore Synthesis A10, France) was used throughout for solution preparation. All glassware was soaked in 10 % (v/v) $HNO_3$ and rinsed with deionized water prior to use. A 0.43 mol/L acetic acid (AcOH) working solution used as perfusate and extractant as per the SMT recommendations [235] was prepared by dilution of glacial acetic acid. The perfusate ionic strength

matched that of the extracting reagent so as to prevent unbalanced osmotic pressure in the course of the dialysis-based mass transfer [223,228,236]. For the manufacture of probes, toluene and ethyl acetate were used without any further treatment. Investigation of the monomer ratio of the customized blended probes was performed by nuclear magnetic resonance (NMR) after probe dissolution in deuterated dimethyl sulphoxide (DMSO). Standard solutions of lead for ETAAS calibration were obtained by sequential dilution of a 1002 ± 5 mg/L commercially available stock solution. The matrix modifier for ETAAS measurements consisted of a solution of 20 g/L of $NH_4H_2PO_4$ and 1.2 g/L of $Mg(NO_3)_2$. Different types of commercially available capillary microdialysis membranes (see table 6.1) were assessed in this work for continuous monitoring of bioaccessible Pb. Prior to implementation in the flow-through assembly the dialysis membranes were soaked in Milli-Q water for about 10 min.

*Table 6.1. Physicochemical characteristics of microdialysis membranes (provided by manufacturers) for estimation of lead bioaccessibility in solid substrates*

| *Properties of the membrane* | *Type of membrane* | | |
|---|---|---|---|
| | *Fresenius SPS 400* | *Nephros Allegro H. F.* | *Gambro Polyflux 17L* |
| *Composition* | *Polysulphone* | *Regenerated cellulose* | *Blended polymer fiber (polyarylethersulfone, polyvinylpyrrolidone, polyamide blend)* |
| *Wall thickness (µm)* | *80* | *8* | *50* |
| *Inner diameter (µm)* | *500* | *200* | *215* |
| *MWCO (kDa)* | *5 (Average)* | *5 (Average)* | *30 ± 20* |
| *Supplier* | *Fresenius AG (St. Wendel, Germany)* | *Organon Teknika, (Boxtel, The Netherlands)* | *Gambro (Lund, Sweden)* |
| *Probe type* | *Concentric* | *Capillary-type* | *Capillary-type* |

## 6.2.2. Sampling and characterization of soil samples

Two surface soils from Mallorca, Spain, from different sources, that is, a forestry soil and a soil from scrapyards of discarded vehicles (coded soil 1 and soil 2, respectively) were selected to investigate the reliability of the proposed microdialysis-based flow assembly. A given amount (ca. 5 kg) of individual surface soils (from about

0-30 cm depth) was collected by grab sampling and stored in plastic containers. Prior to chemical analysis, soils were air-dried until constant weight and 2-mm sieved. Soils were characterized in terms of soil suspension pH, organic matter content and particle size distribution. Soil pH was determined in 0.01 mol/L $CaCl_2$ using a 5:1 (w:v) L/S ratio with gentle shaking for 5 min and then allowed to settle for 2 h as endorsed by the ISO 10390 [217]. After shaking the soil suspension again, pH is measured with a combined pH glass electrode. pH values of 7.42 ± 0.03 and 7.55 ± 0.01 were obtained for soil 1 and 2, respectively (figure 6.6). Assays were conducted in triplicate. pH was also monitored within the timeframe of the bioaccessibility test showing an increase from 2.45 to 4.51 and from 2.45 to 4.18 in 135 minutes and 45 minutes for soil 1 and 2, respectively. Organic matter was estimated by resorting to the loss-on ignition gravimetric method [237], involving the calcination of 10 g of dried soil sample at 440ºC overnight. The contents of organic matter were 6.80 ± 0.06 % and 5.46 ± 0.42 % for soil 1 and 2, respectively. Temperatures should not exceed 440 ºC to prevent the loss of inorganic carbon. Particle size distribution of the fraction <2 mm for determination of soil texture was performed with the aid of the Bouyoucos hydrometer method (ASTM type 152H) [218]. Soil 1 consisting of 61% coarse sand (0.2-2.0 mm), 31% fine sand (0.05-0.2 mm), 8% silt (2-50 µm), and non-detected clay (<2 µm) and soil 2 of 49% coarse sand, 10 % fine sand, 23% silt, and 19% clay, respectively, were classified as sand and sandy loam soils, respectively.

## 6.2.3. Microdialysis Probes

Two custom-made microdialysis probe-type designs including concentric [111] and capillary hollow fiber microdialyzers [223,228] made of polysulfone and regenerated cellulose or polysulfone blended, respectively, were investigated for in situ monitoring of bioaccessible Pb in soils (see table 6.1).

The concentric microdialysis probe is built of 5 cm long stainless steel capillary of 0.50 mm outer diameter (OD) and 0.40 mm inner diameter (ID) (G Kinnvall AB, Sweden) and contains a tunable 10 cm nonpolar fused silica inner cannula of 0.25 mm ID and 0.38 mm OD. The probe was fitted with a 3 cm long polysulphone capillary membrane of 0.5 mm ID with average MWCO of 5 kDa (Fresenius SPS 400). Cyanoacrylate instant glue was used to fix the membrane onto the stainless steel capillary tubing. The capillary microdialyzer probes of regenerated cellulose (Nephros Allegro H.F) were constructed using the experimental procedure described elsewhere [228]. Blended polymer membranes of 3, 4, or 5 cm effective dialysis length were cut from a single hollow-fiber of a bundle type artificial kidney (Gambro Polyflux 17L). Both ends of the capillary were housed in 5 mm long Tygon tubing (Ismatec, IDEX Health & Science, Glattbrugg, Switzerland) of 0.25 mm ID and 1.95 mm OD. For the sake of mounting the probe, the Tygon tubing was swollen by soaking it in ethyl acetate for 5 min prior to use. The capillary membrane gets extremely soft when ethyl acetate

enters into the lumen jeopardizing the assembling procedure. Hereto, the capillary was gently squeezed against filter paper before probe manufacture. After at least 30 min and to facilitate the connection with the liquid handling system, the ends of the small bore Tygon tubes were inserted into 5 mm long Tygon tubing of 1.52 mm ID and 3.22 mm OD furnished with 10 mm long PTFE tubing of 0.25 mm ID and 1.6 mm OD. The manufactured probes were allowed to air-dry completely for 24 h before incorporation in the flow manifold. Diagrammatic descriptions of both the concentric and linear type probes are available in figure 6.1.

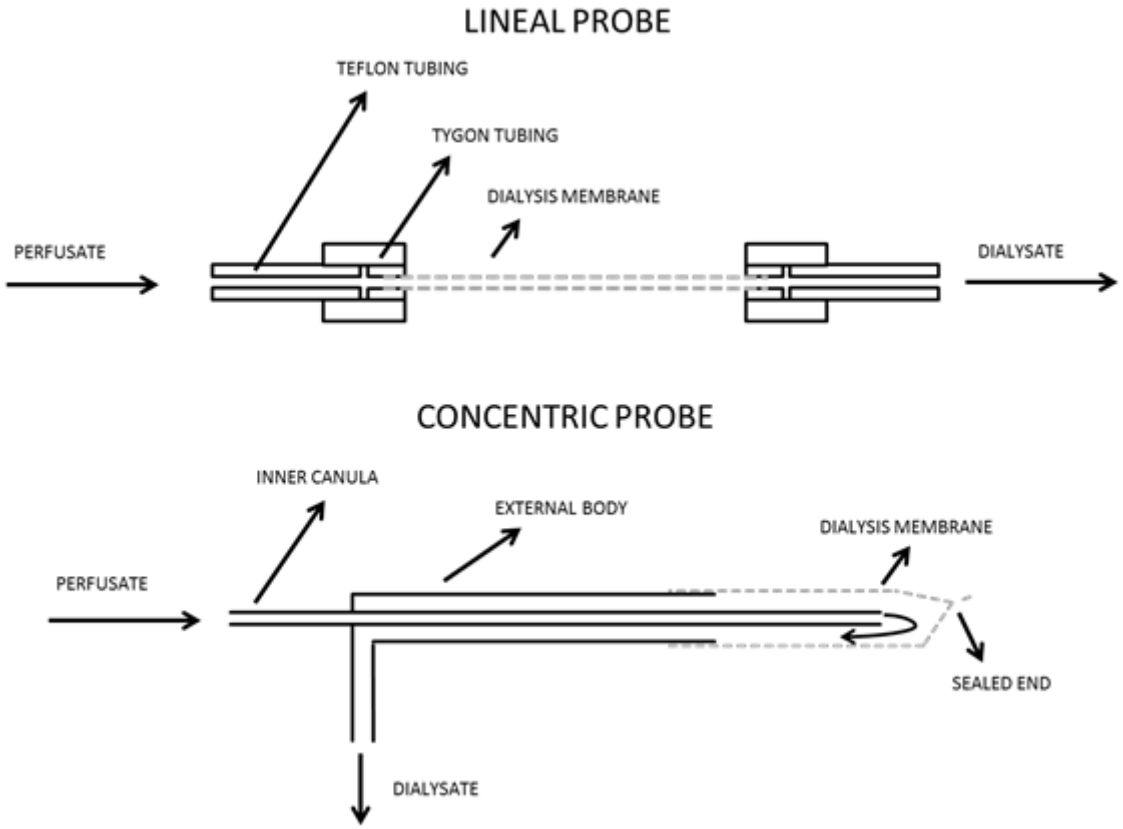


*Figure 6.1. Schematic illustration of operational modes in linear and concentric-type microdialysis probe configurations.*

## 6.2.4. Multivariate Analysis

A multivariate mapping through a Doehlert matrix scheme [238] was carried out so as to investigate the effect of perfusate flow rate ($Q_p$) and effective probe length ($L_{ef}$) upon microdialysis efficiency over the experimental domain ($Q_p$: 3−6 µL/min; $L_{ef}$: 3−5 cm). This design was chosen for minimizing the number of experiments needed for mapping as the neighboring domain might be easily explored adding minimum extra experimental points. Further, it offers different resolution degrees for the various variables [239]. In this work, $L_{ef}$ was studied at three levels, whereas $Q_p$ was studied at

five levels because of expected strong dependence of flow rate upon dialysis efficiency [228]. These experiments were carried out first using lead standards (200 µg/L in 0.43 mol/L AcOH) and later in a filtered leachate of forestry soil to evaluate potential matrix effects on the dialysis rate. Three sequential dialysate aliquots (120 µL each) were collected after probe equilibration for a preset time frame in the sample (usually 10 min), so as to stabilize the dialysis recoveries, from two microdialyzers inserted simultaneously in the probing medium. The Doehlert matrix variables and averaged relative recovery results are listed in table 6.2.

*Table 6.2. Uncoded variables and averaged relative microdialysis recoveries obtained by multivariate optimization using Doehlert matrix mapping.*

| $L_{ef}$, (cm) | $Q_p$, ( µL/min) | $L_{ef}/Q_p$ | RR (%) |
|---|---|---|---|
| 3 | 3 | 1 | 87.8 |
| 3 | 5 | 0.6 | 76.9 |
| 4 | 2 | 2 | 99.8 |
| 4 | 4 | 1 | 90.3 |
| 4 | 6 | 0.66 | 87.4 |
| 5 | 3 | 1.66 | 98.9 |
| 5 | 5 | 1 | 95.3 |

## 6.2.5. Instrumentation

The microdialysis module consisted of a CMA 102 microdialysis pump (DP, CMA/Microdialysis AB, Stockholm, Sweden) equipped with a 10 mL gastight syringe (Hamilton Gastight 1010) to which the capillary microdialysis probe is attached via a 30 cm long PTFE spacer tubing (0.25 mm ID). The outlet of the probe was connected to a 15 cm long PTFE tubing of 0.25 mm ID to deliver the dialysate toward the sampling cup of the flow setup (see figure 6.2).

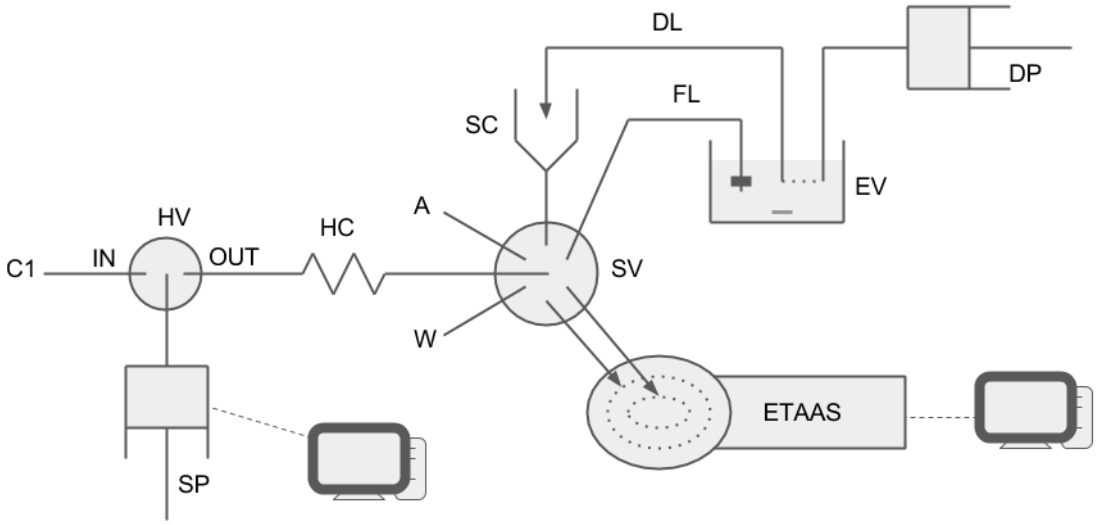


*Figure 6.2. Diagrammatic description of the microdialysis system capitalized on SIA for automatic monitoring of the kinetic batchwise extraction of Pb in soils using the SMT 0.43 mol/L AcOH single extraction protocol. SP: Syringe Pump, HV: Head Valve, C: Carrier, HC: Holding Coil, SV: Selection Valve, SC: Sampling Cup, DP: Dialysis Pump, A: Air, W: Waste, ETAAS: Electrothermal Atomic Absorption Spectrometer, DL: Delivery line, FL: Filtrate line, EV: Extraction Vessel.*

An SIA system based on programmable (bi-directional) flow is used in this work for automatic at-line hyphenation of continuous microdialysis sampling with discrete ETAAS detection. The SIA platform illustrated in figure 6.2 is composed of a Cavro XP 3000 bidirectional SP (Tecan group, Männedorf, Switzerland) furnished with a 5 mL-Cavro glass syringe and a 6 port IDEX V-1451-DC SV (Lake Forest, IL), and controlled by an early version of CocoSoft, written in Visual Basic 6 (Microsoft, Redmond, WA). All manifold tubing was built of 0.8 mm ID PTFE (VICI AG International, Schenkon, Switzerland) tubing. The sampling cup consisted of a 1 mL universal pipet tip connected to the selection valve (port 1) through a 10 mm long-Tygon tubing (Ismatec) and 5 mm long PTFE tubing. A nylon syringe filter (25 mm diameter, 0.45 µm pore diameter, Scharlab, Barcelona) for in-line microfiltration of the leachate was coupled to the SV (port 6) through a male luer lock–barbed fitting and 250 µm ID PTFE tubing, bearing a total dead volume of ca. 600µL. Port 5 was left open for air aspiration in the experimental procedure in order to separate sample (leachate) and carrier segments and port 3 served as a waste. Ports 2 and 4 were used to deliver the sampled leachate aliquots to the ETAAS autosampler using two 150 cm long PTFE tubes, mounted on a tailor-made autosampler lid, each one connecting a selection valve port with a different autosampler row (port 2 with the outer row and port 4 with the inner row). The homemade lid was shaped from a 5 mm PTFE sheet with the same pattern as the original ETAAS lid.

A PerkinElmer PinAAcle 900Z Spectrometer equipped with a transversely heated graphite tube with end-caps and integrated pyrolytically coated L'vov platform (PerkinElmer, part code B3000653) and a Lumina Coded Lead Lamp (part no. N3050157) was used as a detection system. The lamp operated at 10 mA with a 0.7 nm slit. Analytical readouts were taken at 283.3 nm. For sample introduction, the autosampler AS900 with a 148 position rack was used. The ETAAS and autosampler were controlled by the manufacturer's software (Winlab32 for AA). The manufacturer's recommended ETAAS temperature procedure was employed for lead assays unless otherwise stated using a combined matrix modifier (0.050 mg $NH_4H_2PO_4$ and 0.003 mg $Mg(NO_3)_2$). The ETAAS temperature program lasts about 6 min per two sample replicates. The analytical signals were processed in the peak area mode after Zeeman background correction.

The temperature and pH of the leachate were monitored in real-time every 5 s for 16 h using a Eutech PC 2700 multimeter (Eutech Instruments Europe B. V., Nijkerk, Netherlands), composed of a Hamilton "Polylite Lab" pH electrode (Hamilton Bonaduz AG, Bonaduz, Switzerland) and the manufacturer's temperature probe. It was controlled by a custom-made data logger, coded in Visual Basic 6.

## 6.2.6. Analytical Procedures

The analytical method started by turning on the microdialysis pump to deliver the perfusate (0.43 mol/L AcOH) at 3 µL/min through the lumen of the microdialysis probe, which was settled in a polypropylene extraction vessel containing 240 mL of extractant (0.43 mol/L AcOH) subjected to controlled mechanical agitation (500 rpm). This step was performed for stabilization of the diffusive mass transfer. The dialysate stream in this step was directed to waste. After 10 min, 6.0 g of dried soil were added to the extraction vessel and both the microdialysis flow-system and the ETAAS detector were triggered simultaneously.

The batchwise kinetic extraction method was monitored for 16 h to comply with the standard SMT test. The temporal resolution was 80 min/dialysate, excepting for the first hour for evaluation of the so-called easily mobilizable Pb fraction, whereby it was increased to 20 min/dialysate. To assess the reliability of time-course microdialysis sampling or as a quality control of the performance of the graphite tube analyses of in-line filtrates or lead standards were also performed. In this way, alternate filtrate/lead standards and dialysate samples were collected and analyzed in the course of the procedure as described below.

### 6.2.6.1. Microdialysis Procedure

During the first hour the microdialysis pump is programmed to dispense the perfusate solution for 20.0 min at 3 µL/min, so that a 60 µL plug of dialysate is

automatically brought to the sampling cup on the port 1 of the SV (see figure 6.2). Then the SIA setup is activated to dispense 180 µL of carrier (0.43 mol/L AcOH) to the sampling cup to facilitate the automatic handling of the otherwise minute quantity of sample. After that, the holding coil is filled with air and the total content of the sampling cup (diluted sample) is aspirated into the holding coil and dispensed through the delivery line to the ETAAS vial. This line was previously loaded with 760 µL of carrier for additional sample dilution. Therefore, the initial 60 µL-sample segment is diluted to a final volume of 1000 µL. The above analytical protocol is repeated three times to obtain the first three data of the leaching profile. After the first hour, collection/detection of microdialysates is undertaken every 80 min, so the entire procedure described above is repeated by collecting a microdialysate volume of 240 µL, without diluting the dialysate in the sampling cup.

### 6.2.6.2. Microfiltration QC Procedure

Before initialization of the microfiltration procedure 940 µL of diluent, that is, the carrier solution, is dispensed inside a vial of the ETAAS autosampler. Afterward, the syringe pump from the SIA manifold is set to draw 1.5 mL of the leachate through the microfilter inside the extraction vessel, from port 6 of the selection valve into the holding coil. After waiting 10 s to stabilize the pressure drop, 60 µL of the resulting microfiltrate are dispensed to the diluent containing ETAAS vial. The remaining microfiltrate plus a surplus of 60 µL of fresh extractant are returned to the extraction vessel, maintaining the volume unaltered throughout. The large volume aspirated through the microfilter ensures the analysis of a fresh microfiltrate plug without concerns about the filter dead volume. By pushing extractant back to the extraction vessel, clogging of the filter is also alleviated, thereby preventing the increase of flow backpressure over time. During the first hour the microfiltration QC protocol is repeated every 6 min and synchronized with the microdialysis sampling procedure in such a way that three microfiltrates are collected between each individual microdialysate.

### 6.2.6.3. Detection Protocol

Time synchronization between the automatic microdialysis system and ETAAS was employed in this work as the spectrometer hardware do not allow for relay triggered measurements. Taking into account that a single microdialysate/microfiltrate or standard measurements takes 6 min (3 min per replicate, two replicates) and that the standards/microfiltrates are analyzed every 40 min, the synchronization between the spectrometer program with the fluidic part is ensured using the “multimethod sequence” available in the ETAAS software. At the end of the detection of the two replicates the lamp is turned off and immediately after is set to stand by for 34 min in a warming step. Because of the higher sample frequency during the first hour, the

analyses of the microdialysates/filtrates are performed in a conventional mode without shutting down and subsequent preheating of the lamp.

All the methods described above were initially assayed with standards and soil extracts using on-line dilution with recoveries >95% in volume and lead amount. Is important to point out that the dilution ratio might be readily modified as per the assays needs so as to modify the temporal resolution of the sampling or analyze highly contaminated soils.

## 6.3. Results and discussion

### 6.3.1. Selection of the Microdialysis Membrane and the Probe Design

To prevent dilution of the microdialysate and omitting calibration of the sampling step, preliminary investigations were conducted aimed at selecting the probe design affording the greatest microdialysis efficiency. The microdialysis efficiency, also called relative recovery (RR), is defined as the ratio of the concentration of target species in the dialysate ($C_d$) to that in the external medium ($C_{ext}$) as follows:

$$RR = 100\frac{C_d}{C_{ext}}$$

The optimum recovery is 100%, that is, the analyte concentration in the dialysate matches that of the outer probe environment.

Two different geometries of microdialysis probes, namely, the linear-type hollow fiber and the concentric arrangements furnished with permselective membranes of variable physicochemical properties were tested for in situ sampling of lead in soil leachates. The concentric microdialysis probe was furnished with a polysulfone membrane with average MWCO of 5 kDa, while two distinct flow-through linear hollow fiber probes were constructed using a blended polysulphone capillary of MWCO of 30±20 kDa and with a cellulose regenerated membrane of average 5 kDa, respectively.

The configuration and microdialysis membrane type were selected on the basis of RR for lead in the batchwise kinetic extraction of soil 1 (see the experimental section) using 0.43 mol/L AcOH as extractant rather than using standard solutions. The L/S ratio was 40:1 as specified by the SMT test. In preliminary experiments the fiber length and perfusate flow rate were fixed in all instances to 30 mm and 2 µL/min, respectively. Six consecutive microdialysate fractions (1 h sampling each) were collected in a 6 h time-course extraction. The $C_{ext}$ of target element was determined by ETAAS using manual microfiltration. The microfiltrate was sampled right after the

collection of the microdialysate to evaluate the RR in every single fraction.

The $C_d$ of Pb in the cellulose regenerated linear-type dialysis probes was surprisingly higher than that of $C_{ext}$. This is most likely a consequence of the thick soil layer attached to the membrane outer shell, which leads to a higher concentration of Pb in the vicinity of the probe as compared to the bulk medium. Regenerated cellulose hollow fibers were thus deemed unsuitable for probing the target metal in soil extracts. Further, cellulose-type membranes are prone to fast degradation by microbial activity [230].

The polysulphone concentric microdialyzer and the blended polysulphone linear-type dialysis probe were proven to be less immune to soil particle adhesion, yet repeatability (19.8% vs 6.9%) was significantly improved using the linear-type configuration. Further, as the smaller inner volume of the linear probe in comparison to the concentric design assures low mass depletion and accurate measurements with minimal impact on the outer microenvironment, the blended polysulphone capillary microdialyzer (Gambro Polyflux 17L) was selected for the remainder of the studies.

The blended polysulfone microdialyzers were characterized in terms of morphology, pore size and chemical composition using scanning electron microscopy (SEM) with backscattered electron detection and energy dispersive X-ray spectroscopy. Regarding morphology, 1 cm-long membrane pieces of artificial kidney capillaries were gold sputtered and micrographed to study the inner surface, thickness and superficial pore dispersion. SEM micrographs revealed that the blended polysulfone fibers are composed of two different layers: an inner dialysis layer and an outer porous support layer (see figure 6.3) that ensures the stability of the capillary. The pores in the support layer are much larger than in the separation layer, up to 1000 nm (see figure 6.3. and 6.4). Figure 6.4 also shows the extremely high dispersion of pore size of the outer layer between two segments of different fibers. Clay particles in soils might be trapped in the outer porous layer and retain by electrostatic interactions free metal species that would be in turn excluded from dialysates. The higher the cationic exchange capacity of the soil the most likely is the influence of the external medium resistance to dialytic mass transfer

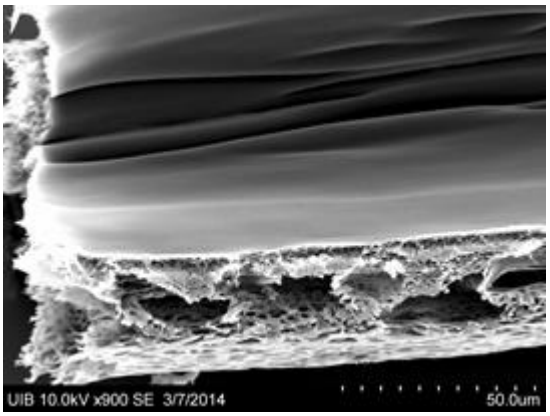


*Figure 6.3. SEM micrographs (x900 magnification) of polysulphone blended microdialysis membrane capillaries (Gambro Polyflux 17L) illustrating the two layer structure of the capillary: the outer porous support layer and the inner dialysis layer.*

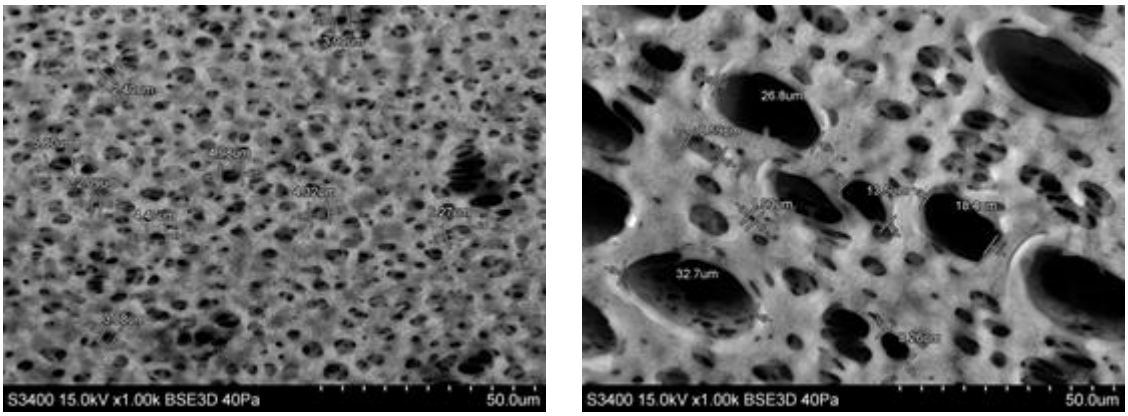


*Figure 6.4. SEM micrographs (x1k magnification) of polysulphone blended microdialysis membrane capillaries (Gambro Polyflux 17L) illustrating the different porosity of the outer layer of two different membrane pieces.*

Wet chemical analysis was also performed to elucidate potential chemical heterogeneity in dialysis layers when handling short pieces cut from the long artificial kidney capillaries. To this end, three 5 cm-long fiber capillaries (Gambro Polyflux 17L) were dissolved in deuterated DMSO and analyzed individually by NMR. The monomers (polyarylethersulfone, polyvinylpyrrolidone and blended polyamide) were in all instances in the same ratio. The composition of the short capillaries used in probe construction is thus proven to be virtually the same.

As the microdialysis mathematical framework has been already studied elsewhere [230,240] the experimental data obtained by Doehlert mapping were fitted to the equation relating RR with $Q_p$ and $L_{ef}$ (in mass transfer resistances to dialysis) as follows:

$$RR = 100 - \frac{100}{e^{\left(\frac{1}{Q_p(R_m+R_e+R_d)}\right)}}$$

Where the resistances of mass transfer through the dialysate ($R_d$), membrane ($R_m$) and external medium ($R_e$) into the microdialysis probe are given below:

$$R_D = \frac{K(r_o - r_o)}{\pi L_{ef} r_i D_d}; \qquad R_m = \frac{ln(r_o/r_i)}{2\pi L_{ef} \phi_m D_m}; \qquad R_e = \frac{1}{2\pi D_{ef}\sqrt{2L_{ef} r_o}}$$

Being $r_i$ and $r_o$ the inner and outer radius, respectively, K a constant, $\varphi_m$ the accessible volume fraction for analytes, $D_m$ the diffusive transport of analyte through the membrane, $D_d$ the diffusive transport through the dialysate fluid, and $D_{ef}$ the diffusive transport through the external medium.

The above fixed terms for a given linear-type probe are combined in merely two constants terms called A and B, so the RR might be expressed as:

$$RR = 100 - \frac{100}{e^{\left(\frac{1}{\frac{Q_p}{L_{ef}}\left(\frac{A}{\sqrt{L_{ef}}}+B\right)}\right)}}$$

The parameters A and B were obtained by minimization of the residual squares (Newton method) using experimental results shown in table 6.2, being 0.36 and 0, respectively. Since B is the term associated with $R_e$, we can conclude that the thickness of the diffusion layer in the outer microdialyzer shell is negligible as a result of efficient mechanically stirring conditions so the equation can be realigned to:

$$RR = 100\left(1 - e^{\left(\frac{-Lef}{AQ_p}\right)}\right)$$

Therefore, RR is merely influenced by the $L_{ef}/Q_p$ ratio. Taking this new parameter as the single significant factor, the multivariate Doehlert mapping was then revisited in univariate format at five different levels (see table 6.2). Figure 6.5 shows that RR of ca. 100% is afforded at $L_{ef}$(cm)/$Q_p$ (µL/min) of about 1 within the investigated experimental domain. Preliminary experiments were conducted by affixing the $L_{ef}$ and $Q_p$ to 5 cm and 4.5 µL/min, respectively, as a compromise between RR and dialysate sampling frequency. However, the increase of backpressure observed at this flow rate resulted in most cases in probe leaking, thus, $Q_p$ was decreased to 3 µL/min.

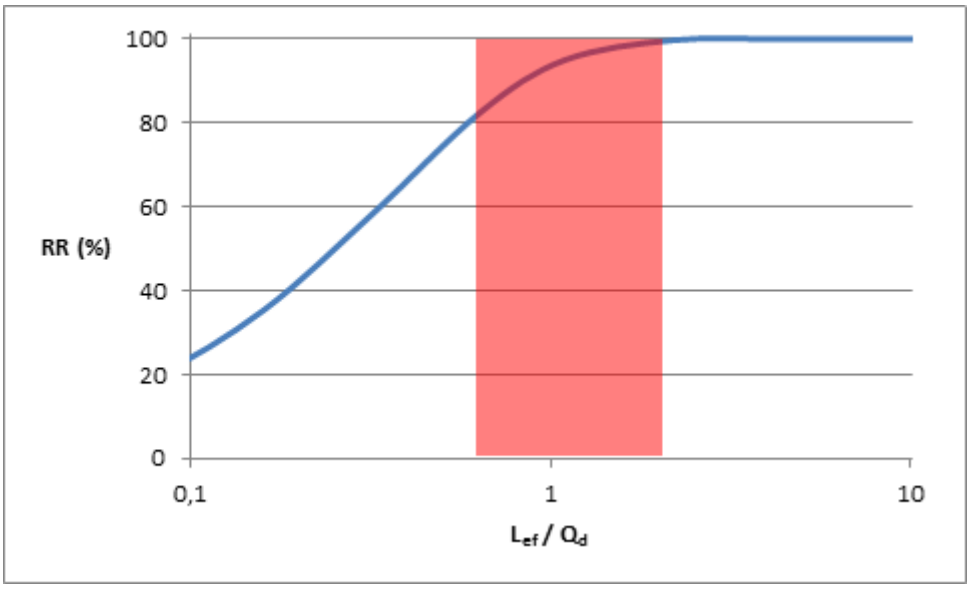


*Figure 6.5. Mathematical dependence of the microdialysis relative recovery (RR) versus the probe length to perfusate flow rate ratio ($L_{ef}/Q_p$). The shadowed zone denotes the experimental domain studied.*

## 6.3.2. Automatic Monitoring of Lead Bioaccessibility in Soils Using Microdialysis Sampling

The proposed SIA setup features the hyphenation of continuous microdialysis sampling with discontinuous ETAAS detection for analysis of the minute volumes of dialysates collected. Automatic filtrate collection and analysis, or injection of recalibration standards into ETAAS were used as QC tools. Even though the newly developed polysulfone-based capillary probes are proven to operate under steady-state dialytic regime analysis for lead assays, that is, RR∼100%, in standard solutions and filtered soil leachates, the presence of soil particles in the probed medium decreased RRs to an average of 0.58 and 0.89 for soil 1 and 2, respectively. The two RRs values however are significantly more elevated than those reported previously using other microdialysis probe designs for metal assays [232,241]. The probes were thus (re)calibrated in each individual sample using the average of two in-line filtrates, one after the first extraction hour and the other at the end of the experiment.

The release of lead from soil in 0.43 mol/L AcOH is deemed to follow first order reactions in which the metal is mostly released whenever the mineralogical phase to which is associated is dissolved [61]. Notwithstanding the fact that parallel reactions as redistribution or readsorption in newly generated surfaces are likely to occur, the extraction itself is supposed not to be disturbed by sampling of minute volumes of target species. In order to evaluate the effect of microdialysis sampling over the extraction process, the last experimental raw concentration of lead (sampling after 16 h extraction) was compared through a t-test to the same concentration after sampling correction, employing the following equation:

$$[Pb]_{sampling,t} = \frac{[Pb]_{exp,t}V + \sum_{i=1}^{t}[Pb]_{exp,i}V_{sample,i}}{V}$$

Where $[Pb]_{sampling,t}$ stands for the sampling corrected lead concentration at a time t, V the total volume of extraction medium, $[Pb]_{exp}$ the experimental lead concentration at a given time, V sample the volume of dialysate drawn at a given time. No significant differences were obtained between them at a 0.05 significance level (p = 0.52 >> 0.05) demonstrating the negligible depletion conditions in which microdialysis sampling does work.

The decrease in the volume of extraction milieu due to evaporation was also corrected. The equation for evaporation correction was based on Fick's law taking into account the decrease of the extractant level over time:

$$[Pb]_{evaporation,sampling,t} = \frac{m_0}{m_0 - z_0 S\rho + S\rho\sqrt{z_0^2 - \frac{2DP_t t}{\rho RT} ln\left(\frac{P_{Air2}}{P_{Air1}}\right)}}[Pb]_{sampling,t}$$

Where $m_0$ is the initial extractant mass, $z_0$ the initial level of extractant from the vessel top, S the section of the vessel, ρ the density of the extractant, D the diffusivity of the extractant in air, Pt the total pressure, R the ideal gas constant, T temperature in K, $P_{Air2}$ (air pressure at the vessel top, that is, away from the liquid interface), and $P_{Air1}$ (air pressure at the gas–liquid interface). All parameters were replaced except diffusivity, which was adjusted by the Newton method to the experimental final mass value.

After recovery, sampling and evaporation corrections, the extraction profile of lead (three replicates) in the soils as determined by automatic microdialysis sampling was adjusted to a double first order kinetic equation as follows:

$$C = A_1(1 - e^{-k_1 t}) + A_2(1 - e^{-k_2 t})$$

With C as the total bioaccessible lead measured at a time t, $A_1$ as the readily extractable (labile) lead pool, $A_2$ as the slowly extractable (moderately labile) lead pool with $k_1$ and $k_2$ as the kinetic constants associated with the previous pools.

The model parameters were obtained from the fitting of the experimental data to the previously described equation through a weighted minimum squares algorithm programed in MS Excel, and their respective standard deviations were calculated with a Monte Carlo method [242], programmed ad hoc in an MS Excel macro with Visual Basic for Applications (VBA). The hypotheses testing the significance of regression and the goodness of fit were accepted at the 0.05 significance level (see table 6.5). As there is no significant variance unexplained by the model, we could conclude that any of assayed soils undergo significant readsorption or redistribution processes for lead in the course of the 16-h extraction test as endorsed by SMT. In soil 1 the residual sum of

squares for the double first order kinetic model was virtually the same than that of the equation with the $A_2$ constant equal to zero. The model was thus reduced to a single first order kinetic equation based on the $A_1$ parameter, which is deemed the most relevant metal pool in ecotoxicological tests. This soil was sampled from a former hunting forest, wherein lead contamination most likely stems from bullets. Taking into account that the carbonate content of the soil is about 47% (see experimental section), the lead is associated with a great extent to the carbonate soil phase, which is readily released under the action of the SMT extractant. The pH rise observed in the course of the extraction process (see figure 6.6) demonstrates that the carbonate phase is dissolved within the first 2 h in which time frame 99.97% of bioaccessible lead (associated with carbonate) is released. The leaching profile of lead in the soil as determined by coupling in-line microdialysis with ETAAS is shown in figure 6.7 along with the mathematical model fitting.

*Table 6.5. Mathematical model for estimation of fast and slowly mobilizable lead in soils using 0.43 mol/L AcOH as extractant*

| *Soil* | *Forest (soil 1)* | *Industrial (soil 2)* |
|---|---|---|
| *$A_1$ (mg/kg soil)* | *10.9 ± 0.3* | *2.66 ± 0.05* |
| *$_{K1}$ ($min^{-1}$)* | *0.067 ± 0.008* | *0.18 ± 0.01* |
| *$A_2$ (mg/kg soil)* | *---* | *1.28 ± 0.08* |
| *$k_2$ ($min^{-1}$)* | *---* | *2.66E-3±1.9E-4* |
| *p Lack of Fit (>0.05)* | *0.25* | *0.39* |
| *Predicted bioaccessible lead (mg Pb/kg soil) (t=16 h)-Standard SMT* | *10.9* | *3.8* |
| *Bioaccessible lead at 16 h (mg Pb/kg soil) determined by microdialysis* | *11.5 ± 0.5* | *3.8 ± 0.5* |
| *Bioaccessible lead at 16 h (mg Pb/kg soil) determined by in-line filtration* | *11.5 ± 0.9* | *4.3 ± 0.5* |
| *p Significance of Regression (>0.05)* | *0.997* | *0.051* |
| *p Expected value (mg Pb/kg soil) vs microdialysis (mg Pb/kg soil) at 16h (>0.05)* | *0.06* | *0.89* |
| *p Expected value vs filtrate at 16h (>0.05)* | *0.136* | *0.095* |
| *Time for reaching 99% of bioaccessible Pb (min)* | *1 h, 9 min* | *21 h, 49 min* |

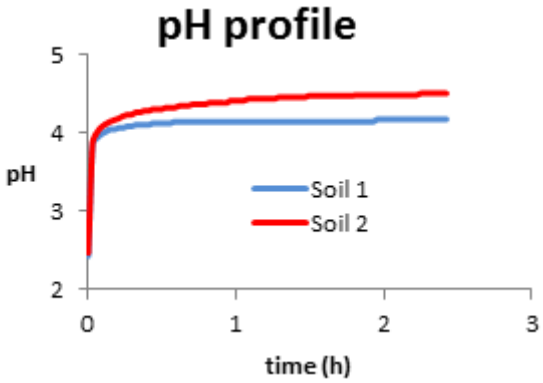


*Figure 6.6. pH profiles of the leachates of the two soils investigated in the course of the bioaccessibility test.*

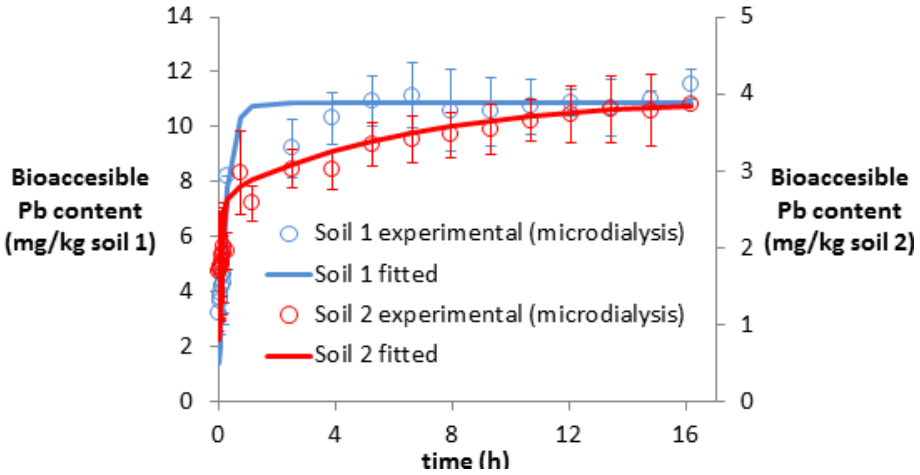


*Figure 6.7. Leaching profiles of bioaccessible lead in soils using the single extraction SMT standard test as determined by coupling microdialysis sampling to ETAAS. (Error bars are given as the standard deviation of 3 replicates).*

As for the soil 2, the two first order kinetic model was fitted to the microdialysis-based experimental data (see figure 6.7). The significance of the two kinetic leaching constants ($k_1$ and $k_2$) as determined by a lack-of-fit test ($p > 0.05$) indicates lead sorption to distinct mineralogical soil phases as a result of the long-term occurrence of the heavy metal in the soil, most likely originated from lead-acid batteries. The contribution of the rate constant associated with the moderately labile lead ($k_2$, see table 6.5) suggests the presence of metallic splinters in the assayed sample. Experimental results demonstrate that steady state extraction conditions as assumed in the standard method by mechanical agitation of a soil or solid material in 0.43 mol/L AcOH for 16 h are not assured whenever metal species are associated with slowly leachable fractions (e.g., soil 2) whereby the magnitude of overall bioaccessible pools (worst-case scenarios) is not accurately quantified. In fact, the extraction time should be increased up to 21.8 h for releasing up to 99% of bioaccessible lead (using 0.43

mol/L AcOH) in soil 2. On the other hand, steady-state conditions might be reached in about 69 min (e.g. soil 1) in those samples bearing solely readily extractable lead-soil phase associations. In contrast to conventional end-point leaching tests, our automatic kinetic leaching method allows for monitoring the leaching profiles at near-real time so as to get relevant insight on the leaching rates and the actual time frame for reaching the thermodynamic extraction equilibrium to support environmental risk assessment programs.

Trueness of the microdialysis sampling-based automatic bioaccessibility method for lead was ascertained by statistical comparison, via the Student's t test, of the microdialysate experimental data with that determined by in-line filtration after extraction for 16 h in compliance with the requirements of the SMT standard method yielding a filtrate concentration of 11.5 ± 0.9 mg/kg and a dialysate concentration of 11.5 ± 0.5 for soil 1, with an associated p-value of 0.997, and 4.3 ± 0.5 mg/kg for the filtrate and 3.8 ± 0.5 mg/kg for the dialysate in soil 2 with a $p = 0.051$. The concentration predicted by the first order reaction mathematical framework was also compared with that of filtration. The concentrations determined by the microdialysis method and the mathematical model were proven not to be significantly different to that obtained by in-line filtration at a significance level of 0.05 (see table 6.5), thus denoting the reliability of the proposed SIA method and of the first order kinetic equation.

Investigation of the relationship between dialysable and bioaccessible lead species in the extraction milieu (0.43 mol/L ACOH) was effected by splitting the in-line filtered leachate samples (collected at 16 h) into two aliquots. The two aliquots were subjected to microdialysis sampling, yet one was prior acidified to pH 1.3 to release potential associations of lead to dissolved organic matter. No significant differences at the 0.05 significance level were found in any of the assayed samples for both soils which allow us to conclude that the bioaccessible lead fractions in the acid extraction milieu are to be estimated accurately by microdialysis sampling.

# 7. Assessing oral bioaccessibility of trace elements in soils under worst-case scenarios by automated in-line dynamic extraction as a front end to inductively coupled plasma atomic emission spectrometry

## 7.1. Introduction

Anthropogenic activities, such as industrial emissions, mining or smelting, increase the levels of trace elements (TE) in terrestrial environments, which may pose severe health hazards to humans. Soil ingestion is deemed a potential route of exposure to soilborne contaminants especially to children. In fact, accidental ingestion via hand-to-mouth behavior results in the uptake of on average 50–200 mg soil per day, while 60 g per day are estimated for children deliberately ingesting soil [243].

It is well recognized that the impact of soil contamination by TE on human health cannot appropriately be assessed by measuring only the total concentration of individual metals [244,245]. Hereto, TE bioavailability, that is, the fraction of the total amount of TE ingested that reaches the systemic circulation is studied in human health-risk assessment scenarios. The concept of bioavailability encompasses bioaccessibility – defined as the fraction of target species that is mobilized from the solid matrix in the human gastrointestinal tract – besides the fraction of species permeated across a physiological membrane (e.g., intestinal epithelium) and that metabolized in the liver [246].

Taking into account that current EU programs promote *in-vitro* assays rather than *in-vivo* animal testing [17], several in-vitro oral bioaccessibility tests aimed at simulating the enzymatic actions in the mouth, stomach and intestines have been reported [54,247–249]. In vitro testing frequently is restricted to bioaccessibility measurements on the assumption that absorption across physiological membranes is not rate limiting [14,246].

The unified bioaccessibility method (UBM) [250] from BARGE (Bioaccessibility Research Group in Europe [251] ) is a validated method [15] for evaluation of the oral

bioaccessibility of TE in soils. The human gastrointestinal tract in the UBM is simulated through two different compartments (stomach and small intestine) applying the physiological temperature of 37º C, and using synthetic digestive fluids with biochemical composition similar to human saliva, gastric fluid, duodenal fluid and bile. BARGE suggests however that the "stomach" compartment alone is a good analogue of maximum in-vivo TE bioaccessibility [15].

The International Organization for Standardization (ISO) [246] also recommends that any test method used for measuring the bioaccessibility of soil contaminants should enable quantification of TE dissolution under "realistic worst-case conditions", that is, mimicking the highest TE leachability that can be expected [246,252]. On the other hand, the UBM method recommends equilibrium based batch wise tests for the stomach and the intestinal phases, which cannot reliably simulate the increase in TE leachability by fast absorption of mobilized metals [221].

To simulate the equilibrium displacement to the liquid phase in extraction procedures (e.g., because of permeation of bioaccessible TE across membranes) several teams of researchers have over the past few years dedicated a vast amount of effort to propose appealing alternatives based on dynamic (on-line continuous) extraction of TE in solid environments [226,253–257] that have been extended to oral bioaccessibility tests of food commodities by Beauchemin's team in Canada [257–261]. In contrast to steady-state methods, fresh portions of leaching agents are continuously provided in dynamic methods to solid samples that are contained in flow-through microcolumns or chambers. The dissolution equilibrium is thus driven to the right thereby affording insight into the maximum amount (worst-case extraction) of bioaccessible TE [14,225,226].

Entirely enclosed and (semi)automatic flow-based extraction methods also simplify the operational bioaccessibility tests, minimize accidental errors (e.g., sample contamination and analyte losses) and foster time-resolved (kinetic) data of the ongoing extraction. Further, TE readsorption phenomena onto remaining or freshly generated sorptive soil surfaces are circumvented [14,225,226]. Notwithstanding the attractive features of dynamic flow through extraction methods reported so far for oral bioaccessibility tests of TE they are merely applicable to highly homogeneous solid samples (e.g., reference materials) inasmuch as only sample amounts of 100–200 mg are admitted [258,259], in some instances in combination with high pressure pumps as liquid drivers, or with the wrapping of the solid material in quartz wool for alleviating back-pressure effects [260]. As a result of the minute amounts of sample loaded, sample representativeness of the test aliquot might be not entirely assured. Moreover, the above dynamic oral bioaccessibility tests [257–261] used overly simplistic extraction media with selected enzymes and salts as promulgated by the United States Pharmacopeia XXIII for simulation of gastrointestinal dissolution of pharmaceuticals

rather than those endorsed for leaching of inorganic and organic contaminants in soils, soil-like materials or foodstuffs [246,250].

In this work, a hybrid flow assembly for automation of the complex UBM-like method using different enzymes, inorganic salts and organic acids so as to mimicking physiologically-based extraction procedures accurately is herein presented for expeditious assessment of the gastric bioaccessible of TE (Cu, Zn, Pb, Ni, Cr) in real soil samples. The flow manifold capitalizing upon the hyphenation of a sequential injection manifold accommodating a stirred flow-cell reaction to inductively coupled plasma-optical emission spectrometry (ICP-OES) is devised for quantification of the oral bioaccessible TE in a conservative assessment while getting insight into the leaching kinetics as well. A novel at-line interface is proposed for handling of the leachates at will (e.g., allowing dilution in highly contaminated soils). To the best of our knowledge, this is the first time that the UBM-like gastric digestion protocol has been automated in a dynamic flow through extraction format for the assessment of oral bioaccessibility of TE in soils.

# 7.2. Experimental

## 7.2.1. Reagents and solutions

All reagents were of analytical grade and Milli-Q water (Millipore Synthesis A10, Millipore Corporation, Billerica, MA, USA) was used throughout. All glassware and polyethylene containers were previously soaked in 10% (v/v) $HNO_3$ and rinsed three times with deionized water.

The inorganic salts, the organic reagents and the distinct enzymes for the preparation of the synthetic saliva and the gastric biofluid were specified by BARGE [250]. The chemical composition of the saliva as per UBM guidelines is as follows: 896 mg/L KCl, 888 mg/L $NaH_2PO4$, 200 mg/L KSCN, 570 mg/L $Na_2SO_4$, 298 mg/L NaCl, 72 mg/L NaOH, 145 mg/L alpha amylase, 50 mg/L mucin, 15 mg/L uric acid with a final pH 6.5 ± 0.5. The chemical composition of the gastric juice is as follows: 824 mg/L KCl, 266 mg/L $NaH_2PO_4$, 2752 mg/L NaCl, 400 mg/L CaCl2, 306 mg/L $NH_4Cl$, 3.6 g/L HCl, 85 mg/L urea, 650 mg/L glucose, 20 mg/L glucuronic acid, 330 mg/L glucosamine hydrochloride, 3000 mg/L mucin, 1000 mg/L pepsin, 1000 mg/L bovine serum albumin with a final pH of 1.1 ± 0.1. Full experimental details in reagent preparation have been reported elsewhere [250].

A multielement standard solution for inductively coupled plasma spectrometry (Standard solution-5, Fluka, Sigma–Aldrich, Saint Louis, USA) was employed for external calibration. Diluted working solutions were prepared daily in 2% $HNO_3$(v/v).

A combination of acids involving nitric acid (69%, Sigma– Aldrich) and hydrochloric acid (37%, Scharlab, Barcelona, Spain) was used for microwave digestion of soils and extraction residues.

## 7.2.2. Soil samples, sampling and soil characterization

Surface layers of forest and ornamental soils (coded soil 1 and soil 2, respectively) from Bellver Castle (Palma de Mallorca, Illes Balears, Spain) and Santa Ponça (Calvià, Illes Balears, Spain) with the geographic coordinates 39º33'50.6"N2º37'4.4"E and 39º30'37.9"N2º27'57.5"E, respectively, were selected to investigate the reliability of the proposed in-line oral bioaccessibility procedure.

A given amount (ca. 5 kg) of individual surface soils (from about 0–30 cm deep) was collected by grab sampling and stored in plastic containers. Prior to chemical analysis, soils were oven-dried at 105ºC until constant weight and 2 mm sieved. Before analysis using digestive fluids, the soils were sieved to 250 mm as endorsed by the UBM method [250] because this is the upper limit of particle size for adhering to fingers and becoming available for accidental ingestion during hand-to-mouth activity.

Soils were characterized in terms of soil suspension pH, organic matter content, inorganic carbon content and particle size distribution. Soil pH was determined in 0.01 mol/L $CaCl_2$ in a 5:1 L/S ratio after shaking for 5 min, whereupon the suspension was allowed to settle for 2 h, with further shaking prior to measurement as endorsed by ISO 10390, using a combined pH electrode (Eutech Instruments, Nijkerk, Netherlands) [217]. The pH values of 7.42±0.03 and 7.05±0.02 were obtained for soils 1 and 2, respectively, for experiments performed in triplicate. Organic matter contents of 6.80 ± 0.06 and 4.7 ± 0.3% for soils 1 and 2, respectively, were estimated by resorting to the loss-on ignition gravimetric method [237], wherein 10 g of dried soil sample was mineralized at 440ºC overnight. Temperatures should not exceed 440ºC to prevent the destruction of any inorganic carbonates. The inorganic carbon content, determined using a volumetric method based on the dissolution of carbonates with a 10% (v/v) HCl solution and measurement of the volume of carbon dioxide released [262], was 468 ± 4 and 448 ± 19 g/kg, for soils 1 and 2, respectively. Measurement of particle size distribution of the fraction < 2 mm for determination of soil texture was performed with the aid of the Bouyoucos hydrometer method (ASTM type 152H) [218]. Soil 1 was composed of 61% coarse sand (0.2 – 2.0 mm), 31% fine sand (0.05 – 0.2 mm), 8% silt (2 – 50 mm), and non-detected clay (< 2 mm), whilst soil 2 was composed of 34% coarse sand, 22% fine sand and 44% silt. Therefore, soils 1 and 2 were classified as sand and sandy loam soil, respectively.

## 7.2.3. Analytical instrumentation

The automated flow system for assessment of oral bioaccessibility of TE in soils is schematically illustrated in figure 7.1. It comprises a 3000-step bidirectional SP (Cavro XP3000, Tecan group, Männedorf, Switzerland) for automatic handling of the biomimetic leaching reagents and delivery of well-controlled volumes to the solid sample as contained in a stirred chamber. An eight-port SV (Crison Instruments, Barcelona, Spain) was used for the selection of appropriate digestive extractants. For quantitative injection of a metered digestive juice volume into the detection system, a six port rotary IV integrated in selection single valve module, was furnished with a 500 µL injection loop. The SV and the IV were connected via a 100 µL transfer line (0.8 mm ID PTFE).

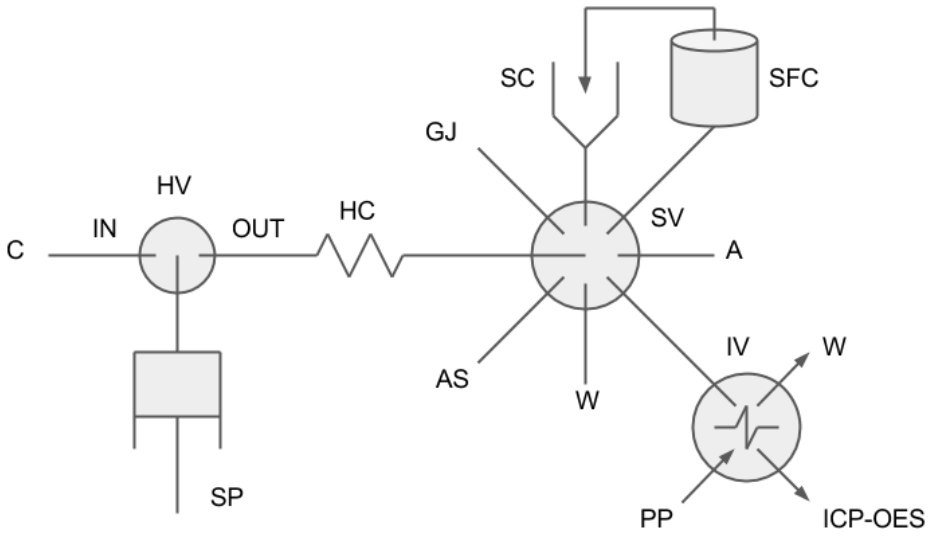


*Figure 7.1. Diagrammatic description of the hybrid flow setup hyphenated to ICP-OES for automated bioaccessibility tests of trace elements in soils using biomimetic fluids based on unified BARGE method (UBM). SP: Syringe pump; HV: Valve on head of the syringe; SV: selection valve; IV: injection valve; HC: holding coil; W: waste; C: carrier ($H_2O$); ICP-OES: inductively coupled plasma-optical emission spectrometer; SFC: Stirred flow cell; AS: Autosampler; GJ: Gastric Juice; W: Waste; A: Air*

The automatic SP was furnished with a 5 mL syringe (Hamilton, Switzerland) and a three-way valve at its head, which allowed connection with either the manifold or the carrier (water) reservoir. The central port of the V2 was connected to SP via a holding coil (HC), which consisted of a 3.0 m-long PTFE tubing (1.5 mm ID), with an approximate internal volume of 5.3 mL. The outlets of V2 were connected to the digestive extractant reservoirs, soil container, extract cup consisting of a 5 mL polypropylene pipette tip, or waste through PTFE tubing (1.5 mm ID) using PEEK fittings.

The flow-through chamber for containing the soil was constructed as described elsewhere [222,253] from borosilicate glass to have a capacity of ca. 15 mL (see figure 7.1). A rubber gasket was placed on top of the chamber followed by a nylon filter (GE Osmonics Labstore, MN, USA) of 0.45 mm pore size and 47 mm diameter to allow dissolved matter to flow through but retain soil particles. The setup was completed with a second rubber gasket and the cover on top of the flow chamber. The inlet of the chamber was connected to SV, while the outlet to the extract cup (see figure 7.1) using small pieces of Tygon tube and PTFE tubing of 1.5 mm ID A weighed soil sample (400, 600, or 800 mg) was transferred to the flow chamber together with a small magnetic bar (1 cm long), and the overall components of the container were securely clamped. A heating and magnetic stirring device (actuated at 480 rpm to ensure a homogeneous soil dispersion) coupled to a digital thermoregulator (VELP Scientifica, Usmate Velate Monza e della Brianza, Italia) was employed for the control and the stabilization of the temperature of the digestive biofluids in the extraction device, placed in a water bath, within the range of 27 – 37ºC for optimization studies.

All the programmable flow sequences were executed by a personal computer running an early version of CocoSoft software written in Visual Basic 6.0 (Microsoft, Redmond, WA, USA). The software permits through an RS232 interface the control of SP motion and speed, the selection of distinct ports at the SV and IV as well as the relay activation of the detection instrument (ICP-OES) via the digital output of the SP.

The digestive juice containing leachates (bioaccessible TE), the residual (non-bioaccessible TE) soil fraction and the original soil samples (total TE content) were analyzed using an inductively coupled plasma-optical emission spectrometer (ICP-OES, PerkinElmer Optima 5300 DV) furnished with a cross-flow pneumatic nebulizer. The operating conditions for ICP-OES detection were 1300W of RF generator at 40 MHz, flow rates of nebulizer, coolant and auxiliary gases of 0.5, 15 and 1 L/min, carrier ($HNO_3$ 2%) flow rate was 1 mL/min, and times of reading, rinsing, flushing and sample uptaking were 1, 60, 0 and 0 s respectively. The measurements were taken axially at following wavelengths (nm) and sensitivities given as the slope of regression lines obtained by plotting the peak area of standards readouts in a continuous flow mode at 1 Hz for a 0.5-mL injection loop against standard concentration for each metal: Cr: 267.716, 2669. Cu: 324.752, 4129. Ni: 231.604, 990. Pb: 220.353, 202 and Zn: 213.857, 2913. The instrument readouts were recorded in a continuous mode at 1Hz for the measurement of the overall leachate/standard content of the injection loop. The area of the transient peak in each leachate subfraction was used for plotting the oral bioaccessibility leaching profile or cumulative extraction profile for the suite of analyzed TE.

## 7.2.4. Analytical procedure

The stirred-flow chamber was initially loaded with a given amount of weighed soil sample (400, 600 or alternatively 800 mg in optimization studies). The peristaltic pump of the ICP-OES instrument is activated providing the spectrometer with a constant flow of 2% $HNO_3$ (v/v) throughout via the IV turned to the load position.

The automatic analytical procedure for on-line oral bioaccessibility measurements starts with the aspiration of 100 mL of air (port 6 of the SV) into the HC so as to prevent dispersion of a given biomimetic extractant reagent into the carrier solution. In worst case scenarios, 4900 mL of the simulated gastric biofluid is aspirated (from port 8 in figure 7.1) into the HC at 10 mL/min. Thereafter, the flow is reversed and the extractant plug perfused the soil sample contained in the stirred chamber at a fixed flow rate (0.5, 1 or 1.5 mL/min in optimization studies) while retaining the air segment within the HC. The gastric leachate (after filling up of the chamber and connecting tubes) is collected into the extractant cup nested to port 1 of the SV. The extractant cup allows the collection of the gastric leachate without the introduction into the flow setup of nuisance $CO_2$ bubbles generated at the low pH of the gastric biofluid in the course of soil extraction because of the carbonaceous nature of the two analyzed soils. For physicochemical homogenization of the content of the cup, a 2.5 mL air zone was pumped up-flow into the extract volume at 5 mL/min. The extract cup is next emptied by aspiration of the overall content (leachate plus a 100 µL air) into HC. The SP is then activated to dispense a 2 mL-leachate volume toward the IV so as to fill the injection loop. The ICP-OES is then triggered via the relay and the IV activated to the injection mode whereupon the transient readout is recorded. The ICP-OES detection is synchronized with the collection of the next leachate subfraction.

The above-mentioned automatic procedure was repeated fortyfold for the gastric-soluble fraction but we have proven that 30 subfractions suffice for exhaustive extraction of overall TE in the analyzed soils with sub estimation of worst-case bioaccessibility by 15% at most. The dynamic extraction method lasts 6.3 min per subfraction, thereby amounting to a total extraction and analysis time of ca. 189 min for 30 subfractions.

The non-dissolved soil was removed from the stirred flow cell as a soil water suspension and dried subsequently at 105ºC prior to further processing.

A ten-point external standard calibration (in 2% $HNO_3$ medium) was selected for determination of oral bioaccessible TE in real soils. Analysis of the UBM-like extraction fractions by ICP-OES was conducted without the need of matrix matched calibration because the application of a 3-level standard addition method to batch UBM extracts revealed comparable sensitivity (slope of the calibration graph) to that of external standard calibration.

To this end, a set of 10 multielemental standards (0, 5, 10, 20, 30, 40, 50, 100, 200 and 500 mg/L) were aspirated from an autosampler (AIM 3200, Aim Lab Automation Technologies, Brisbane, Australia) via port 3 of the SV (rather than port 1 for leachates) and processed likewise.

For evaluation of the three different extraction modes, off-line detection, that is, via automatic collection of the extraction subfractions in autosampler vials was performed. Further details of the analytical protocols using the distinct flow configurations (see figure 7.3) are given in the 7.3.2 section.

### 7.2.5. Dissolution of residues and determination of total concentration of metals

The original soil samples and solid residues leftover after extraction in the gastric phase were digested for quantification of total TE concentrations and immobilized TE under conservative extraction conditions, respectively, using a closed-vessel microwave digestion system (CEM MARS 5, CEM Corporation, Matthews, NC, USA). The pseudo digestion procedure employed is a modified version of EPA Method 3051 [263] for microwave-assisted aqua regia digestion of sediments, sludges, soils, and oils. In brief, weighed solid samples (0.30 g) or the overall remnant solid were digested using 2.5 mL of concentrated $HNO_3$ and 7.5 mL of concentrated HCl. The samples in the aqua regia extraction milieu were heated to 200ºC in 15 min and kept to this temperature for further 15 min. After cooling, the digests were filtered through 0.45 mm cellulose acetate filters (Whatman 40). The clear digests were diluted to 50 mL with Milli-Q water and stored in 50 mL polyethylene bottles prior to ICP-OES analysis.

## 7.3. Results and discussion

### 7.3.1. System configuration

Preliminary investigations using a large-bore cylindrical column extractor [117] were conducted on-line so as to analyze sample amounts > 200 mg that were not feasible in previous flow configurations [257–261]. As a result of the carbon dioxide bubbles generated in the reaction of soil inorganic carbon with the acid gastric juice, loading of 600 mg soil into the column reactor, resulted in the entrapping of excessive amount of gas that eventually led to the breakage of the filter membrane (Fluoropore TM, 25 mm diameter, 1.0 mm pore size, Millipore) because of increased flow back pressure.

On the contrary, the improved surface area of the filter membrane in the proposed chamber design (47 mm diameter) along with the use of a high precision syringe pump allowed the extraction of up to 800 mg soil with negligible pressure

drop. In line with a recent review article [226], the main asset of stirred flow chambers against prevailing microcolumn designs is the continuous mechanical agitation of the sample within the bulk of extractant that facilitates the release of gases out of the flow manifold and decreases the pressure inside the extraction container. On the other hand, the generation of nuisance bubbles in the course of the extraction in gastric biofluids detrimentally affects the performance of in-line/on-line extraction systems coupled to ICP-OES/MS detection. Hereto, at-line collection in an external sample/extract cup of the leachates that might be further processed at will is herein proposed. We would like to stress the fact that previous oral bioaccessibility systems with in-line/on-line atomic spectrometry detection [258–261] were merely applied to foodstuff, where no appreciable carbon dioxide is evolved as a consequence of the absence of carbonates in the sample matrix.

The synthetic digestive fluids recommended by BARGE are composed of large amounts of salts, organic compounds and digestive enzymes that give rise to suspended colloidal dispersions. The handling of the UBM surrogate biofluids in the flow network is thus troublesome because of the progressive clogging of the tubing and membrane filter by suspended matter. This most likely explains the fact that previously reported on-line continuous extraction systems for oral bioaccessibility assays of metals and metalloids resorted to overly simplistic milieus with scarcity of enzymes [257–261].

Preliminary investigations were conducted to investigate the solubility of every enzyme endorsed by UBM in saline solutions of saliva and gastric fluid surrogates. Turbid and viscous solutions were generated with mucin added to either media at the concentration levels detailed under the experimental section. In-vitro batchwise UBM tests were undertaken in the presence or absence of mucin for getting insight of the role of this enzyme in the extractability of TE from soil samples. In brief 0.6 g of soil was mixed with 9.0 mL of saliva and after shaking for 5 min, 13.5 mL of gastric juice were added. The resulting gastric digestion phase was maintained at 37ºC with agitation at 480 rpm. Experimental results for soil 1 are illustrated in figure 7.2. A good agreement is found for the overall TE between confidence intervals [264] of oral bioaccessible concentrations at the 95% level in biomimetic digestive fluids with mucin and those obtained in digestive juices excluding mucin. This is probably a consequence of the lack of digestive action by mucin acting as lubricant in the mouth and stomach. Digestive juices without mucin were thus selected for the ensuing studies inasmuch as the remaining organic and enzyme components were water soluble and no flow impedance effects were observed.

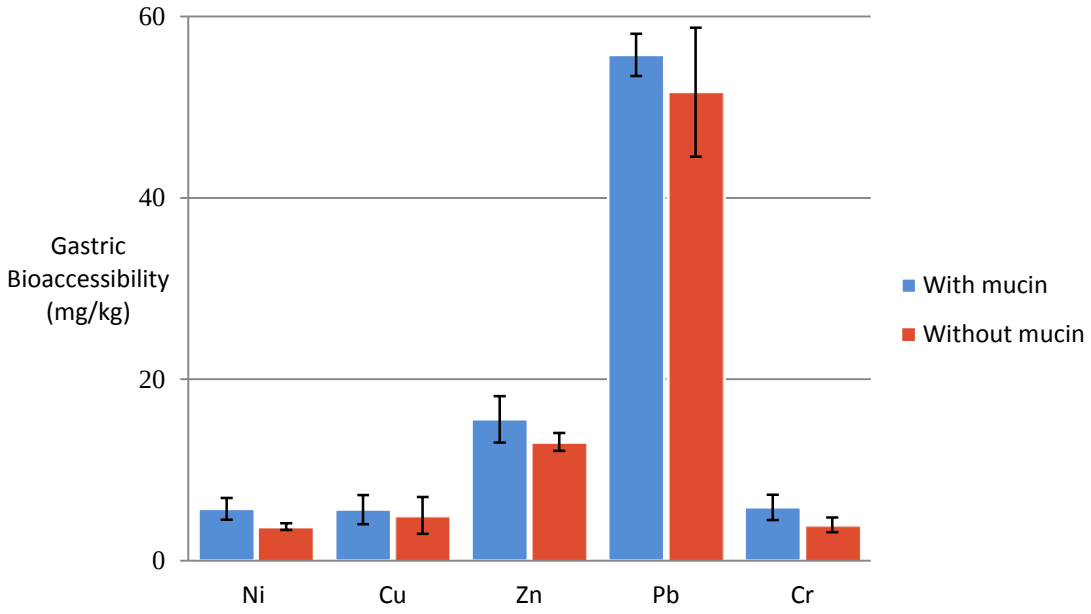


*Figure 7.2. Bioaccessible TE concentrations in the gastric phase in the presence or absence of mucin. Error bars represent confidence intervals at the 95% level (n = 3).*

## 7.3.2. Investigation of distinct in-line dynamic extraction modes

Surrogate digestive juices in the harmonized UBM are not mixed individually with the soil material as is the case with usual sequential extraction procedures for TE fractionation in soil [221], rather the gastric juice is added to the saliva plus soil composite without prior separation of the saliva extract [250]. To mimic UBM specifications, a novel flow-through additive extraction mode capitalizing upon biofluid recirculation was evaluated. In this approach, the saliva extract was collected in an external container and combined with a metered fresh gastric juice volume, whereupon the composite mixture is used as a new extractant and brought to the flow-through sample container (see figure 7.3). Several aliquots (4.9 mL each) of saliva extract were also automatically collected in an ancillary autosampler and further analyzed by ICP-OES. In contrast to the observations by Dufailly [257] from on-line bioaccessibility tests of metalloids (namely, arsenic), wherein the saliva surrogate alone was sufficient to release all of the bioaccessible pools, our results revealed that the concentration of bioaccessible TEs for the overall target metals was below the limit of detection of the instrument. These discrepancies should be attributed to the ionic nature of the arsenic species and their readiness for mobilization in solid substrates in mild extractants as compared with transition and heavy metals. To evaluate the effect of the leached soil matrix by saliva and the behavior of mobilized metals on further TE extractability at the acidic gastric pH, the recirculation mode was compared for soil 1 against two unidirectional operational extraction modes using gastric juice alone and a saliva–gastric biofluid composite at the 2:3 volume ratio so as to select the dynamic

method affording the greatest TE extractability (worst case scenarios) to cope with ISO/TS 17924:2007 requirements [246].

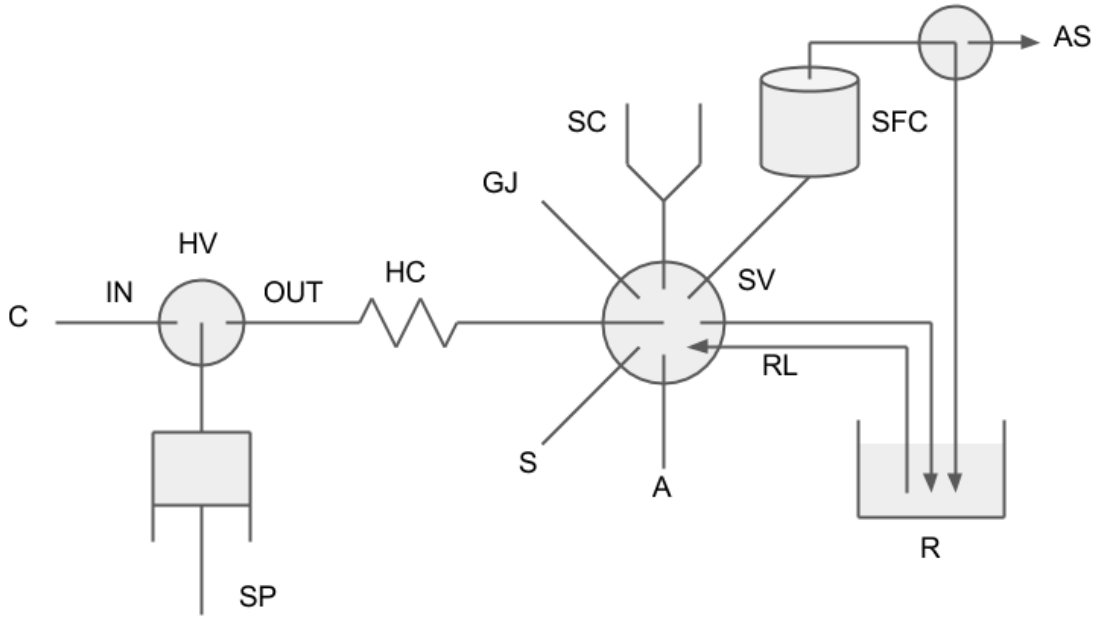


*Figure 7.3. Diagrammatic description of the hybrid flow setup hyphenated to ICP-OES for automated bioaccessibility tests of trace elements in soils using recirculation of the saliva + gastric leachates. SP: Syringe pump; HV: Valve on head of the syringe; SV: selection valve; HC: holding coil; W: waste; C1: carrier ($H_2O$); PP: peristaltic pump; SFC: Stirred flow cell; AS: Autosampler; GJ: Gastric Juice; A: Air; S: Saliva; R: Reservoir; RL: Recirculation line.*

The average cumulative concentration of bioaccessible TE in a given extractant at time t (C**,** mg/kg) (see figure 7.4) is proven to fit an exponential decreasing function (first-order reaction kinetic model) [59,61] in every configuration:

$$C = A(1 - e^{-kt})$$

Where A is the maximum leachable concentration of TE (mg/kg), that is, the actual worst-case conditions, and k the associated rate constant ($min^{-1}$). Only experimental data of subfractions in which the extract pH was ≤ 1.5 were taken for the model as this is the upper pH limit tolerance set by UBM.

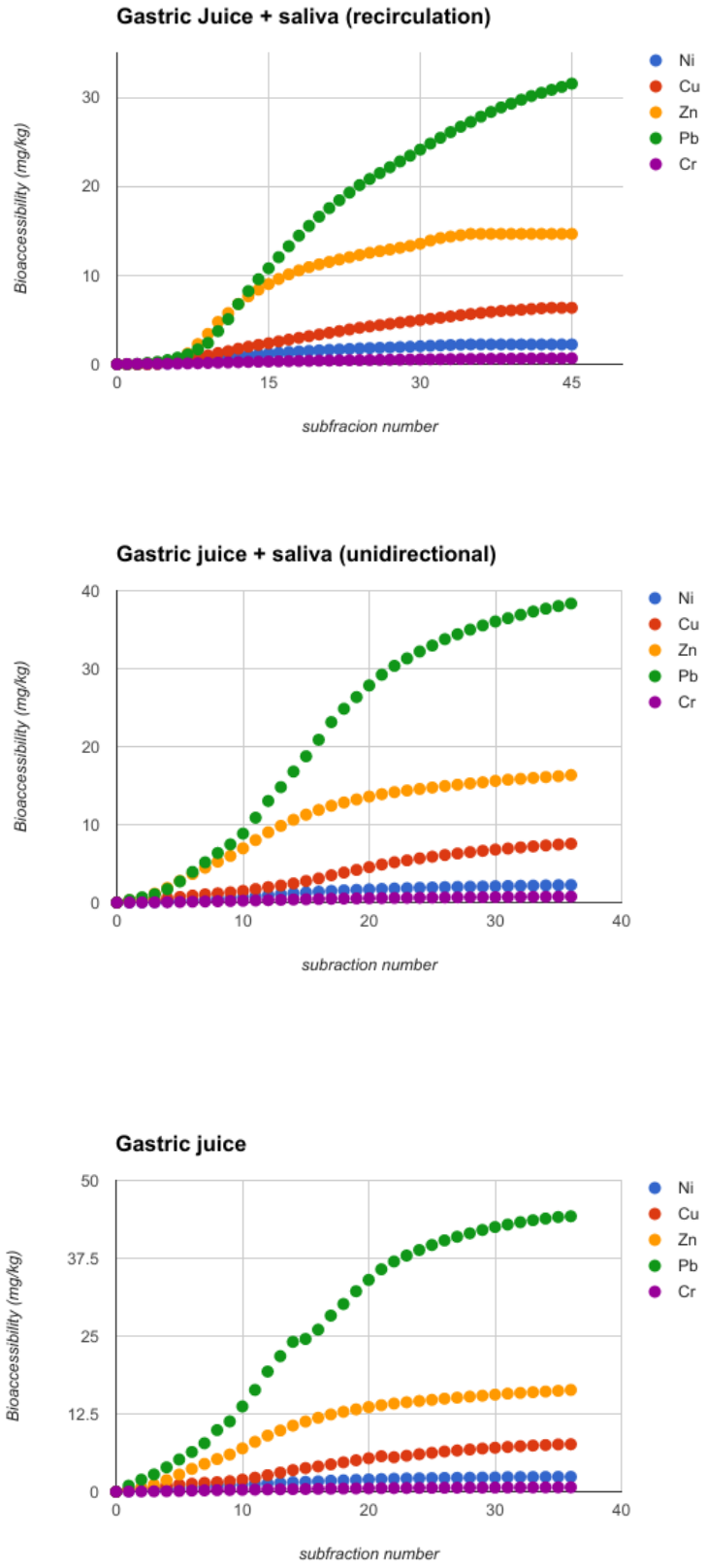


*Figure 7.4. Cumulative extraction profiles of Cu, Cr, Pb, Zn and Ni in saline biomimetic fluids using distinct dynamic operational extraction modes. Average subfraction time = 1.65 min.*

Table 7.1 lists the calculated model parameters for the distinct in-line operational extraction modes tested for Ni, Pb, Cu, Cr and Zn. In most instances (80% of investigated conditions), the lack of fit test revealed p ≥ 0.07 demonstrating that the mathematical model is appropriate for describing the analytical system regardless of the TE and extraction mode at the 0.05 significance level (see table 7.2).

*Table 7.1. Estimation of the maximum gastric leachable concentration (A), the associated rate constant (k) of TE in soil 1 using a first-order kinetic reaction model and $p_{LOF}$, the probability of lack of fit (> 0.05).*

| *Element* | *Parameter* | *Extraction mode* | | |
|---|---|---|---|---|
| | | *saliva + gastric juice (recirculation)* | *gastric juice alone* | *saliva + gastric juice (uni-directional)* |
| *Ni* | *A ( mg/kg)* | *4 ± 1* | *3.0 ± 0.3* | *3.0 ± 0.1* |
| | *k ($min^{-1}$)* | *0.04 ± 0.01* | *0.05 ± 0.01* | *0.06 ± 0.02* |
| | *$p_{LOF}$* | *0.83* | *1.00* | *1.00* |
| *Cu* | *A ( mg/kg)* | *12 ± 3* | *11 ± 2* | *13 ± 5* |
| | *k ($min^{-1}$)* | *0.022 ± 0.003* | *0.05 ± 0.02* | *0.04 ± 0.02* |
| | *$p_{LOF}$* | *1.00* | *0.94* | *2.5E-06* |
| *Zn* | *A ( mg/kg)* | *18 ± 3* | *17 ± 3* | *18 ± 2* |
| | *k ($min^{-1}$)* | *0.06 ± 0.01* | *0.09 ± 0.02* | *0.08 ± 0.01* |
| | *$p_{LOF}$* | *1.00* | *0.99* | *1.00* |
| *Pb* | *A ( mg/kg)* | *51 ± 8* | *55 ± 9* | *54 ± 12* |
| | *k ($min^{-1}$)* | *0.03 ± 0.01* | *0.05 ± 0.02* | *0.06 ± 0.02* |
| | *$p_{LOF}$* | *0.98* | *1.00* | *2.4E-05* |
| *Cr* | *A ( mg/kg)* | *1.0 ± 0.2* | *0.90 ± 0.08* | *1.1 ± 0.1* |
| | *k ($min^{-1}$)* | *0.03 ± 0.01* | *0.051 ± 0.005* | *0.04 ± 0.01* |
| | *$p_{LOF}$* | *1.00* | *2.5E-06* | *0.07* |

The one-way ANOVA test [264] revealed the inexistence of significant differences in the maximum leachable concentrations of Ni, Zn, Cr, Pb and Cu using gastric juice alone, the saliva–gastric composite or the recirculation mode at the 0.05 significance level ($F_{exp,Ni}$=1.96, $F_{exp,Cu}$=1.47, $F_{exp,Zn}$=1.59, $F_{exp,Pb}$=1.93, $F_{exp,Cr}$=1.34 against $F_{crit}$(0.05, 2, 6)=5.14). It should be borne in mind that the underlying principle of in-line dynamic leaching is the multistage extraction nature of the method affording exhaustive (non-equilibrium) TE leachability. As the gastric fluid accounts for the chemical aggressiveness of the digestive juices and the overall configurations/extractants

contained the gastric phase, worst-case leachable pools of Ni, Zn, Cr, Pb and Cu in soil 1 were statistically identical in the three extraction modes investigated. The length and extractant volume for reaching worst-case extraction conditions however greatly differ from the various procedural tests. The gastric juice alone in unidirectional mode allowed for determination of as much as half of the maximum amount of bioaccessible TE in average 14 fractions (70 mL), against 21 fractions (105 mL) and 27 (135 mL) for the saliva–gastric juice composite, at uni-directional and recirculation mode, respectively, as a consequence of the lower pH of undiluted gastric juice. For the sake of setup simplicity and test expediting, the gastric juice alone in unidirectional flow mode was selected as a single extractant for the remainder of the work.

### 7.3.3. Investigation of critical variables in dynamic oral bioaccessibility of TE in soils

Taking into account that one-at-a-time univariate optimization procedures do not necessarily ensure experimental conditions for worst-case extraction scenarios on a short notice in dynamic bioaccessibility tests [265], a two-level full factorial design with three replicates of the center point was undertaken for screening of critical variables.

A multivariate optimization procedure was undertaken for evaluating the effects of the sample weight, the extractant flow rate and the extraction temperature upon oral bioaccessibility of targeted metal species under dynamic extraction mode. The criterion was to maximize TE extractability in soils to mimic worst-case gastrointestinal extraction conditions. A two-level full factorial screening design was employed to detect the main factors that significantly influence the dynamic extraction process and discard the remainder from further studies (table 7.2). Three replicates of the center of the design (center point) were also included to ensure that the variability found is on account of the factor effect rather than the random error. Along with the main effects associated with individual factors, the 3 two-term interactions were calculated to explore the potential degree of twisting of the first-order planar model [265].

A lack-of-fit or curvature test [238] of the first-order model to evaluate the magnitude of predicted errors will elucidate whether or not second-order polynomial models should be selected. The statistical computer package StatGraphics Centurion XV (Statpoint Inc., Herndon, VA, USA, 2005) was used to build the two-level factorial design with 11 runs including center points ($2^3$+3). The solid sample weight, the extractant (gastric phase) flow rate and the extraction temperature were selected as the main factors.

The soil mass domain of 400–800 mg and the temperature spanning from 27ºC (room temperature) to 37ºC were taken as per UBM specifications [250,251], wherein 600 mg of soil is analyzed at 37ºC. The extraction flow rate was investigated within the range of 0.5–1.5 mL/min on the basis of preliminary experiments that revealed the absence of flow impedance under dynamic gastric extraction conditions. For handling multiple response data, a desirability function as the geometric mean of the cumulative bioaccessible pools of Ni, Zn, Pb, Cu and Cr in the gastric phase, [265,266] was calculated in each individual run (see table 7.2):

$$D = \sqrt[5]{d_{Ni} d_{Zn} d_{Pb} d_{Cu} d_{Cr}}$$

with $d_M$ calculated as:

$$d_M = \frac{R_{M,i} - R_{M,min}}{R_{M,max} - R_{M,min}}$$

where $R_i$ is the response (extractability) of run i for metal M and $R_{max}$ and $R_{min}$ the maximum and minimum extractability identified for metal M, respectively. The gastric phase extractability of the overall TE in each individual run is given in table 7.2. The desiderability function equals:

$$D = 0.40 - 0.16A - 0.11B + 0.03C + 0.01AB + 0.19AC - 0.03BC$$

*Table 7.2. Screening design for multivariate investigation of critical variables in oral bioaccessibility of metal species using gastric juice surrogate as extractant in a unidirectional flow extraction format. TE, trace elements; D, desirability function; U, uncoded values; C, coded values.*

| *Sample amount (mg)* | *Extractant flow rate (mL/min)* | *Extraction temperature (ºC)* | *TE oral bioaccessibility (mg/kg)* | | | | | *D* |
|---|---|---|---|---|---|---|---|---|
| | | | *Ni* | *Cu* | *Zn* | *Pb* | *Cr* | |
| *800* | *1.5* | *37* | *2.3* | *4.9* | *16.0* | *43.2* | *0.7* | *0.3* |
| *800* | *1.5* | *27* | *1.9* | *3.0* | *14.6* | *32.8* | *0.5* | *0.0* |
| *800* | *0.5* | *37* | *3.6* | *14.1* | *24.4* | *38.9* | *0.7* | *0.6* |
| *800* | *0.5* | *27* | *3.8* | *11.1* | *21.5* | *34.3* | *0.4* | *0.0* |
| *400* | *1.5* | *37* | *2.8* | *7.3* | *17.3* | *38.0* | *0.5* | *0.3* |
| *400* | *1.5* | *27* | *3.1* | *9.5* | *22.4* | *39.2* | *0.8* | *0.6* |
| *400* | *0.5* | *37* | *3.0* | *11.5* | *21.2* | *39.7* | *0.6* | *0.5* |
| *400* | *0.5* | *27* | *5.6* | *11.7* | *28.7* | *42.6* | *0.7* | *0.9* |
| *600* | *1* | *32* | *2.9* | *5.4* | *17.4* | *37.2* | *0.8* | *0.3* |
| *600* | *1* | *32* | *3.1* | *7.0* | *19.5* | *42.3* | *0.7* | *0.5* |
| *600* | *1* | *32* | *3.1* | *6.0* | *18.8* | *38.9* | *0.9* | *0.4* |

Assessment of the significance of main factors' influence and second-order interactions thereof on the analytical response was explored using an ANOVA test. The standardized factor effects are readily visualized using Pareto histograms (see figure 7.5), where the standardized effects of main factors and interactions are arranged in descending order and each bar length equates the value of a calculated Student's *t*. The cross vertical line indicates the *t*-critical value at a 0.05 significance level corresponding in our case to 4.30 for two degrees of freedom. The positive (light grey) or negative (white) bars denote those scenarios where TE gastric bioaccessibility increases or diminishes, respectively, when increasing a given factor from the lowest to the highest coded level in the experimental domain. The relationship between D and the factors examined is given in figure 7.5. According to ANOVA results the soil weight was deemed statistically significant at the 0.05 significance level (its bar in the chart exceeds the t-critical value), while the extractant flow rate and digestion temperature proved not to be significant because of fast TE gastric bioaccessibility under a dynamic leaching format. The lower the amount of soil loaded in the flow-through sample container the better was the desirability function. This is in good agreement with earlier observations in dynamic column extraction methods [117] in which the effective surface area of the solid material for extraction is ameliorated with the decrease of the solid to free column volume ratio. Mechanical agitation at 480 rpm most likely does not suffice for the reactor to behave as a perfectly mixed continuous-stirred tank when increasing the mass of soil up to 800 mg. Soil amounts below 400 mg were not explored in this work so as to ensure that the processed sample aliquot is representative of the bulk medium.

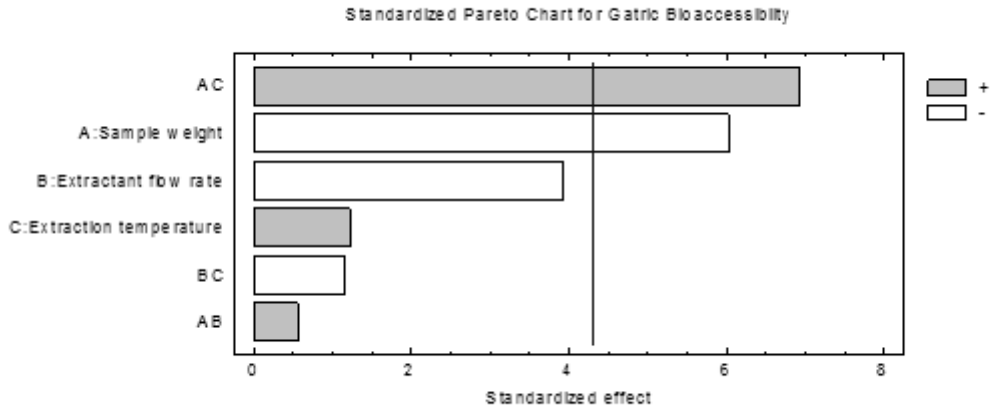


*Figure. 7.5. Pareto chart of standardized effects (α = 0.05) for two-level screening of the influence of main factors and two-term interactions upon TE gastric bioaccessibility.*

The Pareto chart revealed that the two-factor interaction between sample amount and extraction temperature is the one having a more significant influence upon TE extractability. As a result, the univariate approach might have rendered unreliable information as to the maximum TE gastric bioaccessibility in real soils. The effect of the temperature on the TE leaching rates is merely appreciable in those scenarios (in our case, leaching of 800 mg soil) where solid particles are not entirely dispersed in the gastric extractant.

A lack of fit test [238] was undertaken to determine whether the selected first-order model is adequate to describe the observed data or whether a second-order model should be used instead. The test is performed by comparing the variability of the current model predicted errors against the variability between observations at replicate settings of the factors. As the calculated p-value ($p = 0.276$) was greater than 0.05, the first-order model appears to be appropriate to describe the analytical system at the 95.0% confidence level with no need of further optimization.

On the basis of the screening design the sample amount, extraction temperature, and flow rate were fixed to 400 mg, room temperature (27ºC), and 1.5 mL/min for unbiased estimation of worst-case TE gastric leachability on a short notice.

### 7.3.4. Application and validation of the in-line oral bioaccessibility method

The reliability and ruggedness of the dynamic leaching procedure for TE gastric bioaccessibility conservative assessment was ascertained through the analysis of two environmental soils with different matrix complexity and origin as detailed under the experimental section.

The leaching profiles (so-called extractograms) are obtained by the graphical plot of the bioaccessible TE against time, subfraction number or cumulative extractant volume [118,267]. figure 7.6 depicts the average extractograms of Ni, Cu, Zn, Pb and Cr in the two soils assayed using dynamic gastric extraction as a front-end to ICP-OES. Fresh gastric juice is delivered to the soil containing extraction chamber until the bioaccessible TEs are completely leached out as seen from the signal gradually leaving off to baseline level, thereby simulating worst-case scenarios that coped with ISO/TS 17924:2007 specifications [246]. Similar trends in leaching patterns were recorded for the suite of analytes in both soils. Maximum extractability is observed after seven or eight 4.9 mL subfractions (35–40 mL gastric juice) in the two soils as a result of the time needed to reach $pH < 1.5$ for the gastric extracts. The volume capacity of the stirred flow chamber is 15 mL, which implies the need of a minimum of 3 subfractions to renew completely the extractant phase.

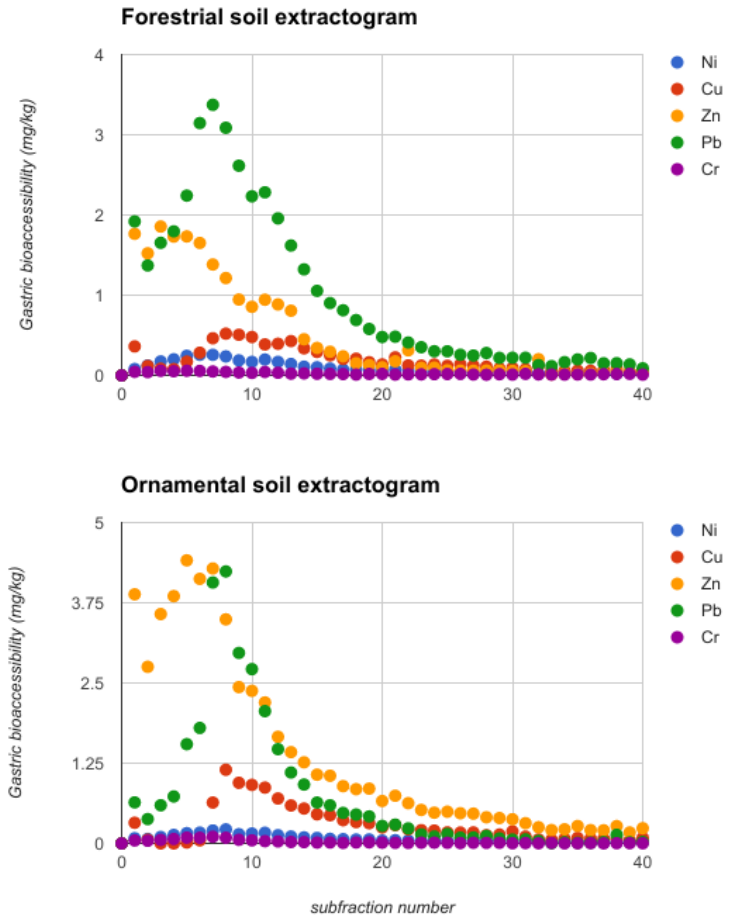


*Figure 7.6. Average extractograms of Cr, Cu, Ni, Pb and Zn in soils for evaluation of leaching kinetics and bioaccessible elements under worst-case gastric digestion scenarios (n = 3).*

It should be noted that the final pH of the gastric phase in UBM bioaccessibility tests has to be < 1.5 otherwise the procedure should be restarted from the beginning with steady control of pH throughout. This is an important limitation in the investigation of TE gastric bioaccessibility of alkaline soils – or those highly carbonated – and solid wastes [116,117] using batchwise UBM tests. However, the dynamic gastric bioaccessibility method herein proposed circumvents this limitation because it involves a continuous solid/liquid equilibrium shift whereby the leachate pH gradually decreases until reaching the nominal pH of the gastric biofluid regardless of the alkalinity of the solid sample. Despite the high pH of the extracts of the two calcareous soils assayed, the nominal gastric juice pH, that is, 1.1 ± 0.1, is attained after 20 subfractions (100 mL) in soil 1 and 12 subfractions (60 mL) in soil 2, respectively, as shown in figure 7.7.

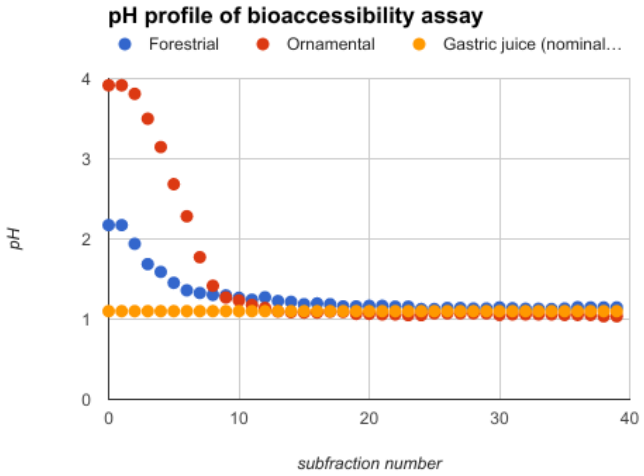


*Figure 7.7. Leachate pH profiles of the two soils analyzed as obtained by exploiting in-line leaching of TE in the gastric phase*

The mean values of the bioaccessible fractions of Cr, Cu, Ni, Pb and Zn for soils 1 and 2 are 2.7, 33.0, 16.5, 71.4, 25.6% and 3.5, 45.6, 15.5, 76.9, 44.7%, respectively, of the total metal concentration as determined by microwave digestion (see table 7.3). The most and least bioaccessible TE in both soils are Pb and Cr, respectively, which is in good agreement with earlier reports of gastric UBM tests in soil substrates [268,269].

For validation purposes, the intermediate precision and the trueness of the dynamic gastric bioaccessibility method were ascertained. Relative standard deviations for bioaccessible TE concentrations in the gastric phase were in all instances below 14% for both soils (see table 7.3), thereby confirming that the in-line extraction method is reliable for conservative evaluation of TE oral bioaccessibility in soils. Notwithstanding the fact that the proposed automated method analyzes 400 mg soil against 600 mg for the harmonized batchwise UBM test, the dynamic system gives rise to similar intermediate precision on Pb gastric bioaccessibility (Relative Standard Deviation (RSD) of 8.5% and 11.4% for non-contaminated soils 1 and 2, respectively) and better for Cr (RSDs of about 11% in both soils) than the batchwise UBM gastric protocol with RSDs up to 8.8% for Pb [268] and ≤ 36% for Cr [269] in urban and/or contaminated soils. This corroborates the fact that 400 mg of soil suffice in our system to ensure sample representativeness.

The trueness of the in-line gastric bioaccessibility test was ascertained through the use of mass balance as applied to individual target elements. To this end, the sum of the gastric bioaccessible concentration and the residual (immobilized) fraction was statistically compared against total metal concentration determined by microwave digestion. As shown in table 7.3, relative recoveries spanning from 96–110% and 96–109% were obtained for soils 1 and 2, respectively. The *t*-test of comparison of means [264] revealed the inexistence of significant differences at the 0.05 significance level

for the overall trace elements in the two soils. The in-line oral bioaccessible method is thus free from both additive and multiplicative matrix interferences, making the use of the standard addition method for determination of TE in the gastric leachates unnecessary.

*Table 7.3. Extractable amounts in gastric phase (worst-case concentrations) and mass balance validation of Cr, Cu, Ni, Pb and Zn in soils exploiting a hybrid flow extraction system coupled to ICP-OES.*

| *Sample* | *Element* | *Gastric bioaccessibility (mg/kg) (% referred to total amount)* | *Residue (mg/kg)* | *Total microwave digestion (mg/kg)* | *RR (%)* |
|---|---|---|---|---|---|
| *Forestrial* | *Ni* | *3.8 ± 0.5 (16.5%)* | *20 ± 2* | *23 ± 1* | *104* |
| | *Cu* | *7.8 ± 0.7 (33.0%)* | *18 ± 2* | *23.6 ± 0.8* | *110* |
| | *Zn* | *20 ± 1 (25.6%)* | *55 ± 5* | *78 ± 6* | *96* |
| | *Pb* | *40 ± 3 (71.4%)* | *15 ± 5* | *56 ± 5* | *98* |
| | *Cr* | *1.0 ± 0.1 (2.7%)* | *35 ± 3* | *36 ± 1* | *100* |
| *Ornamental* | *Ni* | *2.9 ± 0.4 (15.5%)* | *15 ± 2* | *18.7 ± 0.7* | *96* |
| | *Cu* | *11.4 ± 0.6 (45.6%)* | *16 ± 1* | *25 ± 3* | *109* |
| | *Zn* | *54.1 ± 0.9 (44.7)* | *64 ± 2* | *121 ± 2* | *97* |
| | *Pb* | *30 ± 3 (76.9%)* | *9 ± 3* | *39 ± 2* | *100* |
| | *Cr* | *1.0 ± 0.1 (3.5%)* | *27.2 ± 0.8* | *28.7 ± 0.7* | *98* |

# 8. Rapid estimation of readily leachable triazine residues in soils using automatic kinetic bioaccessibility assays followed by on-line sorptive clean-up as a front-end to HPLC

## 8.1. Introduction

Atrazine and ametryn are triazine herbicides often applied to weeds control, especially in maize and sugarcane crops [270].These herbicides have been used in pre- and post-emergency periods, normally at 1.0–3.25 kg/ha doses [271]. Ametryn is usually applied once a year to maize and three-times a year to sugarcane crops [272], and residues after 198 days from initial application were estimated as 0.05 mg/kg [273]. Also, 0.08 ± 0.02 μg/g atrazine residues were determined at 100 days after applying 2.0 kg/ha of atrazine to a maize crop [274]. These data confirmed the high environmental persistence of these herbicides, which are then potential contaminant sources of river and ground-waters. Adsorption and desorption [275], photodegradation [276] and biodegradation [277] are the main processes controlling the persistence of ametryn and atrazine in soils. The adsorption and desorption processes are influenced by pH, surface area, organic matter content, particle size and porosity [278]. After desorption, the herbicides are accessible to interact with food webs. Bioaccessibility is defined as the maximal concentration of target species potentially available to biota under simulated environmental conditions and might serve as a conservative measure (worst-case scenario) of freely dissolved species [6,13,221,226]. There is an increasing interest in analytical partitioning methodologies to measure the fractions of bioaccessible inorganic and organic contaminants in environmental solid substrates [6,14,221,223,279–281]. Dilute saline solutions, such as 0.01 mol/L $CaCl_2$, 0.1 mol/L $Ca(NO_3)_2$,1.0 mol/L $NH_4OAc$ or 1.0 mol/L $(NH_4)_2SO_4$ have been used to correlate the bioaccessibility with the assimilation pathways of the contaminants by living organisms [14,221,223,224]. Classical batchwise procedures to access the contaminant pools of herbicides and other environmental contaminants

usually use 0.01 mol/L $CaCl_2$ as extracting solution to mimic soil pore water or the percolation of rainwater through soil profiles [282–284]. These procedures however are based on endpoint measurements. They do not provide information on the kinetic aspects, in spite of the fact that the involved kinetics (fast, slow or very slow) plays a fundamental role in understanding the actual hazardous effects of environmental contaminants.

For getting relevant insight into pools of bioaccessible contaminants in environmental solids, the flow analysis concept and its sequels [285] showcase advantages such as fast analysis, simple operation, minimum analyst intervention, low cost and low residues production in good agreement with the twelve principles of green chemistry [286]. The analyses are carried out in a closed environment without operator interferences, thus contaminations and/or sample losses are avoided. Flow analysis manifolds are characterized by a rigid time control and good measurement repeatability [174,287]. The sequential injection analysis (SIA) concept [288–290], an advanced modality of flow analysis, features versatile flow-programming linked to pressure-driven flow as precisely controlled by user-friendly software. The sample aliquot and reagents can be driven to other manifold compartments, such as reaction coils, SPE columns [289,291,292] or ancillary modules for on-line/in-line sample processing.

The goal of this work was then to propose an automatic bioaccessibility assay by harnessing an SIA analyzer for real-time monitoring of herbicide residues readily leachable from agricultural soils under simulated environmental conditions and investigation of leaching kinetics. To this end, the herbicides were extracted with a mild extractant, the extracts underwent in-line clean-up via restricted access material for removal of dissolved organic matter and colloidal species while retaining freely dissolved triazines, followed by separation with a HPLC. A six-way valve with a sampling loop was accountable for both eluate heart-cut and injection of the isolated target compounds into a monolithic C18 column for reversed-phase LC separations. To the best of the authors' knowledge, this is the first report of automatic kinetic bioaccessibility assays for organic pollutants in environmental solids with in-line extract processing prior to fast LC separation and expedite quantification of readily mobile pools.

# 8.2. Experimental

## 8.2.1. Standards and reagents

Ultrapure water was obtained from a Milli-Q water generator (Synthesis A10, Millipore, Billerica, MA), whereas HPLC-grade methanol, acetonitrile and acetic acid were supplied by Sigma Aldrich (Steinheim, Germany). Atrazine [2-chloro-4-

(ethylamino)-6-(isopropylamino)-1,3,5-triazine], ametryn [2-ethylamino-4-(isopropylamino)-6-(methylthio)-1,3,5-s-triazine] and prometon [2-methoxy-4,6-bis(isopropylamino)-s-triazine], this later used as internal standard, were also obtained from Sigma-Aldrich. The stock solutions, 500 mg/L of the above-mentioned triazines, were prepared by dissolving each individual compound in pure methanol, and maintaining the solution in darkness at ca.4°C.

The extractant used in the bioaccessibility assays was a 0.01 mol/L $CaCl_2$ solution (also the carrier stream in the flow system) as per test 106 endorsed by Organisation for Economic Cooperation and Development (OECD) [293]. Working standard solutions of the target herbicides were daily prepared in this medium by stepwise dilutions of the corresponding stocks.

Non-polar styrene-divinylbenzene, copolymeric core, sorbent with hydroxylated shell with restricted access material (RAM)-like characteristics as a result of its mesopore structure (Bond Elut Plexa, Agilent, Santa Clara, CA) and hydrophilic-lipophilic balanced copolymer [poly(divinylbenzene-co-N-vinylpyrrolidone)] (Oasis HLB, Waters, Mildford, MA) were evaluated for in-line clean-up of leachates and concentration of triazines. Nylon syringe filters (0.45-µm pore size, Fisherbrand, Fisher Scientific, Pittsburgh, PA) were used for in-line filtration of soil leachates prior to automatic sorptive clean-up.

The SPE column (8.0 x 4.6 mm ID) was prepared from commercially available polypropylene cartridges whereby minimal preparation was needed. The column contained about 30 mg of packed sorbent, and was connected to the flow system via an SPE tube adapter (57020-U, Sigma Aldrich) fitted to the column large bore inlet and a barbed female luer lock fitting (Teknokroma, Barcelona) to the outlet. Polyethylene frits (10-mm pore size, Mo Bi Tec, Göttingen, Germany) were used at both ends of the column to prevent sorbent losses during system operation.

## 8.2.2. Samples

About 1.0 kg of forest soil samples were collected in agricultural areas of Piracicaba SP (Brazil) at depths of 0–20 cm. Geographic coordinates of the sampling sites were 22°37′27″S47°36′67″W and 22°45′18″S47°53′75″W for clayey and sandy soils, respectively.

Physicochemical characterization was accomplished by standard methods [294,295]. In brief, the samples were dried to constant weight at 45°C, sieved (2.0 mm mesh) and analyzed. For pH measurements, the soil suspension (5:1 L/S ratio in 0.01 mol/L CaCl2) was stirred for 5 min, allowed to settle for 2 h, and stirred again prior to measurement using a combined pH electrode (Eutech Instruments, Nijkerk, The Netherlands). The pH was determined as ca. 3.8 for both assayed soils.

Total carbon content was determined titrimetrically as 0.8% and 2.1% for sandy and clayey soils, respectively. Regarding texture analysis using the Bouyoucos hydrometer method [294], the sandy soil was 92% sand (0.05 – 2.0 mm), 2% silt (2–50 μm) and 6% clay (< 2μm), whereas the clayey soil was 26% sand, 9% silt and 65% clay.

For validation purposes, the soil samples were doped with ametryn and atrazine at the 5.0 mg/kg level [271]. To this end, 500mL of both triazine stock solutions were added to a 25-mL volumetric flask; thereafter 12.5 mg sodium azide previously solubilized in methanol were added, and the volume was completed with methanol. The role of sodium azide is to avoid biodegradation of the triazines during the time course analysis and, hence, prevent underestimation of the concentration of potentially leachable species. The solution was dropwise added to accurately weighed 50 g of soil until the soil particles were completely covered; homogenization was ensured by gently mixing the soil with a glass rod. The doped soils were air-dried at room temperature in darkness and aged for three weeks for stabilization.

For the bioaccessibility assays, 2.0 g of raw or doped soils were magnetically stirred with 50.0 mL of 0.01 mol/L $CaCl_2$ extracting solution, thus the 1:25 soil: extractant ratio recommended by OECD 106 [283] was maintained. A cylindrical magnetic stirrer (1.0 cm long, 2.0 mm ID) was used for homogenization purposes.

## 8.2.3. Apparatus

A μSIA flow analyzer (FIALab Instruments, Bellevue, WA) equipped with a 3000-step syringe pump (Cavro, Sunnyvale, CA) and a 5.0 mL gas-tight glass syringe was used for solution propelling and aspiration. The syringe was connected to an eight-port multi-position selection valve (SV) accountable for handling the solutions involved in the batchwise soil extraction and in the in-line SPE procedure. The connection between the syringe pump and the selection valve was accomplished with a 5.0 mL holding coil made from 1.5 mm ID PTFE tubing. The remaining manifold tubing was of 0.8 mm ID. The soil extracts were in-line aspirated at preset time intervals through a 0.45-mm pore size nylon syringe filter (Fisher Scientific) fixed in a PTFE tube connected to SV. The flow system comprised two additional valves: the three-way valve (HV), accountable for connection with the flow system or filling the syringe pump with carrier; and the IV six-port valve, for injection of the processed extract into HPLC. The system was designed to permit in a fully automatic mode the accommodation of the entire analytical method encompassing: sampling of extract aliquots, in-line filtration, SPE of the target analytes, elution towards a sampling loop, heart cutting and injection into HPLC, triazine separations and data recording. A diagrammatic description of the flow analyzer for automatic bioaccessibility tests of triazines in soils as a front end to HPLC is shown in figure 8.1.

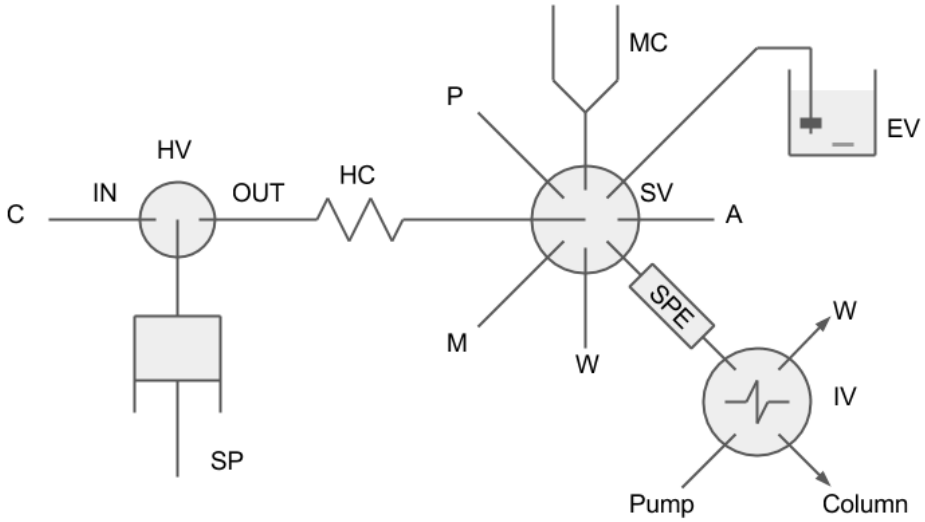


*Figure 8.1. Flow diagram of the automatic system for kinetic bioaccessibility assays of triazines in soils as a front end to HPLC. HV: three-way valve; SV: 8-port selection valve; IV: High pressure 6-way injection valve with 300 µL injection loop; SP: syringe pump; C: carrier stream (0.01 mol/L $CaCl_2$ solution); IN, OUT: optional path ways; HC: holding coil; EV: Extraction vessel, containing sample, extractant, magnetic stirrer and filtering unit; M: 99:1 (v/v) methanol/water; P: prometon (0.25 mg/L); W: outlet towards waste; MC: mixing chamber (Pipet tip); A: air; SPE: column for solid phase extraction; For details and system operation, see text.*

For hyphenating the flow analyzer with HPLC, a model RH-7000L two-position, six-port, high-pressure injection valve (Rheodyne, IDEX Corporation, Oak Harbour, WA) was used. This valve was housed inside a Crison module (Alella, Spain) and comprised a 300-mL PEEK sampling loop (0.75-mm ID, 68-cm long), and a stainless steel stator. Both the SIA analyzer and the Crison module were controlled by the CocoSoft software [164], and the commands transmission from computer to both instruments were accomplished via a USB-RS232 converter (Future Technology Devices International Limited, Glasgow, UK). Although HPLC and SIA were interrelated with each other through relay connection, the HPLC software was used for controlling the mobile phase flow rate, column temperature, and data acquisition and treatment.

Chromatographic separations were accomplished by an HPLC instrument (Waters Technologies, Milford, MA) comprising a helium purger, a high-pressure pump, a thermostat and a model 2996 UV/Vis photodiode-array detector.

## 8.2.4. Chromatographic separation

### 8.2.4.1. Evaluation of HPLC stationary phases for triazine separation

Preliminary experiments were conducted to evaluate the performance of three reversed-phase C18-columns for triazines separation. The criteria to choose the appropriate column were to obtain the best resolution for the target species with the shortest separation time. To this end, 40 µL of 100 µg/L triazines (including prometon) solutions were prepared in 100% methanol and injected in HPLC. The isocratic separation was performed using a mobile phase (40:60 v/v acetonitrile/water) at 1.0 mL/min:

- Onyx monolithic silica-based column (100 x 4.6 mm) (Phenomenex, Inc., Torrance, CA, USA): Retention times of 5.2, 5.9 and 8.0 min were obtained for atrazine, prometon and ametryn, respectively. All triazines were completely separated in 9.0 min.
- Particle-packed silica column (150 × 4.6 mm) (Kromasil 100 C18, 3.5 µm, Scharlab, Barcelona, Spain): the peaks of prometon and atrazine were not completely separated. Besides, the retention times were longer: 5.9, 6.2 and 9.2 for prometon, atrazine and ametryn, respectively.
- Particle-packed hybrid (inorganic/organic) column (150 x 3.9 mm, 3.5 µm) (X-Terra, Waters Corporation, Milford, MA, USA): the chromatographic run time was too long: About 13 min for elution of the three triazines. The peaks of prometon and ametryn were not completely separated.

Considering the resolution and the shortest run time, column 1 was chosen. To avoid polar interactions with potential free silanol groups, 0.4% (v/v) concentrated acetic acid was added to the mobile phase, whereupon the target herbicides were eluted in less than 6 min.

### 8.2.4.2. Selected chromatographic method

Triazines were separated by the Onyx C18 silica monolithic column preceded by a guard column (10 x 4.6 mm) of the same chemical composition. Isocratic elution was carried out in 6 min by a 40.0:59.6:0.4 (v/v/v) acetonitrile/water/acetic acid solution (pH = 3.2) flowing at 1.0 mL/min. The monolithic column underwent a 60-min pre conditioning step before starting the chromatographic separation, and the temperature was kept at 24°C throughout. Triazines were monitored at 220 nm in order to attain maximum sensitivity. Quantification was based on a matrix-matched calibration curve using prometon at the 250 mg/L level as internal standard, viz. standards were processed alike samples using the same flow setup (see experimental section 8.2.4) and peak areas constituted the measurement basis. The dynamic linear

range for both herbicides with retention times of 3.8 min and 4.7 min for ametryn and atrazine, respectively, extended from 10 to 400 mg/L with correlation coefficients ≥ 0.9971.

## 8.2.4.3. Chromatographic characterization parameters

Chromatographic parameters for characterization of the separation of triazine species using the on-line system integrating the Onyx monolithic C18 silica-based column (100 x 4.6 mm) with a mobile phase composition of 40:59.6:0.4 (acetonitrile/water/acetic acid, v/v/v) and injection volume of 300 µL, were calculated following the specifications of USP 37 [296] as indicated in table 8.1. Notwithstanding the fact that some parameters are slightly deteriorated (e.g., peak symmetry) compared to off-line methods because of the injection of methanolic eluate volumes as high as 300 µL, the peak resolution is not compromised and therefore the HPLC characterization parameters do suffice for reliable quantification of the target species in soil extracts after on-line SPE-RAM clean-up.

*Table 8.1. Chromatographic separation parameters of the on-line hyphenated system.*

| | *Equation/acronym* | *Ametryn* | *Atrazine* |
|---|---|---|---|
| *Hold-up time (min)* | $t_M$ | *1.40* | |
| *Retention Time (min)* | $t_R$ | *3.76* | *4.70* |
| *Width at 0.05 height (min)* | $W_{0.05h}$ | *0.40* | *0.58* |
| *Width at 0.5 height (min)* | $W_{0.5h}$ | *0.15* | *0.24* |
| *Leading edge to peak maximum (min)* | $f$ | *0.10* | *0.12* |
| *Symmetry factor (As)* | $W_{0.05}/2f$ | *2.00* | *2.41* |
| *Resolution (R)* | $1.18*(t_{R2}-t_{R1})/(W_{0.5h,1}+W_{0.5h,2})$ | *2.84* | |
| *Number of theoretical plates (N)* | $5.54*(t_R/W_{0.5h})$ | *3481* | *2124* |
| *height equivalent to a theoretical plate (HETP)(µm)* | $L/N$ | *28.7* | *47.0* |
| *Retention factor (k)* | $(t_R-t_M)/t_M$ | *1.68* | *2.35* |
| *Separation factor (α)* | $k_2/k_1$ | *1.40* | |

## 8.2.5. Analytical procedure

2 mL of soil extract were aspirated through in-line filter at 5 mL/min. From this extract, 1 mL was delivered to the mixing chamber (see figure 8.1) and the other was returned along with 1 mL of fresh extractant (carrier) to the extraction vessel, assuring the L/S ratio maintenance in the extraction medium and filter unclogging. The extract in the mixing chamber was mixed with 100 µL of prometon as internal standard at 5.0 mL/min and air bubbled for the sake of the homogenization. The extract with internal standard were aspirated and delivered to the RAM type SPE for analyte retention and matrix cleanup. The solid phase was then rinsed with 1.4 mL of carrier at 2.0 mL/min and the triazines were eluted with 450 µL of methanol; 300 of those were injected on-line into the HPLC in a heart-cut fashion for separation and detection.

### 8.2.5.1. System washing

This step was accomplished by filling the aspirating tubes associated with the soil extract, methanol and prometon solutions with the corresponding solutions (5.0 mL/min). The syringe pump was programmed to permit 1.0 mL of the extracting solution (carrier) to flow through the filter, this volume being selected to exceed the inner volume of the filtering unit, about 650 µL. Next, 3.5 mL of 99:1 (v/v) methanol/water were aspirated towards HC and half of this volume was pumped towards the SPE column for sorbent conditioning. Thereafter, 200 mL of prometon (250 mg/L) were pulled in HC. For HC cleaning, a metered volume of 1.75 mL of methanol and 3.0 mL carrier were propelled towards waste of the selection valve.

### 8.2.5.2. Automatic sampling of soil extract

A 5.0 mL/min flow rate was set for carrying out this step. Initially, the syringe pump aspirated 1.0 mL of 0.01 mol/L $CaCl_2$ (carrier stream), the filter was placed inside the soil suspension, and 2.0 mL of crude extract were aspirated through the in-line filter towards HC. Then, 1.0 mL of the extract was dispensed into the 10 mL polypropylene pipette tip attached to the selection valve (V2). In order to maintain the volume of the extracting solution at 50.0 mL throughout, to avoid filter clogging, and to circumvent leachate fraction overlapping as consequence of dead volume effects of the filtering line, the pump dispensed the remaining 1.0 mL extract plus 1.0 mL carrier inside HC back to the stirred extracting solution. Thereafter, 2.0 mL of air and 100 µL of 0.25 mg/L prometon were aspirated towards HC at 5.0 mL/min. The syringe pump was programmed to dispense 2.1 mL at a high flow rate (50 mL/min), to mix prometon with the soil extract in the external pipette tip.

### 8.2.5.3. In-line SPE and heart-cut protocol

Subsequently, V1 valve was switched to permit the syringe pump to be filled with carrier, and the entire volume of soil extract in the pipette tip was aspirated backward into HC at 5.0 mL/min. For in-line concentration and extract cleanup, the syringe pump dispensed 1.1 mL of prometon containing extract plus 1.4 mL carrier solution (0.01 mol/L $CaCl_2$), respectively, through the SPE column at 2.0 mL/min towards waste of V3 valve. The syringe pump sequentially aspirated 1.0 mL of carrier and 2.0 mL of 99:1 (v/v) methanol/water at 5.0 mL/min towards HC. For elution of the triazines and heart-cut protocol, a total volume of 450 µL of methanol, at 2.0 mL/min, was dispensed through the SPE column with the front eluate fraction filling the 300-µL sampling loop of the V3 injection valve in the loading position. Thereafter, the valve was automatically switched to insert the selected eluate aliquot into the LC mobile phase that acted also as a secondary carrier stream. The remaining volume of methanol plus carrier inside HC was directed to rinse and conditioning the SPE cartridge for the following leachate aliquot.

### 8.2.5.4. Triazine separation

Separation of triazines by monolithic-column based LC required 6.0 min. During this process, the next extract aliquot was aspirated at a preset time through the filter and then in-line cleaned-up and concentrated. This means that the system was designed to operate continuously. When the eluate aliquot was injected into the chromatographic column, the separation of previous aliquot had been already completed. In relation to sampling frequency for the kinetic bioaccessibility assays, the first aliquot of the extracting solution was sampled 1.5 min after the extraction process was started. The following aliquots were aspirated after about every 10 min for on-line monitoring of the extraction profile of triazines aiming at detecting and ascertaining the maximum concentration of bioaccessible triazines under batchwise extraction conditions at near-real time.

## 8.2.6. Selection of the sorptive phase

The sorbent material was selected in preliminary experiments performed with the flow setup in combination with off-line LC separation. To this end, 5.0 mL of a 250 mg/L ametryn, atrazine plus prometon in 0.01 mol/L $CaCl_2$ were processed as above described and the eluate was collected into a dark vessel and offline analyzed by HPLC. In these experiments, the cartridge was packed with 30 or 60 mg of two different copolymeric sorbent materials indicated above.

First, the sorbent material was conditioned by aspirating 400 µL of 0.01 mol/L $CaCl_2$ to fill the syringe (V1 valve IN), followed by 600 µL of 99:1 (v/v) methanol/water (valve OUT) towards HC, all at 5.0 mL/min. Next, 1.0 mL of eluent plus carrier was

forwarded towards the SPE column, followed by aspiration of air (100 µL) towards HC aiming at avoiding dispersion of solutions inside HC. The above-mentioned standard solution (4.9 mL) was aspirated at 3.0 mL/min towards HC and then forwarded at 1.0 mL/min towards the SPE column for in-line uptake of triazines. To rinse the sorbent after this step, 600 µL of carrier were aspirated and delivered at 1.2 mL/min towards the SPE column. To dry the sorbent, 1.5 mL of air were aspirated at 3.0 mL/min towards HC and forwarded through the SPE column at 1.0 mL/min. Elution was accomplished in four fractions, aiming at collecting the most concentrated portion for further heart-cut based LC injection protocols. Hereto, 150 µL of air were aspirated at 3.0 mL/min towards HC with the objective of minimizing the ensuing eluent/ eluate dispersion. Next, 125 µL of 99:1 (v/v) methanol/water were aspirated towards HC at 3.0 mL/min. The first eluted fraction flowing through the column was collected in a dark vial by pumping 275 µL of methanol plus air through the sorbent at 1.0 mL/min. For complete recovery of the first eluate fraction, 500 µL of surplus air were aspirated at 3.0 mL/min and dispensed through the sorbent column at 1.0 mL/min. The remaining three fractions were analogously accomplished. To analyze the collected eluate aliquots, 40 out of 125 µL contained in the each vial were injected into LC.

# 8.3. Results and discussion

## 8.3.1. Automatic SPE extraction

Regardless of the sorbent material assayed, the second heart-cut fraction was the most concentrated one (see figure 8.2). More favorable (narrow elution peaks) and reproducible results were noted for the copolymeric Bond Elut Plexa sorbent. Recoveries in the second fraction for ametryn and atrazine using 30 mg of this sorbent were 71% and 62%, respectively, whereas for Oasis HLB, these values were calculated as 57% and 52%, respectively. Repeatability values (RSD) of measurements for Bond Elut Plexa were about 0.8% for both triazines, whereas larger variability (RSD: 5.9–20.8 %) was noted for Oasis HLB. The Plexa sorbent was deemed more selective because of the RAM-like characteristics as a result of its mesopore structure, which retained the triazines by reversed-phase interactions, while macromolecules, such as humic and fulvic acids in soil extracts, were wasted during the cleanup step. The Oasis HLB sorbent has a polar core due to the presence of hydrophilic monomers, thus a high capacity to retain triazines but at the expense of the likelihood of increased matrix interfering effects.

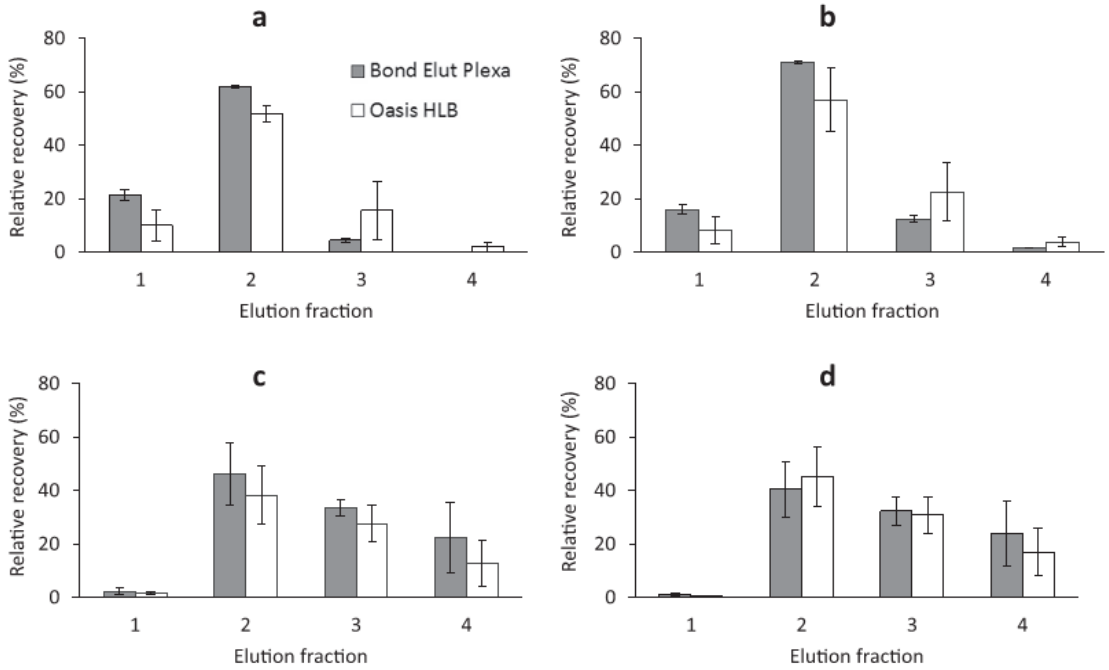


*Figure 8.2. Relative recoveries (%) for in-line SPE of atrazine and ametryn at the 0.25 mg/L level normalized to 100% for a 600 µL-eluent volume: (a, c) atrazine and (b, d) ametryn using 30 mg (a, b) and 60 mg (c, d) of Bond Elut Plexa and Oasis HLB. Numbers 1–4 correspond to the sequentially eluted fractions (125 µL of 99:1 (v/v) methanol/ water each).*

With a larger sorbent amount (60 mg), a wider elution pattern was observed for both sorbents because of the increased sorptive capacity, which impaired the analytical reproducibility and elution efficiency associated with the second fraction (see figure 8.2). A larger eluent volume would then be necessary, but the concentration efficiency would be reduced in heart-cut detection mode due to pronounced peak broadening. A column packed with 30 mg of Bond Elut Plexa sorbent was then selected for the remainder of the work.

## 8.3.2. Heart-cut injection

The volume (within 300 and 800 µL) pumped at 2.0 mL/min through SPE into the HPLC loop of V3 (see figure 8.1) demonstrated to be a relevant parameter in the heart-cut injection, as demonstrated by dispensing different eluent volumes towards the SPE column and maintaining the transmission line (10 cm long, 0.8 mm ID) between SPE and V3 fixed for a 300 µL sampling loop. Increasing the volume from 300 to 550 µL led to a three-fold increase in the recorded peak area; maximum area was attained within the 450–500 µL range, but a 13% decrease in peak area was noted for 600 µL. Beyond this value, a pronounced signal lessening was observed. This effect held true for both triazines, and was analogous to a zone sampling process [297] where either the trailing, central or front edge of a dispersing sample/composite zone volume is sampled. The volume for inserting the most concentrated eluate fraction into LC was

then selected as 450 µL.

## 8.3.3. Modelling of leaching kinetics

Extract aliquots were sampled automatically 1.5, 10, 21, 31, 42 and 52 min after initialization of the extraction, allowing the real time generation of leaching profiles of the target herbicide residues, as illustrated in figure 8.3 and figure 8.4. All extracts were subjected to in-line RAM-type solid phase extraction followed by fast monolithic column-based liquid chromatographic separations.

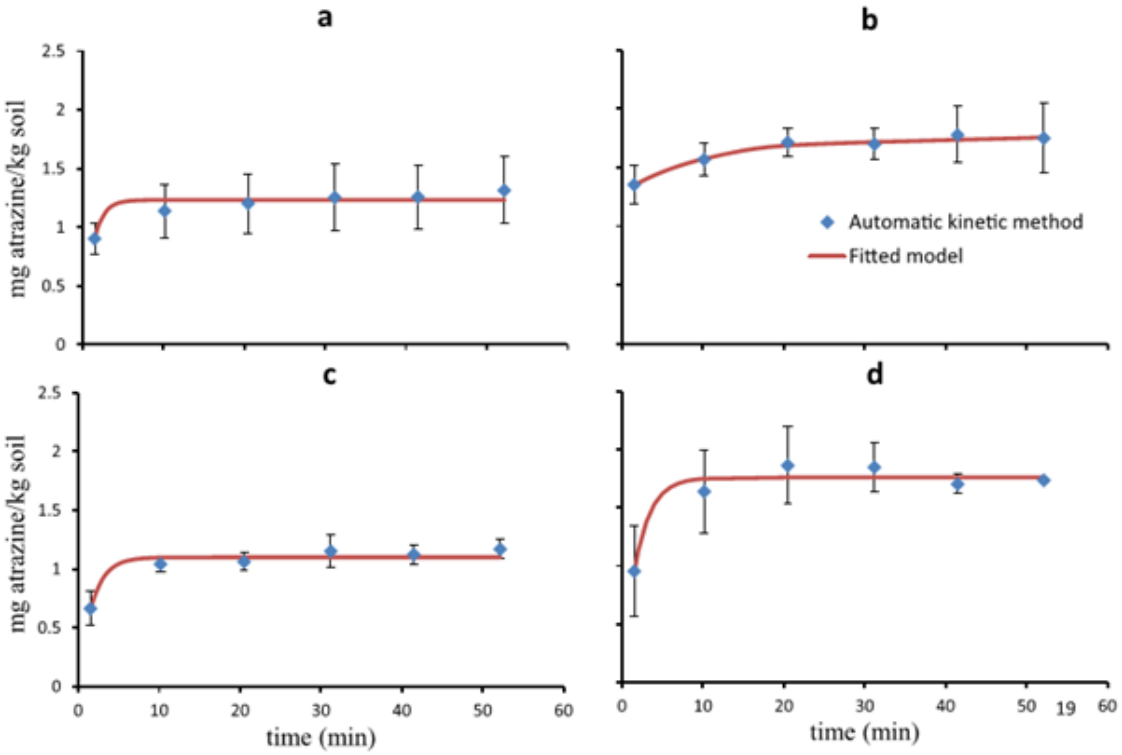


*Figure 8.3. Experimental leaching profiles of bioaccessible pools of atrazine (a,c) and ametryn (b,d) in sandy (a,b) and clayey (c,d) agricultural soils as obtained by automatic batchwise kinetic tests with in-line sorptive concentration/clean-up as a front end to HPLC. Mathematical curve fitting by is given as a solid line.*

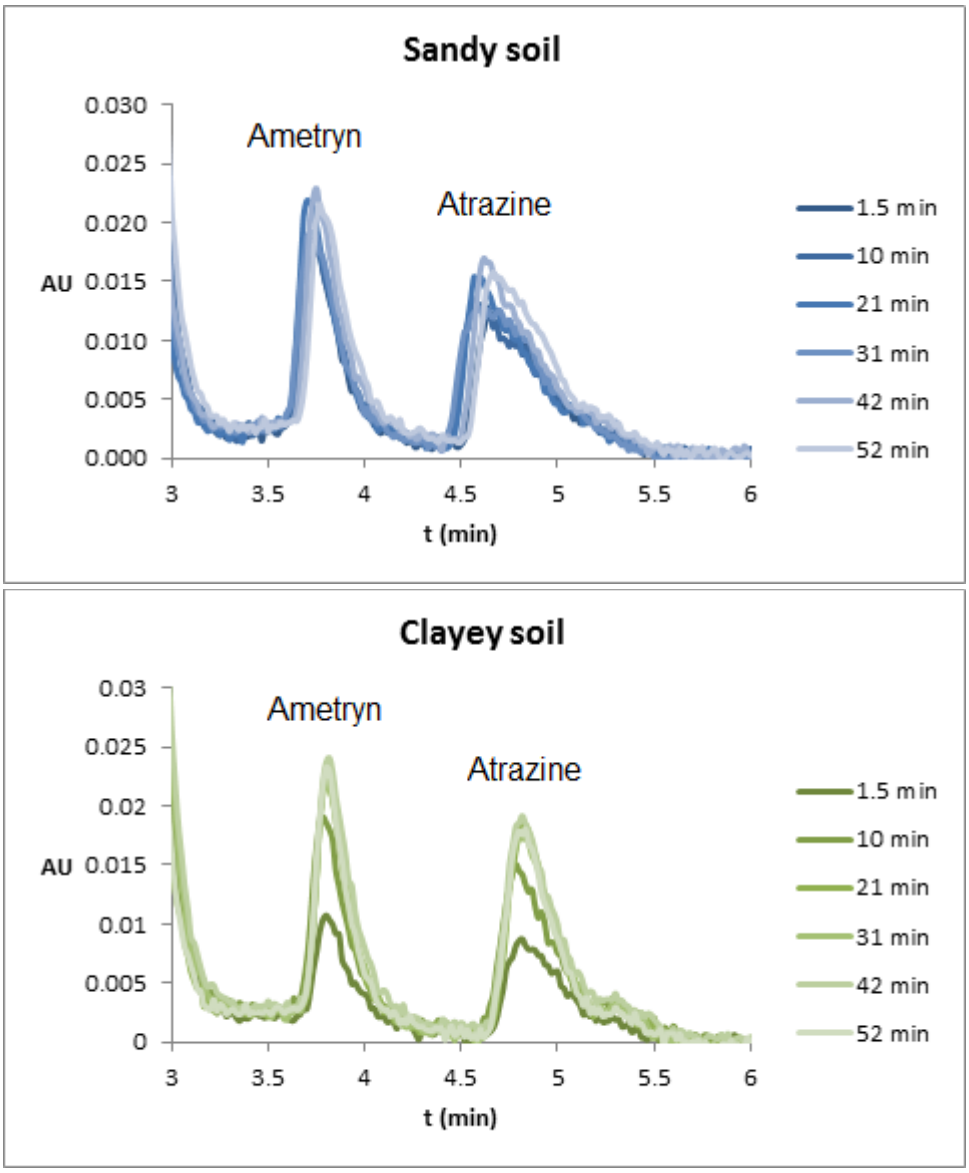


*Figure 8.4. Overlap of chromatograms for the investigation of the leaching kinetics of readily bioaccessible triazine and atrazine in extracts of clayey and sandy soils as obtained from the on-line hyphenated flow-batch system. Extract aliquots were sampled automatically 1.5, 10, 21, 31, 42 and 52 min after starting the bioaccessibility test as indicated in the figure legends.*

The average cumulative concentration of ametryn and atrazine in the pore water simulated extractant after rainfall at time t [C, mg/kg] is proven to fit a first-order exponential function [59,61] with the potential contribution of a secondary steady compartment ($A_2$) (see figure 8.3 and Table 8.3):

$$C = A_1\left(1 - e^{(-kt)}\right) + A_2$$

Where $A_2$ is the concentration of extremely fast leachable triazines (mg/kg); $A_1$ the maximum concentration of readily leachable triazines (mg/kg); k is the associated rate constant of $A_1$ ($min^{-1}$), and t is the time coordinate (min).

Coefficients estimated for the investigated soil/herbicide systems (table 8.2) revealed a fast and steady-release of the triazine herbicides, which is attributed to the particularly high water solubility of the target compounds and the low abundance of organic matter components in the soil substrates. The maximum pool of available residues was noted in most instances after about 6 min, confirming the high mobility of the target triazines, which may spread on the surface of the soils with potential percolation through soil bodies into aquifers in a short time interval. Soil texture, clay content, permeability and organic matter content, especially this later one, are the main characteristics influencing the herbicides adsorption and mobility in soils [298]. Soils with low percentages of total organic carbon (about 2% or less) tend to bear insufficient capacity to retain organic species, as is the case in the assayed soils (figure 8.3).

The lack of fit test [299] of every individual profile (see table 8.2) indicated that almost all variance at the 0.05 significance level was accounted for the variables $A_1$, $A_2$ and k specified in the model with p values ranging from 0.70 to 0.92, that is, $p > 0.05$ in all instances. The rate constants of the two herbicides in the clayey soil were very similar to each other and ranged from 0.51 to 0.60 $min^{-1}$. Most importantly, the actual extraction times for identification of steady-state available concentrations of ametryn and atrazine, ($C(t_{95\%})=0.95\ (A_1+A_2)$), ranged from 3.4 to ca. 33 min, indicating the needlessness of using the recommended OECD conditions, especially the ≥ 4h duration of leaching tests. The experimental results emphasized that, regardless of the soil analyzed, the maximum bioaccessible pools (in the absence of biotic degradation) for ametryn and atrazine amounted to 22–35% from the original dose application after 3 weeks. This aspect indicates a potential short-term contamination of the phreatic zone in agricultural soils if appropriated measures are not taken.

*Table 8.2. Parameters of the mathematical model for the leaching profiles*

| *Analyte* | *Soil* | *$A_1$ (mg/kg)* | *k ($min^{-1}$)* | *$A_2$ (mg/kg)* | *$t_{95\%}$* | *p (> 0.05)* |
|---|---|---|---|---|---|---|
| *Ametryn* | *Sandy* | *0.47* | *0.09* | *1.29* | *32.7* | *0.72* |
| *Atrazine* | *Sandy* | *1.23* | *0.87* | *0* | *3.4* | *0.93* |
| *Ametryn* | *Clayey* | *1.76* | *0.51* | *0* | *5.9* | *0.91* |
| *Atrazine* | *Clayey* | *1.10* | *0.60* | *0* | *5.0* | *0.70* |

## 8.3.4. Figures of merit and comparison with previous analytical methods

As a result of extract processing by in-line SPE, no artifact peaks from soluble components of natural organic matter, which were identified in previous communications in the determination of triazine herbicides in soils without extract clean-up [300,301], were observed here.

In-line sampling, mixing with internal standard, extract cleanup and heart-cut injection of SPE eluate into LC loop lasted about 4.3 min for every extract aliquot. As the chromatographic run lasted 6 min, the sampling throughput for extracts inherent to the proposed procedure is 10/h. This implies 3-fold improvement as compared to a previous flow system with sorptive concentration and monolithic column separation of herbicides [302].

The proposed analytical procedure was validated under near equilibrium conditions ($t > t_{95}$) attained for the various samples after 3.4 – 33 min upon starting the bioaccessibility test (see Table 8.2). Relative recoveries for target triazine herbicides were estimated for the sandy and clayey soils by spike additions at the 100, 200 and 300 μg/L levels of ametryn and atrazine to the soil extract after completing the bioaccessibility assay. Experimental results and recovery data calculated on the basis of the concentrations found in the spike solutions and the leachable pools in the soil microcosm studies are given in table 8.3. Recoveries were in all instances within the range of 70 – 120%, *viz.* 86 – 104% (see table 8.3), which is deemed acceptable for the determination of herbicides and pesticides in soils [300]. The t-test of comparison of relative recoveries against the theoretical value, namely 100%, for every individual spike level and soil, indicated the lack of biased results (e.g., absence of matrix effects) at the 0.05 significance level for the suite of analyzed samples, since the p-value was > 0.05 in all instances (see table 8.3). Recoveries below 100% might be however indicative of association of triazines to dissolved organic matter or colloidal particles, which are not retained by the RAM-SPE copolymer.

*Table 8.3. Spike recoveries (RR) of atrazine and ametryn in soil leachates after steady-state bioaccessibility assays*

| *Soil* | | *Sandy* | | *Clayey* | |
|---|---|---|---|---|---|
| *Analyte* | | *Ametryn* | *Atrazine* | *Ametryn* | *Atrazine* |
| *Steady state bioaccessible concentration (µg/L) ($A_1$+$A_2$)* | | *70* | *49* | *71* | *44* |
| *spike 100 (µg/L)* | *found (µg/L)* | *155 ± 15* | *156 ± 16* | *164 ± 6* | *128 ± 8* |
| | *RR (%)* | *91 ± 9* | *104 ± 11* | *96 ± 3* | *89 ± 5* |
| | *p (> 0.05)* | *0.40* | *0.67* | *0.37* | *0.20* |
| *spike 200 (µg/L)* | *found (µg/L)* | *263 ± 25* | *222 ± 19* | *254 ± 5* | *220 ± 10* |
| | *RR (%)* | *87 ± 9* | *89 ± 8* | *94 ± 1* | *90 ± 4* |
| | *p (> 0.05)* | *0.30* | *0.29* | *0.06* | *0.19* |
| *spike 300 (µg/L)* | *found (µg/L)* | *320 ± 45* | *300 ± 27* | *337 ± 23* | *311 ± 30* |
| | *RR (%)* | *86 ± 12* | *86 ± 8* | *91 ± 6* | *90 ± 9* |
| | *p (> 0.05)* | *0.36* | *0.23* | *0.29* | *0.36* |

Enhancement factors were estimated as the sensitivity ratio of the proposed flow-based system with in-line SPE against a conventional manual LC strategy with 40-µL standard injection by autosampler (see figure 8.5. for illustrative chromatograms). With the proposed system, there were partial losses of triazines due to heart-cut injection, which was confirmed by the enhancement factors of 10.2 and 18.8 for ametryn and atrazine, respectively. The difference in enrichment factors is attributed to the higher solubility of ametryn in water (1850 mg/L) in relation to atrazine (33 mg/L) [272,303] with the potential pre-elution of the former in the course of the sorbent rinsing prior to elution as a result of the inferior sorption coefficient onto reversed-phase copolymeric sorbents.

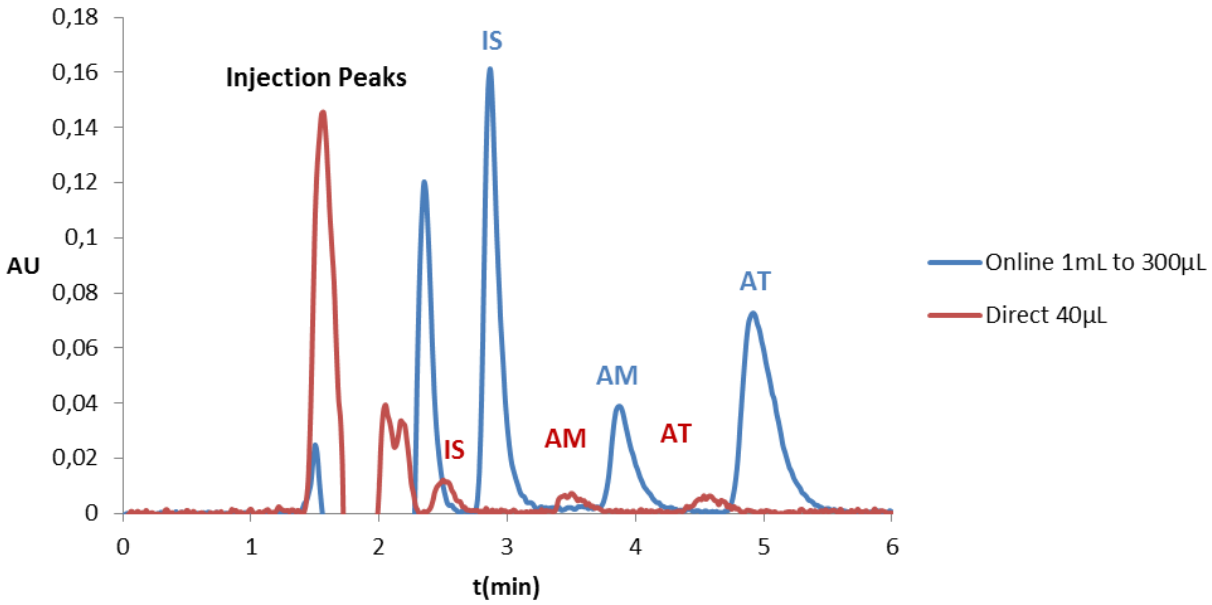


*Figure 8.5. Chromatogram of the on-line hyphenated system (blue line) obtained by injection of a 1.0 mL standard at the 200 µg/L level through the RAM-like sorbent followed by elution and hear-cut HPLC injection of 300 µL methanolic eluate as compared with direct off-line injection (red line) of the same standard. AM: Ametryn. AT: Atrazine, IS: Prometron (Internal standard at 250 µg/L level)*

The LOD of the on-line SPE-LC method based on the 3 σ/s criterion (σ = estimate of the standard deviations of results related to 10 consecutive measurements of the blank or baseline noise around the retention time of targeted species; s = slope of the analytical curve) [304] were estimated as 0.40 and 0.37 mg/kg for ametryn and atrazine, respectively. These data correspond to 0.016 and 0.015 mg/L in the extracting solution for ametryn and atrazine, respectively. The LOD (for 1 mL sample) and relative recoveries are better than those reported for a flow-based system encompassing in-line sorptive retention of atrazine from spiked waters onto C18 membranes using a 3-fold increased sample volume (sample volume: 3 mL, LOD: 22 µg/L, recoveries: 85 – 106%) [302]. It should be stressed that the samples in [302] are less prone to interfering effects as compared to soil extracts, and that the spike levels (600 µg/L) used in recovery tests were far exceeding the maximum allowed concentration of triazine in waters, set at 3 µg/L by US-EPA.

Good intermediate (inter-day) precision was obtained for five replicate measurements of steady-state concentrations in bioaccessibility tests of atrazine and ametryn with relative standard deviations ranging from 8.6 to 14.0% and 2.0 – 9.6% for sandy and clayey soil, respectively.

With the proposed system, detectability can be improved by increasing the sample volume (> 1.0 mL) of the soil extract submitted to SPE. Consequently, the determination of herbicides residues is possible even several weeks after the initial application in crops.

# 9. On-line coupling of dynamic accessibility tests to HPLC using bead-injection mesofluidic platform for monitoring leaching kinetics of xenobiotics in environmental solids

## 9.1. Introduction

As indicated in the introduction of this dissertation and chapter 3, bioaccessibility tests serve to elucidate the chemical hazard of an environmental solid sample potentially contaminated with organic compounds more accurately than total extractions with organic solvents and harsh extraction conditions, which usually overestimate the associated risks to biota. Bioaccessibility tests for organic pollutants consist of a mild extraction of the sample with a given extractant under operationally defined conditions. Recently it has been demonstrated (also by us in chapter 6) that the prescribed duration of the assay can be not sufficient for some samples [110], with the consequent artefacts for risk assessment studies, and waste of resources it implies. Monitoring of the leaching kinetics allows to custom fit experimental conditions (e.g., steady state regime) to every sample, avoiding operationally defined conditions stated by regulations or other authors in studies with a limited number of samples. However, conventional methodologies for monitoring leaching kinetics tend to be cumbersome or require substantial resources or sample amount [14] so there is a trend to automate them using a minimum of added dedicated instrumentation.

It has also been demonstrated that the analyte solubility in the leaching medium can limit the test applicability, rendering the so-called sink problem [305]. There are two distinct steps involved in any extraction process involving solid samples, that is release of target species from their original binding sites and diffusion through the sample pores toward the particle surfaces, and partitioning of the species from the surface into the extraction solvent. The bioaccessibility concept assumes that the rate limiting step of the overall extraction is the analyte desorption step [306] and therefore practical measures should be adopted to circumvent saturation of the

extraction phase.

Several attempts reported in the literature to ameliorate the sink capacity usually involve the incorporation of sorptive sinks in a three-phase sorptive extraction model [25,49,53,55–57,307] so as to maintain concentration gradients driving the desorption process, however they are not free from drawbacks as pinpointed in the introduction of chapter 3. An elegant and straightforward alternative to the batch counterparts to alleviate sink issues is the fast removal of desorbed compounds by continuous flowing of the extractant. This is readily accomplished in dynamic extraction/fractionation methods [226], where the sample is inserted in a fluidic manifold and perfused continuously. While the desorbed compound are removed from the medium in contact with the sample, the activity gradient of the analyte between the sample and the medium and thus desorption flux is maintained, mimicking closely the continuous removal of the analyte as occurring in the nature. By doing do, flow-through partitioning does serve for augmenting the sink capacity with the added advantage of potential monitoring of the leaching kinetics.

In this chapter, we propose an automatic methodology for the determination of the bioaccessible fraction of hydrophobic organic pollutants in solid samples of environmental interest. PAH have been used as model analytes because of its ubiquity, large range of partitioning coefficient (log $K_{ow}$) and inclusion in the priority pollutant list by EPA because of its toxic properties, being cancer its main endpoint, but also producing pulmonary, gastrointestinal, renal and dermic chronic effects. Benz(a)anthracene, benzo(b)fluoranthene, benzo(a)pyrene, dibenz(a,h)anthracene, and indeno(1,2,3-c,d)pyrene are carcinogenic for animals and possibly for humans, according to World Health Organization (WHO) [308], U.S. Department of Health and Human Services (HHS), International Agency for Research on Cancer (IARC) [309], the National Institute for Occupational Safety and Health (NIOSH), the US Agency for Toxic Substances and Disease Registry (ATSDR) [310] and the European Food Safety Authority (EFSA) [311]. Our method is based on the *in-vitro* beta-hydroxy-cyclodextrin assisted extraction [36,280,312–315], which is recommended in literature on the basis of strong correlations between chemical extraction data and microbial degradability or mineralization of PAHs in environmental solids [30].

Our proposal is capitalized on an SIA [288]-LOV [85,316] platform for automation and miniaturization of the bioaccessibility test in a dynamic format. The on-line extract is clean-up and analytes preconcentrated on a dedicated reversed-phase SPE for PAHs so as to obtain a cleaner matrix and adequate concentrations for detectability by instrumental methods. We have demonstrated that the organic matter remains irreversibly bound in the resin, so it is automatically disposed and renewed between successive fractions using less than 10 mg of resin each time through a BI [86,317] approach. The clean and concentrated extract is eluted and automatically analyzed by

HPLC separation through an on-line heart-cut hyphenation. The new method has been optimized, validated and applied successfully to a natural sediment sample.

# 9.2. Experimental

## 9.2.1. Reagents

All chemicals were of analytical grade or better and used without further purification. HPLC gradient BASIC grade methanol and acetonitrile were obtained from Scharlab (Barcelona, Spain). Envisolv grade dichloromethane was from Honeywell Research Chemicals (Morris Plains, New Jersey, US). (HPCD) with average molecular weight of 1380 g/mol was from Sigma-Aldrich (332593-100G, Saint Louis, Missouri, USA). Water was doubly distilled. $NaN_3$ was purchased from Sigma Aldrich, naphthalene from Panreac (Barcelona, Spain) and dibenzo(a,h)anthracene from Supelco (48574). Multicomponent calibration mixture of PAH (16 EPA priority) in acetonitrile (10µg/mL) was acquired from Sigma Aldrich (CRM 47940) and used both for the calibration and spiking of samples. Common abbreviations for the name of individual PAH have been used throughout this contribution: NAP (naphthalene), ACY (acenaphthylene), ACE (acenaphthene), FLU (fluorene), PHE (phenanthrene), ANT (anthracene), FLT (fluoranthene), PYR (pyrene), BaA (benzo(a)anthracene), CHR (chrysene), BbF (benzo(b)fluoranthene), BkF (benzo(k)fluoranthene), BaP (benzo(a)pyrene), DaA (dibenzo(a,h)anthracene), BgP (benzo(g,h,i)perylene), and I1P (indeno(1,2,3-cd)pyrene). EnvirElut PAH resin, from Agilent Technologies (Santa Clara, CA, US), is a reversed-phase styrene-divinylbenzene modified silica, designed specially to extract PAH congeners from aqueous or biological fluids, with average particle size of 40 µm, ranging from 15 to 60 µm as per SEM micrograph (see results and discussion section). Neutral polymeric divinylbenzene-N-vinylpyrrolidone Oasis HLB (Waters, Milford, Massachusetts) was used because of its balanced hydrophilic-lipophilic polarity, and featured spherical beads of average 33.5 µm particle size, 798 $m^2/g$ surface area, 7.9nm average pore size and total pore volume of 1.25 mL/g. Puriflash 50 µm spherical C18 covered silica resin from Sugelabor SA (Madrid, Spain) with 500 $m^2/g$ was also used during the experimental work. The high density of C18 (21 %C), the pore structure (6 nm average size) and the high specific surface (500 $m^2/g$) is expected to serve for expedient uptake of hydrophobic compounds. SEM micrographs were obtained from the EnvirElut PAH and Puriflash C18 in order to ascertain their shape and foresee their behaviour upon fluidic manipulation (see figures 9.3 and 9.4 in the section 9.3.2).

## 9.2.2. Samples

A marine sediment was sampled from a harbour near Cala Figuera (39º19'54.9804''N, 3º10'2.856''E), in the east coast of Mallorca and used for validation of the proposed method. The leaching agent was prepared by dissolving 75 g/L of HPCD in water [23–35] along with 0.5 g/L of $NaN_3$ used as a biocide for preventing the biotic degradation of analytes in the course of the extraction.

In order to characterize the packed resin under worst case scenario conditions for further use in LOV, a matrix matched extract containing no detectable amount of analytes was prepared by extracting 5 g of the marine sediment with 100 mL of extracting agent (L/S ratio of 20) during 24 h under 300 rpm magnetic stirring at room temperature. The extraction medium was vacuum-filtered through 0.45 µm Nylon filter and stored at 4ºC until use.

The marine sediment containing no native PAH was spiked and aged for validation purposes. To this end, 20 g of dry sediment were weighed in 50 mL amber vials. 200 µL of 16 EPA priority PAH mixture at the 10 mg/L level were added as well as 20 mL MeOH in order to get a final spiking level of 100 µg/kg, far below the maximum allowed concentrations and standards for for the declaration of contaminated solids by PAHs according to National regulations [4]. The vials were capped with a teflon lined cap and shaken vigorously during 2 min. The vials were uncapped and let air dry in a fume-hood until the methanol content evaporated completely and the sediment appeared loose. Then, 5 mL of water containing 0.5 g/L of $NaN_3$ were added to restore the natural hydration of the sediment. The so prepared sediment was allowed to age for 12 months in order to mimic environmental conditions.

## 9.2.3. Fluidic manifold

The fluidic setup was composed of a LOV stator furnished on a multiposition rotary valve and hyphenated with HPLC equipment through an injection valve (see figure 9.1). The LOV was ad hoc milled from transparent piece of hardened PVC in order to fit the stator of a standard 6 multiposition Vici-Valco Cheminert valve, and was mounted on a commercial µSIA setup. The µSIA module was purchased from Fialab Instruments (Bellevue, WA) and was equipped with a 5mL gastight glass syringe (Tecan, Männedorf, Switzerland). The left port of the syringe was connected to the carrier reservoir (75g/L HPCD solution). The right one was connected to the central port of the LOV via a 500-µL, 1.6 mm ID Fluorinated Ethylene Propylene (FEP) tubing from IDEX Corporation (lake Forest, Illinois, USA). Port no. 1 of the LOV was connected to a 1-mL plastic syringe body through a 1/4'' 28 male to female luer lock adapter from IDEX. Port no. 2 was connected to a methanol reservoir through a 300-µL, 1.6 mm ID FEP tube. Port no 3 was used as waste. Port no 4 was let air open as air was needed in some steps of the automatic method. Port 5 was a dual port. One end was connected

to the outlet of the sediment column through a 200 µL, 1.6 mm ID tube, and the other end was connected to the loading port of the injection valve through a 20 cm long 0.8 mm ID FEP tube through a 20 µm polypropylene frit (MoBiTec GmbH, Göttingen, Germany), that would serve for retaining the beads in the bead injection protocol. Port no 6 was connected to the inlet of the sediment column through a 1/4'' 28 male to 1/4'' 28 male adapter from IDEX. The soil holder was a PEEK biconical column described elsewhere [216], that proved in previous works to fluidize the soil bed and thus enhance the extraction speed when perfused in an upright position [318]. The injection valve was a H7000L high pressure steel Valco Injection valve furnished with a 0.8 mm ID PEEK injection coil (300 µL) mounted on a Crison Valve module (Alella, Spain). The HPLC system was composed of a Waters E600 pump and a Waters 474 spectrofluorimetric detector, controlled by the manufacturer's software (Empower Pro, Waters). The chromatographic column was a Pursuit 3 PAH, 4.6 x 100 mm (Agilent, Santa Clara, CA). During early experiments, an autosampler AIM 3200 (AIMLab, Queensland, Australia) with up to 120 positions was also used. A diagrammatic representation of the system can be found on figure 9.1 and the setup is visualized in figure 9.2.

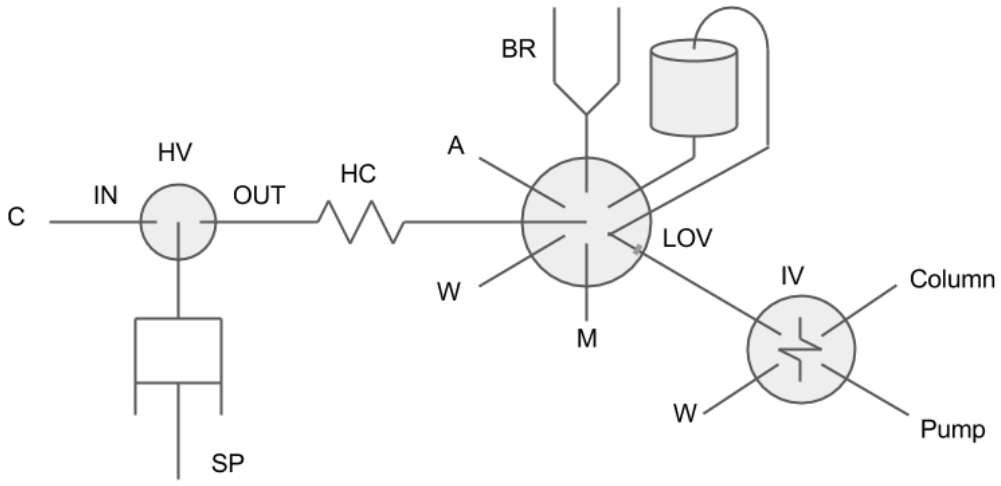


*Figure 9.1. Diagrammatic description of the LOV-SIA fluidic manifold. SP: Syringe pump, HV: Head valve, IV: High pressure injection valve, LOV: Lab on valve monolithic manifold on selection valve. HC: holding coil, BR: resin Bead Reservoir, Column: chromatographic column Pursuit 3 PAH from Agilent. Note that there is the frit in the LOV channel leading to the IV valve.*

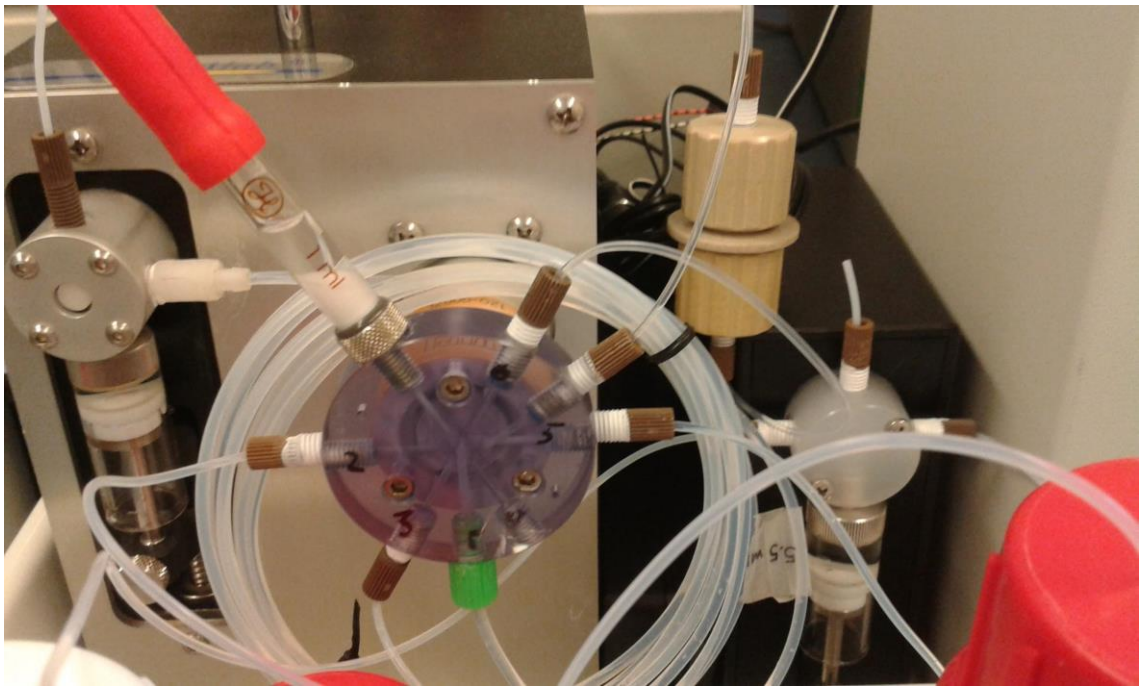

*Figure 9.2. Close-up of the LOV monolith connected to the microsyringe pump and external biconical microcolumn for on-line dynamic bioaccessibility tests.*

## 9.2.4. Fluidic control

The µSIA equipment and the high pressure-injection valve communicated with the computer through USB-RS232 adapters and were controlled by CocoSoft [164], software designed to automate analytical methodologies as well as to automate data processing (see chapter 4). The chromatographic injection was programmed in the manufacturer's software (Empower PRO) and triggered from CocoSoft in the automatic method, by means of a contact closure signal given by a relay attached to the µSIA module and the E600 pump.

The method for controlling the fluidic manifold consisted of three routines that could be called in any order depending on the specific experiment. The routines for packing and unpacking the sorbent column are comprehensively discussed in the section 9.2.8. Once the sorbent column is reproducibly packed in the channel 5 of the LOV monolithic manifold, the 0.2 g sediment-loaded biconical column on position 6 is perfused with 5 mL of HPCD solution (carrier of the LOV system) at 1 mL/min. As the extract emerges from the column, it passes through the LOV dual port where the analytes are selectively retained as cyclodextrin complexes in the previously packed SPE column, and the extract matrix is discarded. The valve position is set to 'load' position and the retained analytes are eluted with a methanol plug of 450 µL at 1 mL/min into the injection coil (see section 9.2.13, coupling of LOV-BI to HPLC). A 5 seconds delay is included for let the pressure equilibrate and then the valve is turned to the 'injection' position. The HPLC is instructed to start the gradient program through

a contact closure, and the packed microcolumn of sorbent is then discarded (see section 9.2.8). The whole process is repeated for each fraction until quantitative extraction of the bioaccessible PAHs. The chromatographic data is extracted manually but evaluated automatically with a Python script ad hoc.

## 9.2.5. HPLC procedure

The HPLC method lasts 23 minutes using acetonitrile:water mobile phase at a flow rate of 2 mL/min, T=30ºC, and gradient with an initial composition of acetonitrile of 50% and lineal segments to (acetonitrile): 80% (t = 16 min), 100% (t = 18 min), 100% (t = 21 min) and 50% (y = 23 min). PAH were detected at EX/EM (nm): 275/350 (NAP, ACE, FLU, 0-6.7 min), 274/365 (PHE, 6.7-7.8 min), 260/420 (ANT, 7.8-8.9 min), 270/400 (FLT, PYR, 8.9-12.0min), 260/420 (BaA, CHR, 12.0-15.0 min), 290/430 (BbF, BkF, BaP, DaA, BgP,15.0-20.2 min), and 250/500 (I1P, 20.2-23.0 min).

## 9.2.6. Band broadening in HPLC analysis

The effect of increasing the injection volume in the HPLC separation was studied in order to ascertain the maximum injectable volume of eluate from LOV-BI µSPE. Volumes in the range of 50 to 500 µL with concentrations from 10 to 1 ng/mL were injected from standards prepared in methanol from the same stock in order to maintain constant the amount of analyte injected but variable solvent volumes. Recoveries of the amount injected and the overall chromatogram shape were evaluated.

## 9.2.7. SPE selection

The suitability of three different SPE materials, namely Envir Elut, C18 and Oasis HLB was evaluated by packing commercial SPE cartridges with 30 mg of each resin, loading 8 mL of standard prepared in 75 g/L HPCD and 0.5 g/L $NaN_3$ in an automated fashion, from a sampling cup connected to port 6 of the selection valve, and the second channel of the port 5 closed with a blind stopper and eluting sequentially in 2 fractions of 300 µL each with methanol. NAP and DaA were used as individual standards at 25 ng/mL in order to ascertain the resin behavior for compounds with a broad spectrum of polarity bearing distinct log $K_{ow}$ values (3.30 [319] and 6.75 [320] respectively). The distribution of the analytes into the eluted subfractions was used to evaluate the performance of the resin in the elution step aiming at reliable on-line HPLC coupling. The EnvirElut PAH resin was used for the remaining of the research. Further details are discussed under the results and discussion within SPE selection section.

## 9.2.8. Packing reproducibility

The beads were stored in methanol medium (ca. 0.5 g of beads and 2 mL of methanol) in a sampling cup on port 1 of the LOV, composed of a polyethylene syringe body of 5 mL and a female luer lock to 1/4 28'' adapter. The reproducibility of the packing and unpacking of the microcolumn in an LOV format was deemed the pivotal aspect of method development and was achieved by resuspending the beads before each column packing within LOV by dispensing a 100 µL plug of methanol at 6 mL/min just before the aspiration of the beads for packing into the LOV microcolumn. The methanol plug was separated from the carrier by a 10 µL air segment in order to prevent the diffusion of the aqueous HPCD solution into the bead reservoir. 30 µL of bead slurry were aspirated at 300 µL/min and a 5 seconds delay was introduced in order to let the pressure equilibrate and let the beads draw into the holding coil reproducibly. The previous air bubble served at this point for preventing the free entry of the beads into the holding coil lumen, because of surface tension reasons. The segment of beads in methanol, followed by air and carrier was dispensed to the port number 5, where a frit prevented the bead passage and trapped them into the sorptive microcolumn.

For allowing the Bead Injection mode, a method for discarding the beads after every use was developed. The method consisted of aspirating sequentially a 50 µL air bubble and 200 µL of methanol. This tandem was pushed through the packed column at 2 mL/min for wetting the beads with a low-viscosity solvent. Then the flow was reversed and the wetted column (200 µL) was aspirated at 2 mL/min. The beads were then unpacked and remained in the holding coil. The coil content was emptied toward the waste port. For preventing the beads to stick to the tubing wall, the holding coil contained previously 4 consecutive tandem segments of 20 µL air and 20 µL methanol each, so during the discarding step, the dispersed beads into the coil faced 8 methanol-air interfaces that swept them away. The whole unpacking method was repeated twice in order to ensure that no beads remained in the holding coil or the channels of the monolithic LOV manifold.

The evaluation of repeatability/reproducibility in packing and unpacking was evaluated by recovering the discarded beads, evaporating the solvent and weighing the solid material.

## 9.2.9. Microcolumn breakthrough characterization - maximum resin capacity

In order to elucidate the maximum retention capacity of the LOV sorbent column, 450 µL of the sediment extract matrix solution, obtained as described in the samples section by batch extraction during 24 h, spiked with 500 µg/L of the PAH

mixture were loaded in the LOV microcolumn. The concentration was higher than that expected in a single fraction of real samples in order to be in the worst case scenario and to saturate the sorbent microcolumn. The volume was smaller than that of real fractions to avoid chromatographic pre-elution. Once the column was loaded with the analytes, they were eluted in a very large volume (2 mL) in order to recover them quantitatively. The amount of analyte recovered will let us know the maximum capacity of the column.

## 9.2.10. Elution volume optimization

In order to get insight into the minimum volume needed for eluting quantitatively a saturated column, the column was loaded with 450 µL of sediment extract containing no native PAH, and spiked at 500 µg/L level of each EPA priority PAH. After loading and drying with 300 µL of air, the column was eluted with 50 µL of methanol with help of a 150 µL plug of air. The packed sorbent column was then discarded even if the analytes were not quantitatively eluted. The experiment was repeated with a freshly packed sorbent column for different volumes of eluting plug: 100, 150, 200, and 250 µL (see section 9.3.1, 'Band broadening of HPLC readouts').The experiments were undertaken in duplicate. The recoveries are expected to increase with increasing elution volumes up to a maximum. The minimum volume that yields the maximum recovery will be selected for the on-line heart-cut hyphenation.

## 9.2.11. Chromatographic pre-elution characterization

When the sample is being loaded into an SPE column, along with the sorption of the target analytes in the solid phase by reversed-phase interactions, there is also a parallel chromatographic elution (mass transfer) as per Van Deemter equation by the sample medium itself. This preelution effect could cause partial losses of the less hydrophobic analytes from the sorptive column before the sample is fully loaded. In order to investigate the maximum volume of extract that can be loaded into the packed column avoiding preelution of target analytes, an equimassic mixture of each of 16 EPA priority PAH (ca. 20 ng each) was loaded in increasing volumes of the sediment extract prepared in HPCD as described in the sample section. Concentrations and volumes loaded into the LOV SPE microcolumn for each elution were of 50, 5, 2.5, 1.67 ng/mL and 0.450, 4.8, 9.6 and 14.4 mL respectively in order to maintain a constant loading of ca. 24 ng of each PAH in the column. The column was then eluted with 2 mL of methanol (in order to assess the quantitative elution and minimize the manipulation steps required for bringing the sample to the HPLC) at 1 mL/min and the eluate analyzed to quantify the amount of PAH retained on the column.

### 9.2.12. Irreversible sorption of matrix components and reuse

For studying the potential interfering effects of the sediment extract upon the retention capacity of the sorbent material in a LOV configuration, the sorbent microcolumn was packed and loaded with 5 mL of 5 ng/mL of each PAH doped to the HPCD sediment extract and eluted with 900 µL of methanol that suffices for quantitative elution. The eluates were analyzed and the PAH amount quantified. The same microcolumn was reused up to 4 times.

### 9.2.13. Coupling of LOV-BI to HPLC

For hyphenating the characterized and optimized LOV-BI system described in the previous sections with HPLC, an injection valve was used as the on-line interface. The eluate of the LOV-SPE microcolumn was directed to the injection valve furnished with a 200 µL PEEK tubing. The volume of methanol used for eluting and delivery of the eluted plug to the injection loop was optimized. The volumes of tubing of the injection coil plus the tube from the packed column till the injection valve amounted to 325 µL. The sorption column was perfused with a plug of methanol ranging from 325 and 500 µL in increments of 25 µL, in order to see which volume trapped successfully the most concentrated segment of SPE eluate into the injection loop. The selected volume was 450 µL.

## 9.3. Results and discussion

### 9.3.1. Band broadening of HPLC readouts

The injection of 50 µL of PAH standard at 10 ng/mL level prepared in methanol was taken as reference. Injection of standard volumes greater than 300 µL deformed the naphthalene peak (the first coming out) significantly. The overlapping of other PAH peaks also prevented accurate quantification. Volumes larger than 50 µL but lower than 300 µL afforded smooth peak shapes with respect to the reference chromatogram, and allowed for a baseline resolution ($R > 1.5$) except for the pair ACE - FLU. Even if that pair of analytes were not baseline separated, relative recoveries ranged from 92% to 112%.

### 9.3.2. Selection of the sorbent material for µSPE in LOV-BI configuration

A SEM micrograph was obtained from the Puriflash C18 beads (figure 9.3 left), showing their spherical shape, thus anticipating easy manipulation of the slurry in the fluidic manifold. Another SEM micrograph was obtained of the EnvirElut resin (figure

9.3 right) that proves it is composed of chunks instead of spherical particles, which in turn might jeopardise the on-line handling of beads in the fluidic manifold, namely the packing and unpacking methods.

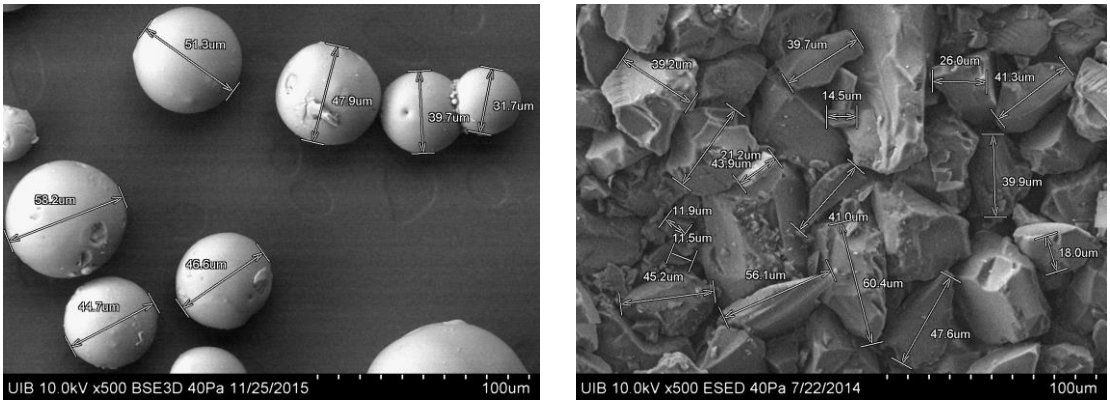


*Figure 9.3. SEM micrograph of the Puriflash C18 resin (left) and Envir Elut PAH resin (right) at x500 magnification with individual particle size measurements.*

The loaded cartridges were eluted in two subfractions of 300 µL methanol each. Those fractions were analysed by HPLC and the distribution of the analytes between the two subfractions was used for evaluating the feasibility of the resins for the BI setup (see figure 9.4).

The Oasis HLB resin required a larger volume to elute the NAP than the DaA and in general, it required more methanol to elute the naphthalene than the other two resins, because of the mixed mode hydrophilic-hydrophobic balance of this reversed-phase material. As a result, Oasis HLB was deemed inappropriate in our system because the PAH with small number of rings tend to be more bioaccessible than the PAH of large number of rings. The elution in a large volume of the small congeners would complicate the on-line hyphenation of the LOV-BI to the HPLC. Thus, the elution of the low-membered ring congeners in a small eluent volume was prioritized and the Oasis HLB resin was discarded. The EnvirElut PAH resin (EE) was selected as the most suitable resin against C18 because of the lower volume of methanol needed for eluting both the low and high-membered ring congeners (see figure 9.4). An average mass of 9.5 mg was packed for every microcolumn with an RSD of 14.6% (n = 12), thus highlighting significant sorbent savings compared with commercially available SPE cartridges with amounts > 30 mg.

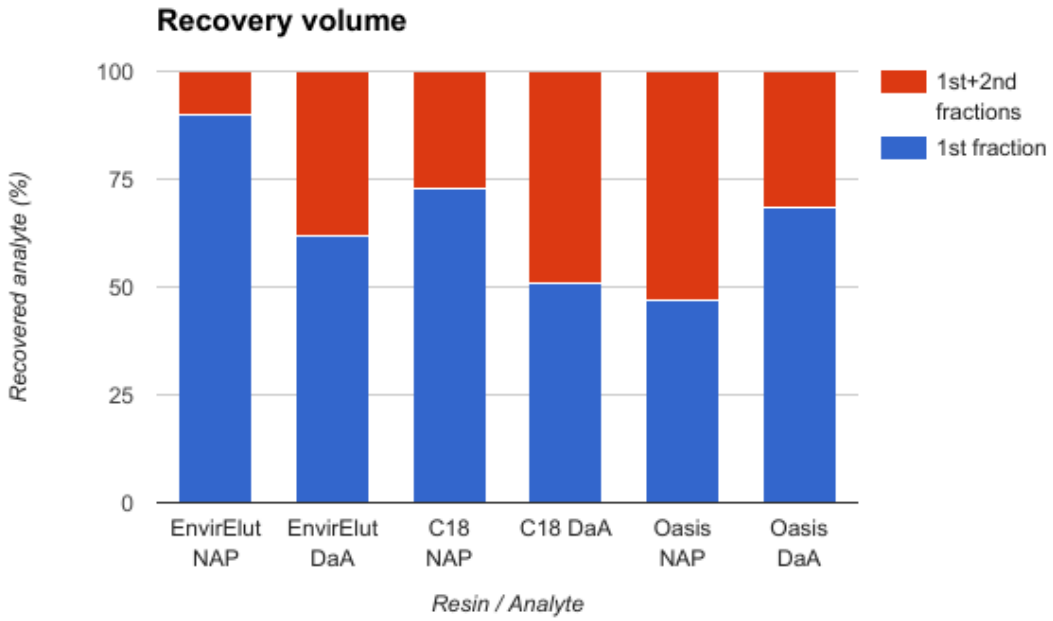


*Figure 9.4. Distribution of the recovered analytes from LOV-BI using EnvirElut, C18 and Oasis HLB materials into the 2 eluent subfractions of 300 µL methanol each.*

### 9.3.4. Microcolumn breakthrough characterization - maximum resin capacity

The analysis of the HPCD sediment extract revealed that an average of 74% in weight of the loaded compounds was recovered with 2 mL of eluent (see figure 9.5). As this volume is higher than the volume recommended for the analysis (see Elution volume optimization section), the non-recovered analytes are deemed to have passed through the column because of the saturation of the available binding sites. The summation of analyte mass of all 16 loaded compounds unveils a maximum capacity of 260 pg/mg when loaded with an equimassic mixture containing ca. 20 ng of each PAH. Note that in a competitive mode across low and high-numbered ring PAHs, the resin retains more strongly the smaller congeners than the six-membered ring counterparts, as expected because of the possibility of penetration into the pores of the sorptive beads without sterical hindrance.

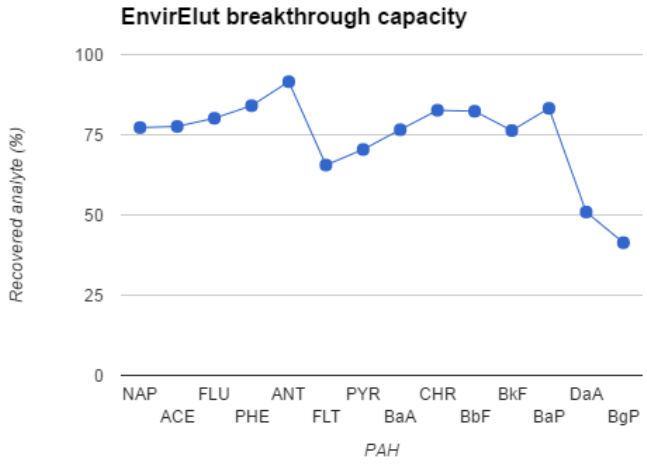


*Figure 9.5. Recovered mass of each analyte from the methanolic eluate in an LOV packed microcolumn upon saturation loading with equimassic mixture.*

## 9.3.5. Elution volume optimization

The results of the experiment described in section 9.2.10, 'Elution volume optimization', are depicted in figure 9.6. For the sake of clarity, only a representative compound for each number of rings is represented (NAP (2), PHE (3), FLT (4), BkF(5), BgP(6)). The minimum elution volume that depletes a saturated column can be set to 200 µL for the overall analytes. Note that the lower the number of rings of the molecule the higher is the amount extracted with lesser eluent. This is the expected behaviour, as PAHs with greater log $K_{ow}$ require stronger eluotropic conditions to elute quantitatively from reversed-phase materials: more volume of a given solvent or more eluotropic solvents.

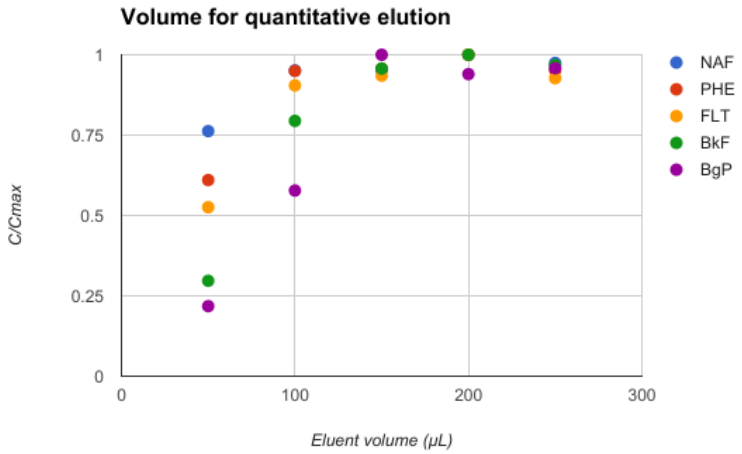


*Figure 9.6. Experimental relationship between the elution volumes and the amount of analyte released in a saturated column under LOV-BI conditions.*

## 9.3.6. Chromatographic preelution characterization

The results of the pre-elution experiments are shown in figure 9.7. For the sake of simplicity only a representative of each number of rings is depicted. Experimental revealed that the only preeluting compound in the studied range of extract volumes is the most polar specie, that is, NAP. While a mere 87.5% NAP is recovered with 5 mL of loaded extract, this volume was selected for the remaining of the study as the trade-off between the nominal preconcentration factor for the overall compounds and the wash out (pre-elution) of the most polar target species. It should be however taken into account that this experiment has been carried out under worst case conditions, thereby the amount of organic matter in every subfraction of the real sample will be lower than that of the extract used herein obtained after stirring for 24 h. Thus, the sorbent column will be exposed to less matrix interferences and the NAP will be retained strongly. The presence of NAP at high concentrations in aged natural samples is unexpected because this is the most biodegradable and soluble PAH, and bears a high vapor pressure. Thus, the fraction volume could be increased up to 15 mL for further applications, especially when dealing with low concentration of PAH with higher number of rings, otherwise the accurate quantitation of bioaccessible pools in real samples might be jeopardized by falling down to the LOQ of this work.

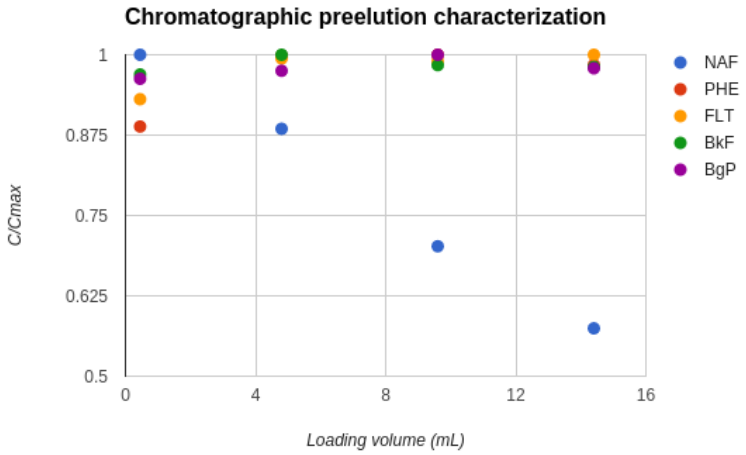


*Figure 9.7. Relationship between the recovered mass of each model PAH and the sample volume loaded into the packed sorbent. Note that NAP is the only compound to be preeluted in the considered volume range.*

## 9.3.7. Irreversible sorption of matrix components and reuse of LOV microcolumn

Except for NAP, the absolute sorptive recovery diminished severely after the first fraction and down to 12% for NAP and 35% for other PAHs in the 4th fraction, thereby indicating the need for on-line disposal of the sorptive LOV column in a bead injection format after each 5 mL extract fraction. The decrease in absolute recoveries may be due to the irreversible sorption of matrix components that block binding sites by strong hydrophobic interactions, thus decreasing the maximum capacity of the resin after every single fraction for determination of bioaccessible pools in the dynamic extraction method.

## 9.3.8. Application to real samples

The cumulated experimental data illustrating the on-line dynamic extraction of most hazardous PAHs for humans in 100 µg/mL spiked and 12 months aged marine sediment using HPCD extraction as a front end to LOV-BI-HPLC can be seen in figure 9.8 for the 15 fractions analyzed. The concentrations recovered after quantitative extraction of available pools are lower than the initially spiked because of the aging of sediment, during which a part of the bioaccessible pool became non-extractable.

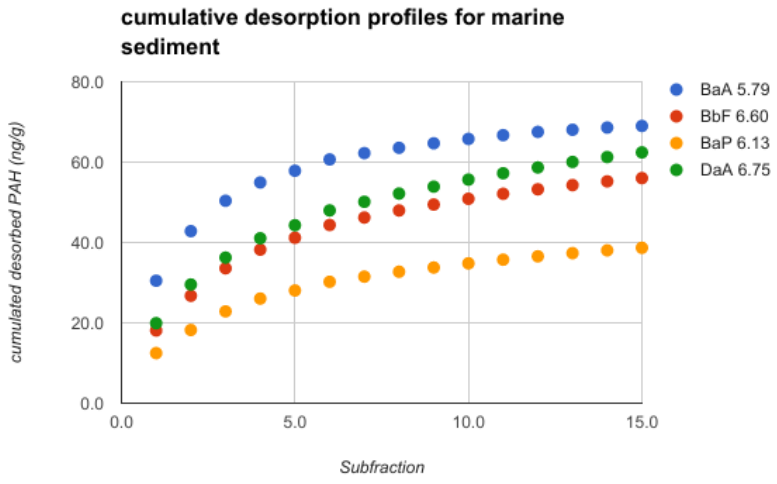


*Figure 9.8. Cumulated kinetic profiles of bioaccessible PAH from the doped sediment using dynamic flow-through extraction*

The experimental data was fitted to different theoretical equations describing desorption kinetics for one, two or three compartments (n = 1, 2 or 3 in the equation down here) into the extraction medium, in order to predict the final concentration upon exhaustive extraction of the bioaccessible pool from the sediment:

$$C = \sum_{i=1}^{n} A_i(1 - e^{-k_i t})$$

This was done in a custom made Python script exploiting the numpy's wrapper of MINPACK's lmdif [321] and lmder [322] algorithms. The deviations of the fitted parameters were also calculated by a Jacobian approximation around the solution included in the same package, instead of the Monte Carlo method described in chapter 6. Regression statistics were performed on each fit. The $R^2_{adjusted}$ parameter was used to ascertain the best fit between different models for each PAH. This statistic takes into account the number of variables present in the model, so while $R^2$ increases when more variables are added to the model, biasing the interpretation, $R^2_{adjusted}$ can be used for comparing regressions to models with different number of variables. The two compartment was the model that yielded the higher $R^2_{adjusted}$ parameter for every PAH (n=2), unveiling that two different bioaccessible pools or bioaccessibility mechanisms operate simultaneously in the desorption of the whole bioaccessible fraction, so this was the model chosen for calculating the total desorbed analyte mass upon depleting the bioaccessible PAH pools.

The readily leachable fraction of PAH is associated to $A_1$ and $k_1$ whereas the parameters $A_2$ and $k_2$ are linked to the slowly leachable fraction. The expected concentrations of every pool are shown in table 9.1 along with the associated kinetic constants, the $R^2$ parameter, the probability of Goodness of Fit ($p_{GF}$<0.05) and probability of Lack of Fit ($p_{LOF}$>0.05). The $R^2$ parameter measures the fraction of variance explained by the regression, the probability of goodness of fit indicates whether the regression is more suitable for describing the experimental data than its average, and the lack of fit indicates whether the error of the residuals is within the range of the deviation of the experimental data itself, that is, if the model fits the data properly.

*Table 9.1. Values of the bioaccessible pools of the 4 PAH carcinogenic for humans, along with the kinetic constants, the number of fractions needed for exhaustive extraction and the statistics related to the fitting: $R^2$, $p_{GF}$, $p_{LOF}$ as QC*

| PAH | BaA | BbF | BaP | DaA |
|---|---|---|---|---|
| $A_1$ (ng/g) | 35 ± 5 | 23 ± 5 | 16 ± 5 | 25 ± 4 |
| $k_1$ (fraction$^{-1}$) | 1.09 ± 0.16 | 0.79 ± 0.18 | 0.8 ± 0.2 | 0.86 ± 0.16 |
| $A_2$ (ng/g) | 35 ± 4 | 37 ± 3 | 26 ± 2 | 45.1 ± 1.7 |
| $k_2$ (fraction$^{-1}$) | 0.20 ± 0.03 | 0.13 ± 0.04 | 0.11 ± 0.05 | 0.11 ± 0.03 |
| fractions for exhaustive extraction | 13 | 24 | 28 | 27 |
| $R^2$ | 0.9526 | 0.9293 | 0.9704 | 0.8905 |
| $p_{GF}$ (<0.05) | 1.11E-16 | 4.1E-15 | 1.11E-16 | 7.1E-13 |
| $p_{LOF}$ (>0.05) | 0.99 | 0.99 | 0.99 | 0.99 |

After calculating the desorption constants for the two bioaccessible pools in the model, the number of fractions needed for depleting the pool (that is, the number of fractions for extracting more than the 95% of the overall pool) was calculated by ceiling the ln(20)/k value, on which k is the smaller kinetic constant (in our case $k_2$). The PAH whose bioaccessible fraction required a greater number of fractions to be exhausted was the BaP, that required 28 fractions. Corresponding this number of fractions to an extraction time of 11 h, the proposed method decreases the analysis time significantly as compared to the equilibrium-based batch methods proposed in the literature, with the added advantages of obtaining kinetic information, avoiding sink issues by the dynamic exhaustive method and the use of a larger L/S ratio, and less sample and extracting agent consumption, as can be seen in table 9.2:

*Table 9.2. Comparison of the proposed method against batch extraction methods reported in the literature*

| Parameter | Proposed method | Reference method [23–35] |
|---|---|---|
| Sample amount (g) | 0.2 | 1.25 - 25 |
| HPCD volume (mL) | 140 | 20 - 500 |
| L/S ratio (w:v) | 1:700 | 1:3 - 1:20 |
| Extraction time (h) | 11 | 20 - 240 |
| Kinetic information | Yes | No |

This work has potential for application of soil samples with incurred PAHs in

forensic studies for identification of potential soil uses as we have obtained of a former industrial site from the Conselleria of Environment of the Balearic Islands. Further perspectives and prospects of the hyphenated LOV-BI/HPLC binomial for dynamic fractionation of solid materials are discussed in the general conclusion section.

# 10. On-line monitoring of *in-vitro* oral bioaccessibility tests as front-end to HPLC for determination of chlorogenic acid isomers in dietary supplements

## 10.1. Introduction

Nowadays, healthy eating and good nutrition are topics of major interest worldwide. Therefore, pharmaceutical companies invest considerable efforts in developing novel food supplements, usually served in capsules or tablets that contain one or several dietary ingredients to enhance nutritional supply. They might include vitamins, minerals, herbs or other botanicals, amino acids, and additional substances, such as enzymes, glandular tissues, metabolites, or probiotics [323].

Unlike tablets, capsules are favoured in pharmaceutical and medical therapies because of their“easy-to-swallow” properties supplemented by the advantage of active substance enclosure. Therefore, consumers do not experience neither odour nor bitterness of drugs [324]. Capsules could be made using hard or soft shell components [325,326]. Hard-shelled capsules are typically made of gelatin, a naturally occurring polymer with notable hygroscopic properties [327], because of its biodegradability [328,329] and biocompatibility [330,331] in physiological environments. Shells of gelatin capsules are prepared from a molten gel mass (gelatin) and a plasticizer dissolved in an aqueous vehicle [324]. The most usual sources of gelatin production are pig skin (46%), bovine hides (29.4%) and pig and cattle bones (23.1%) [332].

Gelatin capsules are readily melted in water at a temperature above 30°C. Drug release formulations are thus expected to dissolve in the human digestive tract at the physiological temperature under the action of gastric pH and digestive enzymes [333]. In fact, the dissolution behaviour of gelatin capsules is extraction medium and experimental conditions dependent. According to US Pharmacopoeia (USP) [334], the addition of enzymes, such as pepsin or pancreatin, to the dissolution medium is allowed in dissolution testing. The addition of pepsin is recommended when the

medium is water or, alternatively, a physiologically relevant medium with a pH below 6.8. The critical factor, however, is the activity of pepsin. The recommended activity in drug dissolution testing is to not exceed 750,000 USP units per liter [325].

Green coffee extract has attracted a great deal of attention over the past few years as a food supplement commonly delivered in gelatin capsules for quick weight loss. Significance of green coffee is attributed to the presence of chlorogenic acids (CGAs), naturally occurring phenolic compounds found largely in the majority of higher plants [335,336]. They are a family of esters formed between quinic and certain trans-cinnamic acids, mostly caffeic, ferulic and p-coumaric acids. CGAs account for many positive health effects on the human body with recognised antioxidative and anticancer properties, and, most importantly, for promoting weight loss on the basis of their capacity to slow the release of glucose into the bloodstream after a meal [337,338]. Green coffee beans are the highest source of CGA, particularly caffeoylquinic acids (CQAs), ranging from 4 to 14% [339].

There have been a plethora of studies dealing with CGAs content in coffee or other foodstuffs, such as sweet potatoes [339,340], tomatoes [341], apples, and oranges [342], just to name a few. The most abundant and concomitantly most effective CGA related to health promotion as a functional food ingredient is 5-caffeoylquinic acid (5-CQA), often inaccurately called “chlorogenic acid”. It is however reported that this compound might lead to up to 9 isomers–particularly 3 – CQA and 4 - CQA in aqueous heated solutions [343].

In this chapter, a novel fully automated flow-setup integrating on-line tangential filtration as a front-end to HPLC separations is proposed for chemical and temporal profiling of dissolution tests of green coffee bearing food supplements and investigation of the release rates of three CQA acids (mostly 5-CQA, but 3-CQA and 4-CQA as well) using biomimetic digestive fluid as a proxy for bioaccessibility in the human gastric fluid. To the best of our knowledge, this is the first work reporting TFF as automatic sample processing approach in real-time monitoring of oral bioaccessibility/dissolution test assays of drugs or dietary supplements coupled to HPLC.

In contrast to pharmaceutical dosage forms, food supplements are not subjected at present to stringent regulatory control and quality assurance tests [344]. Our system is presented as a viable approach to speed up assays of green coffee bean-based food supplements to quantify the actual content of 5-CQA and isomers thereof (3-CQA and 4-CQA), detect potential cases of product adulteration and characterize the rates of CQA release under physiologically simulated experimental conditions.

## 10.2. Experimental

### 10.2.1. Samples, chemicals and materials

5-caffeoylquinic acid (5-CQA), HCl (37%), $CH_3COOH$ (100%), $NH_3$ solution (25%), orthophosphoric acid (85%), acetonitrile (HPLC gradient) and Coomassie Blue G250 dye were purchased from Sigma Aldrich (St. Louis, USA). Hard-shelled capsules of green coffee extracts, namely, Vieste-Zelená káva (Volt Retail Ltd., Great Britain) and Café Slank (Espadiet SL, Granollers, Spain), were purchased in local Czech and Spanish pharmacies. These samples are further identified as ZK (Zelená káva) and CS (Café Slank) capsules, respectively, throughout.

Two diafiltration modules in series (Vivaflow 50, Sartorius Stedim Biotech, Goettingen, Germany) housing a polyethersulfone (PES) hydrophilic membrane each with a molecular-weight cut-off of 5 kDa and featuring low binding protein characteristics-to prevent membrane fouling in the course of dissolution testing were selected for on-line tangential filtration/sample clean-up. The active membrane surface area of a single module for transfer of low molecular weight species is about 50 $cm^2$, with 15 mm wide and 300 µm deep flow channels for the donor compartment integrated in a polycarbonate case. The two modules with a nominal transfer area of 100 $cm^2$ are interconnected via an 8 cm-long PVC tubing (4.0 mm ID). Syringe filters made of PTFE, Nylon, polyvinylidene difluoride (PVDF) (Merck Millipore, Madrid, Spain) with pore size of 0.22 or 0.45 µm and cartridge diameters ranging from 17 to 33 mm were also tested in in-line sampling protocols.

The physiologically based extraction medium was prepared by dissolving a metered amount of pepsin (1.34 g) with an activity of 559 USP units/mg (Sigma) in 1 L of 0.1 mol/L HCl so as to cope with USP specifications of biomimetic gastric fluid composition containing <750,000 USP units of pepsin per litre [325].

### 10.2.2. Flow system and software for automation of unit operations

A diagrammatic description of the flow-through setup accommodating in-line diafiltration for automatic monitoring of dissolution testing of dietary supplements as a front end to HPLC separations is illustrated in figure 10.1. The flow system was assembled as follows: A 1 L glass beaker filled with a given volume of digestive fluid surrogate was placed into a water bath preheated at 37°C. A paddle stirrer set to a stirring speed of 50 rpm was inserted into the vessel and activated throughout. The donor chambers of the tandem tangential filtration units, with an inner volume of 1.5 mL each, were also fed with the sample laden dissolution medium that mimics gastric digestion as propelled by a peristaltic pump (Minipuls 3, Gilson, Middleton, Wisconsin)

operating as a liquid driver. The peristaltic pump is furnished with polypropylene-based tubing of 1.85 mm ID (PharMed Ismaprene, IDEX Health & Science GmbH, Wertheim, Germany) connected to the first module via luer inlet fitting. The retentate outlet of the second module accommodates a 0.6 mm polypropylene flow restrictor connected to 4.0 mm ID PVC tubing for sample recirculation to the extraction vessel (see figure 10.1).

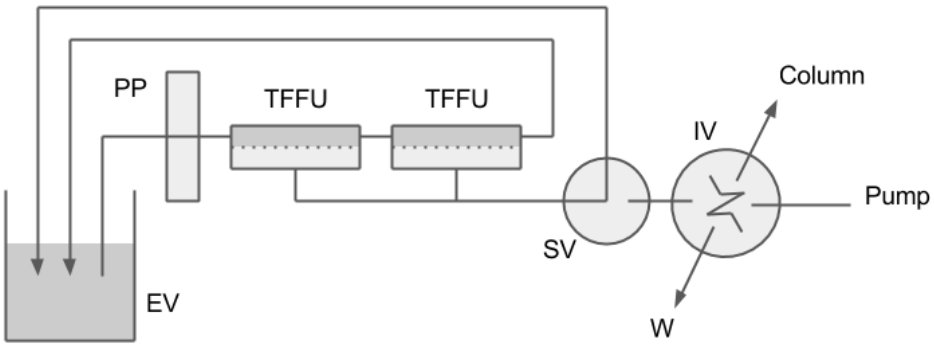


*Figure 10.1. Diagrammatic description of the flow setup with on-line tangential filtration for automatic kinetic dissolution tests of food supplements as a front end to HPLC. PP: peristaltic pump, TFFU: TFF units, SV: selection valve, IV: injection valve, W: Waste, EV: extraction vessel.*

The acceptor channels of the tandem filtration units were joined to a Y-barbed fluidic junction (1.58 mm OD, 0.75 mm ID) using a 5-cm long Tygon flexible tubing (1.14 mm ID). The outlet of the flow confluence was connected to the central port of a multiposition valve (SV, Cheminert, VICI AG international, Schenkon, Switzerland) for directing the filtrate back to the extraction vessel (port 8, see figure 10.1) or alternatively (port 2), under precise time control, to a two-position, high-pressure IV with large bore 10–32 ports (model RH-7000L, stainless steel stator, Rheodyne, IDEX Corporation, Oak Harbour, WA) for chromatographic separations of CQAs isomers in protein-free samples (see figure 10.1). The high-pressure injection valve is furnished with a PEEK injection coil (1.58 mm OD, 0.75 mm ID, 15 cm long) with an inner volume of ca. 67 µL. The low-pressure V1 and the high pressure V2 valves were precisely controlled by the CocoSoft freeware (version 4.3) described in chapter 4.

## 10.2.3. Chromatographic equipment and experimental conditions

The HPLC setup is composed of a Waters 600 high-pressure gradient pump, flow controller, column thermostat, and a Waters 2996 photodiode array detector. LC eluents were degassed by means of helium (99.999%) flow at 30 mL/min prior to use. Reversed-phase separations were performed at 40°C using a Kinetex C18 core-shell analytical column (250 x 4.6 mm, 5µm, Phenomenex. Torrance. CA, USA) preceded by a C18 Security Guard™ ULTRA precolumn (2 x 4.6 mm, Phenomenex). Eluent A consisted of water and eluent B of acetonitrile/water (97:3, v:v), both containing 0.2% (v:v) of acetic acid. Gradient elution at a flow rate of 1 mL/min was performed as follows: 0–7 min with 15% B, increase to 100% B in 2 min, 2 min hold at 100% B, decrease to 15% B in 5 min and finally an equilibration step with 15% B lasting 10 min before the next injection. The detection of CQAs isomers was accomplished by a PDA at 330 nm and quantitation was done using peak area measurement. Positive identification of bioaccessible CQA isomers in dietary supplements was done by using pure standards of 5-CQA and isomerization results for 3-CQA and 4-CQA as per literature data [345]. Running of the LC-gradient sequence, chromatogram recording, and data processing were performed automatically by a PC operated under the Empower software (Waters). The chromatographic run was started by *ad hoc* contact closure input on the Waters 600 high pressure pump, controlled by a custom made relay operated by CocoSoft [164].

## 10.2.4. Analytical procedure

*In-vitro* oral bioaccessibility/dissolution testing was carried out in this work using 500 or 900 mL of simulated gastric fluid (0.1 mol/L HCl and 749,060 USP units of pepsin/L) as contained in USP type 2 (paddle) apparatus as described above. A water bath fostered holding the temperature inside the vessel at 37 ± 0.5°C. All these conditions were used according to USP general chapters 711, 1092 and 2040 [326,334,346] for dissolution tests of drug formulations.

The analytical procedure initiates with pre-heating of the gastric biofluid at 37°C for ca. 15 min, whereupon a single hard shelled gelatin capsule containing CQA is allowed to sink to the bottom of the vessel before starting blade rotation at 50 rpm. A piece of metal wire is coiled around the solid dosage form to preclude floating. The peristaltic pump is then activated at 11.8 mL/min to recirculate the extractant medium through the tandem tangential flow-through filtration unit. The outlet pressure is controlled by the flow restrictor indicated above so as to receive a protein-free filtrate flow at 0.6 mL/min. The filtrate is continuously brought back to the feed beaker unless in-line sampling and LC analysis are undertaken. At the sampling time, the switching valve is turned automatically to the port communicating with the high pressure HPLC

valve (see figure 10.1). Temporal extract profiles were recorded by probing the leachates at 10, 20, 40, 80, 120, 160, and 200 min. In every sampling cycle, the filtrate solution first cleaned the IV loop so as to avoid sample cross-contamination effects and then filled the loop. The sampling step lasted merely 1 min so only 0.6 mL of the filtrate were used. Because of withdrawing of such a small sample volume from the overall extraction milieu (viz., 500 or 900 mL), its replacement was not performed, but the decrease of the extraction volume (in the order of millilitres) was included in the calculation of the concentration of bioaccessible pools of CQAs in every sampling step. The evaporation of the extraction medium throughout the dissolution process was also taken into consideration. At every sampling time, the volume of solvent evaporated was estimated by the weight loss of the extractant containing beaker and the average density of the gastric fluid surrogate (1.05 g/mL). In the preheating step, the evaporation effect was proven negligible.

Once the IV loop was filled, the HPLC valve was automatically switched to the inject position for 30 s for introduction of the extract into the chromatographic column, whereupon it was turned back to the load position. Notwithstanding the fact that the three target CQA isomers eluted approximately in 5.1 min the chromatographic run was extended to 26 min for eluting other food supplement ingredients out of the column and conditioning the stationary phase to initial conditions. Taking into account the temporal resolution set in this work, the filtrates collected at 20 and 40 min had to be parked in the loop of the HPLC valve and remained there until completion of the previous chromatographic run.

After recording of the temporal profiles, the tandem tangential filtration unit was cleaned with 250 mL of 0.5 mmol/L NaOCl in 0.5 mol/L NaOH according to manufacturer's recommendations. The units were also rinsed with 100 mL of a fresh extraction medium so all the tubes and module channels were filled with gastric fluid surrogate prior to the ensuing assay. The overall inner volume of the donor compartment (tubing and two tangential filtration units) was 12.5 mL. Therefore, the volume of digestive fluid used in every assay was set to 512.5 and 912.5 mL for 500-mL and 900-mL dissolution testing, respectively.

## 10.2.5. Method validation

The on-line sample processing method coupled to HPLC for oral bioaccessibility/dissolution testing and quantitation of CQA isomers in dietary supplements was validated for specificity, linearity, trueness and precision as endorsed by USP guidelines [346] along with the investigation of the mass transfer efficiency of the tandem flow-through tangential filtration unit.

Method specificity was evaluated by analysis of a placebo sample. This was effected by removing the active substance out of the hard-shelled gelatin capsule. The

placebo was transferred to a separated vessel with 500 mL of dissolution medium at 37 ± 0.5°C and stirred for 200 min at 50 rpm using the same unit operations as for the real samples. Afterwards, aliquots were analysed on-line by HPLC.

The regression equation was established by matrix matched calibration of standards of 5 - CQA at the 1, 5, 10, 20, 40 and 80 mg/mL level in 0.1 mol/L HCl without pepsin. Method trueness was evaluated by spike recoveries because no commercially available reference standard materials for CQAs in food supplements were found in the major CRM manufacturers. Once steady state extraction conditions were identified by the on-line monitoring system, a known metered amount of 5 - CQA was added to the dissolution medium. The mixture was let to re-circulate through the tangential filtration units for 45 min, whereupon the filtrate was analysed on-line by HPLC using the very same flow system configuration. The spikes were extractant volume dependent. For a 500 mL medium, two spike additions of ca. 10 mg of 5 - CQA each were effected so that the concentration of the most abundant CQA in green coffee beans increased by about 20 mg/mL over the background concentration (namely, 5 - CQA leached from the dietary supplement) at the first, and 40 mg/mL at the second spike level. For 900 mL, two spike additions of 20 mg each were effected, whereby the 5-CQA concentration in the vessel increased by ca. 22.2 mg/mL and 44.4 mg/mL, respectively.

To evaluate the precision of the method, working solutions of 5 - CQA at concentrations levels of 5, 10 and 40 mg/mL in 0.1 mol/L HCl were analysed with the fully automated system. Repeatability (intra-day) and intermediate precision (inter-day) were evaluated based on RSD of six replicated data values.

The mass transfer efficiency of the tandem flow-through PES diafiltration unit for CQAs in 0.1 mol/L HCl was evaluated by comparing direct HPLC injection of standard solutions at three different concentration levels (5, 10 and 40 µg/mL, n = 3) against injection preceded by on-line tangential filtration (n = 3). This study was performed with the as-received filtration unit and compared against the very same unit after recording the temporal dissolution profiles for 200 min each of 9 individual green coffee bean capsules at a loading flow rate of 11.8 mL gastric juice/min, so as to evaluate the potential reuse of the diafiltration membrane for oral bioaccessibility tests with appropriate chemical conditioning and rinsing procedures.

## 10.2.6. Isomerization and determination of CQA isomers

With the pursuit of identifying and quantifying CQAs isomers in green coffee bean supplements, 5-CQA was used as the single standard and subjected to isomerization prior to HPLC analysis. The isomerization procedure is as follows: 200 mg of 5 - CQA were dissolved in distilled water (20 mL) and the pH was then adjusted to 8.0 with 4 mol/L of $NH_3$. This solution was heated for 30 min in a boiling water bath

and, after cooling to room temperature, the pH was adjusted to 2.5 with 4 mol/L HCl. A mixture of 5, 4 and 3 - CQA as major isomers was then obtained and analysed by our HPLC method. Quantification was based on peak-area measurement and by comparison with a 5 - CQA standard and literature data for reversed-phase separations of CQAs [345]. The concentration of individual isomers, also in real sample analysis, was calculated using molar extinction coefficients, according to the equation below:

$$c = \frac{RF\varepsilon_1 A}{\varepsilon_2}$$

Where c is the concentration of the target isomer in mg/mL; RF is the response factor of the 5-CQA standard (viz., concentration of the isomer in milligrams per millilitre per unit area); A is the peak area of the isomer at the corresponding retention time; $\varepsilon_1$ is the molar absorptivity of 5-CQA; $\varepsilon_2$ is the molar absorptivity of the target isomer. Molar absorptivity coefficients at λmax=330 nm are as follows: 5-CQA=1.95 x$10^4$ L/mol/cm, 4-CQA=1.80 x$10^4$ L/mol/cm, 3-CQA=1.84 x$10^4$ L/mol/cm [345]. Results were calculated as mg/g of the individual target isomer in the solid dosage form.

# 10.3. Results and discussion

## 10.3.1. On-line sampling and sample clean-up protocols

Bearing in mind that cross-linked gelatin from hard-shelled capsules is composed of approximately 90% (w/w) of proteins [347] appropriate unit operations should be ascertained for efficient removal of dissolved proteins in the extraction milieu in the course of the assays so as to protect the HPLC reversed-phase particulate column from clogging. Sample preparation is in fact deemed imperative in on-line chemical profiling of drug formulation dissolution processes coupled to modern analytical instrumentation [348]. To this end, syringe filters of varied hydrophobic/hydrophilic materials and pore size as indicated in Experimental were assayed for in-line cross-flow filtration after steady-state leaching or complete dissolution of the ZK and CS green coffee capsules and compared against TFF using a 5 kDa PES membrane. Taking into account that the composition of the dissolution medium is not provided by USP for food supplements, three different extraction milieus (namely, deionised water; 0.1 mol/L HCl; and 0.1 mol/L HCl containing 749,060 USP units/L of pepsin, 100 mL each) were examined due to expectations of different leaching behaviour of the gelatin-laden hard capsules. A variety of filtration devices (see Experimental) under virtually identical experimental conditions as for the real sample analyses were assayed. Analysis of the protein content in the several filtrates was effected by the colorimetric Bradford test using the microassay method by Kruger [349]. The concentration of protein was determined as the ion-paired complex with Coomassie Blue G-250, which was detected spectrophotometrically at 595 nm. Bovine serum albumin (BSA) was

used as a model protein with a regression line spanning from 10–250 µg/mL.

Experimental results compiled in table 10.1 revealed that there were no significant differences in the concentration of dissolved proteins using either distilled water or 0.1 mol/L HCl as extractants. On the other hand, a slight decrease of the amount of Bradford proteins was identified by the proteolytic action of pepsin. Out of the varied filtration materials and modes, TFF was proven to afford protein-free filtrates throughout. The concentration of Bradford proteins in the filtrates were in all tested media below the LOQ of the analytical procedure. On the contrary, percentages of dissolved proteins within the range of 47 – 73% and 76 – 100% were measured for Nylon and PVDF syringe filters respectively with dead-end filtration. Moreover, PTFE syringe filters with pore size of 0.22 mm were proven inappropriate due to filter clogging after processing of a mere few millilitres of extracts. Taking into account that direct injection of proteolytic enzyme digests into HPLC is not practicable, TFF using a PES membrane with a 5 kDa cut-off was accommodated as on-line unit operation for the remainder of the studies. The transfer efficiency of the TFF unit for 5 - CQA at the 5, 10 and 40 µg/mL levels in 0.1 mol/L HCl (n = 3 for each level) expressed in terms of concentration ratio between acceptor and donor solutions were 98.1 ± 0.4%; 96.9 ± 1.3% and 95.1 ± 1.5%, respectively, for a fresh filtration unit with only a minor decrease in performance down to 94.1 ± 0.8%; 92.9 ± 1.7% and 92.1 ± 3.1%, respectively, after on-line processing (n = 3 in each level) and re-circulating of more than 21 L of CQA-laden gastric juice, thus denoting the utility of the regeneration protocol detailed in Experimental.

*Table 10.1. Concentration of proteins in filtrates (mg/g) for comparison of tangential and dead end filtration using distinct materials for protein depletion of dissolved hard-shelled capsules using a variety of extraction milieus*

| | | *Distilled Water* | *0.1 mol/L HCl* | *0.1 mol/L HCl + pepsin* |
|---|---|---|---|---|
| *PES tangential flow 5 kDa* | *CS* | *<LOQ* | *<LOQ* | *<LOQ* |
| | *ZK* | *<LOQ* | *<LOQ* | *<LOQ* |
| *NYL 0.45 µm syringe filter* | *CS* | *121 ± 5* | *110 ± 4* | *85 ± 12* |
| | *ZK* | *92 ± 9* | *84 ± 5* | *62 ± 4* |
| *PVDF 0.45 µm syringe filter* | *CS* | *19 ± 9* | *192 ± 6* | *180 ± 11* |
| | *ZK* | *110 ± 9* | *96 ± 10* | *73 ± 5* |
| *Without filtration* | *CS* | *193 ± 8* | *201 ± 10* | *179 ± 9* |
| | *ZK* | *132 ± 7* | *115 ± 10* | *96 ± 4* |

*CS average weight = 0.43 g, ZK average weight = 0.52 g, LOQ = 1.2E-2 µg/mL of BSA, LOD = 3.9E-3 µg/mL of BSA. Results are expressed as mean ± standard deviation (n=3)*

## 10.3.2. Effect of L/S ratio on the dissolution/oral bioaccessibility test

Monitoring of the dissolution rates of green coffee capsules and release of CQA isomers at real time was conducted at two distinct volumes of digestive fluid for the CS type hard capsules, taken as a model sample. Extractant volumes of 500 [350] and 900 mL [351–353], which are in compliance with USP dissolution tests of drug formulations, were explored. The larger the L/S ratio the greater the mimicry of physiological extraction conditions is [54,354]. The expected dissolution profiles of CQA isomers (see figure 10.2) were calculated on the basis of the chromatographic datasets of filtrates obtained by on-line discrete sampling and the temporal variation of the extractant volume in the course of the assays as a consequence of solvent evaporation and the sampling step itself. The decrease in extractant volume within the experimental timeframe (0-200 min) was < 4.5% and < 2.5% for the 500-mL and 900-mL assay, respectively. The chromatographic readouts of 3, 4, and 5-CQA isomers for the dynamic samples collected during the dissolution/bioaccessibility test within the timeframe of 10 – 200 min are illustrated in figure 10.2.

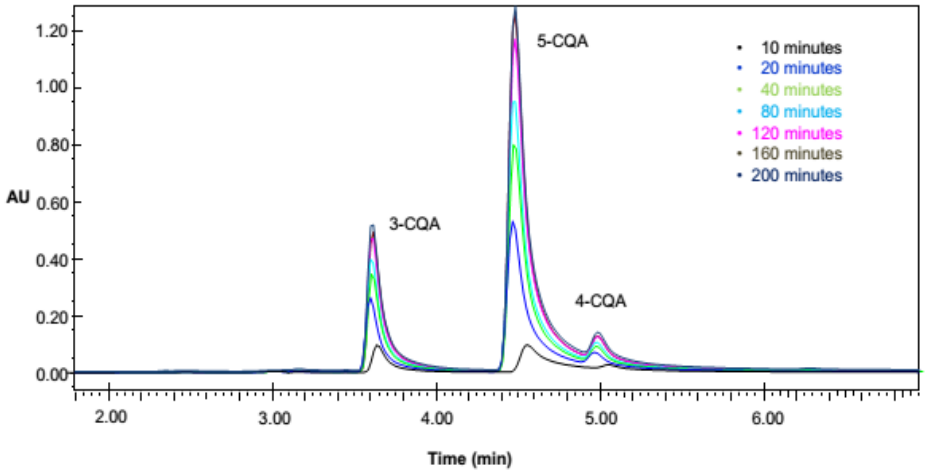


*Fig. 10.2. On-line temporal dissolution profiles of CQA isomers from dietary supplements (CS capsule) as determined by TFF as a front end to reversed-phase chromatography at increasing monitoring times (10, 20, 40, 80, 120, 160 and 200 min).*

Experimental results in figure 10.3 indicated that the L/S ratio does not have a statistically significant influence at the 0.05 significance level onto the bioaccessible pool of 5-CQA and the overall bioaccessible amount of CQA isomers under steady-state conditions for the CS dietary supplement (76.1 ± 1.8 mg/g for the 500-mL test against 73.1 ± 1.2 mg/g for 900-mL test), yet dissolution rates are strongly dependent upon the L/S ratio (see section 10.3.5). Slight differences in steady-state concentrations are found for the two less abundant CQA isomers in the CS capsule as a result of undue sample dilution in the 900 mL-test.

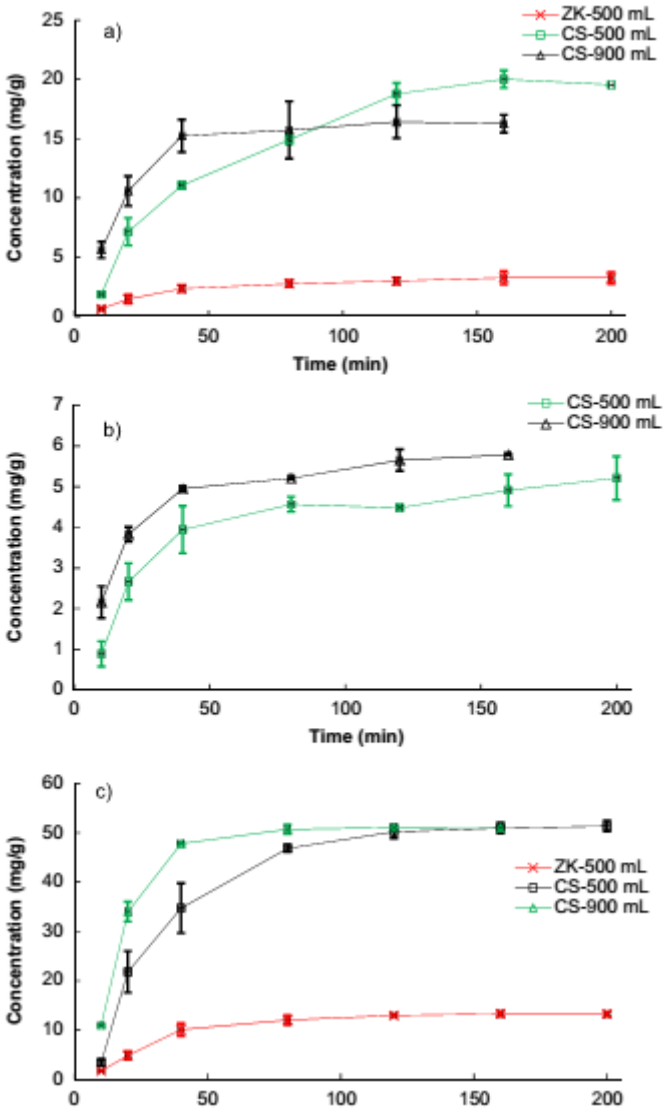


*Fig. 10.3. On-line temporal dissolution profiles as obtained by TFF as a front end to HPLC for CS and ZK capsules: (a) 3 - CQA; (b) 4 - CQA and (c) 5 - CQA (n = 3).*

## 10.3.4. Validation of the on-line dissolution/bioaccessibility test

The automatic flow method incorporating on-line sample processing prior to HPLC for unattended temporal profiling of the dissolution process of coffee bean extract-containing dietary supplements was validated for specificity, linearity, LOD, LOQ, trueness and precision according to the USP recommendations and ICH guidelines [355].

### 10.3.4.1. Linearity, LOD and LOQ

According to USP 1092 chapter on validation of dissolution procedures [346], the recommended concentration range in calibration curves should be +20% above the highest and -20% below the lowest expected drug concentration in the dissolution

test. A six point practical calibration curve spanning from 1.0 to 80 µg/mL of 5-CQA for use in real samples was evaluated by plotting peak area versus concentration. The sensitivity of the calibration graph was 214898 (in mL/µg) with a determination coefficient of 0.9990. LOD and LOQ of 5-CQA calculated on the basis of the signal to noise ratio (S/N) of 3 and 10, respectively, were 8.5 µg/L and 28.3 µg/L, respectively. The concentrations of 3-CQA and 4-CQA isomers in the gastric fluid extracts were calculated on the basis of the equation given in the Experimental section. Based on the LOQ of 5-CQA and the molar absorptivity ratio between 5-CQA and each of the less abundant isomers, LOQs for 3-CQA and 4-CQA were estimated as 30.0 and 30.7 µg/L, respectively.

## 10.3.4.2. Specificity

The specificity of the on-line tangential filtration/HPLC method for real-time monitoring of the dietary supplement dissolution process was evaluated by placebo analysis. Shells of CS and ZK capsules underwent this test. A comparison of chromatograms from placebo analysis (0.1 mol/L HCl and 749,060 USP units/L of pepsin with empty hard-shelled CS-type capsule) and the standard solution after isomerization analysis containing a mixture of CQA isomers is given in figure 10.4. Identical results were obtained with ZK placebo. Experimental data demonstrated that the proteolytic extract of gelatine shells by pepsin in 0.1 mol/L HCl did not contain any interfering species of molecular weight <5 kDa that might interfere with the chromatographic separation of 3-CQA, 5-CQA and 4-CQA.

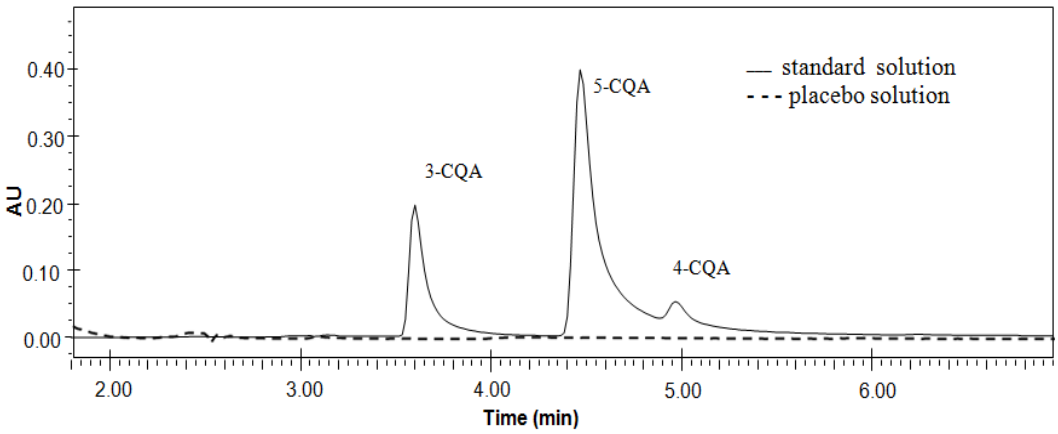


*Fig. 10.4. Method specificity evaluated by comparison of chromatographic readouts of a 20 µg/mL standard solution after isomerization (3-CQA, 5-CQA and 4-CQA) against placebo (gelatin capsule without active ingredient)*

## 10.3.4.3. Precision, trueness and comparison with previous methods

The repeatability (intra-day) and intermediate precision (interday) of the on-line sample processing/HPLC method obtained by replicate analysis of 5-CQA standards in 0.1 mol/L HCl at the 5.0, 10, and 40 µg/mL level were 3.4%, 2.0% and 0.2% and 4.2%, 5.5%, and 3.9%, respectively.

Trueness of the analytical method was evaluated by spike recoveries at two concentration levels upon reaching steady-state dissolution conditions as indicated in the experimental section 10.2.5. Relative recoveries for 5-CQA ranging from 91.5% to 104.0% were obtained in all instances regardless of the dietary supplement supplier and the L/S ratio (see table 10.2), which indicates that the analytical results herein reported lack bias.

*Table 10.2. Trueness of the on-line TFF method coupled to LC as determined by spike recoveries of 5-CQA in physiologically based gastric fluid upon quantitative dissolution of the hard-shelled capsule.*

| *Capsule* | *Added (µg/mL)* | *Measured (µg/mL)* | *RR (%)* |
|---|---|---|---|
| | | *14.1 ± 0.6* | |
| *ZK (500 mL-test)* | *20* | *32.4 ± 0.5* | *91.5* |
| | *40* | *53.0 ± 1.4* | *97.2* |
| | | *49.7 ± 1.2* | |
| *CS (500 mL-test)* | *20* | *68.0 ± 1.2* | *91.5* |
| | *40* | *91 ± 2** | *104.0* |
| | | *26.0 ± 0.4* | |
| *CS (900 mL-test)* | *20* | *48.5 ± 0.5* | *101.4* |
| | *40* | *69.1 ± 1.2* | *97.1* |

*Results are expressed as the mean of three replicates ± standard deviation. *This sample was diluted 1:4 in gastric juice prior to injection into HPLC.*

A variety of methods capitalising on HPLC and capillary zone electrophoresis separations and voltammetric assays have been reported earlier in the literature for quantification of CQA in coffee bean extracts, beverages, drug formulations and tobacco residue powers. Notwithstanding the fact that the previous procedures were not harnessed to assays of CQA-containing digestive fluids extracts our method features improved relative recoveries as compared to capillary zone electrophoresis and electrochemical methods with recoveries ranging from 89–117% [356,357], three orders of magnitude better LOD (8.5 µg/L against 10 mg/L) with respect to a previous liquid chromatographic method [358] and superior precision as compared to voltammetric methods in which RSD values spanned from 2.6–6.7% [356,359] in contrast to 0.2–5.5% in our case.

## 10.3.5. On-line temporal dissolution profiles and measurement of dissolution rates

Proteolytic extract aliquots of green coffee bean supplements were subjected to on-line TFF followed by HPLC separation at 10, 20, 40, 80, 120, 160 and 200 min (see figure 10.2) to generate temporal dissolution profiles of individual CQAs at real time.

A first-order dissolution model was evaluated to fit the experimental data to non-linear regression. The cumulative concentration of individual isomers extracted with digestive fluid at time t (C(t), mg/g) is proven to fit an exponential decreasing function as described previously in chapters 3 to 9:

$$C = A(1 - e^{-kt})$$

where A is the maximum concentration of CQA isomer released under steady-state conditions (mg/g) and k the associated kinetic constant. Those parameters can be found in table 10.3 along with its standard deviation obtained by Monte Carlo simulations, and the lack of fit test of every individual profile, which indicated that almost all variance is accounted for with the variables A and k specified in the model ($p >> 0.05$ in all instances), and this is corroborated with the determination coefficients listed in table 10.3 with $R^2 > 0.9$ in all but 3 - CQA in ZK capsule. The rates of release of the three isomers spanned from 1.25 – 5.13 $h^{-1}$ with no statistically significant differences at the 0.05 level between CS and ZK capsules for 5 - CQA. The dissolution rates of 3 - CQA and 5 - CQA were more than 2.2-fold increased by operating at a large L/S ratio (900-mL vs 500-mL extractant test). Likewise, the nominal timeframes ($t_{95\%}$) for quantitative release of the overall amount (viz., C ($t_{95\%}$) = 0.95 A) of 3-CQA and 5-CQA as contained in the CS capsule were 3.4 and 2.2-fold reduced by increasing the L/S ratio and decreased from 144 to 43.8 min and from 78 to 34.8 min for 3 - CQA and 5 - CQA, respectively. This is the expected trend when increasing the extractant volume - operating equally to a sink- in bioaccessibility tests, yet the extractability of 4-CQA remained virtually unalterable on the basis of the kinetic variables listed in table 10.3.

*Table 10.3. First-order dissolution mathematical model for investigation of the release kinetics of CQA isomers in coffee-bean extracts following on-line tangential filtration.*

| *Isomer* | *Capsule* | *Volume* | *A (mg/g)* | *k ($h^{-1}$)* | *$R^2$* | *$p_{LOF}$* | *$t_{95\%}$ (h)* |
|---|---|---|---|---|---|---|---|
| *3-CQA* | *ZK* | *500* | *3.2 ± 0.5* | *1.73* | *0.806* | *0.84* | *1.73* |
| *5-CQA* | *ZK* | *500* | *13.2 ± 1.0* | *2.33* | *0.965* | *0.68* | *1.29* |
| *3-CQA* | *CS* | *500* | *20.2 ± 3.1* | *1.25* | *0.945* | *0.38* | *2.40* |
| *4-CQA* | *CS* | *500* | *4.8 ± 0.5* | *3.13* | *0.906* | *0.44* | *0.95* |
| *5-CQA* | *CS* | *500* | *50.8 ± 3.7* | *2.30* | *0.972* | *0.55* | *1.30* |
| *3-CQA* | *CS* | *900* | *16.2 ± 0.9* | *4.11* | *0.965* | *0.65* | *0.73* |
| *4-CQA* | *CS* | *900* | *5.6 ± 0.4* | *3.59* | *0.956* | *0.10* | *0.84* |
| *5-CQA* | *CS* | *900* | *50.9 ± 1.1* | *5.13* | *0.996* | *0.99* | *0.58* |

On the basis of the experimental results illustrated in figure 10.2 and/or values of the parameter A from the mathematical model, the sum of oral bioaccessible 3 - CQA, 4 - CQA and 5 - CQA for CS and ZK capsules were ca. 76 mg/g and 16.4 mg/g, respectively, which represent < 40% and about 70% of the overall CQA concentration labelled by the manufacturers. These values serve as quality control of the green coffee content of dietary supplements and signaled the expected amounts of the most abundant CQA isomers released in the gastrointestinal tract.

# 11. General conclusions

In the following the merits of the several analytical approaches, techniques and automatic flow-systems for accurate evaluation of accessible species in environmental samples for risk assessment purposes are described:

In chapter 3, the MEBE approach offers a novel insight into the bioaccessibility equilibria for organic contaminants by proving that separating the sample and the final extraction medium/acceptor with a thin membrane, offers an enhanced extraction speed for accessible species without sink constraints, usually observed in cyclodextrin-based leaching tests.

In order to ease the design and automation of the different fluidic manifolds, 'CocoSoft' as an automation suite has been developed in chapter 4. By using CocoSoft, the real-time data acquisition was exemplified with potentiometric feedback for maintaining a constant extractant pH during a bioaccessibility extraction (pH-stat method), demonstrating the applicability of fully automated methods involving feedback controlled processes, which have not been developed as of yet for bioaccessibility tests. Several manifolds based on flow methods have been devised and validated in chapters 5 to 10 for the real time monitoring of extraction kinetics in bioaccessibility tests, by automating the sample extraction, conditioning, and analysis or detection through at-line or on-line hyphenation to instrumental equipment and exemplified by the determination of phosphate, lead, nickel, zinc, chromium, copper, 16 EPA priority PAH, atrazine and ametryn in soils, PAH in sediments and caffeoylquinic acids in solid pharmaceutical preparations.

It has been proven in chapters 6 to 9, that the kinetic monitoring of accessibility extraction profiles yields more decision-taking relevant information than the classical steady-state accessibility methods, as far as it offers early estimation of the equilibrium conditions, deconvolution of several components with environmental significance and, in general, allows to detect experimental artefacts as readsorption and redistribution phenomena.

Different extraction schemes have been successfully applied throughout the experimental work in this dissertation, including the Hieltjes-Lijklema for phosphate, one-step SMT for trace metals, UBM for trace metals, 0.01 mol/L $CaCl_2$ for organic

pollutants as recommended by OECD, cyclodextrin assisted extraction for PAH and USP synthetic gastric juice extraction for food supplements. The success of the implementation of methods resorting to the aforementioned water-based saline, acidic, alkaline, sugary, protein, surfactant and enzymatic mediums, highlights the versatility of the designed manifolds, thanks to the inert materials of the flow micro conduits, as PTFE, FEP, PVC, Kel-F,polyethylene and polypropylene, predicting a good compatibility with other bioaccessibility extraction mediums.

Regarding the flow methods, FIA, SIA and LOV have been used in chapters 5-10. FIA was used for the derivatization and detection of bioaccessible inorganic P in chapter 5, but the reagent waste was very high, and the low pressure of the peristaltic pump does not allow to exploit the FIA approach for reliable on-line leaching tests. If the sample throughput is not a key parameter in the method development, the sequential derivatization and transport to the detector could be done with an SIA setup. The SIA was used for automating the sample preparation and hyphenation to instrumental equipment steps in most of the works presented in this dissertation. It has proven to be very robust, flexible and allowed to integrate operations requiring up to 8 atm, which allowed sampling, perfusing, filtering and exploiting in-line integrated SPE cartridges (see chapter 8). LOV was used in the experimental setup of chapter 9 because the small size, integration of the channels and lack of connections, allowed to manipulate liquids as well as slurries and thus implementing the BI method, that is, to renew the SPE surfaces from one sample to another. The simplicity of the LOV configuration, along with the robustness of the SIA make the SIA-LOV hyphenation the perfect choice for automatic sample preparation using partitioning resins in all its possible modes. Moreover, the possibility of designing custom LOV platforms as well as the ease of mechanization in the mechanical workshop makes it more appealing than a standard commercial valve stator and will be thus the method of choice for future work.

Regarding the sampling method, both batch (microdialysis, microfiltration, diafiltration, membrane diffusion) and dynamic (packed microcolumn, stirred flow cell) approaches have been exploited throughout chapters 3-10. Microdialysis probes yield a very clean extract, but lack suitable temporal resolution, they are extremely brittle and require specialized microdialysis pumps working at the nL/min range. Diafiltration offers a clean extract and allows efficient removal of large molecular weight species at flow rates higher than microdialysis but requires an initial outlay and dedicated hardware, and suffers from analyte dilution and dead volume effects. Microfiltration exploits an extremely common and inexpensive labware, is very robust and offers a plethora of different casing and filter materials, as well as different sizes, volumes and pore sizes. For those reasons, microfiltration would be the microsampling technique recommended for probing analytes in batch extractions. Regarding the inclusion of the sample in the fluidic manifold, cylindrical or bi-conically shaped microcolumns in SIA

systems allow bidirectional extractions and they are easy to construct in a minimally equipped mechanical workshop. The stirred flow cell in chapter 7 requires a glass workshop, is more brittle than the packed polymeric columns and does not allow to execute bidirectional extractions in the configuration presented in this thesis. Packed columns would be the sample packing method of choice for future work, being their single drawback the potential lack of tightness of the threads. Maybe other configurations focusing in integration and lack of threads for handling solid materials in fluidic systems should be also taken into account in the design of newer systems.

Flow systems have been hyphenated to instrumental apparatus using at-line, on-line fixed loop and heartcut modes. The at-line coupling proved to be very suited for interfacing a continuous sampling technique, such as microdialysis, with a discontinuous detector, such as ETAAS (chapter 6). The time synchronization between both equipments performed properly, but it was delicate and should be avoided if other means of control are available. The hyphenation of flow approaches to ICP-OES and HPLC was performed on-line with low and high pressure injection valves, respectively in both fixed loop (chapters 5,7 and 10) and heart-cut approaches (chapters 8 and 9). Both of them behaved outstandingly in the developed manifolds. The automatic control of instruments for the on-line hyphenation was performed by contact closure between the fluidic apparatus and the instrumental equipment. This kind of control behaved far better than the time synchronization used in the at-line setups, but could be improved. Commercial instruments are usually designed to work in standalone mode, so they are not ready to be controlled externally.. Several functionalities had to be deceived or adapted in both the control and data acquisition steps because manufacturers dissemble information about electronics, software and in general available features of the equipment.

Data treatment scripts have been designed ad hoc for data evaluation of kinetic profiles for sample sets in chapters 8 and 9. While usually the data evaluation is done in a supervised way, the herein presented script allowed for very fast quantification, outlier removal, fitting to several mathematical equations, evaluation of the suitability of such fittings, implementation of regression statistics and plotting. A change in the desired data processing algorithm can be updated immediately by changing the font code and reevaluate the raw data set. This approach compared to the traditional supervised spreadsheet method reduces the data evaluation time significantly.

# 12. Future work

Concepts like bioaccessibility and bioavailability require further insight in order to make them related to (bio)chemical processes and not to operationally defined conditions. Activity measurements are promising because they standardize and unify the underlying principles of the analytical measurements, however they are not directly applicable to inorganic species, because the bioaccessibility/availability of metals is closely related to the disintegration of specific mineralogical phases. Other approaches include the substitution of the actual recommended leaching agents by others environmental or biologically relevant, as in the UBM or FOREShT [360] tests, that mimics closely the human gastrointestinal tract content, or to more generic reagents, e.g. pH gradient or electrogenerated redox gradient in order to comprehensively characterize a sample, instead of discrete measurements at given pH and redox potentials using predefined reagents. Further alternatives include the use of liposomes as membrane cell surrogates, because they present an appealing alternative to *in-vivo* ecotoxicological tests. They can assess the partitioning of a pollutant into a membrane bilayer or elucidating unspecific mechanisms of toxicity and thus expanding the in-vitro tests to bioavailability, permeation and toxicology.

The samples used in this thesis work are limited to soil, marine sediment and dietary supplements, but can be expanded to foodstuff, urban residues, airborne particulate matter and any solid sample of ecological interest without hardware rearrangement.

For improving the performance of the proposed hyphenated systems, the instrumental equipments could be revisited. For allowing a multielemental determination, ETAAS could be replaced by ICP-OES or ICP-MS if the flow-through nature of the ICP does not jeopardize the hyphenation, otherwise, it could be substituted by a continuum source AAS. ICP-OES could be substituted by ICP-MS in order to get better sensitivity and selectivity with possibility of isotopologue resolution. Regarding organics, for identification of bioaccessible pools of emerging organic contaminants and degradation metabolites or for multiresidue analysis at trace levels, untargeted approaches in UHPLC-Orbitrap-MS could be used without hardware modification. Ion mobility spectrometry (IMS) is a 1D detector resorting to

gas-phase electrophoresis that allows resolving organic compounds (even isomers) and elements in the ms range timelapse. The hyphenation with flow techniques for direct measurements, as well as exploiting multidimensional orthogonal approaches looks promising.

In order to improve the miniaturization, portability, versatility and saving costs of automated analysis based in fluidic approaches, several hyphenation-free alternatives exist to commercial standalone, benchtop instrumental equipment that resort to optical components, high pressure or extreme temperatures. The detection system for handheld devices might involve molecular spectrometry with solid state instrumentation (e.g., LED or solid state photomultiplier tubes) and accessory non-selective derivatization or reagentless electrochemical measurements as conductometry, amperometry or voltammetry that might be readily implemented in LOV microdevices.

Aiming at fostering the separation capabilities of low-cost, low-pressure techniques, electrochemical separative techniques such as liquid-phase electrophoresis, isotachophoresis, electrochromatography or electrowetting techniques could be exploited. Another option is to use flow based low/middle pressure separative techniques as medium pressure chromatography [361], advanced schemes of Bead Injection (BI) or Sequential Injection Chromatography focused on multiresidue or emerging pollutant groups or to exploit orthogonal approaches in the BI/SIC-detection as e.g. SIC-Voltammetric analysis for electroactive species.

BI manifolds could benefit of chemistries of new (nano)composite materials, in particular of magnetite/maghemite nanoparticles, that are inexpensive, easy to preparate, have a high specific surface, permit a plethora of surface functionalization, and because of their magnetic susceptibility they can be manipulated in-line with new approaches that unlike the inclusion of frits in the flow manifold, do not increase the backpressure in the system, as retaining them by turning electromagnets on or off, or using permanent neodymium magnets and variable flow-rates for allowing or preventing the trapping of the magnetic nanoparticles in the flow conduits.

3D printing has been proven to be an affordable and fast prototyping aid for flow analysis, especially the stereolithography, where 3D manifold components are watertight and have outstanding chemical and optical properties due to their methacrylate-epoxy based chemistry. The exploitation of this kind of resins in the fabrication of both fluid drivers and solid phase extraction materials [362] opens new dimensions in the low-cost, miniaturization, portability, field measurements, point of care and parallelization of analysis.

Advances in software and information and communication technology (ICT) have also to be included in daily analytical workflow [363]. Examples of already available

applications of ICT to the analytical laboratory by means of algorithms programmable in any control suite or low-cost technologies include remote sensing and control (radio data links), remote operation (TeamViewer [364]), real time transference of raw data and reports (Dropbox [365]), computerless operation (Raspberry pi [366], BeagleBone Black [367]), auto optimization schemes [368], automatic emailing (Google less secure apps access [369] + Python Simple Mail Transfer protocol client [370]), automatic texting, voice and video (Twilio [371]), voice reporting [348] or automatic data treatment (CocoSoft).

# 13. References


1. Emmons RA, McCullough ME. Counting blessings versus burdens: an experimental investigation of gratitude and subjective well-being in daily life. J Pers Soc Psychol. 2003; 84: 377–389.
2. Wood AM, Froh JJ, Geraghty AWA. Gratitude and well-being: a review and theoretical integration. Clin Psychol Rev. 2010; 30: 890–905.
3. Watkins PC, Woodward K, Stone T, Kolts RL. Gratitude and happiness: development of a measure of gratitude, and relationships with subjective well-being. Soc Behav Personal. 2003; 31: 431–451.
4. BOE-A-2005-895; REAL DECRETO 9/2005, de 14 de enero, por el que se establece la relación de actividades potencialmente contaminantes del suelo y los criterios y estándares para la declaración de suelos ontaminados. Available: https://www.boe.es/boe/dias/2005/01/18/pdfs/A01833-01843.pdf
5. Pule BO, Mmualefe LC, Torto N. Analysis of polycyclic aromatic hydrocarbons in soil with Agilent SampliQ QuEChERS AOAC Kit and HPLC-FLD. Agilent Technical Note.
6. ISO 17402 (2008). Soil quality-requirements and guidance for the selection and application of methods for the assessment of bioavailability of contaminants in soil and soil materials ISO/TS. 2008; 17402: 1–35.
7. Tessier A, Campbell PGC, Bisson M. Sequential extraction procedure for the speciation of particulate trace metals. Anal Chem. 1979; 51: 844–851.
8. McLaren RG, Crawford DV. Studies on soil copper. I. The fractionation of copper in soils. J Soil Sci.; 1973; 24: 172–181.
9. Kersten M, Förstner U. Chemical fractionation of heavy metals in anoxic estuarine and coastal sediments. Water Sci Technol.; 1986; 18: 121–130.
10. Krishnamurti GSR, Huang PM, Van Rees KCJ, Kozak LM, Rostad HPW. Speciation of particulate-bound cadmium of soils and its bioavailability. Analyst; 1995; 120: 659–665.
11. Rauret G, López-Sánchez JF, Sahuquillo A, Rubio R, Davidson C, Ure A, Quevauviller P. Improvement of the BCR three step sequential extraction procedure prior to the certification of new sediment and soil reference materials. J Environ Monit. 1999; 1: 57–61.
12. Hieltjes AHM, Lijklema L. Fractionation of inorganic phosphates in calcareous sediments. J Environ Qual. 1980; 9: 405–407.
13. Semple KT, Doick KJ, Jones KC, Burauel P, Craven A, Harms H. Defining bioavailability and bioaccessibility of contaminated soil and sediment is complicated. Environ Sci Technol. 2004; 38: 228A–231A.

14. Fedotov PS, Kördel W, Miró M, Peijnenburg WJGM, Wennrich R, Huang P-M. Extraction and fractionation methods for exposure assessment of trace metals, metalloids, and hazardous organic compounds in terrestrial environments. Crit Rev Environ Sci Technol. 2012; 42: 1117–1171.
15. Denys S, Caboche J, Tack K, Rychen G, Wragg J, Cave M, Jondreville C, Feidt C. In vivo validation of the unified BARGE method to assess the bioaccessibility of arsenic, antimony, cadmium, and lead in soils. Environ Sci Technol. 2012; 46: 6252–6260.
16. REACH Competent Authority Information Leaflet Number. REACH - Minimisation of animal testing. 2016; Available: http://www.hse.gov.uk/reach/resources/18animaltesting.pdf
17. Schoeters G. The REACH perspective: toward a new concept of toxicity testing. J Toxicol Environ Health B Crit Rev. 2010; 13: 232–241.
18. Pelfrêne A, Waterlot C, Douay F. Investigation of DGT as a metal speciation tool in artificial human gastrointestinal fluids. Anal Chim Acta. 2011; 699: 177–186.
19. Bouayed J, Hoffmann L, Bohn T. Total phenolics, flavonoids, anthocyanins and antioxidant activity following simulated gastro-intestinal digestion and dialysis of apple varieties: Bioaccessibility and potential uptake. Food Chem. 2011; 128: 14–21.
20. Carbonell-Capella JM, Buniowska M, Barba FJ, Esteve MJ, Frígola A. Analytical methods for determining bioavailability and bioaccessibility of bioactive bompounds from fruits and vegetables: a review. Compr Rev Food Sci Food Saf. 2014; 13: 155–171.
21. Rosende M, Magalhães LM, Segundo MA, Miró M. Automated microdialysis-based system for in situ microsampling and investigation of lead bioavailability in terrestrial environments under physiologically based extraction conditions. Environ Sci Technol. 2013; 47: 11668–11675.
22. Brand LE, Sunda WG, Guillard RRL. Limitation of marine phytoplankton reproductive rates by zinc, manganese, and iron. Limnol Oceanogr. 1983; 28: 1182–1198.
23. Gao Y, Zeng Y, Shen Q, Ling W, Han J. Fractionation of polycyclic aromatic hydrocarbon residues in soils. J Hazard Mater. 2009; 172: 897–903.
24. Stroud JL, Paton GI, Semple KT. Predicting the biodegradation of target hydrocarbons in the presence of mixed contaminants in soil. Chemosphere. 2009; 74: 563–567.
25. van der Heijden SA, Jonker MTO. PAH Bioavailability in Field sediments: comparing different methods for predicting in situ bioaccumulation. Environ Sci Technol. 2009; 43: 3757–3763.
26. Bernhardt C, Derz K, Kördel W, Terytze K. Applicability of non-exhaustive extraction procedures with Tenax and HPCD. J Hazard Mater. 2013; 261: 711–717.

27. Oleszczuk P. Application of three methods used for the evaluation of polycyclic aromatic hydrocarbons (PAHs) bioaccessibility for sewage sludge composting. Bioresour Technol. 2009; 100: 413–420.
28. Khan MI, Cheema SA, Shen C, Zhang C, Tang X, Malik Z, Ali S, Yang J, Shen K, Chen X, Chen Y. Assessment of pyrene bioavailability in soil by mild hydroxypropyl-β-cyclodextrin extraction. Arch Environ Contam Toxicol. 2011; 60: 107–115.
29. Hickman ZA, Swindell AL, Allan IJ, Rhodes AH, Hare R, Semple KT, Reid BJ. Assessing biodegradation potential of PAHs in complex multi-contaminant matrices. Environ Pollut. 2008; 156: 1041–1045.
30. Rhodes AH, Dew NM, Semple KT. Relationship between cyclodextrin extraction and biodegradation of phenanthrene in soil. Environ Toxicol Chem. 2008; 27: 1488–1495.
31. Cuypers C, Pancras T, Grotenhuis T, Rulkens W. The estimation of PAH bioavailability in contaminated sediments using hydroxypropyl-beta-cyclodextrin and Triton X-100 extraction techniques. Chemosphere. 2002; 46: 1235–1245.
32. Patterson CJ, Semple KT, Paton GI. Non-exhaustive extraction techniques (NEETs) for the prediction of naphthalene mineralisation in soil. FEMS Microbiol Lett. 2004; 241: 215–220.
33. Swindell AL, Reid BJ. Comparison of selected non-exhaustive extraction techniques to assess PAH availability in dissimilar soils. Chemosphere. 2006; 62: 1126–1134.
34. Allan IJ, Semple KT, Hare R, Reid BJ. Prediction of mono- and polycyclic aromatic hydrocarbon degradation in spiked soils using cyclodextrin extraction. Environ Pollut. 2006; 144: 562–571.
35. Khan MI, Cheema SA, Shen C, Zhang C, Tang X, Shi J, Chen X, Park J, Chen Y. Assessment of phenanthrene bioavailability in aged and unaged soils by mild extraction. Environ Monit Assess. 2012; 184: 549–559.
36. Hartnik T, Jensen J, Hermens JLM. Nonexhaustive β-cyclodextrin extraction as a chemical tool to estimate bioavailability of hydrophobic pesticides for earthworms. Environ Sci Technol. 2008; 42: 8419–8425.
37. Yang X, Lv Z, Bian Y, Wang F, Gu C, Song Y, Jiang X. Predicting PAHs bioavailability for earthworms by mild solvents and Tenax extraction. J Environ Chem Eng. 2013; 1: 768–776.
38. McKelvie JR, Wolfe DM, Celejewski M, Simpson AJ, Simpson MJ. Correlations of Eisenia fetida metabolic responses to extractable phenanthrene concentrations through time. Environ Pollut. 2010; 158: 2150–2157.
39. Gomez-Eyles JL, Sizmur T, Collins CD, Hodson ME. Effects of biochar and the earthworm Eisenia fetida on the bioavailability of polycyclic aromatic hydrocarbons and potentially toxic elements. Environ Pollut. 2011; 159: 616–622.

40. Ashton-Acton Q. Advances in Eisenia research and application. ScholarlyEditions; 2012.
41. ISO/TS 21268-3:2007 - Soil quality - Leaching procedures for subsequent chemical and ecotoxicological testing of soil and soil materials - Part 3: Up-flow percolation test. In: ISO. 2007 Last accessed 6 Nov 2016. Available: http://www.iso.org/iso/catalogue_detail.htm?csnumber=44147
42. Reichenberg F, Mayer P. Two complementary sides of bioavailability: accessibility and chemical activity of organic contaminants in sediments and soils. Environ Toxicol Chem. 2006; 25: 1239–1245.
43. Mayer P, Tolls J, Hermens JLM, Mackay D. Equilibrium sampling devices. Environ Sci Technol. 2003; 37: 184A–191A.
44. Gomez-Eyles JL, Jonker MTO, Hodson ME, Collins CD. Passive samplers provide a better prediction of PAH bioaccumulation in earthworms and plant roots than exhaustive, mild solvent, and cyclodextrin extractions. Environ Sci Technol. 2012; 46: 962–969.
45. Arthur CL, Pawliszyn J. Solid phase microextraction with thermal desorption using fused silica optical fibers. Anal Chem. 1990; 62: 2145–2148.
46. Mäenpää K, Leppänen MT, Reichenberg F, Figueiredo K, Mayer P. Equilibrium sampling of persistent and bioaccumulative compounds in soil and sediment: comparison of two approaches to determine equilibrium partitioning concentrations in lipids. Environ Sci Technol. 2011; 45: 1041–1047.
47. Reichenberg F, Smedes F, Jönsson JA, Mayer P. Determining the chemical activity of hydrophobic organic compounds in soil using polymer coated vials. Chem Cent J. 2008; 2: 8.
48. Legind CN, Karlson U, Burken JG, Reichenberg F, Mayer P. Determining chemical activity of (semi)volatile compounds by headspace solid-phase microextraction. Anal Chem. 2007; 79: 2869–2876.
49. Li C, Cui XY, Fan YY, Teng Y, Nan ZR, Ma LQ. Tenax as sorption sink for in vitro bioaccessibility measurement of polycyclic aromatic hydrocarbons in soils. Environ Pollut. 2015; 196: 47–52.
50. Sun M, Ye M, Hu F, Li H, Teng Y, Luo Y, Jiang X, Kengara FO. Tenax extraction for exploring rate-limiting factors in methyl-β-cyclodextrin enhanced anaerobic biodegradation of PAHs under denitrifying conditions in a red paddy soil. J Hazard Mater. 2014; 264: 505–513.
51. Collins CD, Mosquera-Vazquez M, Gomez-Eyles JL, Mayer P, Gouliarmou V, Blum F. Is there sufficient “sink” in current bioaccessibility determinations of organic pollutants in soils? Environ Pollut. 2013; 181: 128–132.
52. ISO - Technical committees - ISO/TC 190/SC 7 - Soil and site assessment. In: ISO. 2016 Last accessed 3 Nov 2017. Available: http://www.iso.org/iso/standards_development/technical_committees/other_bodies/iso_technical_committee.htm?commid=54408

53. Cui X, Mayer P, Gan J. Methods to assess bioavailability of hydrophobic organic contaminants: Principles, operations, and limitations. Environ Pollut. 2013; 172: 223–234.
54. Koch I, Reimer K. Bioaccessibility extractions for contaminant risk assessments. In: Comprehensive sampling and sample preparation. Volume 3; Editors Pawliszyn, J., Le, X.C., Li, X-F., Lee, H.K.. Elsevier Academic Press, Oxford, UK, 487-507 (2012).Academic Press Oxford; 2012; 3: 487–507.
55. Gouliarmou V, Collins CD, Christiansen E, Mayer P. Sorptive physiologically based extraction of contaminated solid matrices: incorporating silicone rod as absorption sink for hydrophobic organic contaminants. Environ Sci Technol. 2013; 47: 941–948.
56. Gouliarmou V, Mayer P. Sorptive bioaccessibility extraction (SBE) of soils: combining a mobilization medium with an absorption sink. Environ Sci Technol. 2012; 46: 10682–10689.
57. Mayer P, Olsen JL, Gouliarmou V, Hasinger M, Kendler R, Loibner AP. A contaminant trap as a tool for isolating and measuring the desorption resistant fraction of soil pollutants. Environ Sci Technol. 2011; 45: 2932–2937.
58. Fangueiro D, Bermond A, Santos E, Carapuça H, Duarte A. Heavy metal mobility assessment in sediments based on a kinetic approach of the EDTA extraction: search for optimal experimental conditions. Anal Chim Acta. 2002; 459: 245–256.
59. Labanowski J, Monna F, Bermond A, Cambier P, Fernandez C, Lamy I, van Oort F. Kinetic extractions to assess mobilization of Zn, Pb, Cu, and Cd in a metal-contaminated soil: EDTA vs. citrate. Environ Pollut. 2008; 152: 693–701.
60. Bermond A, Ghestem J-P, Yousfi I. Kinetic approach to the chemical speciation of trace metals in soils. Analyst. 1998; 123: 785–789.
61. Fangueiro D, Bermond A, Santos E, Carapuça H, Duarte A. Kinetic approach to heavy metal mobilization assessment in sediments: choose of kinetic equations and models to achieve maximum information. Talanta. 2005; 66: 844–857.
62. Varrault G, Bermond A. Kinetics as a tool to assess the immobilization of soil trace metals by binding phase amendments for in situ remediation purposes. J Hazard Mater. 2011; 192: 808–812.
63. Manouchehri N, Besançon S, Bermond A. Kinetic characterizing of soil trace metal availability using Soil/EDTA/Chelex mixture. Chemosphere. 2011; 83: 997–1004.
64. Vakh C, Falkova M, Timofeeva I, Moskvin A, Moskvin L, Bulatov A. Flow analysis: a novel approach for classification. Crit Rev Anal Chem. 2016; 46: 374–388.
65. Cerdà V. Introducción a los métodos de análisis en flujo. SCIWARE; 2006.
66. Kolev SD, McKelvie ID. Advances in flow injection analysis and related techniques. Elsevier; The Netherlands. 2008.
67. Trojanowicz M. Advances in flow analysis. Wiley; New York. 2008.

68. Valcárcel M, de Castro MDL. Automatic methods of analysis. Elsevier Science; The Netherlands1988.
69. Garcia-Mesa JA, Luque de Castro MD, Valcarcel M. Coupled robot-flow injection analysis system for fully automated determination of total polyphenols in olive oil. Anal Chem. 1993; 65: 3540–3542.
70. PAL SYSTEM: Ingenious sample handling. Clinx GmbH; Last accessed 6 Nov 2016. Available: http://www.palsystem.com/index.php?id=1
71. Skeggs LT Jr, Hochstrasser H. Multiple automatic sequential Analysis. Clin Chem. 1964; 10: 918–936.
72. Ŗuzicka J, Hansen EH. Flow injection analyses: part I. A new concept of fast continuous flow analysis. Anal Chim Acta; 1975; 78: 145–157.
73. Ruzicka J, Marshall GD. Sequential injection: a new concept for chemical sensors, process analysis and laboratory assays. Anal Chim Acta. 1990; 237: 329–343.
74. Lenehan CE. Sequential Injection Analysis. In: Reference Module opf Chemistry, Molecular Sciences and Chemical Engineering. Elsevier; 2013.
75. Feres MA, Fortes PR, Zagatto EAG, Santos JLM, Lima JLFC. Multi-commutation in flow analysis: recent developments and applications. Anal Chim Acta. 2008; 618: 1–17.
76. Horstkotte B, Elsholz O, Cerdá V. Review on automation using multisyringe flow injection analysis. J. Flow Injection Anal. 2005; 22: 99.
77. Santos JLM, Ribeiro MFT, Dias ACB, Lima JLFC, Zagatto EEA. Multi-pumping flow systems: the potential of simplicity. Anal Chim Acta. 2007; 600: 21–28.
78. Itabashi H, Kawamoto H, Kawashima T. A novel flow injection technique: all injection analysis. Anal Sci. 2001; 17: 229–231.
79. Mozzhukhin AV, Moskvin AL, Moskvin LN. Stepwise injection analysis as a new method of flow analysis. J Anal Chem. 2007; 62: 475–478.
80. Nacapricha D, Sastranurak P, Mantim T, Amornthammarong N, Uraisin K, Boonpanaid C, Chuyprasartwattana C, Wilairat P. Cross injection analysis: concept and operation for simultaneous injection of sample and reagents in flow analysis. Talanta. 2013; 110: 89–95.
81. Krug FJ, Bergamin FH, Zagatto EAG. Commutation in flow injection analysis. Anal Chim Acta. 1986; 179: 103–118.
82. Ma J, Li Q, Yuan D. Loop flow analysis of dissolved reactive phosphorus in aqueous samples. Talanta. 2014; 123: 218–223.
83. Teshima N, Noguchi D, Joichi Y, Lenghor N, Ohno N, Sakai T, Motomizu S. Simultaneous injection-effective mixing analysis of palladium. Anal Sci. 2010; 26: 143–144.
84. Diniz PHGD, de Almeida LF, Harding DP, de Araújo MCU. Flow-batch analysis. Trends Anal Chem. 2012; 35: 39–49.
85. Wang J, Hansen EH. Sequential injection lab-on-valve: the third generation of flow injection analysis. Trends Anal Chem. 2003; 22: 225–231.

86. Chen X-W, Wang J-H. The miniaturization of bioanalytical assays and sample pretreatments by exploiting meso-fluidic lab-on-valve configurations: a review. Anal Chim Acta. 2007; 602: 173–180.
87. Yu Y-L, Jiang Y, Chen M-L, Wang J-H. Lab-on-valve in the miniaturization of analytical systems and sample processing for metal analysis. Trends Anal Chem. 2011; 30: 1649–1658.
88. Miró M, Oliveira HM, Segundo MA. Analytical potential of mesofluidic lab-on-a-valve as a front end to column-separation systems. Trends Anal Chem. 2011; 30: 153–164.
89. Wang J, Hansen EH, Miró M. Sequential injection–bead injection–lab-on-valve schemes for on-line solid phase extraction and preconcentration of ultra-trace levels of heavy metals with determination by electrothermal atomic absorption spectrometry and inductively coupled plasma mass spectrometry. Anal Chim Acta. 2003; 499: 139–147.
90. Oliveira HM, Grand MM, Ruzicka J, Measures CI. Towards chemiluminescence detection in micro-sequential injection lab-on-valve format: a proof of concept based on the reaction between Fe(II) and luminol in seawater. Talanta. 2015; 133: 107–111.
91. Yang M, Xu Y, Wang J-H. Lab-on-valve system integrating a chemiluminescent entity and in situ generation of nascent bromine as oxidant for chemiluminescent determination of tetracycline. Anal Chem. 2006; 78: 5900–5905.
92. Roda A. Chemiluminescence and bioluminescence: past, present and future. Royal Society of Chemistry; Oxford, UK. 2011.
93. Amorim CG, Souza RC, Araújo AN, Montenegro MCBSM, Silva VL. SI lab-on-valve analysis of histamine using potentiometric detection for food quality control. Food Chem. 2010; 122: 871–876.
94. Jakmunee J, Patimapornlert L, Suteerapataranon S, Lenghor N, Grudpan K. Sequential injection with lab-at-valve (LAV) approach for potentiometric determination of chloride. Talanta. 2005; 65: 789–793.
95. Amorim CG, Araujo AN, Montenegro MCBSM. Exploiting sequential injection analysis with lab-on-valve and miniaturized potentiometric detection Epinephrine determination in pharmaceutical products. Talanta. 2007; 72: 1255–1260.
96. Wang Y, Yao G, Tang J, Yang C, Xu Q, Hu X. On-line coupling of Lab-on-Valve format to amperometry based on polyvinylpyrrolidone-doped carbon paste electrode and its application to the analysis of morin. J Anal Methods Chem. 2012; 2012: 257109.
97. Wang Y, Wang L, Tian T, Hu X, Yang C, Xu Q. Automated solid-phase extraction hyphenated to voltammetry for the determination of quercetin using magnetic

nanoparticles and sequential injection lab-on-valve approach. Analyst. 2012; 137: 2400–2405.
98. Wang Y, Liu Z, Hu X, Cao J, Wang F, Xu Q, Yang C. On-line coupling of sequential injection lab-on-valve to differential pulse anodic stripping voltammetry for determination of Pb in water samples. Talanta. 2009; 77: 1203–1207.
99. Wang Y, Liu Z, Yao G, Zhu P, Hu X, Xu Q, Yang C. Determination of cadmium with a sequential injection lab-on-valve by anodic stripping voltammetry using a nafion coated bismuth film electrode. Talanta. 2010; 80: 1959–1963.
100. Miró M, Hartwell SK, Jakmunee J, Grudpan K, Hansen EH. Recent developments in automatic solid-phase extraction with renewable surfaces exploiting flow-based approaches. Trends Anal Chem. 2008; 27: 749–761.
101. Šatínský D, Solich P, Chocholouš P, Karlíček R. Monolithic columns-a new concept of separation in the sequential injection technique. Anal Chim Acta. 2003; 499: 205–214.
102. Idris AM. The second five years of sequential injection chromatography: significant developments in the technology and methodologies. Crit Rev Anal Chem. 2014; 44: 220–232.
103. Hartwell SK, Kehling A, Lapanantnoppakhun S, Grudpan K. Flow injection/sequential injection chromatography: a review of recent developments in low pressure with high performance chemical separation. Anal Lett. 2013; 46: 1640–1671.
104. Chocholouš P, Solich P, Šatínský D. An overview of sequential injection chromatography. Anal Chim Acta. 2007; 600: 129–135.
105. Ruzicka J, On-line tutorial: Sequential injection chromatography: automated sample preparation, derivatization and separation of amino acids. Available: http://www.flowinjectiontutorial.com/files/SIC%20white%20paper.pdf
106. Huclová J, Šatínský D, Karlíček R. Coupling of monolithic columns with sequential injection technique: A new separation approach in flow methods. Anal Chim Acta. 2003; 494: 133–140.
107. Koblová P, Sklenářová H, Chocholouš P, Polášek M, Solich P. Simple automated generation of gradient elution conditions in sequential injection chromatography using monolithic column. Talanta. 2011; 84: 1273–1277.
108. Miró M, Hansen EH. Miniaturization of environmental chemical assays in flowing systems: the lab-on-a-valve approach vis-à-vis lab-on-a-chip microfluidic devices. Anal Chim Acta. 2007; 600: 46–57.
109. Hashem MA, Takaki M, Jodai T, Toda K. Measurements of arsenite and arsenate contained in mining river waters and leached from contaminated sediments by sequential hydride generation flow injection analysis. Talanta. 2011; 84: 1336–1341.
110. Cocovi-Solberg DJ, Rosende M, Miró M. Automatic kinetic bioaccessibility assay of lead in soil environments using flow-through microdialysis as a front end to

electrothermal atomic absorption spectrometry. Environ Sci Technol. 2014; 48: 6282–6290.
111. Torto N. A Review of Microdialysis Sampling Systems. Chromatographia. 2009; 70: 1305-1309.
112. Torto N, Laurell T, Gorton L, Marko-Varga G. Recent trends in the application of microdialysis in bioprocesses. Anal Chim Acta. 1998; 374: 111–135.
113. Miró M, Frenzel W. The potential of microdialysis as an automatic sample-processing technique for environmental research. Trends Anal Chem. 2005; 24: 324–333.
114. Weiss DJ, Lunte CE. In vivo microdialysis as a tool for monitoring pharmacokinetics. Trends Anal Chem. 2000; 19.
115. Miró M, Frenzel W. Microdialysis in environmental monitoring. In: Applications of microdialysis in pharmaceutical science. John Wiley & Sons, Inc. 2011. pp. 509–530.
116. Boonjob W, Rosende M, Miró M, Cerdà V. Critical evaluation of novel dynamic flow-through methods for automatic sequential BCR extraction of trace metals in fly ash. Anal Bioanal Chem. 2009; 394: 337–349.
117. Rosende M, Miró M, Cerdà V. Fluidized-bed column method for automatic dynamic extraction and determination of trace element bioaccessibility in highly heterogeneous solid wastes. Anal Chim Acta. 2010; 658: 41–48.
118. Rosende M, Miró M, Cerdà V. The potential of downscaled dynamic column extraction for fast and reliable assessment of natural weathering effects of municipal solid waste incineration bottom ashes. Anal Chim Acta. 2008; 619: 192–201.
119. Rosende M, Savonina EY, Fedotov PS, Miró M, Cerdà V, Wennrich R. Dynamic fractionation of trace metals in soil and sediment samples using rotating coiled column extraction and sequential injection microcolumn extraction: a comparative study. Talanta. 2009; 79: 1081–1088.
120. Chomchoei R, Miró M, Hansen EH, Shiowatana J. Automated sequential injection-microcolumn approach with on-line flame atomic absorption spectrometric detection for implementing metal fractionation schemes of homogeneous and nonhomogeneous solid samples of environmental interest. Anal Chem. 2005; 77: 2720–2726.
121. Maia MA, Soares TRP, Mota AIP, Rosende M, Magalhães LM, Miró M, Segundo MA. Dynamic flow-through approach to evaluate readily bioaccessible antioxidants in solid food samples. Talanta. 2017; 166: 162-168
122. Boonjob W, Miró M, Cerdà V. Multiple stirred-flow chamber assembly for simultaneous automatic fractionation of trace elements in fly ash samples using a multisyringe-based flow system. Anal Chem. 2008; 80: 7319–7326.
123. Software - FIAsoft - FlowInjection.com. Last accessed 10 Mar 2017. Available: http://www.flowinjection.com/software/66-test-php-sw

124. Software - SIAsoft - FlowInjection.com. Last accessed 10 Mar 2017. Available: http://www.flowinjection.com/software/118-siasoft
125. FlowInjection.com. Last accessed 10 Mar 2017. Available: http://www.flowinjection.com/
126. Software Autoanalysis basic. Last accessed 10 Mar 2017. Available: http://www.sciware-sl.com/products/software-for-automation/item/115-autoanalysis
127. Becerra E, Cladera A, Cerdà V. Design of a very versatile software program for automating analytical methods. Lab Rob Autom. 1999; 11: 131–140.
128. Software AUTOANALYSIS basic. Last accessed 10 Mar 2017. Available: http://www.sciware-sl.com/products/software-for-automation/item/115-autoanalysis
129. lobal FIA FloZF data acquisition and device control. Last accessed 10 Mar 2017. Available: https://www.globalfia.com/component/virtuemart/view/productdetails/virtuemart_product_id/151/virtuemart_category_id/12
130. Global FIA. Last accessed 10 Mar 2017. Available: https://www.globalfia.com/
131. USB4000-UV-VIS - Ocean Optics. Last accessed 10 Mar 2017. Available: http://oceanoptics.com/product/usb4000-uv-vis/
132. Instruments | PalmSens. Last accessed 10 Mar 2017. Available: https://www.palmsens.com/en/instruments/
133. UNI-T Digital multimeters. Last accessed 10 Mar 2017. Available: http://www.uni-trend.com/productscatelist2.aspx?ProductsCateID=897&CateID=897&CurrCateID=897&showCateID=897
134. Gilbault GG, Hjelm M. Nomenclature for automated and mechanised analysis. Pure Appl Chem. 1989; 61: 1657–1664.
135. Zhang Y, Pignatello JJ, Tao S, Xing B. Bioaccessibility of PAHs in fuel soot assessed by an in vitro digestive model with absorptive sink: effect of food ingestion. Environ Sci Technol. 2015; 49: 14641–14648.
136. Mayer P, Hilber I, Gouliarmou V, Hale SE, Cornelissen G, Bucheli TD. How to determine the environmental exposure of PAHs originating from biochar. Environ Sci Technol. 2016; 50: 1941–1948.
137. Fang M, Stapleton HM. Evaluating the bioaccessibility of flame retardants in house dust using an in vitro Tenax bead-assisted sorptive physiologically based method. Environ Sci Technol. 2014; 48: 13323–13330.
138. Jönsson JÅ, Mathiasson L. Membrane extraction in analytical chemistry. J Sep Sci. 2001; 24: 495–507.
139. Strandberg B, Bergqvist PA, Rappe C. Dialysis with semipermeable membranes as an efficient lipid removal method in the analysis of bioaccumulative chemicals. Anal Chem. 1998; 70: 526–533.

140. Mayer P, Fernqvist MM, Christensen PS, Karlson U, Trapp S. Enhanced diffusion of polycyclic aromatic hydrocarbons in artificial and natural aqueous solutions. Environ Sci Technol. 2007; 41: 6148–6155.
141. Mundt M, Hollender J. Simultaneous determination of NSO-heterocycles, homocycles and their metabolites in groundwater of tar oil contaminated sites using LC with diode array UV and fluorescence detection. J Chromatogr A. 2005; 1065: 211–218.
142. Stokes JD, Anne W, Reid BJ, Jones KC, Semple KT. Prediction of polycyclic aromatic hydrocarbon biodegradation in contaminated soils using an aqueous hydroxypropyl-β-cyclodextrin extraction technique. Environ Toxicol Chem. 2005; 24: 1325–1330.
143. Gomez-Eyles JL, Collins CD, Hodson ME. Relative proportions of polycyclic aromatic hydrocarbons differ between accumulation bioassays and chemical methods to predict bioavailability. Environ Pollut. 2010; 158: 278–284.
144. Dew NM, Paton GI, Semple KT. Prediction of [3-14C] phenyldodecane biodegradation in cable insulating oil-spiked soil using selected extraction techniques. Environ Pollut. 2005; 138: 316–323.
145. Doick KJ, Dew NM, Semple KT. Linking catabolism to cyclodextrin extractability: determination of the microbial availability of PAHs in soil. Environ Sci Technol. 2005; 39: 8858–8864.
146. Papadopoulos A, Paton GI, Reid BJ, Semple KT. Prediction of PAH biodegradation in field contaminated soils using a cyclodextrin extraction technique. J Environ Monit. 2007; 9: 516.
147. Dabbagh N, Bannan-Ritland B. On-line learning: concepts, strategies, and application. Prentice Hall; 2005.
148. Kozaris IA. Platforms for e-learning. Anal Bioanal Chem. 2010; 397: 893–898.
149. Randy Garrison D, Vaughan ND. Blended learning in higher education: framework, principles, and guidelines. John Wiley & Sons; 2008.
150. Garrison DR, Kanuka H. Blended learning: uncovering its transformative potential in higher education. The Internet and Higher Education. 2004; 7: 95–105.
151. Cole J, Foster H. Using Moodle: Teaching with the popular open Source course Management System. O'Reilly Media, Inc.; 2007.
152. Fry H, Ketteridge S, Marshall S. A handbook for teaching and learning in higher education: enhancing academic practice. Med Educ. 2000; 34: 317–318.
153. Fakayode SO. Guided-inquiry laboratory experiments in the analytical chemistry laboratory curriculum. Anal Bioanal Chem. 2014; 406: 1267–1271.
154. Knochen M, Caamaño A, Bentos H. Development of a low-cost SIA-based analyser for water samples. J Autom Methods Manag Chem. 2011; 2011: 943465.
155. Sklenarova H, Svoboda A, Solich P, Polasek M, Karlícek R. Simple laboratory-made automated sequential injection analysis (SIA) device. II. SIA operational

software based on labview® programming language. Instrum Sci Technol. 2002; 30: 353–360.
156. Dominguez R, Muñoz R, Araiza H. Automated analytical system based on the SIA technique. 2010 Pan American Health Care Exchanges. 2010. pp. 117–119.
157. Barzin R, Shukor SRA, Ahmad AL. New spectrophotometric measurement method for process control of miniaturized intensified systems. Sens Actuators B Chem. 2010; 146: 403–409.
158. Jitmanee K, Teshima N, Sakai T, Grudpan K. DRC™ ICP-MS coupled with automated flow injection system with anion exchange minicolumns for determination of selenium compounds in water samples. Talanta. 2007; 73: 352–357.
159. Wagner C, Genner A, Ramer G, Lendl B. Advanced Total Lab Automation System (ATLAS). Modeling, programming and simulations using LabVIEW. 2011; Available: http://cdn.intechopen.com/pdfs-wm/12934.pdf
160. Fangohr H. A. Comparison of C, MATLAB, and Python as teaching languages in engineering. In: Bubak M, van Albada GD, Sloot PMA, Dongarra J, editors. Computational Science - ICCS 2004. Springer Berlin Heidelberg; 2004. pp. 1210–1217.
161. Rigol A, Mateu J, González-Núñez R, Rauret G, Vidal M. pH stat vs. single extraction tests to evaluate heavy metals and arsenic leachability in environmental samples. Anal Chim Acta; 2009; 632: 69–79.
162. Ferreira A, Lima J, Rangel A. Potentiometric determination of total nitrogen in soils by flow injection analysis with a gas-diffusion unit. Soil Res. 1996; 34: 503–510.
163. Python-xy.GitHub.io Downloads. Last accessed 10 Mar 2017. Available: http://python-xy.github.io/downloads.html
164. Cocovi-Solberg DJ, Miró M. CocoSoft: educational software for automation in the analytical chemistry laboratory. Anal Bioanal Chem. 2015; 407: 6227–6233.
165. Built-in Functions — Python 2.7.13 documentation. Last accessed 10 Mar 2017. Available: https://docs.python.org/2/library/functions.html
166. Built-in Types — Python 2.7.13 documentation. Last accessed 10 Mar 2017. Available: https://docs.python.org/2/library/stdtypes.html
167. Mathematical functions — Python 2.7.13 documentation. Last accessed 10 Mar 2017. Available: https://docs.python.org/2/library/math.html
168. Schoumans OF, Chardon WJ, Bechmann ME, Gascuel-Odoux C, Hofman G, Kronvang B, Rubæk GH, Ulén B, Dorioz JM. Mitigation options to reduce phosphorus losses from the agricultural sector and improve surface water quality: a review. Sci Total Environ. 2014; 468-469: 1255–1266.
169. Forsberg C. Which policies can stop large scale eutrophication? Water Sci Technol.; 1998; 37: 193–200.

170. McKelvie ID, Lyddy-Meaney A. Phosphorus. In: Encyclopedia of Analytical Science. Elsevier; 2005. pp. 167–173.
171. Turner BL, Cade-Menun BJ, Condron LM, Newman S. Extraction of soil organic phosphorus. Talanta. 2005; 66: 294–306.
172. Baldwin DS. Organic phosphorus in the aquatic environment. Environ Chem. 2013; 10: 439–454.
173. Barbanti A, Bergamini MC, Frascari F, Miserocchi S, Rosso G. Critical aspects of sedimentary phosphorus chemical fractionation. J Environ Qual. 1994; 23: 1093–1102.
174. Hansen EH, Miró M. How flow-injection analysis (FIA) over the past 25 years has changed our way of performing chemical analyses. Trends Anal Chem. 2007; 26: 18–26.
175. Tiyapongpattana W, Pongsakul P, Shiowatana J, Nacapricha D. Sequential extraction of phosphorus in soil and sediment using a continuous-flow system. Talanta. 2004; 62: 765–771.
176. Buanuam J, Miró M, Hansen EH, Shiowatana J, Estela JM, Cerdà V. A multisyringe flow-through sequential extraction system for on-line monitoring of orthophosphate in soils and sediments. Talanta. 2007; 71: 1710–1719.
177. Novozamsky I, van Riemsdijk WH. The behaviour of silver phosphate as the electroactive sensor in a phosphate-sensitive electrode. Anal Chim Acta. 1976; 85: 41–46.
178. Szemes F, Hesek D, Chen Z, Dent SW, Drew MGB, Goulden AJ, Graydon AR, Grieve A, Mortimer RJ, Wear T, Weightman JS, Beer PD. Synthesis and characterization of novel acyclic, macrocyclic, and calix[4]arene ruthenium(II) bipyridyl receptor molecules that recognize and sense anions. Inorg Chem. 1996; 35: 5868–5879.
179. Cheng W-L, Sue J-W, Chen W-C, Chang J-L, Zen J-M. Activated nickel platform for electrochemical sensing of phosphate. Anal Chem. 2010; 82: 1157–1161.
180. Miró M, Estela JM, Cerdà V. Application of flowing stream techniques to water analysis. Part I. Ionic species: dissolved inorganic carbon, nutrients and related compounds. Talanta. 2003; 60: 867–886.
181. Worsfold PJ, Clough R, Lohan MC, Monbet P, Ellis PS, Quétel CR, Floor GH, McKelvie ID. Flow injection analysis as a tool for enhancing oceanographic nutrient measurements—A review. Anal Chim Acta. 2013; 803: 15–40.
182. Motomizu S, Li Z-H. Trace and ultratrace analysis methods for the determination of phosphorus by flow-injection techniques. Talanta. 2005; 66: 332–340.
183. Karthikeyan S, Hashigaya S, Kajiya T, Hirata S. Determination of trace amounts of phosphate by flow-injection photometry. Anal Bioanal Chem. 2004; 378: 1842–1846.
184. Tzanavaras PD, Themelis DG. Simultaneous flow-injection determination of fluoride, monofluorophosphate and orthophosphate ions using alkaline

phosphatase immobilized on a cellulose nitrate membrane and an open-circulation approach. Anal Chim Acta.; 2002; 467: 83–89.
185. Reis BF, Martelli PB, Krug FJ, Tumang CA. Flow injection preconcentration and spectrophotometric determination of orthophosphate in natural waters. J Braz Chem Soc. 1992; 3: 38–42.
186. Li Z, Oshima M, Sabarudin A, Motomizu S. Trace and ultratrace analysis of purified water samples and hydrogen peroxide solutions for phosphorus by flow-injection method. Anal Sci. 2005; 21: 263–268.
187. Kröckel L, Lehmann H, Wieduwilt T, Schmidt MA. Fluorescence detection for phosphate monitoring using reverse injection analysis. Talanta. 2014; 125: 107–113.
188. Frank C, Schroeder F, Ebinghaus R, Ruck W. Using sequential injection analysis for fast determination of phosphate in coastal waters. Talanta. 2006; 70: 513–517.
189. Dasgupta PK, Eom I-Y, Morris KJ, Li J. Light emitting diode-based detectors: absorbance, fluorescence and spectroelectrochemical measurements in a planar flow-through cell. Anal Chim Acta. 2003; 500: 337–364.
190. Dot Laser Modules, Roithner Lasertechnik, Austria. Last accessed 10 Mar 2017. Available: http://www.roithner-laser.com/deepuv_to_select.html
191. MID-IR LEDs. Roithner Lasertechnik, Austria. Last accessed 10 Mar 2017. Available: http://www.roithner-laser.com/led_midir.html
192. Lindsay RH, Paton BE. Inexpensive photometer using light-emitting diodes. Am J Phys. 1976; 44: 188–189.
193. Mims FM. Sun photometer with light-emitting diodes as spectrally selective detectors. Appl Opt. 1992; 31: 6965–6967.
194. Miyazaki E, Itami S, Araki T. Using a light-emitting diode as a high-speed, wavelength selective photodetector. Rev Sci Instrum 1998; 69; 3751.
195. Anh Bui D, Hauser PC. Absorbance measurements with light-emitting diodes as sources: silicon photodiodes or light-emitting diodes as detectors? Talanta. 2013; 116: 1073–1078.
196. Capitán-Vallvey LF, Palma AJ. Recent developments in handheld and portable optosensing—A review. Anal Chim Acta. 2011; 696: 27–46.
197. Pokrzywnicka M, Koncki R, Tymecki Ł. A concept of dual optical detection using three light emitting diodes. Talanta. 2010; 82: 422–425.
198. Lau KT, Baldwin S, Shepherd RL, Dietz PH, Yerzunis WS, Diamond D. Novel fused-LEDs devices as optical sensors for colorimetric analysis. Talanta. 2004; 63: 167–173.
199. O'Toole M, Lau KT, Shepherd R, Slater C, Diamond D. Determination of phosphate using a highly sensitive paired emitter–detector diode photometric flow detector. Anal Chim Acta. 2007; 597: 290–294.

200. Lau K-T, Baldwin S, O'Toole M, Shepherd R, Yerazunis WJ, Izuo S, Ueyama S, Diamond D. A low-cost optical sensing device based on paired emitter–detector light emitting diodes. Anal Chim Acta. 2006; 557: 111–116.
201. O'Toole M, Lau KT, Diamond D. Photometric detection in flow analysis systems using integrated PEDDs. Talanta. 2005; 66: 1340–1344.
202. O'Toole M, Lau K-T, Shazmann B, Shepherd R, Nesterenko PN, Paull B, Diamond D. Novel integrated paired emitter-detector diode (PEDD) as a miniaturized photometric detector in HPLC. Analyst. 2006; 131: 938–943.
203. Tymecki Ł, Pokrzywnicka M, Koncki R. Paired emitter detector diode (PEDD)-based photometry-an alternative approach. Analyst. 2008; 133: 1501–1504.
204. Tymecki Ł, Koncki R. Simplified paired-emitter–detector-diodes-based photometry with improved sensitivity. Anal Chim Acta. 2009; 639: 73–77.
205. Pokrzywnicka M, Cocovi-Solberg DJ, Miró M, Cerdà V, Koncki R, Tymecki Ł. Miniaturized optical chemosensor for flow-based assays. Anal Bioanal Chem. 2011; 399: 1381–1387.
206. Cocovi-Solberg DJ, Miró M, Cerdà V, Pokrzywnicka M, Tymecki L, Koncki R. Towards the development of a miniaturized fiberless optofluidic biosensor for glucose. Talanta. 2012; 96: 113–120.
207. Strzelak K, Koncki R, Tymecki L. Serum alkaline phosphatase assay with paired emitter detector diode. Talanta. 2012; 96: 127–131.
208. Czugala M, Fay C, O'Connor NE, Corcoran B, Benito-Lopez F, Diamond D. Portable integrated microfluidic analytical platform for the monitoring and detection of nitrite. Talanta. 2013; 116: 997–1004.
209. Tymecki Ł, Korszun J, Strzelak K, Koncki R. Multicommutated flow analysis system for determination of creatinine in physiological fluids by Jaffe method. Anal Chim Acta. 2013; 787: 118–125.
210. Tymecki Ł, Pokrzywnicka M, Koncki R. Fluorometric paired emitter detector diode (FPEDD). Analyst. 2011; 136: 73–76.
211. Pokrzywnicka M, Fiedoruk M, Koncki R. Compact optoelectronic flow-through device for fluorometric determination of calcium ions. Talanta. 2012; 93: 106–110.
212. Fiedoruk M, Mieczkowska E, Koncki R, Tymecki L. A bimodal optoelectronic flow-through detector for phosphate determination. Talanta. 2014; 128: 211–214.
213. de Vargas-Sansalvador IMP, Fay C, Fernandez-Ramos MD, Diamond D, Benito-Lopez F, Capitan-Vallvey LF. LED–LED portable oxygen gas sensor. Anal Bioanal Chem. 2012; 404: 2851–2858.
214. Tymecki Ł, Rejnis M, Pokrzywnicka M, Strzelak K, Koncki R. Fluorimetric detector and sensor for flow analysis made of light emitting diodes. Anal Chim Acta. 2012; 721: 92–96.
215. Pokrzywnicka M, Tymecki L, Koncki R. Low-cost optical detectors and flow systems for protein determination. Talanta. 2012; 96: 121–126.

216. Buanuam J, Miró M, Hansen EH, Shiowatana J. On-line dynamic fractionation and automatic determination of inorganic phosphorus in environmental solid substrates exploiting sequential injection microcolumn extraction and flow injection analysis. Anal Chim Acta.; 2006; 570: 224–231.
217. ISO 10390:2005 - Soil quality - Determination of pH. Last accessed 10 Mar 2017. Available: http://www.iso.org/iso/catalogue_detail.htm?csnumber=40879
218. Dietrich H. Standard operating procedure: procedure for determining soil particle size using the hydrometer method. California Department of Pesticide Regulation, Environmental Monitoring Branch. 2005; 1–10.
219. Ziechmann W. McLaren, A. D., und Peterson, G. H. (Editors): Soil Biochemistry. M. Dekker Inc. 1967; pp. 118–119.
220. Russell SEJ, Wild A. Russell's soil conditions and plant growth. Longman Scientific & Technical; 1988.
221. Bacon JR, Davidson CM. Is there a future for sequential chemical extraction? Analyst. 2008; 133: 25–46.
222. Boonjob W, Zevenhoven M, Ek P, Hupa M, Ivaska A, Miró M. Automatic dynamic chemical fractionation method with detection by plasma spectrometry for advanced characterization of solid biofuels. J Anal At Spectrom. 2012; 27: 841.
223. Rao CRM, Sahuquillo A, Lopez Sanchez JF. A review of the different methods applied in environmental geochemistry for single and sequential extraction of trace elements in soils and related materials. Water Air Soil Pollut. 2007; 189: 291–333.
224. Fedotov PS, Miró M. Fractionation and mobility of trace elements in soils and sediments. In: Violante A, Huang PM, Gadd GM, (Editors). Biophysico-chemical processes of heavy metals and metalloids in soil environments. John Wiley & Sons, New York; 2008.
225. Miró M, Hansen EH, Chomchoei R, Frenzel W. Dynamic flow-through approaches for metal fractionation in environmentally relevant solid samples. Trends Anal Chem. 2005; 24: 759–771.
226. Rosende M, Miró M. Recent trends in automatic dynamic leaching tests for assessing bioaccessible forms of trace elements in solid substrates. Trends Anal Chem. 2013; 45: 67–78.
227. Brunori C, Cremisini C, D'Annibale L, Massanisso P, Pinto V. A kinetic study of trace element leachability from abandoned-mine-polluted soil treated with SS-MSW compost and red mud. Comparison with results from sequential extraction. Anal Bioanal Chem. 2005; 381: 1347–1354.
228. Miró M, Frenzel W. Implantable flow-through capillary-type microdialyzers for continuous in situ monitoring of environmentally relevant parameters. Anal Chem. 2004; 76: 5974–5981.
229. Miró M, Jimoh M, Frenzel W. A novel dynamic approach for automatic microsampling and continuous monitoring of metal ion release from soils

exploiting a dedicated flow-through microdialyser. Anal Bioanal Chem. 2005; 382: 396–404.
230. Miró M, Fitz WJ, Swoboda S, Wenzel WW. In-situ sampling of soil pore water: evaluation of linear-type microdialysis probes and suction cups at varied moisture contents. Environ Chem. 2010; 7: 123–131.
231. Sulyok M, Miró M, Stingeder G, Koellensperger G. The potential of flow-through microdialysis for probing low-molecular weight organic anions in rhizosphere soil solution. Anal Chim Acta. 2005; 546: 1–10.
232. Torto N, Mwatseteza J, Sawula G. A study of microdialysis sampling of metal ions. Anal Chim Acta. 2002; 456: 253–261.
233. Torto N, Mogopodi D. Opportunities in microdialysis sampling of metal ions. Trends Anal Chem. 2004; 23: 109–115.
234. Torto N, Laurell T, Gordon L, Varga GM. A study of a polysulfone membrane for use in an in-situ tunable microdialysis probe during monitoring of starch enzymatic hydrolysates. J Membr Sci 1997; 130: 239–248.
235. Ure AM, Quevauviller P, Muntau H, Griepink B. Speciation of heavy metals in solids and harmonization of extraction techniques undertaken under the auspices of the BCR of the Commission of the European Communities. Int J Environ Anal Chem. 1993; 51: 135–151.
236. Miró M, Frenzel W. Investigation of chemical effects on the performance of flow-through dialysis applied to the determination of ionic species. Anal Chim Acta. 2004; 512: 311–317.
237. Schumacher BA. Methods for the determination of total organic carbon (TOC) in soils and sediments. Ecological Risk Assessment Support Center, EPA. 2002; pp. 1–23.
238. Sarabia LA, Ortiz MC. Response surface methodology. Comprehensive chemometrics. Elsevier. 2009; 1: 345–390.
239. Lundstedt T, Seifert E, Abramo L, Thelin B. Experimental design and optimization. Chemometr Intell Lab. 1998; 42: 3–40.
240. Bungay PM, Morrison PF, Dedrick RL. Steady-state theory for quantitative microdialysis of solutes and water in vivo and in vitro. Life Sci. 1990; 46: 105–119.
241. Mogopodi D, Torto N. Enhancing microdialysis recovery of metal ions by incorporating poly-l-aspartic acid and poly-l-histidine in the perfusion liquid. Anal Chim Acta. 2003; 482: 91–97.
242. Motulsky H, Christopoulos A. Fitting models to biological data using linear and non-linear regression. GraphPad Software. Inc, San Diego. 2003.
243. Oomen AG, Tolls J, Sips AJAM, Groten JP. In vitro intestinal lead uptake and transport in relation to speciation. Arch Environ Contam Toxicol. 2003; 44: 116–124.

244. Casteel SW, Weis CP, Henningsen GM, Brattin WJ. Estimation of relative bioavailability of lead in soil and soil-like materials using young Swine. Environ Health Perspect. 2006; 114: 1162–1171.
245. Oomen AG, Tolls J, Sips AJAM, Van den Hoop MAGT. Lead speciation in artificial human digestive fluid. Arch Environ Contam Toxicol. 2003; 44: 107–115.
246. ISO/TS 17924:2007 - Soil quality - Assessment of human exposure from ingestion of soil and soil material - Guidance on the application and selection of physiologically based extraction methods for the estimation of the human bioaccessibility/bioavailability of metals in soil. 2007. Last accessed 10 Mar 2017. Available: http://www.iso.org/iso/catalogue_detail.htm?csnumber=45728
247. Intawongse M, Dean JR. In-vitro testing for assessing oral bioaccessibility of trace metals in soil and food samples. Trends Anal Chem. 2006; 25: 876–886.
248. Dean JR, Ma R. Approaches to assess the oral bioaccessibility of persistent organic pollutants: A critical review. Chemosphere. 2007; 68: 1399–1407.
249. Wragg J, Cave MR. In-vitro methods for the measurement of the oral bioaccessibility of selected metals and metalloids in soils: A critical review. Environment Agency; 2003.
250. Wragg J, Cave MR, Taylor H, Basta N, Brandon E, Casteel S, Gron C, Oomen A, Van de Wiele T. Inter-laboratory trial of a unified bioaccessibility testing procedure. Nottingham, UK: British Geological Survey; 2007; p. 90.
251. British Geological Survey- BARGE (the Bioaccessibility Research Group of Europe). Last accessed 10 Mar 2017. Available: http://www.bgs.ac.uk/barge/home.html
252. Oomen AG, Rompelberg CJM, Bruil MA, Dobbe CJG, Pereboom DPKH, Sips AJAM. Development of an in vitro digestion model for estimating the bioaccessibility of soil contaminants. Arch Environ Contam Toxicol. 2003; 44: 281–287.
253. Shiowatana J, Tantidanai N, Nookabkaew S, Nacapricha D. A flow system for the determination of metal speciation in soil by sequential extraction. Environ Int. 2001; 26: 381–387.
254. Limbeck A, Wagner C, Lendl B, Mukhtar A. Determination of water soluble trace metals in airborne particulate matter using a dynamic extraction procedure with on-line inductively coupled plasma optical emission spectrometric detection. Anal Chim Acta. 2012; 750: 111–119.
255. Fedotov PS, Savonina EY, Wennrich R, Spivakov BY. A hyphenated flow-through analytical system for the study of the mobility and fractionation of trace and major elements in environmental solid samples. Analyst. 2006; 131: 509–515.
256. Buanuam J, Wennrich R. Study of leachability and fractional alteration of arsenic and co-existing elements in stabilized contaminated sludge using a flow-through extraction system. J Environ Monit. 2011; 13: 1672–1677.
257. Dufailly V, Guérin T, Noël L, Frémy J-M, Beauchemin D. A simple method for the speciation analysis of bioaccessible arsenic in seafood using on-line continuous

leaching and ion exchange chromatography coupled to inductively coupled plasma mass spectrometry. J Anal At Spectrom. 2008; 23: 1263–1268.
258. Leufroy A, Noël L, Beauchemin D, Guérin T. Bioaccessibility of total arsenic and arsenic species in seafood as determined by a continuous on-line leaching method. Anal Bioanal Chem. 2012; 402: 2849–2859.
259. Leufroy A, Noël L, Beauchemin D, Guérin T. Use of a continuous leaching method to assess the oral bioaccessibility of trace elements in seafood. Food Chem. 2012; 135: 623–633.
260. Horner NS, Beauchemin D. A simple method using on-line continuous leaching and ion exchange chromatography coupled to inductively coupled plasma mass spectrometry for the speciation analysis of bioaccessible arsenic in rice. Anal Chim Acta. 2012; 717: 1–6.
261. Chu M, Beauchemin D. Simple method to assess the maximum bioaccessibility of elements from food using flow injection and inductively coupled plasma mass spectrometry. J Anal At Spectrom. 2004; 19: 1213–1216.
262. ISO 10693:1995 - Soil quality - Determination of carbonate content - Volumetric method. 1995. Last accessed 10 Mar 2017. Available: http://www.iso.org/iso/catalogue_detail.htm?csnumber=18781
263. EPA. Microwave Assisted Acid Digestion of Sediments, Sludges, Soils, and Oils. 2007 . Report No.: Test Method 3051A. Available: https://www.epa.gov/sites/production/files/2015-12/documents/3051a.pdf
264. Miller JN, Miller JC. Statistics and chemometrics for analytical chemistry. Prentice Hall, 2000.
265. Montgomery DC. Design and analysis of experiments, 5th edition. Wiley; 2006.
266. Candioti LV, De Zan MM, Cámara MS, Goicoechea HC. Experimental design and multiple response optimization. Using the desirability function in analytical methods development. Talanta. 2014; 124: 123–138.
267. Rosende M, Miró M, Segundo MA, Lima JL, Cerdà V. Highly integrated flow assembly for automated dynamic extraction and determination of readily bioaccessible chromium (VI) in soils exploiting carbon nanoparticle-based solid-phase extraction. Anal Bioanal Chem. 2011; 400: 2217–2227.
268. Pelfrêne A, Waterlot C, Douay F. In vitro digestion and DGT techniques for estimating cadmium and lead bioavailability in contaminated soils: influence of gastric juice pH. Sci Total Environ. 2011; 409: 5076–5085.
269. Broadway A, Cave MR, Wragg J, Fordyce FM, Bewley RJF, Graham MC, Ngwenyaa BT, Farmera JG. Determination of the bioaccessibility of chromium in Glasgow soil and the implications for human health risk assessment. Sci Total Environ. 2010; 409: 267–277.
270. Silva CR, Gomes TF, Andrade GCRM, Monteiro SH, Dias ACR, Zagatto EAG, Tornisielo VL. Banana peel as an adsorbent for removing atrazine and ametryn from waters. J Agric Food Chem. 2013; 61: 2358–2363.

271. Amadori MF, Cordeiro GA, Rebouças CC, Peralta-Zamora PG, Grassi MT, Abate G. Extraction method for the determination of atrazine, deethylatrazine, and deisopropylatrazine in agricultural soil using factorial design. J Braz Chem Soc. 2013; 24: 483–491.
272. EPA. Reregistration Eligibility Decision (RED) for Ametryn. 2005 Sep. Report No.: 7508C. Last accessed 10 Mar 2017.Available: https://archive.epa.gov/pesticides/reregistration/web/pdf/ametryn_red.pdf
273. Vivian R, Queiroz MELR, Jakelaitis A, Guimarães AA, Reis MR, Carneiro PM, Silva AA. Persistence and leaching of ametryn and trifloxysulfuron-sodium on sugarcane soil. Planta daninha. 2007; 25: 111–124.
274. Tandon S, Singh A. Field dissipation kinetics of atrazine in soil and post-harvest residues in winter maize crop under subtropical conditions. J Chem Ecol. 2015; 31: 273–284.
275. Adams RS Jr. Factors influencing soil adsorption and bioactivity of pesticides. Residue Rev. 1973; 47: 1–54.
276. Xu LJ, Chu W, Graham N. Atrazine degradation using chemical-free process of USUV: analysis of the microheterogeneous environments and the degradation mechanisms. J Hazard Mater. 2014; 275: 166–174.
277. Wackett M. Sadowsky B. Martinez L. Biodegradation of atrazine and related triazine compounds: from enzymes to field studies. Appl Microbiol Biotechnol. 2002; 58: 39–45.
278. Mudhoo A, Garg VK. Sorption, transport and transformation of atrazine in soils, minerals and composts: a review. Pedosphere. 2011; 21: 11–25.
279. Templeton DM, Ariese F, Cornelis R, Danielsson L-G, Muntau H, van Leeuwen HP, Lobinski R. Guidelines for terms related to chemical speciation and fractionation of elements. Definitions, structural aspects, and methodological approaches. Pure Appl Chem. 2000; 72: 1453-1470
280. Dean JR, Scott WC. Recent developments in assessing the bioavailability of persistent organic pollutants in the environment. Trends Anal Chem. 2004; 23: 609–618.
281. Ortega-Calvo JJ, Harmsen J, Parsons JR, Semple KT, Aitken MD, Ajao C, Eadsforth C, Galay-Burgos M, Naidu R, Oliver R, Peijnenburg WJ, Römbke J, Streck G, Versonnen B.From bioavailability science to regulation of organic chemicals in session bioavailability. Environ Sci Technol. 2015; 49: 10255-10264
282. Pueyo M, López-Sánchez JF, Rauret G. Assessment of CaCl2, NaNO3 and NH4NO3 extraction procedures for the study of Cd, Cu, Pb and Zn extractability in contaminated soils. Anal Chim Acta. 2004; 504: 217–226.
283. Organisation for Economic Co-operation and Development (OECD). Adsorption - Desorption Using a Batch Equilibrium Method. 2000 Jan. Report No.: Test No. 106. doi:10.1787/9789264069602-en

284. Ettler V, Mihaljevič M, Šebek O, Grygar T. Assessment of single extractions for the determination of mobile forms of metals in highly polluted soils and sediments—Analytical and thermodynamic approaches. Anal Chim Acta. 2007; 602: 131–140.
285. McKelvie ID. In: Kolev SD, D MI, editors. Chapter 4 - Principles of flow injection analysis; In comprehensive analytical chemistry. Elsevier; 2008. pp. 81–109.
286. Gałuszka A, Migaszewski Z, Namieśnik J. The 12 principles of green analytical chemistry and the SIGNIFICANCE mnemonic of green analytical practices. Trends Anal Chem. 2013; 50: 78–84.
287. Miró M, Frenzel W. What flow injection has to offer in the environmental analytical field. Microchim Acta. 2004; 148: 1–20.
288. Lenehan CE, Barnett NW, Lewis SW. Sequential injection analysis. Analyst. 2002; 127: 997–1020.
289. Mesquita RBR, Rangel AOSS. A review on sequential injection methods for water analysis. Anal Chim Acta. 2009; 648: 7–22.
290. Trojanowicz M, Kołacińska K. Recent advances in flow injection analysis. Analyst. 2016; 141: 2085–2139.
291. Miró M, Hansen EH. Solid reactors in sequential injection analysis: recent trends in the environmental field. Trends Anal Chem. 2006; 25: 267–281.
292. Miró M, Hansen EH. On-line sample processing methods in flow analysis in advances in flow analysis. In: Advances in Flow Methods of Analysis. Trojanowicz M. (Editor). Wiley-VCH 2008. pp. 291–320.
293. OECD. Guideline TG 106. OECD Guideline for the testing of chemicals. Adsorption- desorption using a batch equilibrium method. Organization for economic co-operation and development; 2000.
294. Holliday VT. Methods of soil analysis, part 1: Physical and mineralogical methods (2nd edition), A. Klute, Ed., Wiley & Sons. 1990; 5: 87–89.
295. Sparks DL, Page AL, Helmke PA, Loeppert RH, Soltanpour PN, Tabatabai MA, Johnston CT and Sumner ME. Methods of soil analysis. Part 3-Chemical methods. Soil Science Society of America Inc. 1996.
296. United States Pharmacopeia (USP) 37. Chromatography / Physical Tests. Chapter 621. Last accessed 10 Mar 2017. Available: https://hmc.usp.org/sites/default/files/documents/HMC/GCs-Pdfs/c621.pdf
297. Zagatto EAG, Oliveira CC, Townshend A, Worsfold PJ. Flow analysis with spectrophotometric and luminometric detection. Springer-Verlag. 2011
298. Fenoll J, Vela N, Navarro G, Pérez-Lucas G, Navarro S. Assessment of agro-industrial and composted organic wastes for reducing the potential leaching of triazine herbicide residues through the soil. Sci Total Environ. 2014; 493: 124–132.

299. Massart DL, Vandeginste BG, Buydens LMC, Lewi PJ, Smeyers-Verbeke J, Jong SD. Handbook of chemometrics and qualimetrics: Part A. New York, USA: Elsevier . 1997.
300. de Prá Urio R, Masini JC. Evaluation of sequential injection chromatography for reversed phase separation of triazine herbicides exploiting monolithic and core–shell columns. Talanta. 2015; 131: 528–534.
301. Urio R de P, Infante CMC, Masini JC. On-line sequential-injection chromatography with stepwise gradient elution: a tool for studying the simultaneous adsorption of herbicides on soil and soil components. J Agric Food Chem. 2013; 61: 7909–7915.
302. Chávez-Moreno CA, Guzmán-Mar JL, Hinojosa-Reyes L, Hernández-Ramírez A, Ferrer L, Cerdà V. Applicability of multisyringe chromatography coupled to on-line solid-phase extraction to the simultaneous determination of dicamba, 2, 4-D, and atrazine. Anal Bioanal Chem.; 2012; 403: 2705–2714.
303. US-EPA. Decision Documents for Atrazine. United States Environmental Protection Agency Washington, DC; 2006. Last accessed 10 Mar 2017.doi:https://www3.epa.gov/pesticides/chem_search/reg_actions/reregistration/red_PC-080803_1-Apr-06.pdf
304. Currie LA. Nomenclature in evaluation of analytical methods including detection and quantification capabilities. Pure Appl Chem. 1995; 67: 1699–1723.
305. Mayer P, Wernsing J, Tolls J, de Maagd PG-J, Sijm DTHM. Establishing and controlling dissolved concentrations of hydrophobic organics by partitioning from a solid phase. Environ Sci Technol. 1999; 33: 2284–2290.
306. Brack W, Bandow N, Schwab K, Schulze T, Streck G. Bioavailability in effect-directed analysis of organic toxicants in sediments. Trends Anal Chem. 2009; 28: 543–549.
307. Collins CD, Mosquera-Vazquez M, Gomez-Eyles JL, Mayer P, Gouliarmou V, Blum F. Is there sufficient “sink” in current bioaccessibility determinations of organic pollutants in soils? Environ Pollut.; 2013; 181: 128–132.
308. World Health Organization (WHO). Chapter 59: Polycyclic aromatic hydrocarbons (PAHs) in Air Quality Guidelines - Second Edition. Regional Office for Europe, Copenhagen; 2000.
309. World Health Organization (WHO). International Agency for Research on Cancer. Some non-heterocyclic polycyclic aromatic hydrocarbons and some related exposures. Lyon; 2010. Report No.: 92. Last accessed 10 Mar 2017. Available: https://monographs.iarc.fr/ENG/Monographs/vol92/mono92.pdf
310. Agency for Toxic Substances and Disease Registry (ATSDR). Toxicity of polycyclic aromatic hydrocarbons (PAHs): health effects associated with PAH exposure. Last accessed 10 Mar 2017. Available: https://www.atsdr.cdc.gov/csem/csem.asp?csem=13&po=11

311. Polycyclic Aromatic Hydrocarbons in Food, Scientific Opinion of the Panel on Contaminants in the Food Chain. The European Food Safety Agency Journal. 2008; 1–114.
312. Mayer P, Hilber I, Gouliarmou V, Hale SE, Cornelissen G, Bucheli TD. How to determine the environmental exposure of PAHs originating from biochar. Environ Sci Technol. 2016; 50: 1941–1948.
313. Sánchez-Trujillo MA, Morillo E, Villaverde J, Lacorte S. Comparative effects of several cyclodextrins on the extraction of PAHs from an aged contaminated soil. Environ Pollut. 2013; 178: 52–58.
314. Sánchez-Trujillo MA, Lacorte S, Villaverde J, Barata C, Morillo E. Decontamination of polycyclic aromatic hydrocarbons and nonylphenol from sewage sludge using hydroxypropyl-β-cyclodextrin and evaluation of the toxicity of leachates. Environ Sci Pollut Res Int. 2014; 21: 507–517.
315. Liu H, Cai X, Chen J. Mathematical model for cyclodextrin alteration of bioavailability of organic pollutants. Environ Sci Technol. 2013; 47: 5835–5842.
316. Ruzicka J. Lab-on-valve: universal microflow analyzer based on sequential and bead injection. Analyst. 2000; 125: 1053–1060.
317. Ruzicka J, Scampavia L. From flow injection to bead injection. Anal Chem. 1999; 71: 257A–263A.
318. Fiedoruk M, Cocovi-Solberg DJ, Tymecki Ł, Koncki R, Miró M. Hybrid flow system integrating a miniaturized optoelectronic detector for on-line dynamic fractionation and fluorometric determination of bioaccessible orthophosphate in soils. Talanta. 2015; 133: 59–65.
319. Pubchem. naphthalene | C10H8 - PubChem. Last accessed 10 Mar 2017. Available: https://pubchem.ncbi.nlm.nih.gov/compound/naphthalene#section=Top
320. Pubchem. Dibenz [a,h] anthracene | C22H14 - PubChem. Last accessed 10 Mar 2017. Available: https://pubchem.ncbi.nlm.nih.gov/compound/5889#section=Vapor-Pressure
321. Burton S. Garbow, Kenneth E. Hillstrom, Jorge J. More. Documentation for MINPACK subroutine LMDIF. 1980; Last accessed 10 Mar 2017. Available: https://www.math.utah.edu/software/minpack/minpack/lmdif.html
322. Burton S. Garbow, Kenneth E. Hillstrom, Jorge J. More. Documentation for MINPACK subroutine LMDER. 1980. Last accessed 10 Mar 2017. Available: https://www.math.utah.edu/software/minpack/minpack/lmder.html
323. Zuo J, Gao Y, Almukainzi M, Löbenberg R. Investigation of the disintegration behavior of dietary supplements in different beverages. Dissolution Technologies. 2013; 20: 6–9.
324. Marques MRC. Enzymes in the dissolution testing of gelatin capsules. Pharm Sci Tech. 2014; 15: 1410–1416.

325. United States Pharmacopeia. USP chapter: 2040: Disintegration and dissolution of dietary supplements. 2011Last accessed 10 Mar 2017. Available: http://www.usp.org/sites/default/files/usp_pdf/EN/USPNF/revisions/2040disintegrationdissolution.pdf
326. United States Pharmacopeia. USP chapter: 701 Disintegration. 2008 Aug. Report No.: 701. Last accessed 10 Mar 2017. Available: http://www.usp.org/sites/default/files/usp_pdf/EN/USPNF/generalChapter701.pdf
327. Barham AS, Tewes F, Healy AM. Moisture diffusion and permeability characteristics of hydroxypropylmethylcellulose and hard gelatin capsules. Int J Pharm. 2015; 478: 796–803.
328. Ikada Y, Tabata Y. Protein release from gelatin matrices. Adv Drug Deliv Rev. 1998; 31: 287–301.
329. Kawai K, Suzuki S, Tabata Y, Ikada Y, Nishimura Y. Accelerated tissue regeneration through incorporation of basic fibroblast growth factor-impregnated gelatin microspheres into artificial dermis. Biomaterials. 2000; 21: 489–499.
330. Kuijpers AJ, van Wachem PB, van Luyn MJ, Plantinga JA, Engbers GH, Krijgsveld J, Zaat SA, Dankert J, Feijen J. In vivo compatibility and degradation of crosslinked gelatin gels incorporated in knitted Dacron. J Biomed Mater Res. 2000; 51: 136–145.
331. Yao C-H, Liu B-S, Hsu S-H, Chen Y-S, Tsai C-C. Biocompatibility and biodegradation of a bone composite containing tricalcium phosphate and genipin crosslinked gelatin. J Biomed Mater Res A. 2004; 69: 709–717.
332. Gómez-Guillén MC, Pérez-Mateos M, Gómez-Estaca J, López-Caballero E, Giménez B, Montero P. Fish gelatin: a renewable material for developing active biodegradable films. Trends Food Sci Technol. 2009; 20: 3–16.
333. Duconseille A, Astruc T, Quintana N, Meersman F, Sante-Lhoutellier V. Gelatin structure and composition linked to hard capsule dissolution: A review. Food Hydrocoll. 2015; 43: 360–376.
334. United States Pharmacopeia. USP chapter: 711: Dissolution. 2011. Last accessed 10 Mar 2017. Available: http://www.usp.org/sites/default/files/usp_pdf/EN/USPNF/2011-02-25711DISSOLUTION.pdf
335. Clifford MN. Chlorogenic acids and other cinnamates-nature, occurrence and dietary burden. J Sci Food Agric. 1999; 79: 362–372.
336. Clifford MN, Wu W, Kuhnert N. The chlorogenic acids of Hemerocallis. Food Chem. 2006; 95: 574–578.
337. Haghi G, Hatami A, Arshi R. Distribution of caffeic acid derivatives in Gundelia tournefortii L. Food Chem. 2011; 124: 1029–1035.
338. Bakuradze T, Boehm N, Janzowski C, Lang R, Hofmann T, Stockis J-P, Albert FW, Stiebitz H, Bytof G, Lantz I, Baum M, Eisenbrand G. Antioxidant-rich coffee

reduces DNA damage, elevates glutathione status and contributes to weight control: results from an intervention study. Mol Nutr Food Res. 2011; 55: 793–797.
339. Upadhyay R, Rao LJM. An Outlook on Chlorogenic acids—occurrence, chemistry, technology, and biological activities. Crit Rev Food Sci Nutr. 2013; 53: 968–984.
340. Sasaki K, Oki T, Kobayashi T, Kai Y, Okuno S. Single-laboratory validation for the determination of caffeic acid and seven caffeoylquinic acids in sweet potato leaves. Biosci Biotechnol Biochem. 2014; 78: 2073–2080.
341. Dao L, Friedman M. Chlorogenic acid content of fresh and processed potatoes determined by ultraviolet spectrophotometry. J Agric Food Chem. 1992; 40: 2152–2156.
342. Siddiqi AI, Freedman SO. Identification of chlorogenic acid in castor bean and oranges. Can J Biochem Physiol. 1963; 41: 947–952.
343. Dawidowicz AL, Typek R. Thermal stability of 5-o-caffeoylquinic acid in aqueous solutions at different heating conditions. J Agric Food Chem. 2010; 58: 12578–12584.
344. US Food and Drug Administration. FDA 101: Dietary Supplements. Center for Drug Evaluation and Research; 2008. Report No.: 101. Last accessed 10 Mar 2017. Available: https://www.fda.gov/downloads/ForConsumers/ConsumerUpdates/UCM050824.pdf
345. Trugo LC, Macrae R. Chlorogenic acid composition of instant coffees. Analyst. 1984; 109: 263–266.
346. United States Pharmacopeia. USP chapter: 1092 The dissolution procedure: development and validation. 2014. Last accessed 10 Mar 2017. Available: http://www.usp.org/sites/default/files/usp_pdf/EN/gc_1092.pdf
347. Schrieber R, Gareis H. Gelatine Handbook: Theory and Industrial Practice. John Wiley & Sons; 2007.
348. Hsieh K-T, Liu P-H, Urban PL. Automated on-line liquid–liquid extraction system for temporal mass spectrometric analysis of dynamic samples. Anal Chim Acta. 2015; 894: 35–43.
349. Kruger NJ. The Bradford method for protein quantitation. Methods Mol Biol. 1994; 32: 9–15.
350. Adrover A, Pedacchia A, Petralito S, Spera R. In vitro dissolution testing of oral thin films: A comparison between USP 1, USP 2 apparatuses and a new millifluidic flow-through device. Chem Eng Res Des. 2015; 95: 173–178.
351. Qureshi SA, Shabnam J. Cause of high variability in drug dissolution testing and its impact on setting tolerances. Eur J Pharm Sci. 2001; 12: 271–276.
352. Meyer MC, Straughn AB, Mhatre RM, Hussain A, Shah VP, Bottom CB, Cole ET, Lesko LL, Mallinowski H, Williams RL. The effect of gelatin cross-linking on the

bioequivalence of hard and soft gelatin acetaminophen capsules. Pharm Res.; 2000; 17: 962–966.
353. Rossi RC, Dias CL, Donato EM, Martins LA, Bergold AM, Fröehlich PE. Development and validation of dissolution test for ritonavir soft gelatin capsules based on in vivo data. Int J Pharm. 2007; 338: 119–124.
354. Collins CD, Craggs M, Garcia-Alcega S, Kademoglou K, Lowe S. "Towards a unified approach for the determination of the bioaccessibility of organic pollutants." Environ Int. 2015; 78: 24–31.
355. (ICHT) International conference on harmonisation of technical requirements for registration of pharmaceuticals for human use. Validation of analytical procedures: Text and methodology. 2014. Last accessed 10 Mar 2017. Available: http://somatek.com/content/uploads/2014/06/sk140605h.pdf
356. Yardım Y, Keskin E, Şentürk Z. Voltammetric determination of mixtures of caffeine and chlorogenic acid in beverage samples using a boron-doped diamond electrode. Talanta. 2013; 116: 1010–1017.
357. Li Z, Huang D, Tang Z, Deng C, Zhang X. Fast determination of chlorogenic acid in tobacco residues using microwave-assisted extraction and capillary zone electrophoresis technique. Talanta. 2010; 82: 1181–1185.
358. Urakova IN, Pozharitskaya ON, Shikov AN, Kosman VM, Makarov VG. Comparison of high performance TLC and HPLC for separation and quantification of chlorogenic acid in green coffee bean extracts. J Sep Sci. 2008; 31: 237–241.
359. Chao M, Ma X. Voltammetric determination of chlorogenic acid in pharmaceutical products using poly(aminosulfonic acid) modified glassy carbon electrode. J Food Drug Anal. 2014; 22: 512–519.
360. Lorenzi D, Entwistle J, Cave M, Wragg J, Dean JR. The application of an in vitro gastrointestinal extraction to assess the oral bioaccessibility of polycyclic aromatic hydrocarbons in soils from a former industrial site. Anal Chim Acta. 2012; 735: 54–61.
361. Li Y, Dvořák M, Nesterenko PN, Stanley R, Nuchtavorn N, Krčmová LK, Aufartová J, Macka M. Miniaturised medium pressure capillary liquid chromatography system with flexible open platform design using off-the-shelf microfluidic components. Anal Chim Acta. 2015; 896: 166–176.
362. Su C-K, Peng P-J, Sun Y-C. Fully 3D-Printed preconcentrator for selective extraction of trace elements in seawater. Anal Chem. 2015; 87: 6945–6950.
363. Prabhu GRD, Urban PL. The dawn of unmanned analytical laboratories. Trends Anal. Chem. 2017; 88: 41-52.
364. TeamViewer: soporte remoto, acceso remoto, colaboración en línea y reuniones. Last accessed 10 Mar 2017. Available: https://www.teamviewer.com/en/
365. Dropbox. Last accessed 10 Mar 2017. Available: https://www.dropbox.com/home

366. Raspberry Pi - Teach, Learn, and Make with Raspberry Pi. Last accessed 10 Mar 2017. Available: https://www.raspberrypi.org/
367. BeagleBoard - black. Last accessed 10 Mar 2017. Available: https://beagleboard.org/black
368. Horstkotte B, Tovar Sánchez A, Duarte CM, Cerdà V. Sequential injection analysis for automation of the Winkler methodology, with real-time SIMPLEX optimization and shipboard application. Anal Chim Acta. 2010; 658: 147–155.
369. Allowing less secure apps to access your account – Google accounts help. Last accessed 10 Mar 2017. Available: https://support.google.com/accounts/answer/6010255
370. SMTP protocol client — Python 2.7.13 documentation. Last accessed 10 Mar 2017. Available: https://docs.python.org/2/library/smtplib.html
371. Communication APIs for SMS, Voice, Video and Authentication. Last accessed 10 Mar 2017. Available: https://www.twilio.com/